
Electronic Thesis and Dissertation Repository

9-22-2017 12:00 AM

Depositional and Environmental Controls on Oxygen and Carbon Isotope Compositions of Late Pleistocene to Mid-Holocene Shelly Fauna from the Huron Basin, Ontario, Canada

Jane Wilson, *The University of Western Ontario*

Supervisor: Fred Longstaffe, *The University of Western Ontario*

A thesis submitted in partial fulfillment of the requirements for the Master of Science degree in Geology

© Jane Wilson 2017

Follow this and additional works at: <https://ir.lib.uwo.ca/etd>



Part of the [Geochemistry Commons](#)

Recommended Citation

Wilson, Jane, "Depositional and Environmental Controls on Oxygen and Carbon Isotope Compositions of Late Pleistocene to Mid-Holocene Shelly Fauna from the Huron Basin, Ontario, Canada" (2017). *Electronic Thesis and Dissertation Repository*. 4989.

<https://ir.lib.uwo.ca/etd/4989>

This Dissertation/Thesis is brought to you for free and open access by Scholarship@Western. It has been accepted for inclusion in Electronic Thesis and Dissertation Repository by an authorized administrator of Scholarship@Western. For more information, please contact wlsadmin@uwo.ca.

Abstract

The $\delta^{18}\text{O}$ and $\delta^{13}\text{C}$ of aragonitic mollusc shells were analyzed from nine sites in the Huron Basin, Ontario, Canada. These sites represent three lake phases spanning the Late Pleistocene to the mid-Holocene (Algonquin, Transitional, and Nipissing) and three depositional environments (fluvial, estuarine, and lacustrine). Depositional environment controls mollusc $\delta^{18}\text{O}$ more strongly than climate. The source of carbon and climate control the $\delta^{13}\text{C}$ of the shelly fauna. Shells from fluvial sites are most depleted of ^{18}O and exhibit the greatest antipathetic $\delta^{13}\text{C}$ - $\delta^{18}\text{O}$ covariation. This reflects the dynamic nature of this system. Lacustrine sites have the highest $\delta^{18}\text{O}$ and $\delta^{13}\text{C}$ - $\delta^{18}\text{O}$ shows a weak positive covariation with open hydrology, but a distinct $\delta^{13}\text{C}$ - $\delta^{18}\text{O}$ negative covariation when the water body was isolated. Estuarine $\delta^{18}\text{O}$ lies between these two end members. These data demonstrate that depositional environment must be known before climatic interpretations are made using the isotopic compositions of freshwater shells from the Huron basin.

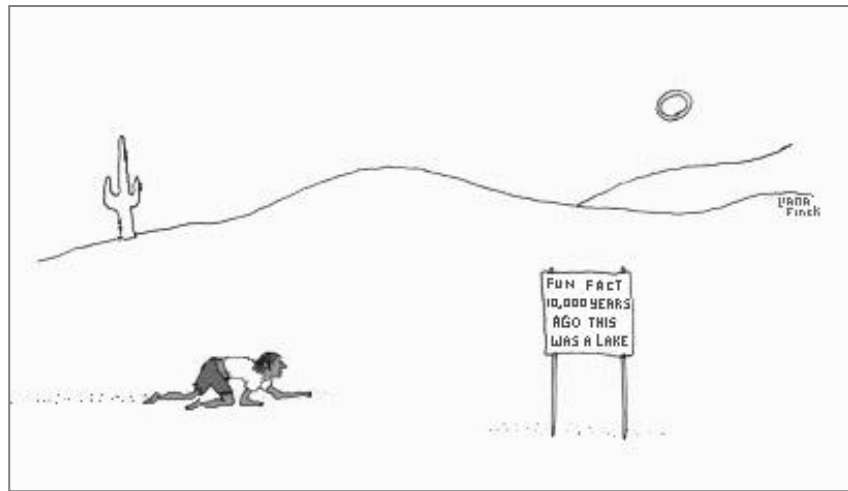
Keywords

Stable isotopes of molluscs, climate, Late Pleistocene to mid-Holocene, Lake Huron

Epigraph

Dedicated to my Grandfather.

There once was a shell from a lake
Whose isotopy looked rather fake
It turns out it differs
From lagoons to rivers,
And that is the point that I make.



Lake Meditation #478 by Liana Finck (2015)

Acknowledgments

First and foremost, I would like to thank my supervisor Dr. Fred Longstaffe whose support and patience (through my many ups and downs) has pushed me steadily towards becoming a better academic. I've also been very fortunate to share in his wisdom and sense of humour. I am truly grateful for the financial assistance given to me during the twilight of my program. With it, I was able to raise the quality of my writing to a level that reflected the quality of my research.

Next it is important to mention the people who retrieved my samples from the many ditches and streams. Without the work of Paul Karrow, Andy Bajc, and Fred Longstaffe identifying these tough-to-find locations, I wouldn't have had such a successful suite of samples. Also, I'd like to thank Rachel Schwartz-Narbonne for lending a hand in their recovery.

The previous research completed by Anita Godwin and Rebecca Macdonald proved to be essential for filling in the gaps of my research. The story would not have been so clear if not for their work.

I would also like to thank the fabulous women who run our Laboratory for Stable Isotopes Science: Kim Law, who has been giving me guidance since my second year of undergraduate studies; and Li Huang and Grace Yau, who have showed infinite patience and perseverance during my time working with the Multiprep.

Thank you as well to Dr. Steve Hicock, who has had his hand in my education, whether it was teaching me the basics about rocks on the first day of my undergraduate studies or hiring me as a teaching assistant to introduce the basics to a new class of students during my last working term. I was very pleased to learn that he was part of my advisory committee.

I would also like to thank the friends I have made in my years in London, with a special thanks to the lucky few of office 1031. Their guidance through the graduate program was not insignificant; however, it was their friendship during that time that was more important. Also, a shout out to the past and present members of the Lake Pod: Jacob Walker, Rebecca Doyle, Zijun Liu, Gila Binyamini, and Ryan Hladynuik.

This project was made possible by the generous funding provided by The Natural Sciences and Engineering Research Council of Canada Discovery Grant (FJL), the Canada Research Chairs Program (FJL), the Canada Foundation for Innovation (FJL) and the Ontario Research Fund (FJL).

Last but certainly not least, I would like to thank my Mom and Dad for their constant support and guidance through my life. Their recognition of my new passion for rocks helped me realize that I could go back to school. I don't know if I could have done it without them.

Table of Contents

Abstract.....	i
Epigraph.....	ii
Acknowledgments.....	iii
Table of Contents.....	v
List of Tables.....	ix
List of Figures.....	x
List of Appendices.....	xvii
Chapter 1.....	1
1 Introduction.....	1
1.1 Project Overview.....	1
1.2 Thesis Structure.....	1
1.3 Research Objectives.....	3
1.4 Sedimentary Environments.....	3
1.4.1 Fluvial Systems.....	3
1.4.2 Estuarine Systems.....	5
1.4.3 Lacustrine Systems.....	6
1.5 Site Locations and Descriptions.....	7
1.5.1 Fluvial Locations.....	8
1.5.2 Estuarine Locations.....	11
1.5.3 Lacustrine Locations.....	12
Chapter 2.....	14
2 Background Information.....	14
2.1 Mollusc Biogenic Carbonate, Oxygen Isotopes and Isotopic Vital Effects.....	14
2.1.1 Mollusc Biogenic Carbonate.....	14

2.1.2	Oxygen Isotopes ($\delta^{18}\text{O}$).....	15
2.1.3	Carbon Isotopes ($\delta^{13}\text{C}$).....	19
2.1.4	Controls on the Oxygen and Carbon Isotope Variations in Water	22
2.1.5	Vital Effects	24
2.2	Assumptions.....	26
2.3	Species Information	27
2.3.1	<i>Valvata</i> spp. (Say, 1817).....	27
2.3.2	<i>Pisidium</i> spp. (Pfeiffer, 1821).....	28
2.3.3	<i>Amnicola limosa</i> (Say, 1817).....	29
2.3.4	Species Assemblages	29
2.3.5	Indicator Fossils	30
2.4	General History of Lake Huron	30
2.4.1	History of the Huron Basin.....	34
2.4.2	Lake Agassiz.....	35
2.4.3	Huron Basin	36
2.4.4	Lake Algonquin	39
2.4.5	Main Lake Algonquin Phase.....	39
2.4.6	Transitional Phase.....	42
2.4.7	Nipissing Phase.....	45
Chapter 3	48
3	Methodology	48
3.1	Field Methods	48
3.2	Laboratory Methods.....	48
3.2.1	Sieving	48
3.2.2	Shell Identification.....	48
3.2.3	Sample Selection.....	48

3.2.4	Powder X-Ray Diffraction (<i>p</i> XRD).....	49
3.2.5	Stable Isotope Sampling	49
3.2.6	Serial Sampling.....	50
3.2.7	Standardisation of Isotopic Results for Biogenic Carbonate	51
3.2.8	Water $\delta^{18}\text{O}$	52
Chapter 4.....		53
4	Results	53
4.1	<i>p</i> XRD Results	53
4.2	Species Identification and Counts by Site	53
4.3	Stable Carbon and Oxygen Isotope Results.....	54
4.3.1	Algonquin Phase	55
4.3.2	Transitional Phase.....	57
4.3.3	Nipissing Phase.....	59
4.4	Consideration of Small Sample Sets ($n \leq 5$).....	63
Chapter 5.....		64
5	Discussion	64
5.1	Vital Effects	64
5.2	Indicator Species.....	65
5.3	Re-evaluating the $\delta^{18}\text{O}$ of Meteoric Water During the Holocene in Southern Ontario	67
5.4	Data Sets from Previous (Unpublished) Theses	71
5.5	Water Oxygen Isotope Compositions	72
5.6	Depositional Environments.....	73
5.6.1	Lacustrine sites.....	74
5.6.2	Fluvial Sites	80
5.6.3	Estuarine Sites.....	91

5.7 Comparison Between Depositional Environments Over Time: Summary	93
Chapter 6.....	95
6 Conclusions and Future Work.....	95
6.1 Major Conclusions	95
6.2 Future Work	96
References.....	98
Appendices.....	114
Curriculum Vitae	144

List of Tables

Table 2.1 - Average growth temperatures of different mollusc species	27
Table 2.2 - Species and environments from Miller et al. (1979) and Mackie (2007).....	29
Table 4.1 - Relative abundance of fossil fauna identified at each site by species and total number of shells counted (n). The absolute and relative abundances of each genera / species are listed in Appendix E.....	53
Table 5.1 - Relative abundance of species found at each site other than ubiquitous <i>Valvata</i> spp. and <i>Pisidium</i> spp. and total number of shells counted (n). Sites 52/53 have been considered together because they both represent the same environment and lake phase. I = Nipissing Indicator species. Appendix E lists the species counts and relative abundances for all species.	66
Table 5.2 - Summary of isotopic data from Godwin (1985) and Macdonald (2012). All data are provided in Appendices H and I, respectively.	72

List of Figures

Figure 1.1 - Idealised diagram illustrating the controls on water input and output and the relative magnitude of their effect on the system within two river regimes. Black arrows indicate input, and yellow arrows indicate output. Size of the arrows indicates relative magnitude.....	4
Figure 1.2 - Idealised model of estuarine sediment sequence (after Fuks and Wilkinson, 1998).	5
Figure 1.3 - Idealised diagram illustrating the controls on water input and output and the relative magnitude of their effect on the system within two lake water regimes that occupied the Great Lakes basin. Black arrows indicate input, and yellow arrows indicate output. (a) Open lakes are supplied by precipitation, inflowing rivers, terrestrial runoff, and ground water that equals water loss from evaporation and outlet channels. (b) Closed or terminal lakes experience a large amount of evaporation that can exceed the input of precipitation, inflowing rivers, terrestrial runoff, and ground water, which results in a fall in lake level.....	6
Figure 1.4 - Site locations. Red - Algonquin Phase; Yellow - Transitional Phase; Blue - Nipissing Phase. (Google Earth, 2016).....	8
Figure 1.5 - Locations of fluvial sites 51-53 (Google Earth, 2016).....	9
Figure 1.6 - Location of Algonquin site 13. (Google Earth, 2016)	10
Figure 1.7 - Location of Algonquin sites K6 and K21 (yellow), and Transitional site K10 (red). (Google Earth, 2016).....	11
Figure 1.8 - Location of Ferndale (FN-1, 2, 8) and Sucker Creek (Google Earth, 2016).....	13
Figure 2.1 - Annual average $\delta^{18}\text{O}$ of meteoric water in southern Ontario (Longstaffe <i>et al.</i> , 2013).	16
Figure 2.2 - (a) Controls on oxygen isotopic composition of meteoric water. Arrows indicate the direction of isotopic change with each control. Light blue arrow indicates that evaporation is most strongly linked to drier conditions. (b) Controls on oxygen isotopic	

composition by depositional environment. (c) Oxygen isotope fractionation of water remaining after evaporation. Starting $\delta^{18}\text{O}$ illustrated is -5‰ ; h is relative humidity. The graph illustrates enrichment of ^{18}O for constant volume, well mixed lakes as a function of the fraction of water lost by evaporation relative to total inflow (after Gonfiantini, 1986). .. 16

Figure 2.3 - (a) Idealised controls on carbon isotopic composition of DIC. (b) Idealised controls on carbon isotopic composition by water energy..... 20

Figure 2.4 - The Niagara Escarpment overland in southern Ontario (Google Earth, 2016)... 22

Figure 2.5 – Shells from site 53 (a) *Valvata tricarinata*. (b) *Valvata sincera*. (c) *Valvata sincera* side shell opening and umbilicus..... 27

Figure 2.6 - *Pisidium* sp. valve. 28

Figure 2.7 - *Amnicola limosa*..... 29

Figure 2.8 - Generalized Palaeozoic bedrock geology map of southern Ontario (after Haeri-Ardakani *et al.*, 2013). 32

Figure 2.9 - Bathymetry map of Lake Huron (after Thomas *et al.*, 1973)..... 33

Figure 2.10 - Lake Agassiz (after Leverington and Teller, 2003). 35

Figure 2.11 - Age-dependent variations in the Huron Basin since the Late Pleistocene. (a) ¹ Change in relative MAT from modern for south-eastern Canada (Terasmae, 1961), ² Change in relative humidity from modern and actual $\delta^{18}\text{O}$ of precipitation in southern Ontario (Edwards *et al.*, 1996). (b) ¹ Change in relative precipitation amount from modern times in Minnesota, USA (Webb III *et al.*, 1987), ² Relative lake level from modern times (Lewis *et al.*, 2008a). 37

Figure 2.12 - Inferred lake level changes and phases in the Huron Basin from the late Pleistocene to present adjusted for isostatic rebound after Eschman and Karrow (1985), Baedke and Thompson (2000), Lewis *et al.* (2008a,b), Brooks *et al.* (2012) and Lewis and Anderson (2012). Full-discharge line is from Lewis and Anderson (2012). Lake water oxygen isotopic data for northern Lake Huron are calculated from ostracode data provided by

Lewis *et al.* (1994, core 37P), Moore *et al.* (2000, core 22P), Wakabyashi (2010, core 181) and Macdonald (2012, core 596). Carbon isotopic data for northern Lake Huron were obtained using ostracod shell data from Lewis *et al.* (1994, core 37P), Wakabyashi (2010, core 181) and Macdonald (2012, core 596). Table insert - Summary of major lake phases in the Huron basin in radiocarbon years from Macdonald and Longstaffe (2008). Map insert shows core locations from above..... 38

Figure 2.13 - Main Algonquin phase [12.2 ¹⁴C ka [14.2 ka cal) BP] lake boundary (light blue) overlain on the modern lake boundary (darker blue). LIS - Laurentide Ice Sheet with arrows showing the direction of retreat (after Prest, 1970; Eschman and Karrow, 1985; Karrow 1987a) and moisture regimes in southern Ontario from pollen data (Shuman *et al.*, 2002)... 40

Figure 2.14 - Transitional phase [7.4 ¹⁴C ka (8.2 ka cal) BP] light blue) lake boundary overlain on the modern lake boundary (darker blue). (after Eschman and Karrow, 1985; Lewis *et al.*, 1994). 43

Figure 2.15 - Nipissing phase [5.0 ¹⁴C ka (5.7 ka cal) BP] lake boundary (light blue) overlain on the modern lake boundary (darker blue) (after Eschman and Karrow, 1985) and moisture regime in southern Ontario (Shuman *et al.*, 2002)..... 45

Figure 3.1 - Schematic for serial sampling of *Pisidium* spp. shell. 50

Figure 4.1 - All shell carbon and oxygen isotopic results produced in this project for southern Ontario. 54

Figure 4.2 - Isotopic composition of fluvial Algonquin site shells by species at (a) site 13, and (b) site K6..... 55

Figure 4.3 - Algonquin sites and their average shell $\delta^{18}\text{O}$ and shell $\delta^{13}\text{C}$. Light blue – Lake Algonquin water. Black lines – modern lake boundary..... 56

Figure 4.4 - (a) Bulk isotopic results for Algonquin estuarine site K21 shells by species. (b) Isotopic results for serial sampling of three *Pisidium* spp. shells. All results and schematics are provided in Appendix G..... 57

Figure 4.5 - (a) Transitional sites and their average shell $\delta^{18}\text{O}$ and $\delta^{13}\text{C}$. Light blue – Transitional phase lake water. Black lines – modern lake boundary. (b) Isotopic results for site 51 shells by species.	58
Figure 4.6 - Isotopic results for site K10 shells by species.	58
Figure 4.7 - (a) Nipissing sites and their average shell $\delta^{18}\text{O}$ and $\delta^{13}\text{C}$. Light blue – Lake Nipissing water. Black lines – modern lake boundary. (b) Isotopic results for Nipissing phase fluvial site 52 by fauna analysed.	59
Figure 4.8 - Isotopic results for one serial-sampled <i>Pisidium</i> sp. shell from site 52. All results and schematic are [provided in Appendix G.	60
Figure 4.9 - (a) Isotopic results for Nipissing phase fluvial site 53 by fauna analysed. (b) Isotopic results for serial-sampled <i>Pisidium</i> spp. shell from site 53. Numbers refer to individual shells analysed. All results and schematics are provided in Appendix G.	61
Figure 4.10 - Isotopic results for shells from Nipissing phase lacustrine sites at Ferndale and Sucker Creek.	62
Figure 5.1 - Carbon vs. oxygen isotope compositions of <i>Pisidium</i> spp. by calculated weighted mean of successive growth layers. Arrows denote the younging direction. Full schematics and isotopic results are provided in Appendix G.	64
Figure 5.2 - Location of sites studied by Edwards <i>et al.</i> (1996) (Google Earth, 2016).	68
Figure 5.3 - (a) average length of the growing season in Ontario from 1971 - 2000. (b) Estimated growing season length based on a 1 to 2 °C increase in monthly averages from 2010 to 2039 (Agriculture and Agri-Food Canada, 2014).	69
Figure 5.4 – Modern contours of equal $\delta^{18}\text{O}$ for meteoric water (VSMOW) for North America. LIS - Approximate boundary of the Laurentide Ice Sheet at the end of the Main Algonquin phase [10.2 ^{14}C ka (12.1 ka cal) BP] (blue line) after Kohn and Dettman (2007). North American map from Google Earth (2016).	70

Figure 5.5 - Effect of precipitation $\delta^{18}\text{O}$ / temperature gradient. Red solid line – present mid-to high-latitude isotopic gradient. Dotted lines – other gradients. The intersection point of the example gradients is based on Edwards and Fritz (1986): annual temperature for southern Ontario 7.1 °C and $\delta^{18}\text{O}$ of annual precipitation –11 ‰. Horizontal dashed lines indicate the minimum and maximum precipitation $\delta^{18}\text{O}$ for southern Ontario during the Holocene from Edwards *et al.* (1996). 71

Figure 5.6 - Study areas of Godwin (1985) and Macdonald (2012) (Google Earth, 2016). 71

Figure 5.7 - Calculated water $\delta^{18}\text{O}$ for each site using the shell-water oxygen isotope fractionation factors of Macdonald (2012). Shapes indicate the mean water $\delta^{18}\text{O}$. Lines indicate the total range of $\delta^{18}\text{O}$. For sites 52 and 53, only the weighted mean results for serially-sampled shells are included. Appendix F lists calculated water $\delta^{18}\text{O}$ for each sample. 72

Figure 5.8 - All isotopic data (including Godwin, 1985 and Macdonald, 2012) for shells presented in terms of calculated water oxygen isotopic compositions and shell carbon isotopic compositions. The results have been categorised by lake phase (red - Algonquin; yellow - Transitional; blue - Nipissing) and by depositional environment (square -fluvial, triangle - estuarine; circle - lacustrine). 73

Figure 5.9 - (a) Lake Algonquin shoreline at time of emergence of the Six Fathom Scarp, which isolated the Goderich sub-basin. The Ipperwash scarp to the south may have further isolated the lake during extreme lowstands. (b) Goderich sub-basin core 594 showing interval 9.8 to 15 m. Black intervals are sections lost to radiocarbon dating. *Pisidium* spp. were restricted to 12.8 to 15.0 m depth (from Macdonald, 2012). 74

Figure 5.10 - Lake water isotopic variations in the Goderich sub-basin (solid lines) and the northern Manitoulin and Mackinac sub-basins (dotted lines) inferred from ostracodes (Lewis *et al.*, 1994; Moore *et al.*, 2000; Lewis and Anderson, 2012) and *Pisidium* spp. (Macdonald, 2012). Inferred lake level variations are also shown, based on the above references. 75

Figure 5.11 - Ferndale and Sucker Creek isotopic compositions of *Valvata* spp. and *Pisidium* spp. Lake water oxygen isotope composition has been determined using ostracode valves from two cores (146: $\delta^{18}\text{O}$ –6 ‰; 594: $\delta^{18}\text{O}$ –7 ‰) in the Goderich sub-basin to the south

of Ferndale site, which has been dated to the Nipissing phase [~ 4.4 ^{14}C ka (5 ka cal) BP] (Macdonald and Longstaffe, 2008).....	77
Figure 5.12 – Water oxygen and carbon isotopic compositions calculated for Algonquin phase Core 594 and Nipissing phase Ferndale and Sucker Creek samples.	78
Figure 5.13 - Direction of idealised isotopic change affecting lake water resulting from various processes. OM = organic matter; DS = dissolved solids.....	79
Figure 5.14 – Location of fluvial Algonquin sites with their average water $\delta^{18}\text{O}$ and $\delta^{13}\text{C}$ shell isotopic compositions. Solid black lines indicate isobases representing predicted deformation in meters from 9.9 ka (11.3 ka cal) BP (after Clark <i>et al.</i> , 2007).	80
Figure 5.15 – (a) Isotopic composition of all species of Algonquin phase fluvial sites. Godwin (1985) data are shown as open squares. (b) Water isotopic compositions derived from <i>Valvata</i> spp. shells for Algonquin-phase fluvial sites.....	81
Figure 5.16 - Topography along transect between K6 and 13 (Google Earth, 2016).....	81
Figure 5.17 - Direction of idealised isotopic change affecting original river water compositions resulting from various processes. OM - organic matter; DS - dissolved solids; Lat - latitude.....	82
Figure 5.18 – Isotopic composition of all species from Transitional- and Nipissing-phase fluvial sites.....	83
Figure 5.19 - (a) Monthly conditions for the Nottawasaga River. Monthly mean of mean daily discharge for a 4-year period of the Nottawasaga River at Baxter (1992-1996) (Thornbush, 2001). Average monthly temperatures for 2008 recorded at Barrie, Ontario (Government of Canada, 2016). Inset - Water temperature of Nottawasaga River recorded on specific dates in 2008 (Nottawasaga Valley Conservation Authority, 2014). (b) Location of fluvial sites and surrounding towns (Google Earth, 2016).	84
Figure 5.20 - Isotopic results for fluvial sites 51-53 by species.	85

Figure 5.21 - Predicted deformation in the Lake Huron region relative to present due to unloading of the LIS. Fluvial sites 51-53 are shown at the estimated time of deposition (after Clark *et al.*, 2007). 86

Figure 5.22 - Water oxygen vs. shell carbon isotopic composition averages (triangles) based on results for *V. sincera* and *V. tricarinata*. Solid line represents a linear regression of all data for each time phase. Dashed lines represent one standard deviation for $\delta^{18}\text{O}$ and $\delta^{13}\text{C}$ of each time phase. 87

Figure 5.23. River water oxygen isotope composition versus temperature ($\text{‰} / \text{°C}$) when mixed with 65 % and 75 % ground water (Algonquin and Transitional -17‰ , Nipissing -13‰) over the growth temperature range of *Valvata* spp. Black line represents average growth temperature for *Valvata* spp (Godwin, 1985; Macdonald, 2012). Gradients are based on a southern Ontario modern average annual temperature of 7.1°C and average annual precipitation $\delta^{18}\text{O}$ of -11‰ (Edwards and Fritz, 1986)..... 89

Figure 5.24 - (a) Locations of estuarine sites. (Google Earth, 2016 (b) Water oxygen and shell carbon isotope compositions of all species from estuarine sites. Godwin (1985) shown as open triangles. Red – Algonquin phase; Yellow – Transitional phase..... 91

Figure 5.25 - Monthly precipitation for Kincardine, Ontario for 2016 (Government of Canada, 2016). 92

Figure 5.26 - *Valvata* spp. and *Pisidium* spp. $\delta^{13}\text{C}$ shell and $\delta^{18}\text{O}$ water results (for $n \geq 6$) categorized by depositional environment and lake phase. Algonquin phase - red; Transitional phase - orange; Nipissing phase - blue. Dash lines bound the range of $\delta^{18}\text{O}$ for each environment. Ellipses represent 60 % data. 93

Figure 5.27 - (a) Location of Algonquin phase sites. (b) Three Algonquin phase [~ 11 to $10.3 \text{ }^{14}\text{C ka}$ (12.9 to 12.1 ka cal) BP] sites from three environments on the east shore of modern Lake Huron. 94

List of Appendices

Appendix A - Site Descriptions and Locations.....	114
Appendix B - Sediment Columns	115
Appendix C - Isotopic Results for Standards.....	122
Appendix D - XRD Pattern.....	124
Appendix E - Absolute and Relative Percent Shell Abundances	125
Appendix F – All Isotopic Results for Samples.....	126
Appendix G - Serial Sampling Schematics and Isotopic Results	138
Appendix H - Oxygen and Carbon Isotope Data from Core 594 from Macdonald (2012)..	141
Appendix I - Oxygen and Carbon Isotope Data from Godwin (1985)	142

Chapter 1

1 Introduction

1.1 Project Overview

Southern Ontario has experienced major hydrological and climatic changes since the retreat of the Laurentide Ice Sheet (LIS). Several studies in this region have utilized isotopic measurements of mollusc shells to determine the isotopic compositions of modern and ancient river and lake systems (Keith *et al.*, 1964; Fritz and Poplawski, 1974; Stuiver, 1970; von Grafenstein *et al.*, 1994, 1999, 2013; Dettman *et al.*, 1995; Li and Ku, 1997; Guiguer, 2000; Macdonald and Longstaffe, 2008; Hyodo and Longstaffe, 2012; Hladyniuk and Longstaffe, 2016). These studies were completed with the overarching goal of interpreting climatic and environmental conditions in the region. While these studies have increased our understanding of southern Ontario's regional climate history, they are each limited to one specific depositional setting. Few studies have compared variations among depositional environments, and even fewer have examined those differences over time.

This study uses the $\delta^{18}\text{O}$ and $\delta^{13}\text{C}$ of shelly fauna contained in sediment samples to reconstruct the climatic and paleoecological conditions of southern Ontario from the late Pleistocene (Main Algonquin phase), to the early Holocene (Transitional phase), to the mid-Holocene (Nipissing phase). The principal objective of this work is to determine if depositional environment or climate is the stronger control on oxygen and carbon stable isotopic compositions of molluscs. This project then endeavours to develop a paleo-environment and paleo-climatic model for the sites to add to our understanding of such change in southern Ontario over the last 12,000 years. To accomplish these goals, sub-fossil shelly fauna were extracted from glacial and post-glacial sediments in three depositional environments across the three time periods of interest.

1.2 Thesis Structure

Chapter 1 introduces the three sedimentary environments that are the focus of this thesis and provides more detailed information about each study site. The research objectives are also presented in this chapter.

Chapter 2 describes biogenic carbonate and introduces the controls on its oxygen and stable carbon isotope compositions. This chapter characterises the environments occupied by the three mollusc genera fauna of interest: *Valvata*, *Pisidium*, and *Amnicola*. It identifies other species that can be used to define environmental setting or geological time of deposition and presents an overview of the geology and geography of the Lake Huron basin and how it has changed over time.

Chapter 3 explains the methodology used in this study. Isotopic analysis of shell carbonate was completed on bulk samples, and serial sampling was performed on bivalve valves of *Pisidium* spp. Water oxygen isotope compositions were calculated for all sites based on species-specific fractionation factors reported by Macdonald (2012).

Chapter 4 reports the results of bulk sampling of the three selected mollusc genera and the serial sampling of *Pisidium* spp. collected from locations around Lake Huron, and further categorises them by lake phase. This chapter also provides information about number of results needed to characterize isotopic variability.

Chapter 5 first establishes that for *Pisidium* spp., vital effects, if present, are too small to affect interpretation of the isotopic results. Indicator species are then used to help constrain depositional environment, as well as geological time of deposition. The oxygen isotopic composition of precipitation, and its systematic variation with geographic location (“isotopic gradient”), is re-evaluated for the periods of geological time considered in this study, relative to the modern pattern known for southern Ontario. Previous work of Godwin (1985) and Macdonald (2012) is introduced allowing for a preliminary interpretation of calculated water oxygen isotopic compositions for all sites. These results demonstrate that depositional environment, rather than climatic conditions, is the stronger control on the isotopic compositions of the shelly fauna analyzed. Further detailed interpretations are then made for each site, categorised by depositional setting and lake phase.

Chapter 6 summarizes the major findings and provides suggestions for future work.

1.3 Research Objectives

This study uses the $\delta^{18}\text{O}$ and $\delta^{13}\text{C}$ of shelly fauna:

- 1) To test for intra-shell variations in *Pisidium* spp. that may arise from vital effects or varying conditions during growth, which could affect the interpretation of isotopic data for this species;
- 2) To identify and compare isotopic variability related to specific geographic and environmental sites dated to specific Late-Pleistocene to mid-Holocene times to elucidate the isotopic controls on shell and water isotopic composition;
- 3) To test the hypothesis that habitat controls are more influential than regional climate controls on the isotopic composition of the shelly fauna studied; and
- 4) To begin reconstruction of a post-glacial climate history for the Lake Huron region, specifically the eastern Goderich and Manitoulin basin areas and surrounding river systems.

1.4 Sedimentary Environments

Three sedimentary environments were studied, which represent upstream fluvial systems to downstream estuarine systems (involving mixing of river and lake water) to the lacustrine environment.

1.4.1 Fluvial Systems

The morphology of streams differs from other open water bodies due to their narrow banks and continuously running water. Fluvial systems provide the primary transport mechanism for weathered debris to be deposited as clastic sediments downstream in lakes and seas (Nichols, 2009). River discharge represents the total volume flowing through a river channel at a given point measured in m^3 / s . The volume includes water, suspended inorganic s (e.g. clays) and organics (e.g. plant matter, diatoms), and dissolved compounds (e.g. CaCO_3 (aq)) (Turnipseed and Sauer, 2010). Figure 1.1 illustrates the types of inputs and outputs of two river systems – one with a higher flow rate, and one with a lower flow rate.

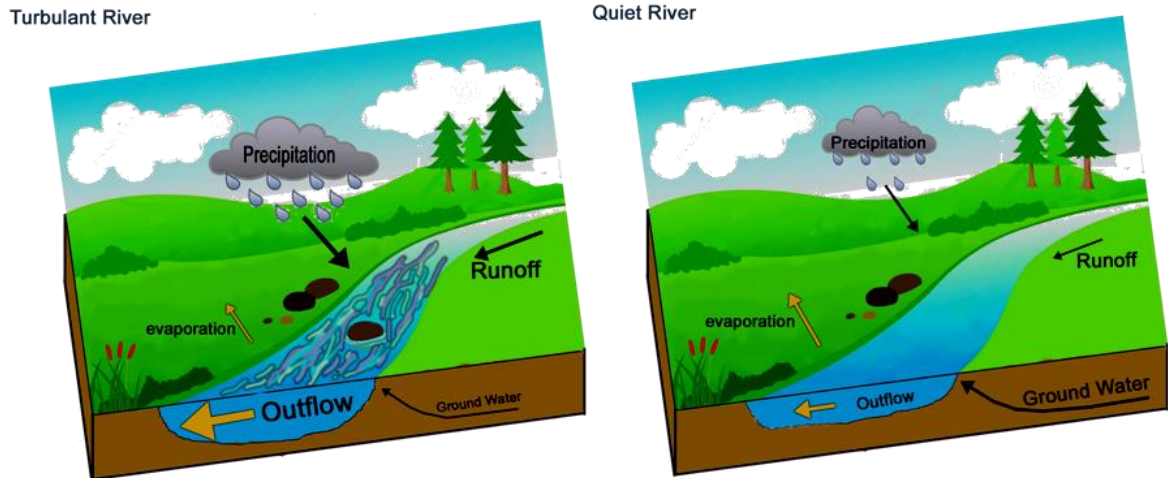


Figure 1.1 - Idealised diagram illustrating the controls on water input and output and the relative magnitude of their effect on the system within two river regimes. Black arrows indicate input, and yellow arrows indicate output. Size of the arrows indicates relative magnitude.

Clastic-dominated sediments, such as sands and silts, accumulate within channels and floodplains and the structure of the sediments is determined by many factors including: (i) the supply of clastic material; (ii) the gradient of the river; (iii) the total river discharge; and (iv) local and regional seasonal variations (Chandler and Kostaschuk, 1994; Thornbush, 2001; Nichols, 2009). Given the changing energy of river systems over time, fossil fauna such as shells can be destroyed, making good preservation uncommon (Nichols, 2009).

Weather, including air temperature, solar radiation, relative humidity, cloud cover, and wind speed, play roles in the heat exchange between the atmosphere and the river water. Air temperature and solar radiation are considered the most significant controls on equilibrium water temperatures (Sinokrot and Stefan, 1993; Magnuson *et al.*, 1997; Mohseni and Stefan, 1999) and strongly affect the river water. Therefore, seasonality has a much greater effect on fluvial systems than estuarine or lacustrine settings. Equilibrium water temperature is more strongly affected by atmospheric conditions with increasing travel time (i.e. low flow rate and/or long reach (Mohseni and Stefan, 1999). Tall vegetation, such as trees, can cause shading effects reducing the effect of daily temperature spikes, and provide shelter from airflow (Sinokrot and Stefan, 1993). The *actual* temperature of the river water at a given location lies between the upstream source water temperature and the equilibrium water temperature (Sinokrot and Stefan, 1993; Mohseni and Stefan, 1999).

In the Great Lakes region, ground water has a temperature range of 8 to 10 °C, which is not

affected by seasonal variations (Rodie and Post, 2009), and contributes 48 to 79 % of water to tributary flows (Lewis, 2016). This percentage is determined by the underlying geology, such as the porosity and permeability of the bedrock, topography and stream gradient (Sinokrot and Stefan, 1993; Mohseni and Stefan, 1999). In all river reaches, ground water input decreases downstream in association with decreasing gradient, indicating that fluvial systems will display a stronger precipitation and evaporative signal downstream (Cerling et al., 1988; Rodie and Post, 2009). As a result, upstream waters are more reflective of cold water regimes compared to downstream waters in summer months (Rodie and Post, 2009).

1.4.2 Estuarine Systems

For the purpose of this thesis, estuarine environments are defined by the regions where distributary channels meet and mix with a standing body of water, such as a lake or ocean (Hough, 1958). There is no requirement that the standing body of water be saline. As water nears the mouth of the river, water velocities approach zero, allowing for suspended clay- and silt-sized particles, as well as abundant nutrients carried from upstream, to be deposited (Fuks and Wilkinson, 1998; Wolfe *et al.*, 2007). Consequently, these areas are generally characterised by greater productivity.

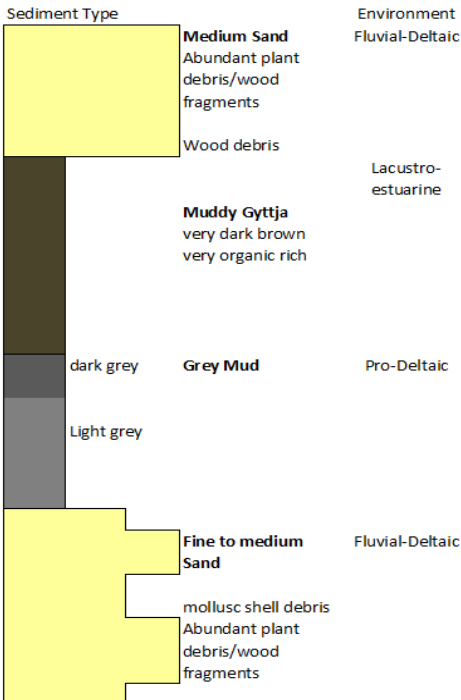


Figure 1.2 - Idealised model of estuarine sediment sequence (after Fuks and Wilkinson, 1998).

Estuaries are commonly mistaken for deltas, mainly because they occupy the same geographic location. The estuary is defined by the water at the mouth of a river, whereas the delta represents the landmass formed by the accumulation of sediments deposited at the river mouth. The resulting landscapes are inextricably linked to spatial and temporal fluctuations of river discharge (Wolfe *et al.*, 2007).

A study conducted on a Lake Michigan transgressive estuary sediment column showed that as the mouth of the river moved towards the lake, the sediment regimes change from a fine- or medium-grained sand to a muddy organic-rich sediment commonly referred to as gyttja (Fig 1.2; Fuks and Wilkinson, 1998). This

sediment sequence is important for identifying where in this depositional environment samples are being collected.

1.4.3 Lacustrine Systems

Lakes form in topographic lows and are recharged by seasonal precipitation (rain or snow), runoff from adjacent land surfaces, and inflow from rivers and ground water (Fig. 1.3; Lewis, 2016). Total ground water volume in the Great Lakes watershed is estimated to be 4900 km³ (International Joint Commission, 2010), but the extent, quantity and, significance of its input are not well known (Lewis, 2016). Modern ground water flows through sediments composed of permeable glacial till and outwashes down to the catchments underlain by relatively impermeable clays. These clays result in no more than 2 % of all meteoric waters permeating into the deeper Paleozoic flow system (McIntosh and Walter, 2005). Consequently, the vast majority of meteoric water flows to the Great Lakes basins, having a distinct impact on the basins' waters.

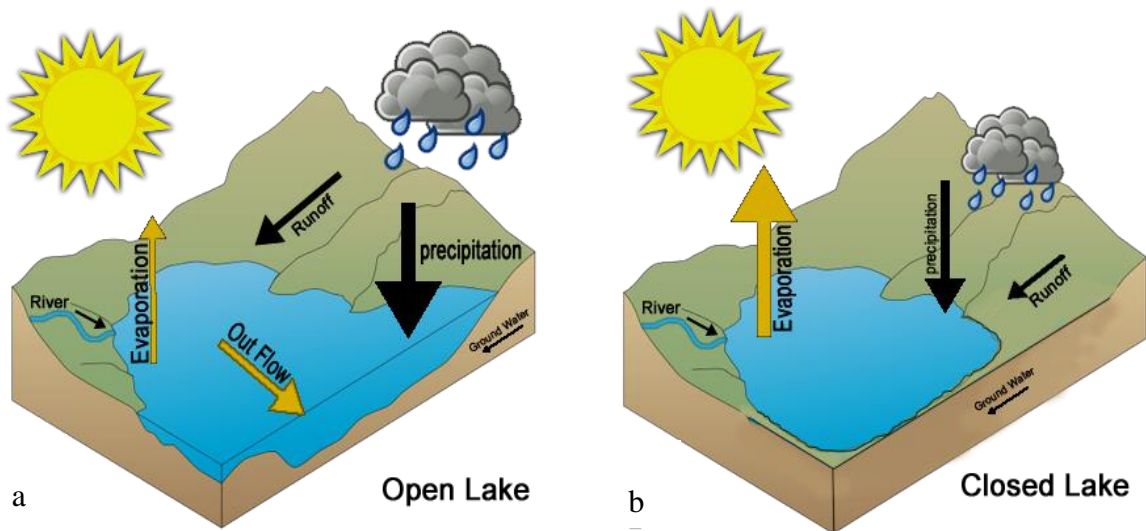


Figure 1.3 - Idealised diagram illustrating the controls on water input and output and the relative magnitude of their effect on the system within two lake water regimes that occupied the Great Lakes basin. Black arrows indicate input, and yellow arrows indicate output. (a) Open lakes are supplied by precipitation, inflowing rivers, terrestrial runoff, and ground water that equals water loss from evaporation and outlet channels. (b) Closed or terminal lakes experience a large amount of evaporation that can exceed the input of precipitation, inflowing rivers, terrestrial runoff, and ground water, which results in a fall in lake level.

Water is lost from lakes by evaporation from water surfaces and from sublimation from ice surfaces. The magnitude of each of these factors contributes to the water level and chemistry of the water body (Nichols, 2009; Lewis, 2016). Bottom water temperatures are generally

consistent throughout the year at ~ 4 °C (Walker, 2004), whereas surface water temperatures vary widely and are closely associated with air temperatures. Lakes in the temperate zone can undergo semi- to annual overturns and this vertical mixing is important for returning nutrients that have been deposited on the lake bottom to the photic zone. Strong surface-water mixing is typically linked to increased productivity (Meyers, 1997).

Smaller lakes are typically more productive than larger ones. Surrounding land resupply nutrients removed by biological activity, especially during times of increased precipitation, deforestation, or fire, which allows for increased erosion of soils (Meyers, 1997). Periods of drier climate may lower water levels and are generally associated with reduced aquatic productivity (Meyers and Lallier-Vergès, 1999).

1.5 Site Locations and Descriptions

This study examined the depositional environments for three different lake phases around the Lake Huron basin in southern Ontario. The earliest phase, the Algonquin Lake Phase (shown in red in Fig. 1.4), is represented by two fluvial sites (K6, 13) and one estuarine site (K21). The Transitional Phase (shown in yellow in Fig. 1.4) is represented by one fluvial site (51), and one estuarine site (K10). The latest phase (Nipissing; shown in blue in Fig. 1.4) is represented by one lacustrine site (Ferndale/Sucker Creek) and two fluvial sites (52, 53). Full site descriptions and GPS coordinates are provided in Appendix A.

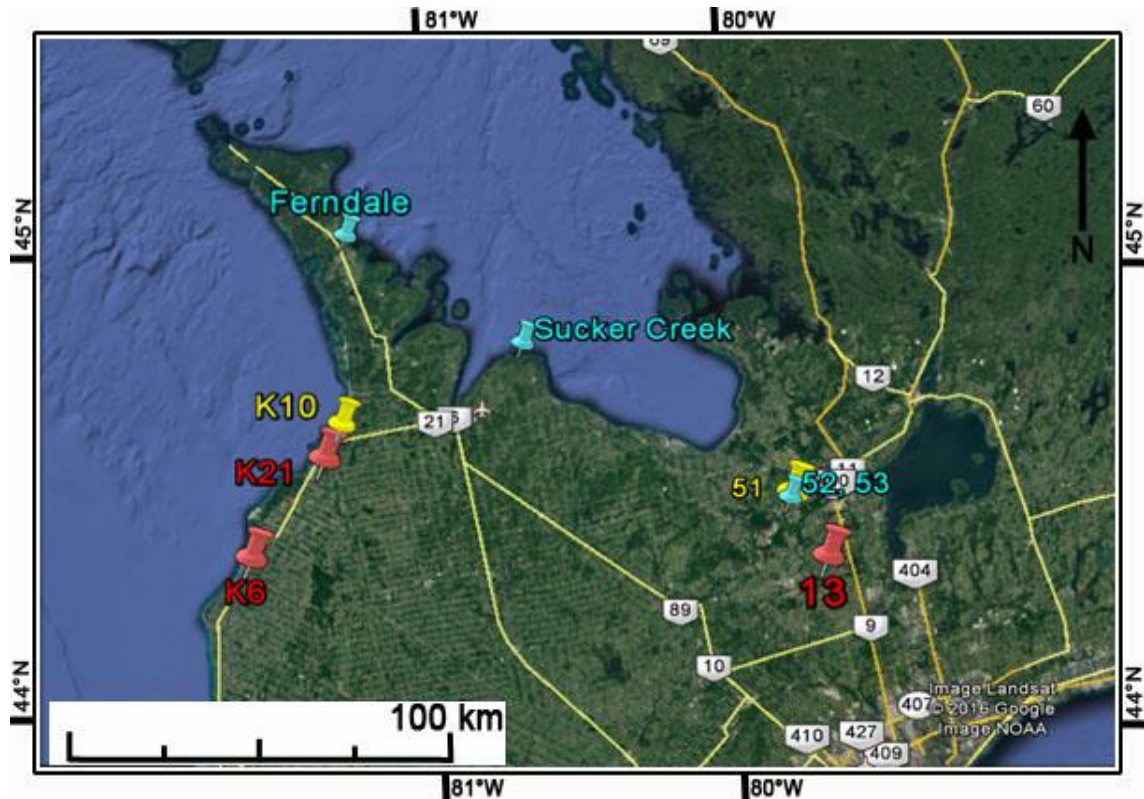


Figure 1.4 - Site locations. Red - Algonquin Phase; Yellow - Transitional Phase; Blue - Nipissing Phase. (Google Earth, 2016).

1.5.1 Fluvial Locations

1.5.1.1 Transitional Phase (51) and Nipissing Phase (52, 53)

These three sites are located on the banks of the Nottawasaga River, south of Angus, Ontario (Fig. 1.5). The Nottawasaga River main branch is ~120 km long (Thornbush, 2001). Much of the river's watershed is located within the west plains of the Simcoe Lowlands. This landscape is characterised by flat to gently rolling plains situated between 177 and 229 masl. The plains meet Georgian Bay at Wasaga Beach at this site (Thornbush, 2001). The gradient of the land that spans from Lake Huron to the sites (~25 km) is extremely low at 0.0001 m/km (Thornbush, 2001; Google Earth, 2016). Thornbush (2001) suggested that the Nottawasaga River is restricted to its downcut valley, where it occupies up to 2/3 of the valley floor, and that its lateral movement was mainly restricted to cutoffs and oxbow lakes within those confines.



Figure 1.5 - Locations of fluvial sites 51-53 (Google Earth, 2016)

Peak monthly discharge occurs in April, but historically, flooding events have occurred in all months except August and September (MacLaren Plansearch Inc., 1988; Thornbush, 2001). Studies at Angus found a five-year major flood cyclicity (MacLaren Plansearch Inc, 1988). Some causes include ice or log jamming of upstream flow, which decreased downstream sediment transport (Thornbush, 2001).

The sediments of the Nottawasaga riverbed consist of coarse gravel and cobbles, but increasingly become more sandy in areas of glaciolacustrine deposits, such as between Alliston and Angus, Ontario (Chandler and Kostaschuk, 1994). Sediments of both Nipissing sites (52, 53) are comprised mostly of well-sorted fine sands, with the bottom ~1 m of the sediment column containing layers of thinly bedded silt and sand. They have been interpreted as prodelta/delta deposits. Site 53 (195 masl; Appendix B) has an unconformity at 3 m, separating a lower sandy unit from an upper gravelly unit with well-developed bedforms that are indicative of a fluvial setting. The mollusc-bearing unit is located within 1 to 3 m of this coarse-grained section. Above this section, a possible aeolian sand cap may indicate the emergence of this site from the water. Site 52 (191 masl; Appendix B) is not topped by aeolian sediments. The Nottawasaga River at this location is only a few meters below site 52 at ~185 masl (Google Earth, 2016), and so it is possible that this site will develop an aeolian sediment layer over time. The mollusc-bearing unit is in the top 2 m of sediment.

The Transitional site 51 (201 masl; Appendix B) comprises a rippled fine sand section with an interbedded sand and silt section to 3 m, changing to massive fine sand to a depth of 7 m. Shells were collected from the top 1 m of the sediment column for this study. An unconformity at 7 m is underlain by very fine sands and silts to the bottom of the studied section.

Gravenor and Couyle (1985) reported sub-laminated silt and clay layers situated atop sites 51 - 53. These were interpreted as Algonquin lake deposits, indicating that the lake boundary extended to the south to engulf these sites.

1.5.1.2 Algonquin Phase (13 and K6)

Site 13 is located on 13th Line, south of Highway #10, and east of Highway #89 (Fig. 1.6). This Algonquin fluvial site sits at 215 masl and has no association with a modern river. The dried river bed may once have been a tributary of the Nottawasaga River or it may have been deposited within a now-vanished river. Approximately 5 km to the west, the Nottawasaga River has a low gradient of 0.0001 m/km (Thornbush, 2001), indicating that this site may have been part of the Nottawasaga river system rather than separate. The sediments consist of well-sorted fine sands (Appendix B).

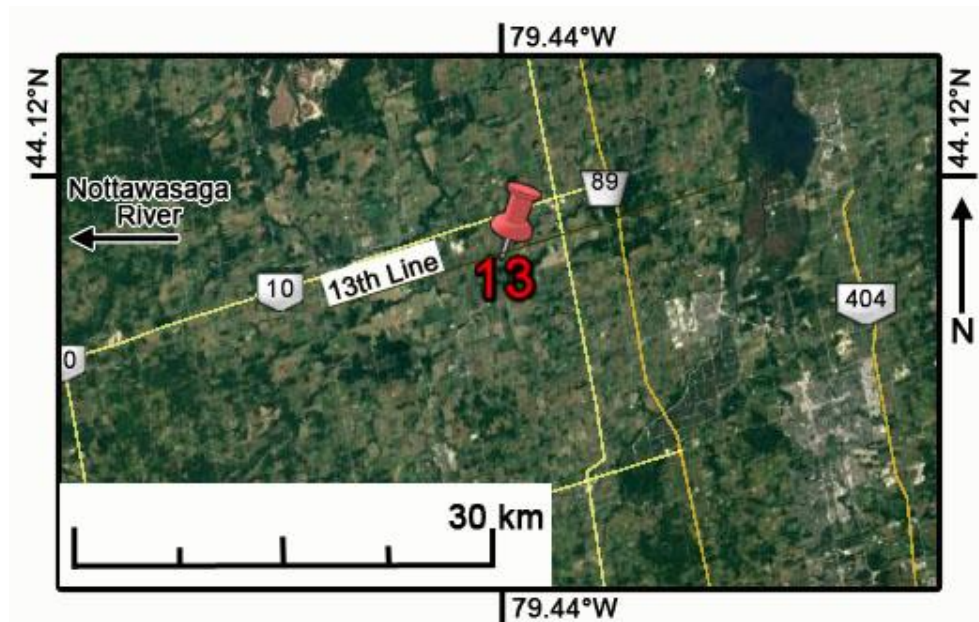


Figure 1.6 - Location of Algonquin site 13. (Google Earth, 2016)

Site K6 is located south of Kincardine, on the banks of the modern Pentagore River (Fig. 1.7) and consists of light brown clays (Appendix B), sitting at 199 masl. Miller *et al.* (1979) first documented this site and found that it was dominated by six aquatic species: *Amnicola limosa*, *Helisoma anceps*, *Lymnea decampi* (syn. *Fossaria decampi*), *Gyraulus parvus*, *Valvata tricarinata* and *V. sincera*. High terraces present at Kincardine also occur in more southern valleys along the Lake Huron shoreline. Karrow (1986a,b) interpreted these terraces as being formed by transgressive waters of Lake Algonquin. Radiocarbon dating of the organic matter yielded an age of $10,800 \pm 110$ BP (GSC-1904, Miller *et al.*, 1979).

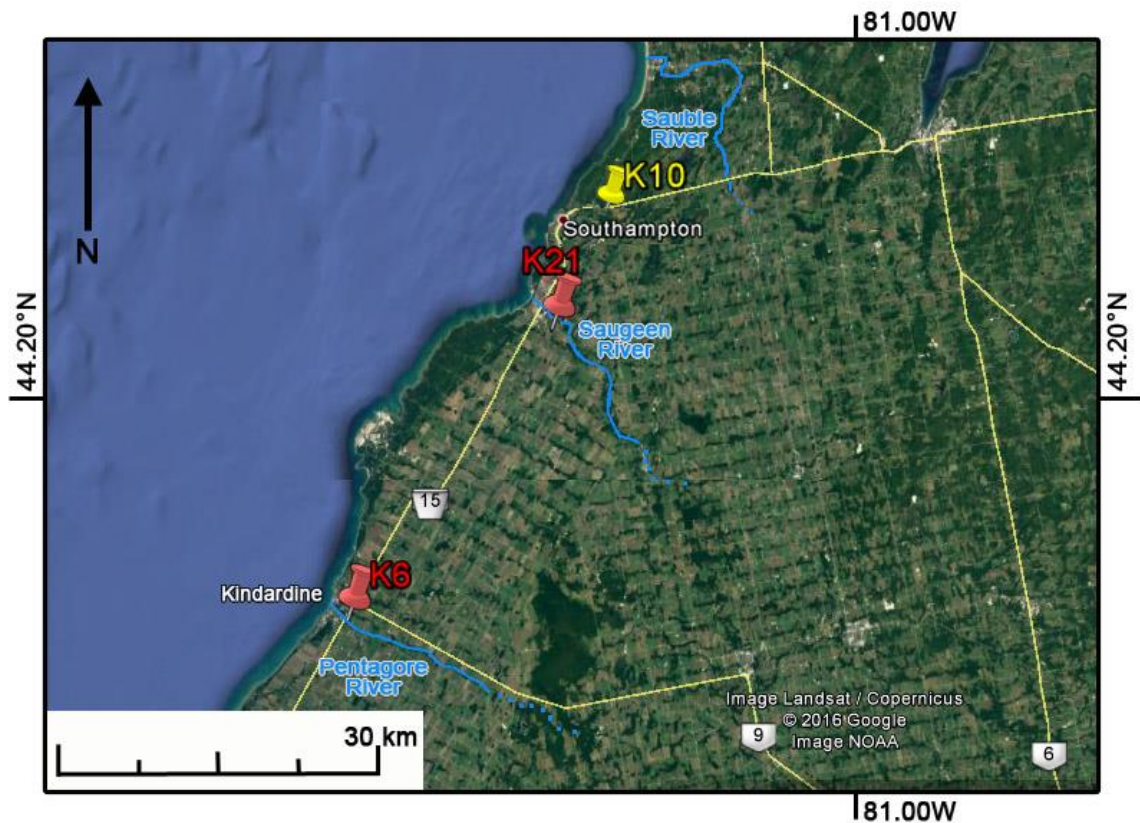


Figure 1.7 - Location of Algonquin sites K6 and K21 (yellow), and Transitional site K10 (red). (Google Earth, 2016)

1.5.2 Estuarine Locations

1.5.2.1 Transitional Phase (K10)

Located north of Southampton, Ontario, this Transitional site sits at 193 masl (Fig. 1.7). Sediments consist of sandy silt and clay with a few rounded pebbles (Appendix B). Miller *et al.* (1979) studied this site and observed *L. decampi*, *Pisidium casertanum*, *P. compressum*,

Sphaerium striatinum, together with an abundance of *V. tricarinata*, *V. sincera*, *G. parvus*, and *Probythinella lacustris*. This study proposed that the assemblage implies a permanent, cool, well-oxygenated, silt-free, lentic water system, with areas of moderate to dense submerged aquatic vegetation. Miller *et al.* (1979) also reported the presence of terrestrial species, suggesting the site represented a near-shore margin. Radiocarbon dates for this site range from 6270 ± 250 BP for a charcoal layer to 5230 ± 100 BP for a shell (Miller *et al.*, 1979).

1.5.2.2 Algonquin Phase (K21)

Karrow (1986a,b) identified a prominent north-trending ridge of sand and gravel that formed a baymouth barrier at the mouth of the Saugeen River, which was sampled at site K21 (Fig. 1.7). This ridge created a large estuary that was protected from the open waters of Lake Algonquin. The Saugeen River has subsequently been rerouted and K21 is now located on the modern shore of Mill Creek (211 masl). The sediments consist mostly of mollusc-bearing silty clays (Appendix B).

1.5.3 Lacustrine Locations

1.5.3.1 Nipissing Phase (Ferndale and Sucker Creek)

Fossil mollusc shells in this general area were first reported by Paul Karrow in 1979. The Ferndale sites FN-1 and FN-2 were found along Highway #6 heading towards Lion's Head and sampled in 2001 (Fig. 1.8). FN-8, found at the same location, was sampled in 2011. All FN sites were located in roadside ditches.

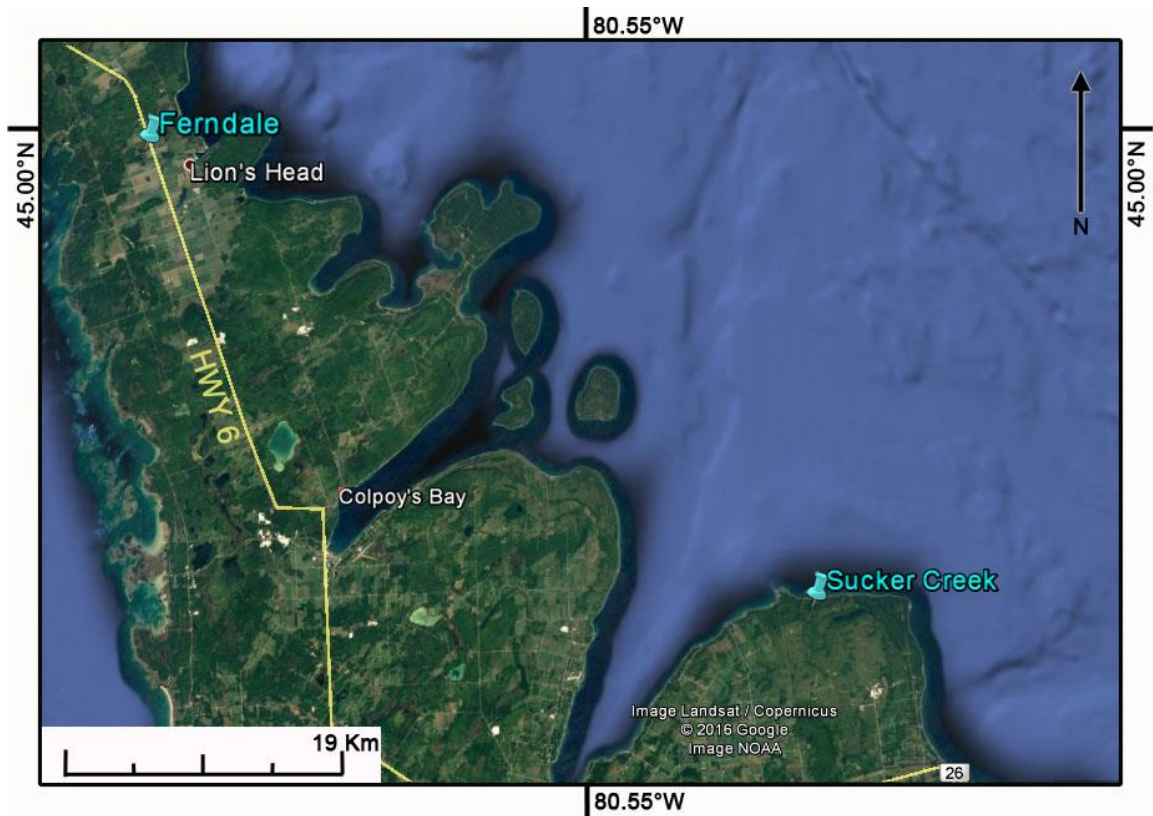


Figure 1.8 - Location of Ferndale (FN-1, 2, 8) and Sucker Creek (Google Earth, 2016)

The fossil fauna recovered were identified as aquatic species (Karrow and Mackie, 2013). Plant and root debris is also common at these sites. A clear water, nearshore or shallow lacustrine plain environment was inferred by Karrow and Mackie (2013). Sucker Creek is an exposed Nipissing beach site open to storm waves and long fetch to the northeast. It is dominated by gastropod fauna, including the indicator species *Pleurocera livescens* (Karrow and Mackie, 2013). Karrow and Mackie (2013) also reported several quiet-water embayments in the area, with a fauna assemblage of gastropods and bivalves, particularly *Pisidium* spp..

Chapter 2

2 Background Information

2.1 Mollusc Biogenic Carbonate, Oxygen Isotopes and Isotopic Vital Effects

Environmental changes can be investigated through the stable isotope compositions of biogenic carbonate. The compositions can provide a proxy for the reconstruction of paleoclimatic and paleo-hydrologic regimes (Stuiver, 1970; von Grafenstein *et al.*, 1994, 1999).

2.1.1 Mollusc Biogenic Carbonate

The Mollusca phylum comprises the second largest group of invertebrates, and contains nearly 100,000 species that inhabit virtually all environments (Burch, 1982; Prendergast and Stevens, 2015). They are among the most visible and ubiquitous fossil biota present in Lake Huron paleo-sediments (Miller *et al.*, 1985). Their widespread nature and the temperature gradients of their habitats make these proxies a valuable paleolimnological tool.

These invertebrate organisms construct their shells using calcite, aragonite, or a combination of the two (McConnaughey and Gillikin, 2008; Prendergast and Stevens, 2015). Molluscs can be divided into two groups based on the structure of their shell. Gastropods, such as snails, have a single shell, which forms throughout their life. This shell is deposited by the mantle in processes that are characteristic to each genus, with overall growth rates decreasing with age (Keith and Weber, 1964; von Grafenstein *et al.*, 1999; Lewis and Leng, 2014; Prendergast and Stevens, 2015). The second group, bivalves, have a two-sided shell (valves), and include clams, oysters, and mussels (Leng and Lewis, 2016). These organisms precipitate their shells relatively continuously throughout their lifetime, in successive outward layers (von Grafenstein *et al.*, 1999; McConnaughey and Gillikin, 2008). For both groups, the carbon and oxygen isotope compositions of the shell represent the water characteristics in the habitat during the shell-forming period (Fritz and Poplawski, 1974).

2.1.2 Oxygen Isotopes ($\delta^{18}\text{O}$)

2.1.2.1 Controls on Oxygen Isotopes of Meteoric Water in Southern Ontario

Urey (1947) first observed in laboratory experiments that carbonate $\delta^{18}\text{O}$ was directly related to the $\delta^{18}\text{O}$ of the solution from which it was precipitated. In 1961, Craig found a relationship between the average hydrogen and oxygen isotope ratios of unevaporated fresh water, principally precipitation, which fell along what is now called the Global Meteoric Water Line (GMWL) (Equation 2.1):

$$\delta^2\text{H} = 8 \times \delta^{18}\text{O} + 10 \text{‰} \quad \text{Equation 2.1}$$

Craig (1961) showed that this relationship reflects the changes in isotopic composition of precipitation due to two main factors: latitude and elevation. Precipitation produced at a lower latitude is more enriched in ^2H and ^{18}O than that produced at a higher latitude. Similarly, precipitation produced at higher elevations (e.g. mountainous regions) is depleted of ^2H and ^{18}O relative to precipitation produced at lower elevations (Craig, 1961; Dansgaard, 1964; Friedman and Smith, 1970). These systematic patterns are due to the process of Rayleigh Distillation. As moisture masses from the south move northward or from low elevation to higher elevation, the heavier isotope water molecules rain out more easily. This depletes the remaining moisture mass of ^{18}O and ^2H , making subsequent rainouts isotopically lighter (Faure and Mensing, 2005; Sharp, 2007). Changes in the isotopic composition of meteoric water at mid- to high-latitudes can be correlated with changes in mean annual air temperature, and averages about $0.65 \text{‰} / 1 \text{ }^\circ\text{C}$ (Dansgaard, 1964; Zuppi, 1981). Stuiver (1970) showed that this gradient can be as high as $1.3 \text{‰} / 1 \text{ }^\circ\text{C}$ in the Great Lakes region. Figure 2.1 shows that, in Ontario, there can be a $> 4 \text{‰}$ difference between the $\delta^{18}\text{O}$ of precipitation at Point Pelee and Sibley. Hence, the source of precipitation, and lake water derived from it, can have a profound effect on the isotopic composition of shelly material formed in these waters.

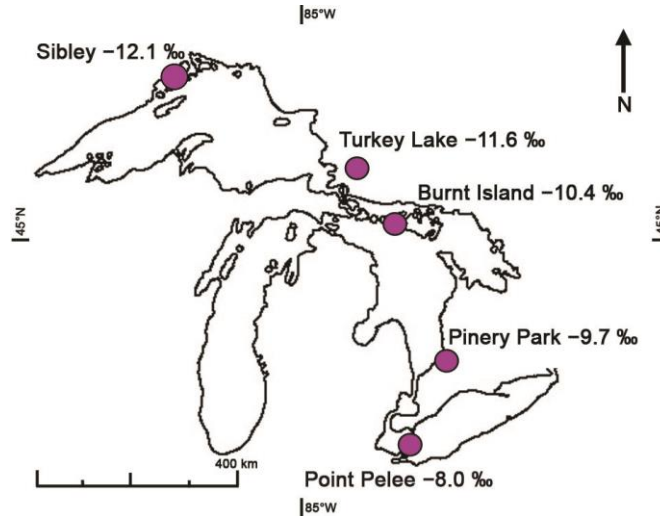


Figure 2.1 - Annual average $\delta^{18}\text{O}$ of meteoric water in southern Ontario (Longstaffe *et al.*, 2013).

2.1.2.2 Environmental Controls on Oxygen Isotope Composition

River and lake water reflects the isotopic composition of local precipitation, which is controlled by temperature, humidity, and seasonality (Fig 2.2a,b; e.g. Rozanski *et al.*, 1993; Faure and Mensing, 2005; Sharp, 2007). Stuiver (1970) determined that the temperature-dependence of oxygen isotopes in fossil shells from river and lake sediments could be utilized to elucidate paleo-climatic changes in the east to mid-west United States, such as the warm period known as the Holocene Hypsithermal (von Grafenstein *et al.*, 1999, 2013).

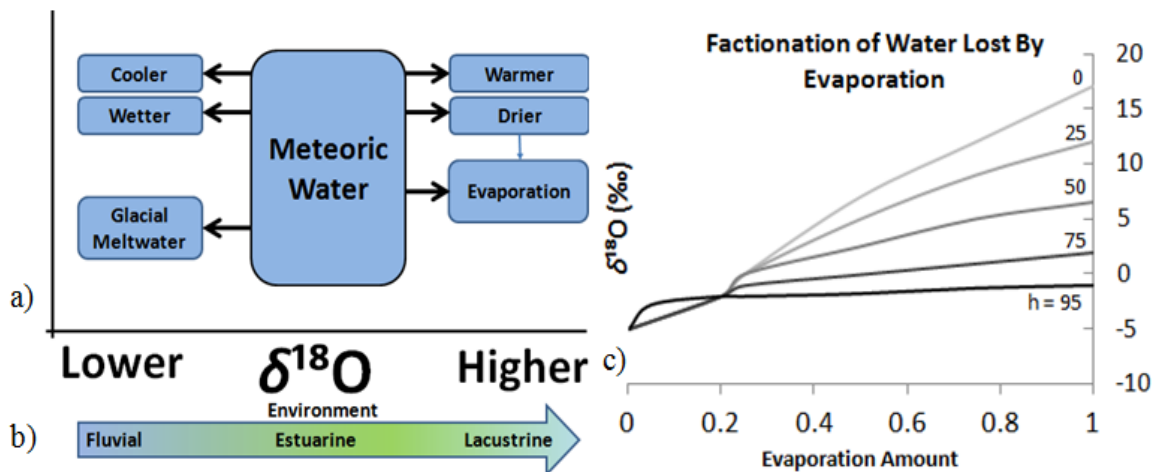


Figure 2.2 - (a) Controls on oxygen isotopic composition of meteoric water. Arrows indicate the direction of isotopic change with each control. Light blue arrow indicates that evaporation is most strongly linked to drier conditions. (b) Controls on oxygen isotopic composition by depositional environment. (c) Oxygen isotope fractionation of water remaining after evaporation. Starting $\delta^{18}\text{O}$ illustrated is -5‰ ; h is relative humidity. The graph illustrates enrichment of ^{18}O for constant volume, well mixed lakes as a function of the fraction of water lost by evaporation relative to total inflow (after Gonfiantini, 1986).

The $\delta^{18}\text{O}$ of lake water is sensitive to changes in water input (I), evaporation (E), and relative humidity (Fig 2.2c; Gonfiantini, 1986). Large changes in $\delta^{18}\text{O}$ can be linked to changing climate, but the lake may display a lag time depending on the volume of water and its residence time. Additional factors such as lake morphology and rate of evaporation must be taken into account when interpreting changes in $\delta^{18}\text{O}$. Inflow to the lake can also be altered by seasonal changes in rainfall distribution (Dansgaard, 1964; Rozanski *et al.*, 1993; Fricke and O'Neil, 1999). Isostatic rebound associated with deglaciation has caused the opening and closing of flow channels into, between and out of the Great Lakes, such as the Port Huron outlet from Lake Huron, and altered the elevation of the ground water table (Covich *et al.*, 1974; Fritz *et al.*, 1975; Eschman and Karrow, 1985; Lewis *et al.*, 2005; Hunter *et al.*, 2006; Clark *et al.*, 2012; Lewis, 2016). This also greatly affected the inflows and outflows from the Great Lakes.

In open lakes, the $\delta^{18}\text{O}$ signal is controlled by the amount, source, and temperature of precipitation available to the lake basin, and to a lesser degree, by evaporation (i.e. low E/I; von Grafenstein *et al.*, 1996, 1999; Sharp, 2007; Mayer *et al.*, 2012; Lewis and Leng, 2014; Leng and Lewis, 2016). The deep waters of Lake Huron have a relatively consistent $\delta^{18}\text{O}$ value (within 1 ‰) below 5 m, although there can be more complex seasonal variation in the surface waters (Dettman *et al.*, 1995).

In closed lakes, the $\delta^{18}\text{O}$ signal is dominated by wet season recharge and dry season evaporation (Covich *et al.*, 1974; Li, 1995; Lewis and Leng, 2014; Leng and Lewis, 2016). The magnitude of ^{18}O -enrichment depends on relative humidity, air-water surface temperature differences, the rate of vapour removal from wind, and the rate of water recharge (Gonfiantini, 1986). In the Mediterranean, oxygen isotopic shifts of up to 7 ‰ during the mid-Holocene were associated with large fluctuations between arid and humid climatic regimes (Leng *et al.*, 2010). Under ideal conditions, higher ^{18}O should correspond to times of warmer and/or drier climate, associated with an increased rate of evaporation (Fritz and Poplawski, 1974; Gonfiantini, 1986; Cerling *et al.*, 1988). These idealised systems, however, can be skewed by short- or long-term changes in temperature, which can act to partially buffer isotopic effects linked to evaporation (Dansgaard, 1964; Rozanski *et al.*, 1993; Fricke and O'Neil, 1999).

Ground water immediately adjacent to a lake displays a $\delta^{18}\text{O}$ composition more closely related to the lake water (Gonfiantini, 1986; Huddart *et al.*, 1999), implying that this area experiences mixing. Fluvial systems would generally remain isotopically unaffected by lake water because their source waters are from a higher elevation than lakes and their reach can travel for many hundreds of kilometers before reaching the river mouth.

The introduction of glacial meltwater through a collapsing ice sheet or through slow ground water seepage also has the effect of lowering the $\delta^{18}\text{O}$ of a lacustrine system. Fluvial systems may also be affected by glacial water outflows if their reaches intersect with the melting glacier. Because of the southern source location of rivers in the study area and the timing of the retreat of the LIS, the rivers of this study likely did not incorporate meltwater. The oxygen isotopic composition of river water typically reflects the weighted mean of precipitation in its watershed (Wolfe *et al.*, 2007). The oxygen isotopic composition of water in fluvial systems is much less affected by evaporation than lakes (Godwin, 1985), unless flow rates are very low.

2.1.2.3 Biogenic Carbonate Controls on Oxygen Isotope Composition

Shell aragonite of many freshwater bivalve species is deposited in oxygen isotopic equilibrium with ambient water (Fritz and Poplawski, 1974; Wefer and Berger, 1991; Dettman *et al.* 1999, 2004). This can therefore serve as a proxy for the oxygen isotopic composition of the water in which it precipitated, which is a function of regional precipitation, evaporation, and temperature (Fritz and Poplawski, 1974; Godwin, 1985; Cerling *et al.*, 1988; Li, 1995; Holmes, 1996; Jones *et al.*, 2002; Macdonald and Longstaffe, 2008; Macdonald, 2012; Hyodo and Longstaffe, 2012; Hladyniuk and Longstaffe, 2016; Leng and Lewis, 2016).

The fractionation between the oxygen isotope composition of calcium carbonate and the water from which it precipitates is temperature dependent. The $\delta^{18}\text{O}$ decreases by $\sim 0.24\%$ for each $1\text{ }^{\circ}\text{C}$ increase at temperatures typical of shell formation (Craig, 1965; Stuiver, 1970; Friedman and O'Neil, 1977). In an idealised system, therefore, shells formed from warmer (summer) water will be more depleted of ^{18}O compared with shells formed at lower (winter) temperatures from water of the same oxygen isotopic composition. Deeper water species in the Great Lakes, for example, will typically have a higher $\delta^{18}\text{O}$ because bottom waters

remain around 4 °C throughout the year (section 1.4.3; Dettman, *et al.*, 1995), whereas shallow and near-shore waters in modern Lake Huron vary in temperature widely and can reach 23 °C (Macdonald, 2012).

For the Great Lakes region, Godwin (1985) suggested that because fluvial systems are not subject to major evaporative effects, mollusc shells formed in that environment should directly reflect the oxygen composition of meteoric water, and thus provide a more accurate proxy for paleo-climatic and paleo-environmental conditions.

2.1.3 Carbon Isotopes ($\delta^{13}\text{C}$)

2.1.3.1 Environmental Controls on Carbon Isotopic Composition

Dissolved inorganic carbon (DIC) is the sum of carbonate (CO_3^{2-}), bicarbonate (HCO_3^-) and dissolved carbon dioxide ($\text{CO}_2(\text{aq})$), which move towards chemical equilibrium with each other and atmospheric CO_2 (Guiguer, 2000). In Lake Huron, the dominant DIC species is bicarbonate (HCO_3^-) (Rea *et al.* 1994a; Dettman *et al.* 1995), which is more enriched in ^{13}C than coexisting $\text{CO}_2(\text{aq})$ by ~8 ‰ (Mook, 1971; Szaran, 1998; Guiguer, 2000). The $\delta^{13}\text{C}$ of DIC is determined by lake processes that alter chemical and isotopic equilibrium among the DIC components (Guiguer, 2000).

DIC content and isotopic composition of the water are a function of primary productivity (photosynthesis and respiration) and subsequent decay of organic matter (OM), degree of exchange between atmospheric CO_2 and dissolved CO_2 , dissolution of surrounding carbonate rocks, and local habitat conditions such as temperature (Fig. 2.3a; e.g. Stuiver, 1968, 1970; Fritz and Poplawski, 1974; Fritz *et al.*, 1975; Cerling *et al.*, 1988; Talbot, 1990; Dettman *et al.*, 1995, 1999; Böhm *et al.*, 1996; Brenner *et al.*, 1999; von Grafenstein *et al.*, 1999; Post, 2002; Leng and Marshall, 2004; Hyodo and Longstaffe, 2011b; Hladyniuk and Longstaffe, 2015).

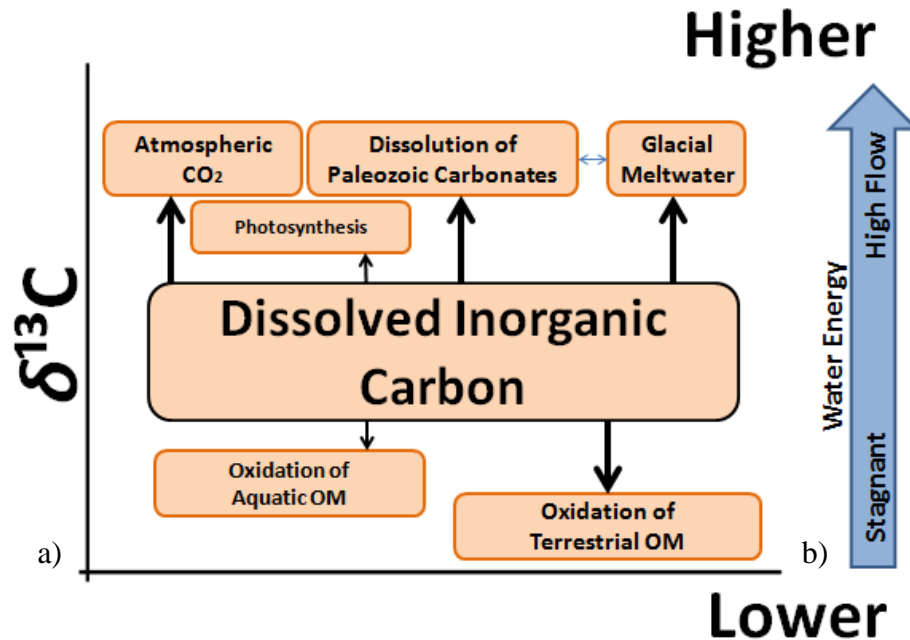


Figure 2.3 - (a) Idealised controls on carbon isotopic composition of DIC. (b) Idealised controls on carbon isotopic composition by water energy.

Figure 2.3b indicates that under ideal conditions, stagnant water, as in sheltered ponds or very slow-moving rivers, would have lower $\delta^{13}\text{C}$, whereas water that is faster moving or experiences wave action, like in lakes, would have higher $\delta^{13}\text{C}$. This variation is due to the concentration of decaying organic matter, which lowers $\delta^{13}\text{C}$ (Fritz *et al.*, 1975), and interaction with atmospheric CO_2 , which drives $\delta^{13}\text{C}$ higher (Li and Ku, 1997).

Primary productivity enriches the DIC pool in ^{13}C as plant matter preferentially consumes ^{12}C during growth in summer months (Leng and Marshall, 2004; Casey and Post, 2011). Warmer temperatures are positively correlated with ^{13}C -enriched plants in both freshwater (Macleod and Barton, 1998) and marine environments (Sackett *et al.*, 1965). In highly productive lakes, $\delta^{13}\text{C}$ DIC may reach as high as +6 ‰ (Li, 1995). Conversely, if the rate of primary production becomes extreme, the photic zone may become depleted of ^{12}C , as it is used up and producers are forced to rely on ^{13}C for their growth (Brenner *et al.*, 1999; Mortsch and Quinn, 1996; Odegaard *et al.*, 2003). The DIC pool can also become enriched in ^{12}C as the newly produced organic matter dies and decays (oxidizes) (Dettman, 1995; Li *et al.*, 2008; Torres *et al.*, 2012).

In closed basin systems, decreasing lake water levels by can increase the concentration of nutrients. This fuels further biological activity, increasing primary productivity (Woszczyk *et al.*, 2014).

Vertical return of nutrient-rich deep waters to the photic zone increases the productivity of aquatic plants (Dettman, 1995; Li and Ku, 1997; Meyers, 1997). This process occurs in lakes that are naturally well mixed, or during times of reduced freshwater input and/or intensified evaporative regimes (Li and Ku, 1997). Conversely, in some small lakes, reduced water volume can result in a lowering of DIC $\delta^{13}\text{C}$ because a relative increase in the contribution from decaying and oxidized OM relative to production (Meyers, 1997; Post, 2002). Such a decrease, however, may also indicate reduced primary productivity (Routh *et al.*, 2009).

Terrestrial OM can be washed into a lake by wave- or wind-action or brought in by inflowing river systems or precipitation runoff (Hammarlund *et al.*, 1997; Leng and Marshall, 2004). They typically have very low $\delta^{13}\text{C}$ of -27‰ (Hyodo and Longstaffe, 2011b), indicative of the C_3 -dominant plant matter of the region, such as trees. Even small contributions of such material can shift the DIC pool to lower $\delta^{13}\text{C}$, especially in smaller lakes and rivers (Keith *et al.*, 1964; Vogel, 1993; Post, 2002; Leng and Marshall, 2004; Hyodo and Longstaffe, 2011b; Hladyniuk and Longstaffe, 2015).

About 1 % of the carbon dioxide in the atmosphere is $^{13}\text{CO}_2$; it diffuses and reacts more slowly, and has a greater tendency toward bicarbonate formation than $^{12}\text{CO}_2$ (aq) (Guiguer, 2000). In addition, strong evaporative regimes can raise the $p\text{CO}_2$ of a lake, causing a net loss of $^{12}\text{CO}_2$ to the atmosphere driving the $\delta^{13}\text{C}$ higher (Talbot, 1990; Li and Ku, 1997; Leng *et al.*, 1999). Atmospheric CO_2 plays a minor part in ground water contribution to rivers because there are few routes for direct contribution from, whereas it can play a major role in lacustrine systems due to wave/storm action and the large interface area between the lake and the atmosphere.

Atmospheric CO_2 during the Pleistocene had $\delta^{13}\text{C}$ of -6.9 to -6.4‰ (Schmitt *et al.*, 2012); thus, under equilibrium conditions the lake DIC would have $\delta^{13}\text{C}$ of $+1$ to $+3\text{‰}$ (Li and Ku, 1997) at typical lake temperatures. There is a lag time in establishing equilibrium between atmospheric CO_2 and aquatic DIC that depends on the volume and turnover time of

the water body (Böhm *et al.*, 1996). The solubility of CO_2 (aq) increases at lower temperatures. Guiguer (2000) reported a greater contribution of CO_2 (aq) to the aquatic system in Colpoy's Bay, located ~27 km south of the Ferndale sites along Highway #6 (Fig. 1.8), in spring than summer. Lower temperatures also aid in the dissolution of carbonate detritus. The Paleozoic carbonate rocks of the Niagara Escarpment (Fig. 2.4) comprise much of the carbonate detritus reaching the Huron basin and have a $\delta^{13}\text{C}$ of +1 to +4 ‰ (Guiguer, 2000). This would have the counteracting effect of enriching the DIC pool in ^{13}C . Isotopic signatures of near-shore and estuarine systems are more affected by such inputs and show more variability (Dettman, 1995; Leng and Marshall, 2004; Michener *et al.*, 2007; Hyodo and Longstaffe, 2011a; Hladyniuk and Longstaffe, 2015).

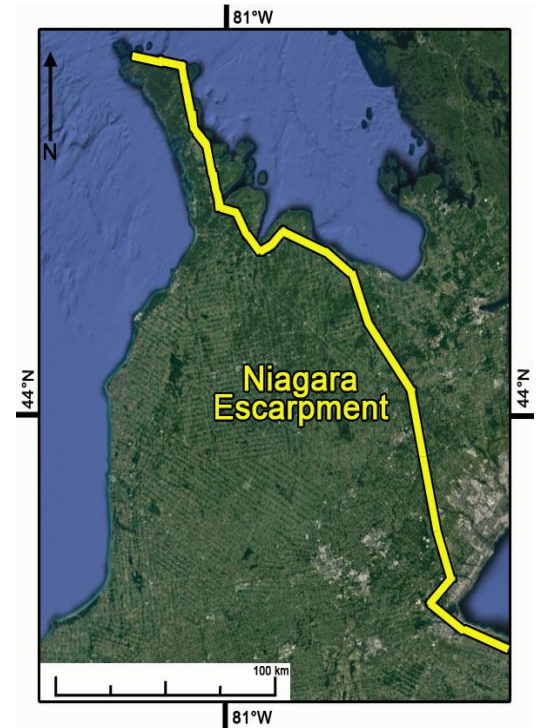


Figure 2.4 - The Niagara Escarpment overland in southern Ontario (Google Earth, 2016).

2.1.3.2 Controls on Carbon Isotope Composition of Biogenic Carbonate

The carbon isotope composition of purely aquatic biogenic carbonates is controlled by the $\delta^{13}\text{C}$ of DIC, with no direct input from atmospheric CO_2 (Keith and Anderson, 1963; Lewis and Leng, 2016). The systematic fractionation of carbon isotopes within the mollusc is not significantly temperature dependent and hence can be used as a proxy for assessing productivity (Fritz and Poplawski, 1974; von Grafenstein *et al.*, 1999; Stott, 2002). Keith *et al.* (1964) suggested that the environment in which a shell was formed (e.g. fluvial, lacustrine) was a more important control on shell $\delta^{13}\text{C}$ than was species.

2.1.4 Controls on the Oxygen and Carbon Isotope Variations in Water

Fresh water inputs and outputs are the main factors controlling the carbon and oxygen isotope compositions of shelly fauna in each environment. The carbon isotope compositions of biogenic carbonate from aquatic environments have been used as proxies for paleo-

environmental and paleo-climatic changes (e.g. Fritz *et al.*, 1975; Talbot, 1990; Poulain *et al.*, 2010; Liu *et al.*, 2013).

In open lakes with stable water levels, $\delta^{18}\text{O}$ and $\delta^{13}\text{C}$ of water and DIC, respectively, remain relatively constant and the covariation between them tends to be weak (Li and Ku, 1997). In closed lake systems, intense evaporation leads to a decrease in lake volume and enrichment in ^{18}O . Residence times of the remaining water increase, which allows for greater exchange and equilibration with atmospheric CO_2 , thus enriching the DIC pool in ^{13}C (Talbot, 1990; Li and Ku, 1997; Hammarlund *et al.*, 2003). Input of OM and CO_2 leached from soil is also reduced as precipitation amounts decrease, which intensifies the positive covariation between $\delta^{13}\text{C}$ and $\delta^{18}\text{O}$ (Hammarlund *et al.*, 2003). It is important to note that as a closed lake system gets smaller, an increasing ratio of OM may become more dominant causing the lake to have a lower $\delta^{13}\text{C}$. Lower water levels can also have the effect of increasing ground water input from the surrounding region, therefore the morphology of the water body can also affect the slope of the covariation trend between $\delta^{13}\text{C}$ and $\delta^{18}\text{O}$. Shallow lakes with a large surface area are more sensitive to precipitation-evaporation conditions and display a steeper slope for this isotopic relationship (Baroni *et al.*, 2006).

The use of $\delta^{13}\text{C}$ - $\delta^{18}\text{O}$ covariance as a measure of hydrological closure is reasonably robust over timescales of 5000 years or longer (Li and Ku, 1997). This does not hold true for shorter time periods, where strong covariance may be a result of dilution arising from a rapid transgression in lake level (Li and Ku, 1997). When the covariance of $\delta^{13}\text{C}$ - $\delta^{18}\text{O}$ shows an antipathetic relationship, this may indicate lake-level oscillations or changes in lake bottom conditions (Baroni *et al.*, 2006).

Relative to lakes, fluvial systems are more likely controlled by seasonal and local environmental variations (Sinokrot and Stefan, 1993; Magnuson *et al.*, 1997; Mohseni and Stefan; 1999). Evaporation and exchange of CO_2 with the atmosphere are less important than in lakes, whereas recharge from ground water and precipitation are much more important (Rodie and Post; Godwin, 1985). Input of terrestrial OM detritus is likely to be a more significant factor during winter/spring months, as the plant canopy is largely absent and root structures are more exposed (Romanek and Grossman, 1989; Mitchell *et al.*, 1994). Primary productivity is also greatly diminished during this time, allowing the low $\delta^{13}\text{C}$ signal from

organic decay to become more dominant. Conversely, cooler temperatures would also allow for greater dissolution of carbonates, driving the $\delta^{13}\text{C}$ of DIC upwards.

Within the Huron Basin, summer months typically experience higher $\delta^{18}\text{O}$ of precipitation but mean daily discharge from rivers in southern Ontario is typically lower than at other times of year (Thornbush, 2001). This has the effect of lowering the flow rates, which leads to an increase in dissolved solids. Warmer water would also see a return of primary productivity, but also an increase in the efficiency of organic decay. It is therefore expected that river water during colder months has lower $\delta^{18}\text{O}$ and variable but commonly higher $\delta^{13}\text{C}$ for DIC, whereas river water in summer months is characterized by higher $\delta^{18}\text{O}$ and lower $\delta^{13}\text{C}$.

Under ideal conditions, an estuarine system represents mixing of a lacustrine and fluvial system. During the summer and fall months, at least in the southern Huron Basin, when there is less input from the fluvial system (Government of Canada, 2016), the water oxygen and carbon isotope signals should reflect more of the lacustrine environment. During winter and spring months, larger amounts of spring melt plus precipitation would enter the estuary, moving its water's isotopic signal towards that of the fluvial system.

2.1.5 Vital Effects

Isotopic compositions that arise from life processes can inhibit isotopic equilibrium with their environment. These "vital effects" (isotopic disequilibrium) may arise from metabolic or kinetic processes (Leng and Marshall, 2004; Sharp, 2007).

2.1.5.1 Metabolic Isotope Effects

Metabolic effects alter the $\delta^{13}\text{C}$ of an organism mainly by the selective addition or removal of ^{12}C by photosynthesis and respiration, respectively (McConnaughey, 1989a; Mitchell *et al.*, 1994). In non-photosynthesizing organisms, these effects would likely be small and would not account for the range of $\delta^{13}\text{C}$ or any covariation with $\delta^{18}\text{O}$, as oxygen would not likely be affected (Mitchell *et al.*, 1994).

Studies of some bivalves and ostracodes have shown that up to 10 % of carbon in their shells may be derived from ingestion of aquatic plants (Dettman, 1994; McConnaughey *et al.*,

1997; Dettman *et al.*, 1999; McConnaughey and Gillikin, 2008; Macdonald, 2012). This typically has the effect of the shell $\delta^{13}\text{C}$ being lower than the ambient DIC pool, with the magnitude of the offset being species-specific (Sharp, 2007). Stott (2002), however, determined that, for gastropods, there was no systematic influence on the isotopic composition of shell carbonate from the ingestion of food with different $\delta^{13}\text{C}$. Instead, the covariation observed between the whole-shell $\delta^{18}\text{O}$ and $\delta^{13}\text{C}$ of *Valvata* spp. reflects derivation of the carbon directly from lake water DIC (Fritz *et al.*, 1975; Jones *et al.*, 2002). This allows for the direct interpretation of the DIC pool of the water in which the shell lived.

Regardless of the influence of metabolic carbon, the isotopic offset from DIC appears to be consistent within each studied species, and therefore intra-species trends in $\delta^{13}\text{C}$ can be used to detect environmental change (Dettman, 1994).

2.1.5.2 Kinetic Isotope Effects

Kinetic isotope effects have been described for both fast-growing biogenic carbonates (McConnaughey, 1989b; Mitchell *et al.*, 1994) and inorganic carbonates (Turner, 1982). This process involves discrimination against heavy isotopes of both carbon and oxygen during hydration and hydroxylation of CO_2 . If the precipitation rate is fast, the carbonate will be unable reach isotopic equilibrium, which results in lower than expected $\delta^{13}\text{C}$ and $\delta^{18}\text{O}$ (McConnaughey, 1989b; Mitchell *et al.*, 1994). McConnaughey (1989b) defined "fast growth" as growth exceeding 2 mm per year, resulting in a strong positive covariation between $\delta^{18}\text{O}$ and $\delta^{13}\text{C}$ (Mitchell., 1994).

2.1.5.3 Other Isotope Effects

Fritz and Poplawski (1974) reported that the purely aquatic genera *Pisidium* and *Valvata* precipitated their shell in oxygen isotope equilibrium with ambient water. McConnaughey *et al.* (1997) suggest that air-breathing molluscs, such as the gastropod *Stagnicola emarginata*, use a proportion of respired CO_2 to build their shells. These species display more variable $\delta^{18}\text{O}$ than purely aquatic organisms living within the same environment (Leng and Marshall, 2004).

Even when disequilibrium fractionation is a factor in the production of the shell, the offset direction and magnitude are generally consistent for a species, and often for the whole genus (Sharp, 2007). Thus, if the offset is known, its effects can be eliminated during comparisons.

2.2 Assumptions

Much published work has made use of the oxygen and carbon isotope compositions of fossil molluscs to reconstruct paleoenvironments. Nonetheless, some caution is needed when interpreting such results. First, and most important, is the assumption that the shell precipitated in isotopic equilibrium with the surrounding water. For $\delta^{18}\text{O}$, this assumption is supported by numerous laboratory and field experiments (Mook and Vogel, 1968; Fritz and Poplawski, 1974; Wefer and Berger, 1991; Carpenter and Lohmann, 1995; Lécuyer *et al.*, 2012; Prendergast and Stevens, 2015). Vital effects can skew shell $\delta^{13}\text{C}$ through kinetic and / or metabolic processes, and can affect different organisms differently. This offset, if applicable, must be correctly determined for each genus (McConnaughey, 1989ab; McConnaughey *et al.*, 1997; Dettman *et al.*, 1999; von Grafenstein *et al.*, 1999; McConnaughey and Gillikin, 2008).

Second, the shell must have preserved its original isotopic compositions, which can be changed during diagenesis, which commonly includes conversion of original aragonite to calcite, and recrystallization more generally. Studies of diagenesis in unconsolidated post-glacial sediments have found this effect to be minimal (Stuiver, 1970; Fritz and Poplawski, 1974; Fritz *et al.*, 1975). Techniques such as powder X-ray diffraction and microscopy can be used to determine whether the original aragonitic mineralogy has been preserved.

Third, traditional interpretation of shell $\delta^{18}\text{O}$ requires assumptions about water $\delta^{18}\text{O}$ or temperature at the time of shell formation. Tracking such changes over time also requires robust chronological information. Such data are commonly difficult to obtain directly, and so must be inferred. Interpretation is further complicated by the possibility that local conditions differed from regional conditions at the time, or that the record preserved in the sediments is biased because of seasonal differences or species habitat preferences (Grootes, 1993; Meyers, 1997).

2.3 Species Information

During the early Holocene when the LIS was in retreat, a group of genera that includes *Amnicola*, *Gyraulus*, *Helisoma*, *Pisidium*, and *Valvata* were already well established in the Huron basin (Miller *et al.*, 1979). This indicates that they must have been able to live on the ice margins prior to deglaciation. Three of these organisms have been included in this study because of their ubiquitous presence over the entire span of geological time considered here. Table 2.2 lists the typical growth temperature ranges for the three genera used in this project.

Table 2.1 - Average growth temperatures of different mollusc species

Species	Growth Range	Source
<i>Valvata</i> spp.	11 - 18 °C	Macdonald, 2012
<i>Pisidium</i> spp.	14 - 22 °C	Macdonald, 2012
<i>Amnicola limosa</i>	12 - 17 °C 18 - 24 °C*	Macdonald, 2012 van der Schalie and Berry, 1973

* experimentally derived

2.3.1 *Valvata* spp. (Say, 1817)

Valvata tricarinata, commonly known as the three-ridged snail, and *Valvata sincera*, commonly known as the turret snail, are members of the *Valvatidae* family of Holarctic snails. They are up to 5 mm in diameter, and have a short, depressed, dextral spiral with umbilicus (Fig. 2.5; Clarke, 1973; Burch, 1982; Perez *et al.*, 2004; Massachusetts Division of Fisheries & Wildlife, 2015).



Figure 2.5 – Shells from site 53 (a) *Valvata tricarinata*. (b) *Valvata sincera*. (c) *Valvata sincera* side shell opening and umbilicus.

Valvata live among submerged vegetation in cool, clean lakes and rivers at a general depth of approximately 2 - 4 m, but can exceed depths of 9 m (Clarke, 1981; Kerr-Lawson *et al.*, 1992; Perez *et al.*, 2004; Foltz, 2013). They have also been found in eutrophic bays and

ponds in the Great Lakes region (Mackie, 1980; Jokinen, 1983). Eutrophic lakes are rich in nutrients and support a dense plant population. Such waters may be darkened by high concentrations of organic materials, but are not necessarily acidic, and populations are not found in waters that become hot, stagnant, or anaerobic (Dillon *et al.*, 2006).

Valvata mate during the warmer months of the year, but have large range of growth temperatures 11 - 18 °C, averaging 15 - 16 °C (Godwin, 1985; Macdonald, 2012). Eggs hatch in early summer and reaching adulthood may take up to four months (Foltz, 2013). Although most cold-water snails have single-year life spans, members of the *Valvata* genus may sometimes live for two years (Foltz, 2013).

V. sincera has the same habitat and life cycle as *V. tricarinata*. The only environmental difference from *V. tricarinata* is possibly a preference for a more calcium-rich environment (Massachusetts Division of Fisheries & Wildlife, 2015).

2.3.2 *Pisidium* spp. (Pfeiffer, 1821)

Pisidium, commonly known as the pea clam, has a shell length of 2 - 4 mm (Fig. 2.6). It can live for two or more years but generally lives only one year (Way and Wissing, 1982; Way, 1988). The size of the shell is not an indication of age, as the variation of individual species adult shell length is only 18 % from the age of six months to death (Holopainen, 1980). This indicates that their shell isotopic compositions should be skewed towards the first six months of growth (Goodwin *et al.*, 2003; Jones and Quitmyer, 1996).

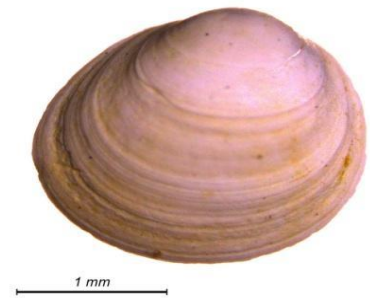


Figure 2.6 - *Pisidium* sp. valve.

Pisidium are benthic organisms that are generally found in water depths from 0.5 - 3 m, but have been collected as deep as 100 m (Mackie *et al.* 1980; Clarke, 1981). This common bivalve species usually lives in the upper few centimeters of the sediment column among vegetation in relatively shallow water with moderate currents within permanent water bodies, such as lakes, ponds, rivers and streams (Mackie *et al.*, 1980; Clarke, 1981; Kerr-Lawson *et al.*, 1992).

Although considered a warm-season carbonate (von Grafenstein *et al.*, 2013), two generations of *Pisidium* are hatched in a year, one in the spring and one in the fall (Way and

Wissing, 1982). Therefore, isotopic compositions of the same species living in the same habitat can vary widely depending on when the bulk of their shell formed (e.g. spring/summer, fall/winter). Dettman *et al.* (1995) found that bivalves grow their shells throughout the year, and so the wide range of growth temperature most likely reflects seasonal changes in temperature. Generally, a greater *Pisidium* abundance is indicative of high productivity and causes shells to grow thicker and longer. Cooler temperatures do not inhibit the organism from shell growth, but the effects alters *Pisidium* spp. demographics (Kilgour and Mackie, 1991).

2.3.3 *Amnicola limosa* (Say, 1817)

Amnicola limosa are gill-breathing organisms, whose adult shells grow to 4 - 5 mm (Fig. 2.7; Van der Schalie and Berry, 1973). This species is found in many types of permanent shallow water bodies, including wave-protected areas in lakes and slow-moving rivers, living among submerged aquatic vegetation (Van der Schalie and Berry, 1973; Mackie *et al.*, 1980; Clarke, 1981; Burch, 1982, 1989; Perez *et al.*, 2004). It is an indicator species for eutrophic lake conditions (Clarke, 1973). This species, similar to *L. decampi*, has a preference for warmer conditions with experimental growth temperatures of 18 - 24 °C (Van der Schalie and Berry, 1973). Macdonald (2012) found an growth range of 12 - 18 °C (average 16 °C), which may indicate that they are heartier than initially thought.



Figure 2.7 - *Amnicola limosa*.

2.3.4 Species Assemblages

Species associated with permanently-wet habitats such as lakes or rivers can be used to interpret depositional environment (Table 2.2). If those species are also associated with vegetation, their presence can also indicate the level of productivity. *Pisidium* spp. live in the top of the substrate, and do not depend on vegetation for their habitat; thus, they can live below the photic zone in deeper parts of lakes.

Table 2.2 - Species and environments from Miller *et al.* (1979) and Mackie (2007)

Medium/Large Lake Very-slow moving river	Small Lake, Estuary Embayment or Slough
---	--

In vegetation	In substrate	<i>Gyraulus parvus</i> <i>Ferrissia</i> spp.
<i>Valvata sincera</i>	<i>Pisidium casertanum</i>	
<i>Valvata tricarinata</i>	<i>Pisidium compressum</i>	

The presence of *G. parvus* and *Ferrissia* spp. indicate a smaller body of water, a lake embayment, or river slough. Absence of littoral lake genera, together with low diversity of aquatic species, suggests a small, slow-moving stream or pond (Miller *et al.*, 1979).

Van der Schalie and Berry (1973) found that eutrophication of the environment in association with warmer waters will tend to favour *Helisoma* spp., allowing them to become dominant, while *Lymnea* spp. tend to disappear. The presence of *G. parvus* is associated with warmer waters and generally found with *Gyraulus deflectus*, *Lymnea stagnalis*, *Physa* spp., *Pisidium* spp. and *Sphaeriidae* spp. (Clarke, 1981). As lake levels fall, a general shift towards more eutrophic species assemblage should occur (Magnuson *et al.*, 1997).

2.3.5 Indicator Fossils

The species assemblages in the Huron basin have changed over time since the Last Glacial Maximum (LGM). This has been a result of changing environmental and climatic factors, the retreat and eventual disappearance of the LIS, and isostatic rebound of the land surface, which has changed the course and depth of water in lakes and rivers (Miller *et al.*, 1985; Clark *et al.*, 2012).

The Algonquin, Transitional, and Nipissing lake phases within the Huron basin have distinctive mollusc assemblages; these indicator species can be used to establish relative time periods. The river-dwelling *Pleurocera livescens* (syn. *Elimia livescens*, *Goniobasis livescens*), commonly known as the slipper shell, is considered a Nipissing zone fossil (Miller *et al.*, 1979; Dillon *et al.*, 2006; Karrow and Mackie, 2013) and the presence of the Nipissing-aged *Unionid* group, commonly known as river mussels, also serves to differentiate between Algonquin and Nipissing deposits (Miller *et al.*, 1985).

2.4 General History of Lake Huron

Lake Huron is the third largest of the Great Lakes by volume (3,540 km³), with an average depth of 59 m, and maximum depth of 229 m (USEPA, 2016). There are many sub-basins, including Goderich, Port Huron, and Manitoulin (Macdonald, 2012). Modern water levels in

Lake Michigan and Lake Huron are interconnected through the Straits of Mackinac with the main outlet for both lakes being the Port Huron outlet at the south end of Lake Huron (Thomas et al., 1973). With continued erosion of this outlet, lake levels have dropped to modern levels of 176 masl (USEPA, 1995). Average lake water has $\delta^{18}\text{O}$ of -7.4‰ (Macdonald and Longstaffe, 2008), and the lake water has a residence time of 21 years (Quinn, 1992). Regional mean annual temperature (MAT) range from $4 - 8\text{ °C}$, with 800 - 1000 mm of precipitation per year (McCarthy *et al.*, 2012).

The modern Great Lakes watershed can be divided into two main regions. The southern region encompasses the entirety of the Erie and Michigan basins and most of the Huron and Ontario basins, and is characterised by relatively gently-dipping Paleozoic sedimentary rocks (Fig. 2.8; Haeri-Ardakani *et al.*, 2013). These relatively thin sections are dominated by carbonate-rich layers intermingled with sandstones and shales, and are remnants of the shallow oceanic environment in this region from ~ 500 to 180 million years ago (Haeri-Ardakani *et al.*, 2013). These rocks are covered by glacial sediments, which are generally 50 m thick but can be up to 350 m in thickness (Breckenridge, 2007).

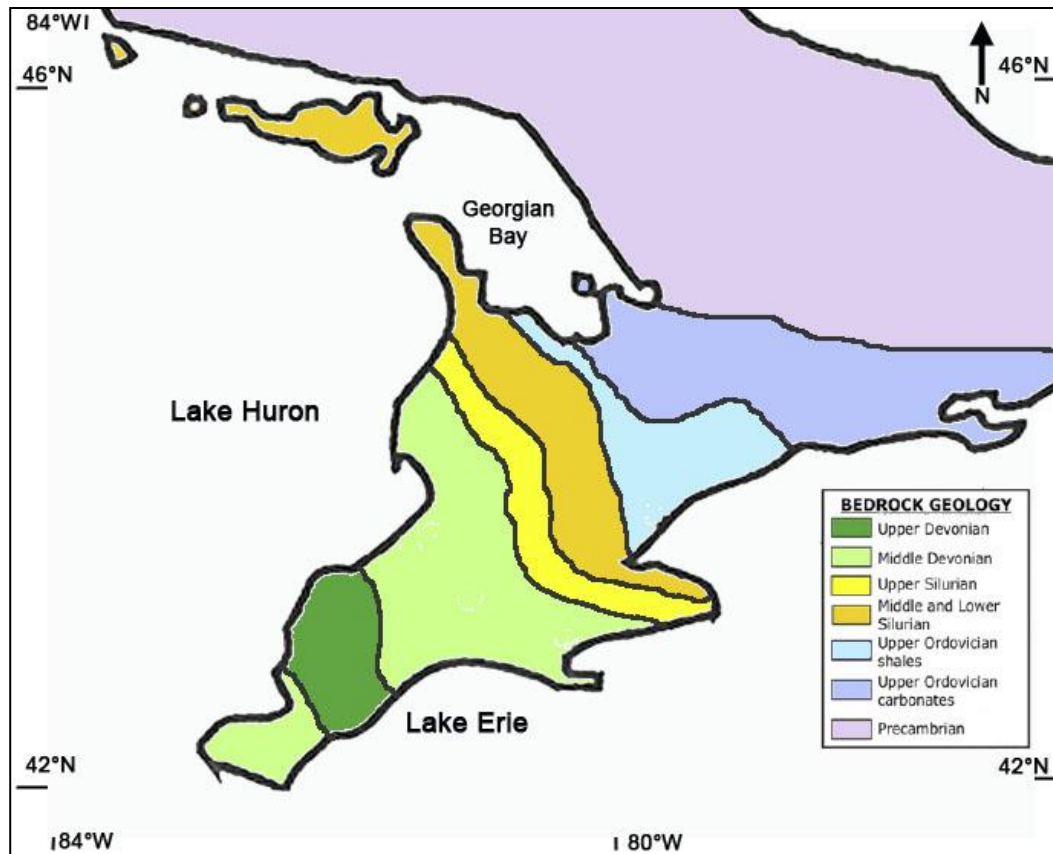


Figure 2.8 - Generalized Palaeozoic bedrock geology map of southern Ontario (after Haeri-Ardakani *et al.*, 2013).

The northern region is underlain by igneous and metamorphic Precambrian rocks of the Canadian Shield and covers the remaining Ontario and Huron basins, including Georgian Bay and the majority of the Superior basin (Breckenridge, 2007). The erosionally resistant nature of the Canadian Shield controls the topography of the region. Differential erosion by glaciers has left much of the rock exposed, with only thin, discontinuous glacial sediments (Larson, 2001).

Lake Huron rests atop both the Paleozoic and Precambrian rocks and is separated into two major sections by an underwater ridge-system known as the Six Fathom scarp (Fig. 2.9; Macdonald, 2012). Lake sediment characteristics, such as grain size distribution, bulk density, and colour, reflect changing sediment sources and lake level changes (Thomas *et al.*, 1973; Odegaard *et al.*, 2003), which can vary considerably across the Huron basin.

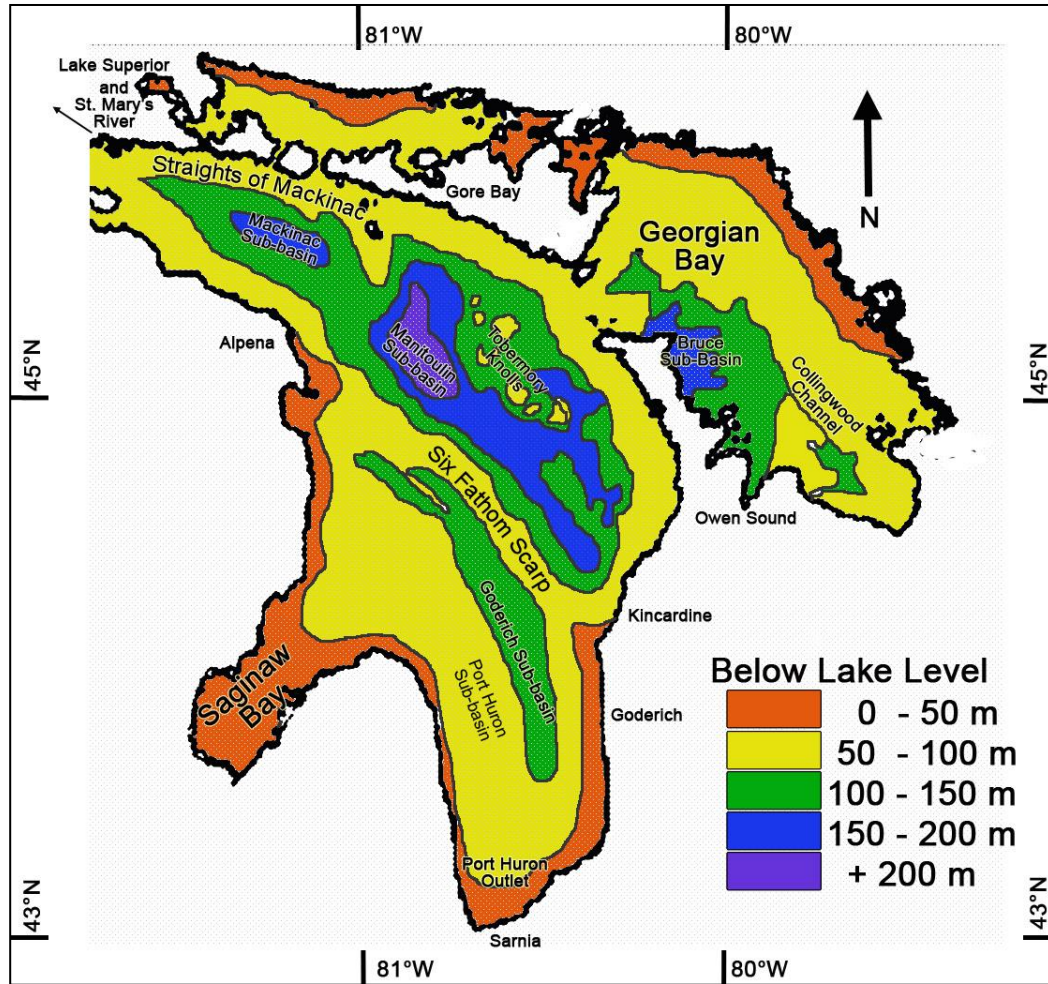


Figure 2.9 - Bathymetry map of Lake Huron (after Thomas *et al.*, 1973).

The lake bottom can be divided into two major categories. The first type is to the south of the ridge and includes the Port Huron and Goderich sub-basins. The lake bottom is relatively flat, generally at 60 to 100 m depth, with the maximum depth of 119 m associated with the Goderich sub-basin (Thomas *et al.*, 1973). The sediments in these sub-basins are mainly derived from erosion of shoreline and shallow subaqueous, glacial till deposits. West of Kincardine there is a large sand deposit. Such larger sand deposits are only present only in the southern portion of the basin. This is because the shallower water facilitates transport of finer grained sediments south through the Port Huron outlet to Lake Ontario rather than allowing for their deposition (Thomas *et al.*, 1973).

The second lake bottom category occurs to the north and includes the Mackinac and Manitoulin sub-basins. These sub-basins have undulating topography with up to 200 m elevation change between adjoining hollows and peaks, known as knolls. In conjunction with

greater water depths, these sub-basins are composed of very fine-grained sediments with >50 % muds (Thomas *et al.*, 1973). To the west, the Mackinac sub-basin has a smoother topography due to the input of sediments from Lake Superior through the St. Mary's River. Georgian Bay, located to the east, has deep channels, such as the Collingwood Channel, indicating possible river systems in this area in the past (Thomas *et al.*, 1973).

2.4.1 History of the Huron Basin

The history of the Great Lakes provides a wide array of examples of changing climate, hydrology and limnology (Lewis *et al.*, 2005). There is extensive documentation of historic lake levels, locations of shorelines, and the isotopic compositions of Lake Algonquin and Lake Nipissing (e.g. Fritz *et al.*, 1975; Miller *et al.*, 1979, 1985; Farrand and Drexler, 1985; Larsen, 1985; Godwin, 1985; Karrow 1986a,b; Lewis *et al.*, 2010; Hyodo and Longstaffe, 2011a,b, 2012; Macdonald, 2012; Karrow and Mackie, 2013). Post-glacial water and pollen records suggest that variations in the lake levels from the latest Pleistocene to the present were commonly climate-related (Larsen, 1985; Yu *et al.*, 1995; Yu and Eicher, 1998; Yu, 2000; Yu and Wright, 2001; McCarthy *et al.*, 2012).

The Great Lakes region of North America consists of five major basins: Superior, Michigan, Huron, Erie, and Ontario. These can be considered relatively new geologic features because their formation coincided with the advance and retreat of ice sheets from ~14.0 to 9.5 ¹⁴C ka (17 to 10.9 ka cal) BP (Miller *et al.*, 1979; Lewis *et al.*, 2005; McIntosh and Walter, 2005). The kilometer-thick Pleistocene ice sheet increased hydraulic gradients and reorganized the ground water flow in Paleozoic aquifers in the underlying geology (McIntosh and Walter, 2005; Clark *et al.*, 2012).

Differential vertical movements of varying magnitudes occurred throughout the Great Lakes region and active uplift is still underway (Larsen, 1985; Lewis *et al.*, 2005; Clark *et al.*, 2007). Former shorelines have been isostatically up-warped towards the north-northeast (Miller *et al.*, 1985; Karrow, 1986a; Lewis *et al.*, 2005). Older shorelines are tilted by greater amounts than younger shorelines (Karrow, 1986a; Karrow, 2004; Coniglio *et al.*, 2006) and those preserved are situated at higher elevations.

Two principal shorelines that have been recognized and mapped regionally are the Main Algonquin shore and the Nipissing Great Lakes coastal zone (Lewis *et al.*, 1994). Extensive erosion of the recent shoreline in most localities has left only the valley terraces of Lake Algonquin and Lake Nipissing to represent the former higher lake levels (Karrow and Mackie, 2013).

2.4.2 Lake Agassiz

Due to its more northern location, Lake Agassiz was subject to inputs from the melting LIS until a much later date than the more southern Great Lakes (Fig. 2.10; Larson, 2001). Waters from this lake intermittently fed glacially-sourced water to the Great Lakes basins (Teller and Thorleifson, 1983; Lewis and Anderson, 1989; Leverington and Teller, 2003). One of the largest of these outbursts to reach the Huron basin occurred at 9.5 ^{14}C ka (10.8 ka cal) BP, with smaller events from 8.5 to 7.7 ^{14}C ka (9.5 to 8.5 ka cal) BP (Prest, 1970; Teller and Thorleifson 1983; Eschman and Karrow, 1985; Teller, 1987; Lewis *et al.*, 1994; Hyodo and Longstaffe, 2012). These far-reaching floodwater events were thought to have produced short-lived but exceptionally high lake levels, known as the Early and Main Lake Mattawa highstands (Lewis *et al.*, 1994; Colman *et al.*, 1994; Lewis and Anderson, 1989; Dettman *et al.*, 1995; Breckenridge, 2007; Macdonald and Longstaffe, 2008; Macdonald, 2012).



Figure 2.10 - Lake Agassiz (after Leverington and Teller, 2003).

Analysis of preserved phytoplankton indicated that Lake Agassiz had a top-water $\delta^{18}\text{O}$ of -18 ± 1 ‰, and bottom water of -24.5 ± 0.5 ‰ (Birks *et al.*, 2007). The difference was suggested to represent evaporative ^{18}O -enrichment of glacial meltwater (Birks *et al.*, 2007).

Nonetheless, the characteristically low $\delta^{18}\text{O}$ composition of this glacially-sourced water can be used as a marker for its contribution to other water systems, as it is much lower than lake water and precipitation from the south (Colman *et al.*, 1990; Lewis *et al.*, 1994; Macdonald, 2012; Hladyniuk and Longstaffe, 2015, 2016). The $\delta^{13}\text{C}$ of the glacial waters was also relatively higher than average lake water in the region prior to meltwater influx. The cold, clear meltwaters typically contained a reduced abundance of low- $\delta^{13}\text{C}$ OM. Additionally, the movement of the LIS comminuted underlying Paleozoic carbonates allowing for enhanced dissolution and high- $\delta^{13}\text{C}$ DIC and associated biogenic carbonates (Guiguer, 2000; Macdonald and Longstaffe, 2008; Macdonald, 2012; Hladyniuk and Longstaffe, 2015, 2016).

2.4.3 Huron Basin

The climate in southern Ontario has changed substantially since the end of the Pleistocene (Fig. 2.11a,b; Terasmae, 1961; Webb III *et al.*, 1987; Edwards *et al.*, 1985, 1996; McCarthy *et al.*, 2012). The Huron basin provided a significant outlet for water from upstream Lake Agassiz and Superior to the St. Lawrence and the Atlantic Ocean for brief periods during the Late Holocene and lake water $\delta^{18}\text{O}$ and DIC $\delta^{13}\text{C}$ in this basin reflect the northern input concurrent with these outwash events (Fig 2.12; Teller and Thorleifson, 1983; Lewis and Anderson, 1989; Lewis *et al.*, 1994, Leverington and Teller, 2003; Birks *et al.*, 2007; Wakabayashi, 2010; Hyodo and Longstaffe, 2012; Macdonald, 2012; Hladyniuk and Longstaffe, 2015, 2016).

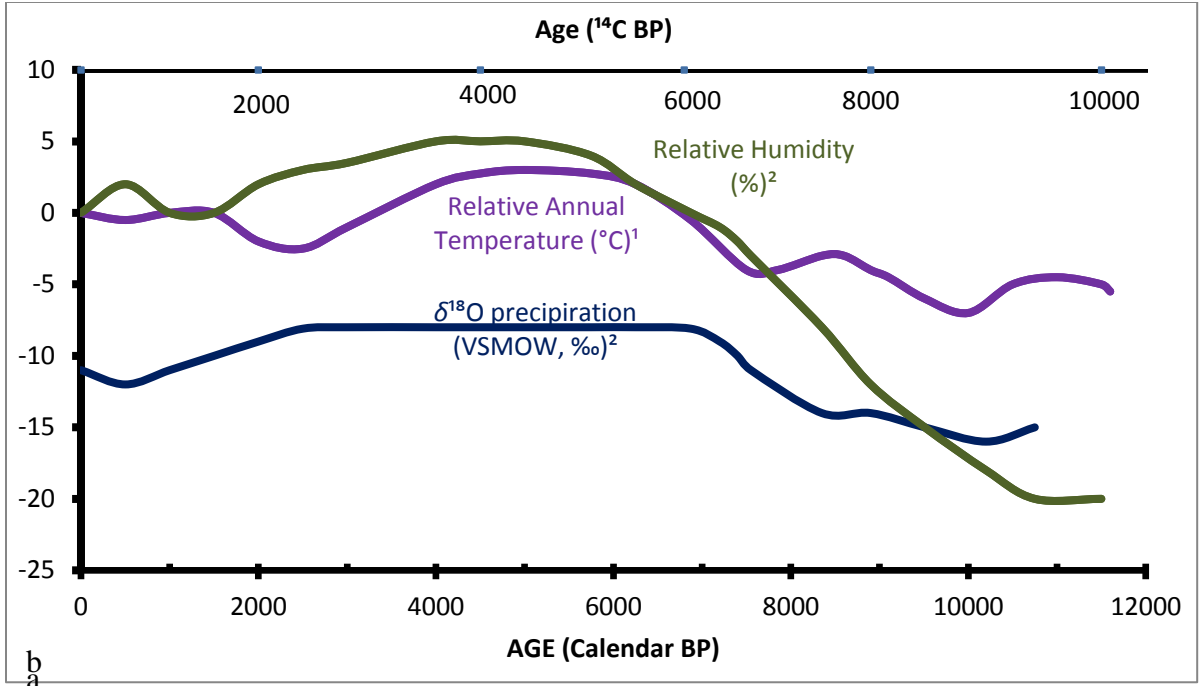
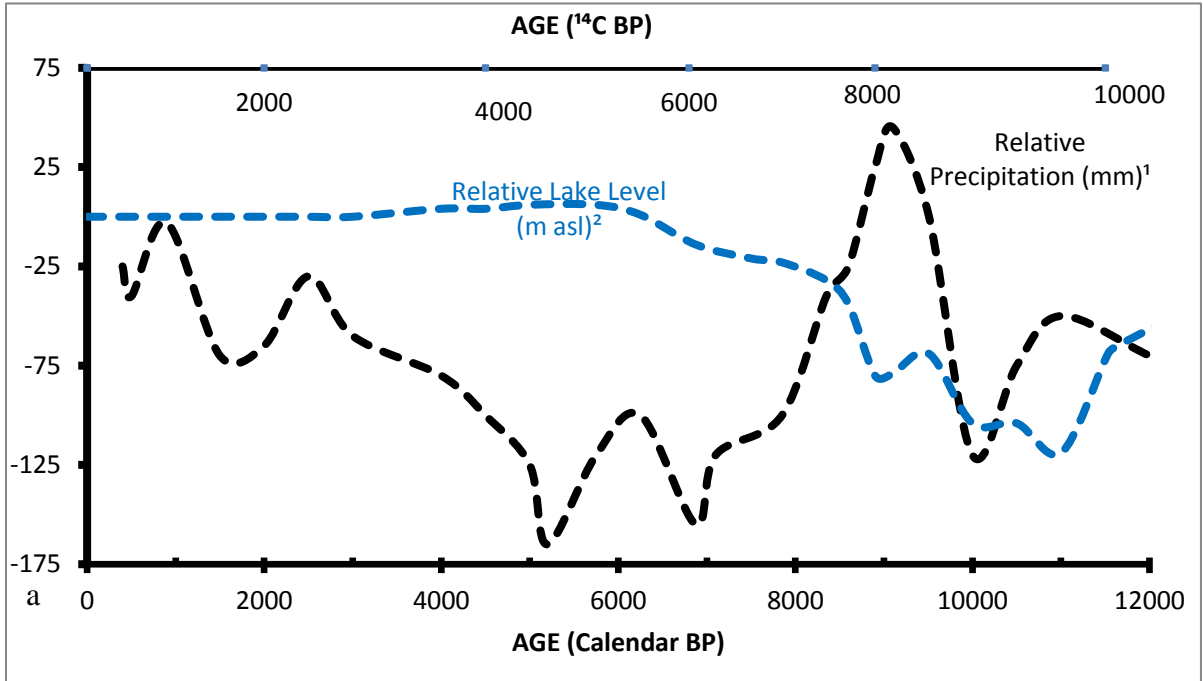


Figure 2.11 - Age-dependent variations in the Huron Basin since the Late Pleistocene. (a) ¹ Change in



relative MAT from modern for south-eastern Canada (Terasmae, 1961), ² Change in relative humidity from modern and actual δ¹⁸ O of precipitation in southern Ontario (Edwards *et al.*, 1996). (b) ¹ Change in relative precipitation amount from modern times in Minnesota, USA (Webb III *et al.*, 1987), ² Relative lake level from modern times (Lewis *et al.*, 2008a).

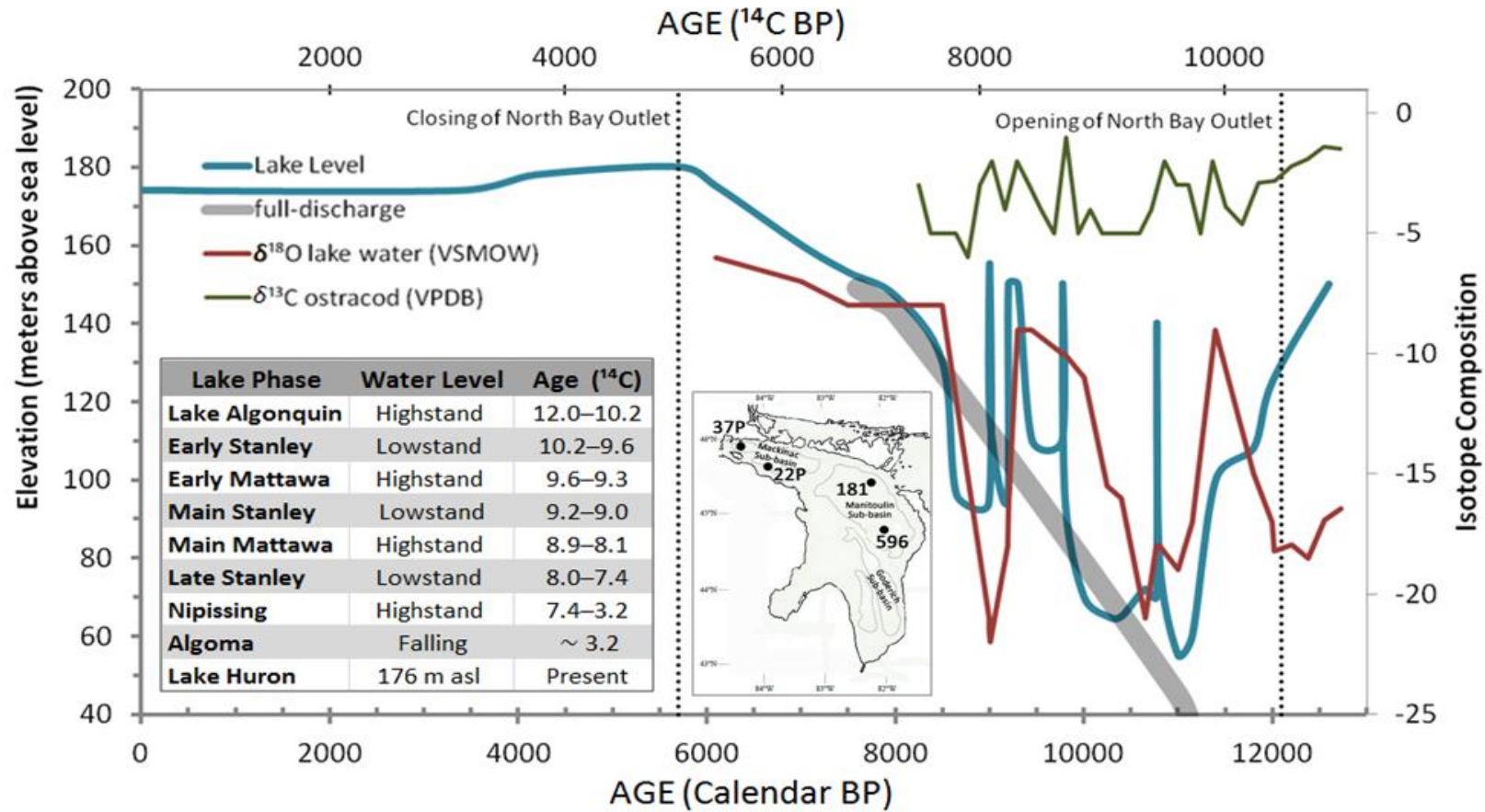


Figure 2.12 - Inferred lake level changes and phases in the Huron Basin from the late Pleistocene to present adjusted for isostatic rebound after Eschman and Karrow (1985), Baedke and Thompson (2000), Lewis *et al.* (2008a,b), Brooks *et al.* (2012) and Lewis and Anderson (2012). Full-discharge line is from Lewis and Anderson (2012). Lake water oxygen isotopic data for northern Lake Huron are calculated from ostracode data provided by Lewis *et al.* (1994, core 37P), Moore *et al.* (2000, core 22P), Wakabyashi (2010, core 181) and Macdonald (2012, core 596). Carbon isotopic data for northern Lake Huron were obtained using ostracod shell data from Lewis *et al.* (1994, core 37P), Wakabyashi (2010, core 181) and Macdonald (2012, core 596). Table insert - Summary of major lake phases in the Huron basin in radiocarbon years from Macdonald and Longstaffe (2008). Map insert shows core locations from above.

2.4.4 Lake Algonquin

The single name Lake Algonquin was applied to several bodies of water present in all or parts of the Michigan, Huron, Superior, and Erie basins. It has since been realized that major changes in lake levels and outlets occurred over time but this broad name has been retained (Eschman and Karrow, 1985).

2.4.5 Main Lake Algonquin Phase

During the LGM [18 to 21 ^{14}C ka (21.3 to 25.4 ka cal) BP], the Great Lakes watershed was completely covered by the southernmost section of the LIS (Lewis *et al.*, 2005). During deglaciation, the ice margin retreated to the north in a series of oscillations and released large quantities of meltwater that pooled in isostatically down-pressed regions created by weight of the ice sheet.

The Main Lake Algonquin phase [\sim 11 to 10.3 ^{14}C ka (12.9 to 12.1 ka cal) BP] occurred at the terminus of the Pleistocene. The lake at that time was the largest of these pro-glacial lakes, and its shoreline is traceable throughout most of southern Ontario and Michigan (Fig. 2.13; Eschman and Karrow, 1985; Hansel *et al.*, 1985; Larsen, 1985, 1987; Karrow and Mackie, 2013). Boundaries of Lake Algonquin followed the retreating margins of the LIS, opening an outlet near North Bay at 10.3 ^{14}C ka (12.1 ka cal) BP. This outlet redirected water movement from the Port Huron outlet causing a sharp drop lake level; the lowest levels were reached at 9.8 ^{14}C ka (11.1 ka cal) BP (Eschman and Karrow, 1985; Larsen, 1987; Lewis and Anderson, 1989; Lewis *et al.*, 1994; Godsey *et al.*, 1999; Karrow, 2004; Lewis, 2016). A second smaller outlet was opened for a short time through Fenelon Falls, but was then closed as isostatic uplift progressed (Finamore, 1985).

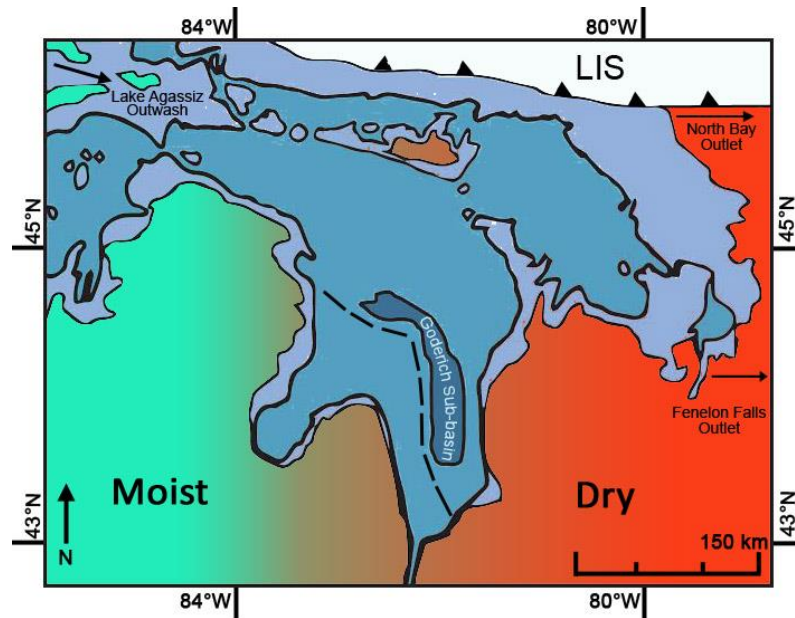


Figure 2.13 - Main Algonquin phase [12.2 ^{14}C ka [14.2 ka cal) BP] lake boundary (light blue) overlain on the modern lake boundary (darker blue). LIS - Laurentide Ice Sheet with arrows showing the direction of retreat (after Prest, 1970; Eschman and Karrow, 1985; Karrow 1987a) and moisture regimes in southern Ontario from pollen data (Shuman *et al.*, 2002).

Analysis of terrestrial plant matter, lake sediments, and fossil diatoms has revealed that the climate in southern Ontario was colder and drier than present during the early Holocene (Godwin, 1985; Edwards *et al.*, 1985, 1996; Magnuson *et al.*, 1997). Pollen data suggest that there was an intense drought in the early Holocene, limiting growth of certain tree species (Baker *et al.* 1992; Shuman, 2001; Shuman *et al.*, 2002). Trends of annual temperature and humidity suggest that dry Arctic air masses prevailed over the region (Edwards and Fritz, 1986; Edwards *et al.*, 1996; Shuman, 2001). The presence of the retreating LIS and associated rapid, drainage induced anticyclonic atmospheric circulation that prevented meridional (northern) flow of moisture-rich air (Kutzbach *et al.*, 1993; Shuman, 2001; Yu and Wright, 2001). This stabilised the jet stream and associated storm tracks, and directed the path of Pacific air masses to the Great Lakes region (Godsey *et al.*, 1999). This had the effect of increasing evaporation in the region, leading to a lowering of lake level (Shuman, 2001). In addition to drier air masses, solar radiation reaching the northern hemisphere during this time was greater than present, possibly facilitating greater evaporation during summer months (Kutzbach *et al.*, 1998).

Over the next 1500 years, a warming climate allowed for the growth of spruce forests along the Great Lakes, reaching north of Sudbury by 10.0 ^{14}C ka (11.5 ka cal) BP (Webb III *et al.*,

1987; Anderson and Lewis, 1992). Miller *et al.* (1985) found fossil mollusc species at Algonquin-dated sites that would require a 4 °C lower temperature than the present mean summer temperatures (Terasmae, 1961; Webb III *et al.*, 1987; Edwards *et al.*, 1996).

A variety of fossils (pollen, diatoms, plant macrofossils, molluscs, insects, ostracodes) have been recovered from Main Algonquin deposits from the Huron basin (Miller *et al.*, 1979; Miller *et al.*, 1985; Macdonald, 2012; Karrow and Mackie, 2013), and demonstrate that life was abundant in the lake at this time. Nonetheless, the cooler air temperatures of this time compared with the Holocene were associated with shorter growing seasons of terrestrial and lake water organisms. Furthermore, lake nutrient concentrations at this time were low because the pine forests surrounding the lake were still immature (Smol and Boucherle, 1985).

2.4.5.1 Previous Carbon and Oxygen Isotope Information for the Algonquin Phase

Great Lakes benthic ostracodes indicate that lake water throughout much of the Huron Basin during the Algonquin phase had $\delta^{18}\text{O}$ -22 to -17 ‰. These low- $\delta^{18}\text{O}$ waters likely originated from upstream and were fed by the melting of the LIS (Lewis *et al.*, 1994; Rea *et al.*, 1994; Dettman *et al.*, 1995; Heath and Karrow, 2007; Macdonald, 2012; Hyodo and Longstaffe, 2011a,b, 2012). This water also seeped into the upper levels of ground water, lowering its $\delta^{18}\text{O}$ to -15 to -13 ‰ (McIntosh and Walter, 2006). In southern Ontario, ground water with $\delta^{18}\text{O}$ of -17 to -14 ‰ is presently known to be at depths of 20 to 40 m in some localities. Based on ^{14}C dating, these characteristically cooler waters likely entered the ground water system between 14 and 11 ^{14}C ka (17 and 12.9 ka cal) BP (Desaulniers *et al.*, 1981).

Cooler temperatures and overland runoff facilitated dissolution of high- $\delta^{13}\text{C}$ Paleozoic carbonates that surround much of the Huron basin (McIntosh and Walter, 2005). This ^{13}C -enriched input coupled with limited contributions of low $\delta^{13}\text{C}$ terrestrial OM (Hyodo and Longstaffe, 2011a; Hladyniuk and Longstaffe, 2015), enriched the DIC pool in ^{13}C . Ground water DIC at the time had $\delta^{13}\text{C}$ ranging from -8 to -3 ‰ (McIntosh and Walter, 2006).

During times when the local precipitation and runoff were the main water sources in the area, lower DIC $\delta^{13}\text{C}$ may reflect a decrease in primary productivity, but more likely it is diagnostic of an increase of DIC derived from terrestrial matter (Vogel, 1993; Post, 2002; Hyodo and Longstaffe, 2011b; Hladyniuk and Longstaffe, 2015). Godwin (1985) found that the Algonquin sites she analysed had a relatively consistent $\delta^{13}\text{C}$, which suggested that the DIC reservoir was stable during this time, and that there were likely no major changes in biological productivity.

2.4.6 Transitional Phase

During the first 2000 years of the Transitional phase [9.0 to 7.4 ^{14}C ka (10.2 to 8.2 ka cal) BP], the Huron Basin was characterised by lingering, dry climatic conditions and warming temperatures (Meyers *et al.*, 1999; Hyodo and Longstaffe, 2012). Mean annual temperatures increased over the period 10.0 to 8.1 ^{14}C ka (11.5 to 8.9 ka cal) BP, generally ranging from 8 to 4 °C below those at present (Magnuson *et al.*, 1997). Studies of terrestrial plant matter have suggested that between 8.8 and 7.4 ^{14}C ka (9.9 and 8.2 ka cal) BP, Georgian Bay basin was 20 to 35 ‰ drier than in modern times (Edwards *et al.*, 1996; McCarthy *et al.*, 2012).

At 9.4 ^{14}C ka (10.8 ka cal) BP, a large outwash from upstream Lake Agassiz raised lake levels by almost 100 m. Some studies have suggested that as much as one-third of Lake Agassiz was released in as little as two years (Teller and Thorleifson, 1983; Farrand and Drexler, 1985; Leverington and Teller, 2003). This highstand lasted only a short time before returning to previous low levels. At 7.4 ^{14}C ka (8.2 ka cal) BP, the LIS retreated northward for the last time and broke up over the Hudson Bay (Karrow *et al.*, 2000; Larsen, 2001). Immense volumes of water stored in the LIS were discharged into the Hudson Bay and out to the Atlantic Ocean at this time, disrupting oceanic circulation patterns, and possibly triggering temporary cool periods (Barber *et al.* 1999; Edwards *et al.* 1996; Shuman *et al.* 2002; Lewis *et al.*, 2005; Gavin *et al.*, 2011; Breckenridge *et al.*, 2007; Yu *et al.*, 2010). Further lowering of lake levels in the Huron Basin may also have occurred at this time (Lewis *et al.*, 2005, 2007, 2008b). Northward shifts in atmospheric circulation and the location of the polar jet stream also occurred (Gavin *et al.*, 2011), which would have reduced the amount of precipitation received by the region (Fig. 2.11).

The Late Stanley phase [8.0 and 7.4 ^{14}C ka (8.9 and 8.2 ka cal) BP] was a period of severely reduced water levels that coincided with regional uplift. This uplift led to the opening and closing of river channels, which altered lake levels by rerouting many of the main sources of incoming and outgoing water (Fig. 2.14; Lewis *et al.*, 2007; Karrow and Mackie, 2013). During this lowstand, Lake Hough was created in the Georgian Bay sub-basin (McCarthy *et al.*, 2012), along with other isolated lakes in the Huron basin, causing the lake level to drop by up to 61 m below maximal Lake Algonquin levels (Prest, 1970; Karrow, 1986a; Miller *et al.*, 1979). This very large drop in water levels transformed previous littoral lacustrine and estuarine environments into locations that were kilometers upstream from the newly developed shoreline. Few Transitional-aged sediment sites preserve any record of lacustrine environments, as most of these were submerged and possibly destroyed during the subsequent, strong and relatively continuous Nipissing transgression (Eschman and Karrow, 1985; Miller *et al.*, 1985; McCarthy *et al.*, 2012).

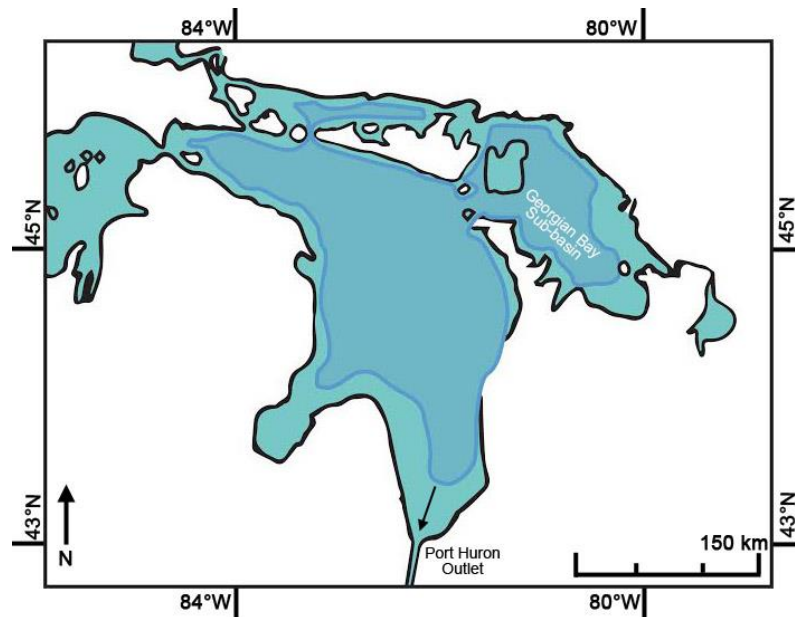


Figure 2.14 - Transitional phase [7.4 ^{14}C ka (8.2 ka cal) BP] light blue) lake boundary overlain on the modern lake boundary (darker blue). (after Eschman and Karrow, 1985; Lewis *et al.*, 1994).

By the end of the Transitional phase [7.4 ^{14}C ka (8.2 ka cal) BP], the regional climate shifted to a warmer regime that saw increased mean annual precipitation and milder winter temperatures; these conditions produced a positive water balance, causing lake levels to gradually rise to several meters above modern conditions (McCarthy *et al.*, 2012).

2.4.6.1 Previous Carbon and Oxygen Isotope Information for the Transitional Phase

Some studies of $\delta^{18}\text{O}$ for biogenic carbonates in the Huron basin suggested that Stanley lowstands were characterized by lower $\delta^{18}\text{O}$, and Mattawa highstands were characterized by higher $\delta^{18}\text{O}$ (Lewis *et al.*, 1994; Rea *et al.*, 1994; Dettman *et al.*, 1995; Godsey *et al.*, 1999; Moore *et al.*, 2000; Odegaard *et al.*, 2003; Macdonald and Longstaffe, 2008). Stanley lowstands may have been dominated by ground water input originating from previous sub-glacial meltwater or lakes with $\delta^{18}\text{O}$ of -13 to -8 ‰, although such values are not typical for glacially-fed lakes (McIntosh and Walter, 2006; Lewis, 2016). Conversely, other studies of this region have correlated high $\delta^{18}\text{O}$ of lake water with lowstands and low $\delta^{18}\text{O}$ with highstands, the latter attributed to inundation of Lake Agassiz meltwater (Lewis and Anderson, 1989; Lewis *et al.* 2005, 2007, 2008a; Breckenridge and Johnson 2009; Brooks *et al.*, 2012). This discrepancy may be attributed to the lake water $\delta^{18}\text{O}$ differing greatly geographically (Macdonald, 2012). Lake water $\delta^{18}\text{O}$ derived from ostracode valves in the Manitoulin basin was -19 to -16 ‰, whereas values of -11 to -8 ‰ were obtained for the Goderich basin to the south. This may indicate that basins in the north and south had different sources of water and hydrologic histories.

Fritz *et al.* (1975) proposed that when a lake is deepening, the effect of evaporation on lake water $\delta^{18}\text{O}$ diminished and it was instead directly linked to the $\delta^{18}\text{O}$ of precipitation. During this time period [7.0 to 6.0 ^{14}C ka (7.8 to 6.9 ka cal) BP], an increase in average $\delta^{18}\text{O}$ of precipitation in the region from -15 to -12 ‰ accompanied rising temperature and humidity (Edwards *et al.*, 1996). Macdonald (2012) found that there was a systematic increase in lake water $\delta^{18}\text{O}$ and $\delta^{13}\text{C}$ upwards in the sedimentary section after 9.0 ^{14}C ka (10.2 ka cal) BP. Godwin (1985) used the carbon and oxygen isotope composition of shelly fauna and fossil plant material to infer an warming trend of 2.5 to 4 °C between Algonquin and Transitional times.

During Transitional times [10.2 to 6.0 ^{14}C ka (9.0 to 6.9 ka cal) BP], the $\delta^{13}\text{C}$ of ostracode valves increased to a maximum of -3 to -2 ‰ (Macdonald, 2012). This increase likely reflects an increase in primary productivity in the basin and / or a decrease of terrestrial OM input (Leng and Marshall, 2004; Macdonald, 2012). Ground water DIC $\delta^{13}\text{C}$ ranged from -14

to -7‰ (McIntosh and Walter, 2006), but with rising lake levels, ground water input would have had a diminished effect on lake water DIC.

2.4.7 Nipissing Phase

The Nipissing phase [7.4 to 3.2 ^{14}C ka (8.2 to 3.4 ka cal) BP] was a period of much more stability than seen in this region over the previous $\sim 5,000$ years. The Nipissing transgression, which began in the Transitional phase, produced a continuous and relatively gradual increase in lake level (Fig. 2.15; Larsen, 1985). Moist air masses from the south became more prevalent and the water supply to the region increased. This influx of moisture raised lake levels in the basin to produce a hydrologically open setting that continues to this day (Lewis *et al.*, 2008b).

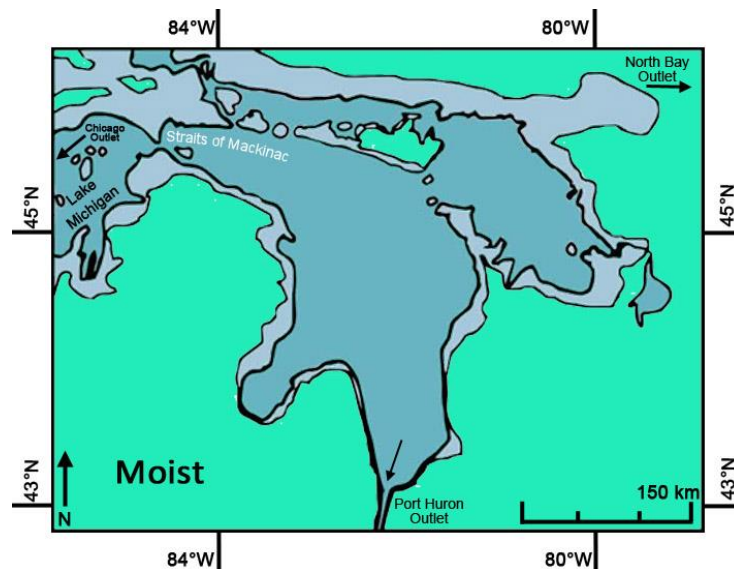


Figure 2.15 - Nipissing phase [5.0 ^{14}C ka (5.7 ka cal) BP] lake boundary (light blue) overlain on the modern lake boundary (darker blue) (after Eschman and Karrow, 1985) and moisture regime in southern Ontario (Shuman *et al.*, 2002).

During the transgression, some studies have suggested that Lake Huron waters may have flowed westward through Lake Michigan and out the Chicago outlet (Lewis and Anderson, 1989; Odegaard *et al.*, 2003). This is further supported by the presence of the Salinac forest in the southern section of the Huron basin; the forest shows evidence of growth until 7.4 ^{14}C ka (8.2 ka cal) BP, several hundred years before the Port Huron outlet is said to have reopened (Fritz *et al.*, 1975; Eschman and Karrow, 1985; Lewis *et al.*, 2005; Hunter *et al.*, 2006; Lewis, 2016).

By 4.2 ¹⁴C ka (4.8 ka cal) BP, isostatic uplift shifted the main water outlet from the Chicago outlet to the southern Port Huron outlet, thus switching flow from Lake Michigan to the Straits of Mackinac and into Lake Huron (Eschman and Karrow, 1985; Hansel *et al.*, 1985; Larson *et al.*, 1985; Thompson and Baedke, 1995; Odegaard *et al.*, 2003; Lewis *et al.*, 2007, 2008a). By 3.4 ¹⁴C ka (3.8 ka cal) BP, the lake level fell by several metres to its modern levels. This lowering may be related to increased erosion of the Port Huron outlet from the additional flow from Lake Michigan; currently, however, there is not enough evidence to indicate for certain why the lake levels fell by more than five times the rate of isostatic rebound (Baedke and Thompson, 2000; Baedke *et al.*, 2004). Satellite-based surface modeling suggests that it wasn't until 3.0 ¹⁴C ka (3.2 ka cal) BP that Port Huron took full control of water movement from the Chicago and North Bay outlets (Clark *et al.*, 2012) .

With lake levels returning to higher levels, the newly-created shoreline allowed for deposition of fossiliferous sediments on top of Transitional and parts of Algonquin sediments (Larsen, 1985; Karrow and Mackie, 2013). Deposits of this age represent a greater abundance of estuarine- and lacustrine-type settings than Transitional-age sites, but should represent essentially the same type of aquatic habitats that were present during the Main Algonquin phase. Nipissing fauna assemblages should also show much similarity to Algonquin-age assemblages, less the colder water aquatic species (Miller *et al.*, 1985).

The Nipissing shorelines generally follow the present Lake Huron and Georgian Bay shorelines but are higher by several metres due to isostatic rebound. Their youth and proximity to the present shoreline make them the most easily recognizable of the paleoshorelines (Coniglio *et al.*, 2006; Lewis *et al.*, 2008a; Karrow and Mackie, 2013).

Most studies agree that the mid-Holocene experienced a warm period between ~9.0 to 4.0 ¹⁴C ka (10.2 to 4.5 ka cal) BP, known as the Holocene Hypsithermal (Yu *et al.*, 1995; Edwards *et al.*, 1996; McFadden *et al.*, 2005; Churcher and Karrow, 2008; Gavin *et al.*, 2011). Studies of pollen suggest that the mean July temperature was 1 - 2 °C warmer than at present, with 10 - 20 % less precipitation, and with slightly cooler conditions on the northern Great Lakes shores (McAndrews and Campbell, 1993; Yu *et al.*, 1995). This climate allowed for the spread of hardwood trees into southern Ontario, and the establishment of forests very similar to what we see today. Some local studies, however, have suggested that Nipissing

temperatures were similar to or ~ 1 °C cooler than during the Transitional Phase (Godwin, 1985).

2.4.7.1 Previous Carbon and Oxygen Isotope Information for the Nipissing Phase

Edwards *et al.* (1996) found that precipitation $\delta^{18}\text{O}$ quickly increased from -12 to -8 ‰ by 6.0 ^{14}C ka (6.8 ka cal) BP, but remained steady for the remainder of the Nipissing phase, despite the increasing temperature and humidity trends reported for the region (Fig. 2.11; Magnuson *et al.*, 1997). A more recent analysis of ostracodes from Nipissing sediments in Lake Huron showed that lake water oxygen compositions had risen to as high as -6 ‰ during this period (Odegaard *et al.*, 2003; Macdonald and Longstaffe, 2008). Studies of shells from a Nipissing-age fluvial site [K45; 4.3 ^{14}C ka (4.9 ka cal) BP] on the Sauble River (Fig. 1.7) found water oxygen and shell carbon isotope averages of -8.6 ‰ and -6.5 ‰, respectively (Godwin, 1985). Ground water at this time also varied. The $\delta^{18}\text{O}$ values increased to range from -13 to -8 ‰, and $\delta^{13}\text{C}$ became lower at -14 to -7 ‰ (McIntosh and Walter, 2006).

Chapter 3

3 Methodology

3.1 Field Methods

Sediments containing fossils were collected from paleo-shorelines spanning three different lake phases during the summer of 2013 by Andy Bajc, and in 2014 by Paul Karrow and Fred Longstaffe (List in Appendix A). Each sample was excavated from horizontal adits into slope faces after first removing slumped material from the slope face. The samples were stored in plastic bags. Photographs and cross sections of sites in Appendix B.

3.2 Laboratory Methods

3.2.1 Sieving

Sediments were sieved through 0.25 mm gauge, by dry or wet methods depending on the consolidation of the sediments. The dry method used agitation to remove sediment, whereas the wet method required running water to remove clay-sized particles characteristic of some sites. Shells were picked from the dried, sieved material using tweezers and stored in dry glass vials.

3.2.2 Shell Identification

Accurate identification of mollusc taxa is important for establishing biostratigraphical zonation for samples, and for consideration of isotopic vital effects associated with certain genera or species. Online resources (Perez *et al.*, 2004; Dillon *et al.*, 2006; Pickering , 2016) and books (Clarke, 1973; Burch, 1982, 1989; Mackie *et al.*, 1980) were used to identify the three genera *Amnicola*, *Valvata*, and *Pisidium*. Species-level identification was also possible for the former two genera. Many *Pisidium* species share very similar shell characteristics, and for some species their soft-body parts are what is used for identification. This made specific identification difficult; therefore, only the genus name is used here.

3.2.3 Sample Selection

The three genera were selected because they were present during all three time periods, and were gill-breathing aquatic organisms. Jones *et al.* (2002) recommended that six or more

shells should be analysed per site so as to capture the full variation of isotopic compositions. The *Valvata* species was sufficiently abundant at all sites. Keith and Weber (1964) noted a large difference in $\delta^{13}\text{C}$ between coeval small and large individuals. Therefore, fully intact adult shells were analyzed, whenever possible.

3.2.4 Powder X-Ray Diffraction (*p*XRD)

Aragonite in shells is thermally unstable and can convert to calcite after death and burial of the organism, which alters its isotopic composition (Leng & Lewis, 2016). To test for preservation of aragonite, ~200 mg of hand-milled powder was front-packed into a glass slide. This approach reduces analytical artifacts arising from preferred crystal orientation and surface roughness during *p*XRD. The samples were analysed using a Rigaku high-brilliance, rotating-anode X-ray diffractometer available in the Laboratory for Stable Isotope Science (LSIS) at the University of Western Ontario. The diffractometer employs $\text{CoK}\alpha$ radiation with monochromation achieved using a curved crystal, diffracted beam, graphite monochromator. The instrument was operated at 45 kV and 160 mA, scanning from 2 to 82° two-theta using a scan rate of 10° two-theta per minute. Mineral identification from the diffraction patterns was achieved by comparison with results available in the JCPDS (Joint Committee on Powder Diffraction Standards) database.

3.2.5 Stable Isotope Sampling

Shells were bulk sampled by powdering a shell in a mortar and pestle. The stable carbon and oxygen isotopic compositions of the shells were obtained by reaction of the powder with orthophosphoric acid at 90 °C, using a Micromass MultiPrep® device coupled to a VG Optima® dual-inlet isotope-ratio mass-spectrometer (IRMS).

The stable isotope ratio of a given element (*R*) is expressed as the ratio of heavy isotope (*R_a*) to light isotope (*R_b*):

$$R = R_a/R_b \quad \text{Equation 3.1}$$

Different isotopes of an element are distributed among various phases by a process called fractionation, which can occur under equilibrium or kinetic conditions. In the biogenic carbonate-water system, the fractionation factor (α) is defined as:

$$\alpha = R \quad \text{Equation 3.2}$$

The oxygen-isotope results are provided in δ -notation relative to Vienna Standard Mean Ocean Water (VSMOW) in parts per thousand (‰):

$$\delta^{18}\text{O} = [(R_{\text{sample}}/R_{\text{standard}}) - 1] \quad \text{Equation 3.3}$$

where $R_{\text{sample}} = {}^{18}\text{O}/{}^{16}\text{O}_{\text{sample}}$ and $R_{\text{standard}} = {}^{18}\text{O}/{}^{16}\text{O}_{\text{standard}}$

The carbon-isotope results are presented in δ -notation relative to VPDB (based on the now exhausted Pee Dee Belemnite standard) in parts per thousand (‰):

$$\delta^{13}\text{C} = [(R_{\text{sample}}/R_{\text{standard}}) - 1] \quad \text{Equation 3.4}$$

where $R_{\text{sample}} = {}^{13}\text{C}/{}^{12}\text{C}_{\text{sample}}$ and $R_{\text{standard}} = {}^{13}\text{C}/{}^{12}\text{C}_{\text{standard}}$

3.2.6 Serial Sampling

Serial sampling was completed on *Pisidium* spp. shells to test for isotopic vital effects. Due to the preservation environment, the surface of most of the shells had become stippled or worn making identification of annual growth bands from seasonal growth bands difficult. *Pisidium* spp. are known to have lifespans of one to two years, with only an 18 % increase of shell size by the second year (Holopainen, 1980). Determining how old the shell was in relation to size was not possible. The age-span of the shell, however, should not significantly affect interpretation of trends in the isotopic data.

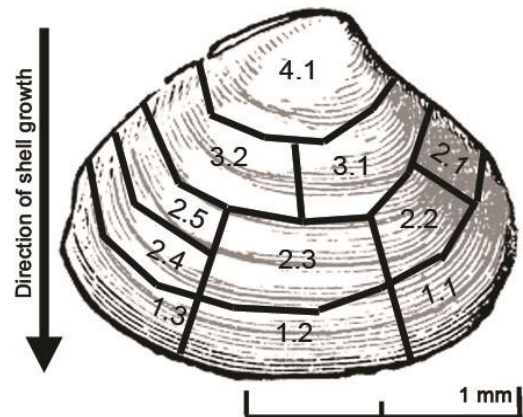


Figure 3.1 - Schematic for serial sampling of *Pisidium* spp. shell.

Small metal tools were used to fracture the shells along growth bands and then divide the shell into small segments for analysis without further crushing (Fig. 3.1). Isotopic compositions were obtained using the same process detailed in section 3.2.5. Results for the centre growing-axis of the shell were compared to the outer portions along growth lines as well as from older (higher numbers) to younger layers (lower numbers).

A weighed mean average was also calculated from serial samples of growth bands. This result was used to compare serial-sampled shells to other bulk-sampled shells.

3.2.7 Standardisation of Isotopic Results for Biogenic Carbonate

A two-point calibration curve was used to convert the oxygen isotope results for aragonite shell material to VSMOW, based on the isotopic compositions of NBS-18 ($\delta^{18}\text{O} +7.2\text{‰}$) and NBS-19 ($\delta^{18}\text{O} +28.65\text{‰}$) (Coplen, 1996). Two calcite standards not included in the calibration curve were used to evaluate accuracy and precision. WS-1 had $\delta^{18}\text{O} +26.30 \pm 0.11\text{‰}$ (SD, $n = 27$), and Suprapur had $\delta^{18}\text{O} +13.24 \pm 0.10\text{‰}$ (SD, $n = 22$), both of which compare well with their accepted values of $+26.23\text{‰}$ and $+13.30\text{‰}$, respectively. To correct for the difference in the oxygen isotope carbon dioxide–acid fractionation factor for calcite versus aragonite at 90°C , data for aragonite samples were further adjusted by subtracting 0.41‰ . The average reproducibility of duplicate analyses of samples ($n=14$) was $\pm 0.2\text{‰}$.

NBS-19 ($\delta^{13}\text{C} +1.95\text{‰}$) and LSVEC ($\delta^{13}\text{C} -46.6\text{‰}$) were used to establish the calibration curve for $\delta^{13}\text{C}$ (Coplen *et al.*, 2006). Calcite standards Suprapur, NBS-18 and WS-1 were used as independent checks on precision and accuracy. Suprapur had $\delta^{13}\text{C} -35.64 \pm 0.28\text{‰}$ (SD, $n = 22$), NBS-18 had $\delta^{13}\text{C} -5.11 \pm 0.16\text{‰}$ (SD, $n = 32$), and WS-1 had $\delta^{13}\text{C} +0.76 \pm 0.06\text{‰}$ (SD, $n = 27$), which compare well with their accepted values of -35.55‰ , -5.0‰ , and $+0.76\text{‰}$, respectively. All results for standards are listed in Appendix C. The average reproducibility of duplicate analyses of samples ($n=14$) was $\pm 0.3\text{‰}$.

Macdonald (2012) determined α for modern samples living in Lake Huron for the four species analyzed in the present study: *A. limosa* $\alpha = 1.0318$, *Pisidium* spp. $\alpha = 1.0315$, *V. sincera* $\alpha = 1.0317$, and *V. tricarinata* $\alpha = 1.0324$. These values of α represent the weighted average oxygen isotope discrimination between shell and water over the period of growth, during which temperature and water isotopic composition likely fluctuated. Nonetheless, these data serve to provide a reasonable estimate for the fractionation between shell and water for the environmental conditions in which these species thrive. In making these determinations, Macdonald (2012) calculated an average growth temperature using the aragonite-water paleothermometer from Böhm *et al.* (1996), and assumed a modern $\delta^{18}\text{O} = -7.4\text{‰}$ for Lake Huron (Macdonald and Longstaffe, 2008). In the application of these values of α to ancient samples from the Huron Basin, it is assumed that the same species grew over

the same temperature range as the modern species, and that there were no oxygen isotope vital effects for the ancient specimens that differed from those (if any) affecting the modern equivalents.

3.2.8 Water $\delta^{18}\text{O}$

The $\delta^{18}\text{O}$ of biogenic carbonates may be used to infer the $\delta^{18}\text{O}$ of a body of water if the following assumptions are met: (Faure and Mensing, 2005; Sharp, 2007):

- 1) The water body has historically maintained a consistent isotopic composition over the time being studied;
- 2) The oxygen isotopic composition of the water and the biogenic calcium carbonate were in equilibrium at the time of shell formation;
- 3) Isotopic vital effects during shell formation are understood and corrected for; and
- 4) Alteration of the shell has been well-studied and found to have had negligible effects on the shell $\delta^{18}\text{O}$.

When those conditions are met, the α of that species and the determined $\delta^{18}\text{O}$ of the carbonate shell are used to infer the composition of the water body. In this thesis, only the composition of whole shell powdered samples and calculated bulk shell of serial samples are calculated into water $\delta^{18}\text{O}$ where:

$$\alpha = (1000 + \delta^{18}\text{O}_{\text{aragonite}} / 1000 + \delta^{18}\text{O}_{\text{water}}) \quad \text{Equation 3.5}$$

rearranged to:

$$\delta^{18}\text{O}_{\text{water}} = [(1000 + \delta^{18}\text{O}_{\text{aragonite}}) / \alpha] - 1000 \quad \text{Equation 3.6}$$

Chapter 4

4 Results

4.1 *p*XRD Results

The mineralogy of five shells from four species (*H. anceps*, *Pisidium* spp., *V. sincera*, *V. tricarinata*), as determined by *p*XRD was entirely aragonite. A typical *p*XRD pattern is shown in Appendix D.

4.2 Species Identification and Counts by Site

Table 4.1 summarizes the abundances of fossil fauna identified at each site. La Rocque (1974) suggested that fossil shell assemblages should be interpreted based on the relative abundances of each species, rather than absolute abundances in the sample.

Table 4.1 - Relative abundance of fossil fauna identified at each site by species and total number of shells counted (n). The absolute and relative abundances of each genera / species are listed in Appendix E.

Depositional Environment	Time Period (Phase)	site	<i>Amnicola limosa</i>	<i>Ferrissia</i> sp.	<i>Gyraulus parvus</i>	<i>Helisoma anceps</i>	<i>Lymnea</i> spp.	<i>Physella gyrina</i>	<i>Pisidium</i> spp.	<i>Sphaeriidae</i> spp.	<i>Pleurocera livescens</i>	<i>Stagnicola catascopium</i>	<i>Valvata sincera</i>	<i>Valvata tricarinata</i>	Total (n)
Fluvial	Algonquin	K6	-	-	10	-	-	-	50	5	-	-	-	35	20
		13	6	-	-	-	10	-	14	2	-	-	24	43	49
	Transitional	51	-	-	-	5	25	-	18	5	-	-	19	29	84
	Nipissing	52	-	-	-	2	8	< 1	15	47	-	-	15	13	171
		53	5	-	4	2	22	< 1	18	3	< 1	-	30	14	547
Estuarine	Algonquin	K21	-	-	43	4	8	-	15	15	-	-	13	1	67
	Transitional	K10	44	8	13	3	-	2	6	-	-	4	-	21	326

In the current study, each bivalve valve was counted as representing one organism because of the difficulty of species identification within *Pisidium* and *Sphaeriidae* and inability of determining whether or not two valves were from the same mollusc. Although it is possible

that two of the valves may have been from the same organism, there is no way to ascertain this.

Fluvial sites have the greatest relative abundances of bivalves and *Valvata* spp. ranging from 65 % at site 53 to 90 % at sites 52 and K6. The Algonquin phase estuarine site (K21) contains the largest percentage of *G. parvus* (43 %), and contains fewer bivalves and *Valvata* spp. (44 %) than the fluvial sites. The Transitional estuarine site (K10) contains the largest percentage of *A. limosa* (44 %) and the second largest percentage of *G. parvus* (13 %). It also contains the smallest percentage of bivalves and *Valvata* spp. (27 %).

4.3 Stable Carbon and Oxygen Isotope Results

The 269 individual shells analysed in this study display a very wide range of $\delta^{18}\text{O}$ (+14.6 to +26.6 ‰) and $\delta^{13}\text{C}$ (-10.6 to +5.0 ‰) (Fig. 4.1). A complete list of isotopic results is provided in Appendix F. To better understand this variation, the data were subdivided by time period (Algonquin, Transitional, Nipissing) and by depositional environments (fluvial, lacustrine, and estuarine)

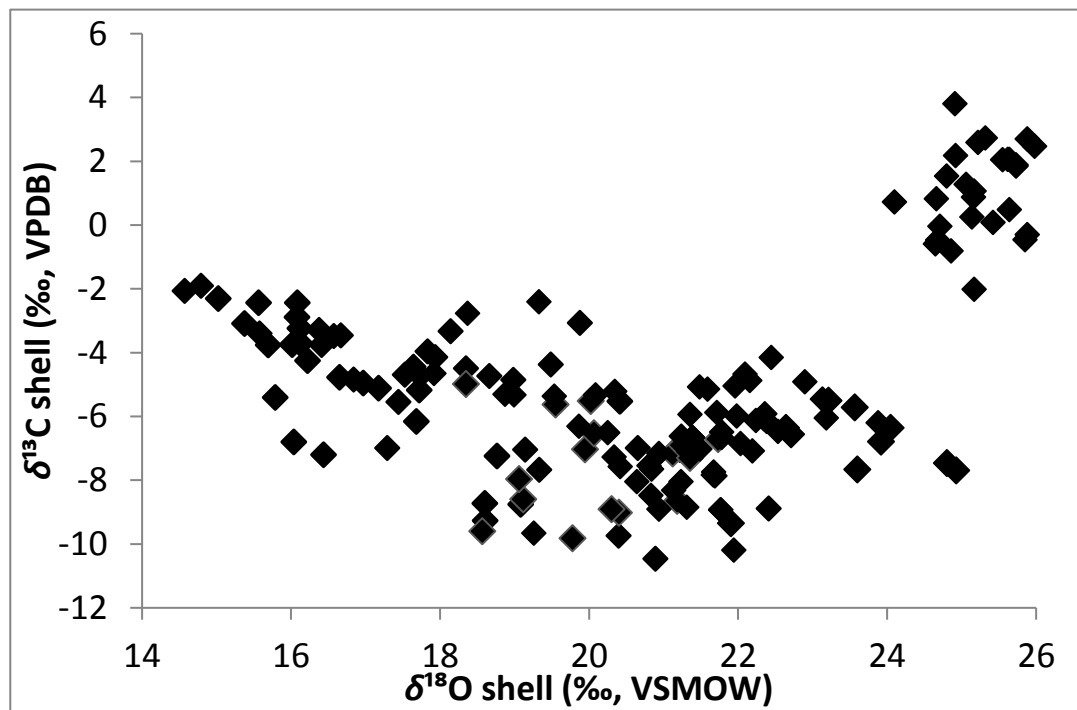


Figure 4.1 - All shell carbon and oxygen isotopic results produced in this project for southern Ontario.

4.3.1 Algonquin Phase

4.3.1.1 Fluvial sites 13 and K6

A total of 28 shells were analysed from the two Algonquin fluvial sites (13 and K6). The $\delta^{18}\text{O}$ range was 4.0‰, and $\delta^{13}\text{C}$ range was 7.4 ‰ (Fig. 4.2a,b; Appendix F). At site 13, three species were analyzed, *A. limosa*, *V. sincera*, and *V. tricarinata*, with a $\delta^{18}\text{O}$ range of +18.3 to +21.7 ‰ (avg +20.1 ‰; SD 1.0 ‰, n = 16) and $\delta^{13}\text{C}$ range of -9.8 to -5.0 ‰ (avg -7.5 ‰; SD 1.5 ‰) (Fig. 4.3). The $\delta^{13}\text{C}$ and $\delta^{18}\text{O}$ of *V. sincera* at this site show an inverse covariation (R^2 0.559; n = 10).

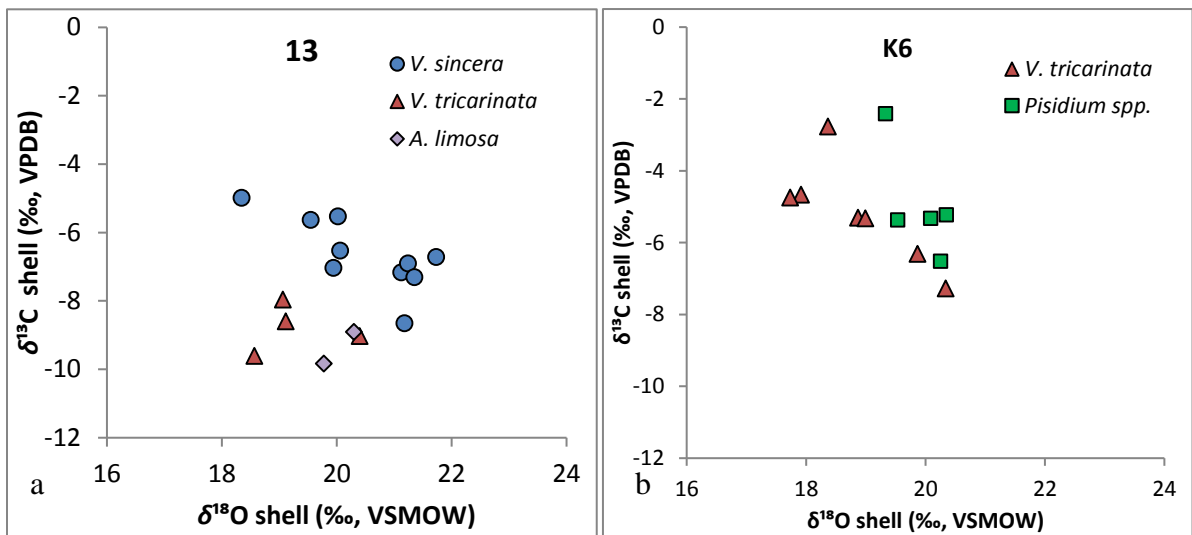


Figure 4.2 - Isotopic composition of fluvial Algonquin site shells by species at (a) site 13, and (b) site K6.

At site K6 (Figs. 4.2b, 4.3), two groups were analyzed, *Pisidium* spp., and *V. tricarinata*, with a $\delta^{18}\text{O}$ range from +17.7 to +20.3 ‰ (avg +19.3 ‰; SD 0.9 ‰, n = 12) and a $\delta^{13}\text{C}$ range from -7.3 to -2.4 ‰ (avg -5.1 ‰; SD 1.4 ‰). The $\delta^{13}\text{C}$ and $\delta^{18}\text{O}$ of *V. tricarinata* at this site show an inverse covariation (R^2 0.614; n = 7).

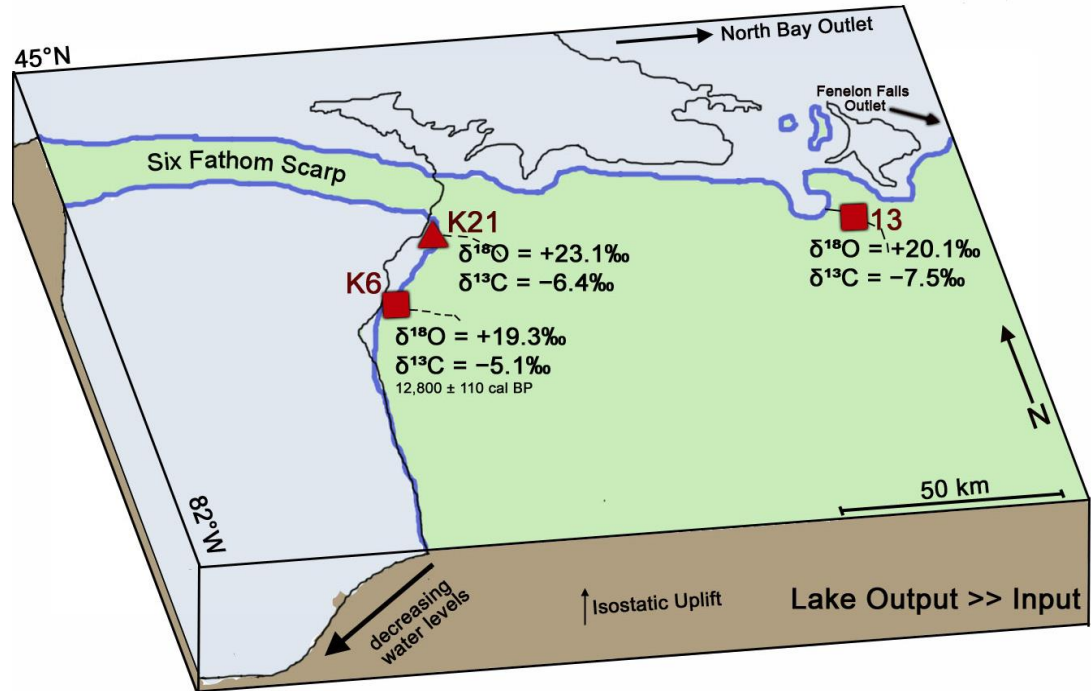


Figure 4.3 - Algonquin sites and their average shell $\delta^{18}\text{O}$ and shell $\delta^{13}\text{C}$. Light blue – Lake Algonquin water. Black lines – modern lake boundary.

4.3.1.2 Estuarine Site K21

A total of 11 shells were analysed at site K21 and have a $\delta^{18}\text{O}$ range of 4.5 ‰ (avg +23.1 ‰, SD 1.1 ‰), and a $\delta^{13}\text{C}$ range of 4.4 ‰ (avg -6.4 ‰, SD 0.8 ‰) (Figs. 4.3, 4.4a,b: Appendix F). Two species were analysed: *Pisidium* spp. and *V. sincera*. All *V. sincera* shells were bulk sampled, whereas the three *Pisidium* spp. shells were also serial-sampled, from which a weighted mean isotopic composition was also calculated. *V. sincera* range in $\delta^{18}\text{O}$ from +21.4 to +24.9 ‰ (avg +23.5 ‰; SD 1.3 ‰; n = 8), and in $\delta^{13}\text{C}$ from -9.9 to -5.5 ‰ (avg -7.2 ‰; SD 1.1 ‰; n = 8). *Pisidium* spp. range in $\delta^{18}\text{O}$ from +21.2 to +25.7 ‰ (avg +23.0 ‰; SD 1.1 ‰, n = 35), and in $\delta^{13}\text{C}$ from -7.0 to -4.9 ‰ (avg -6.2 ‰; SD 0.6 ‰).

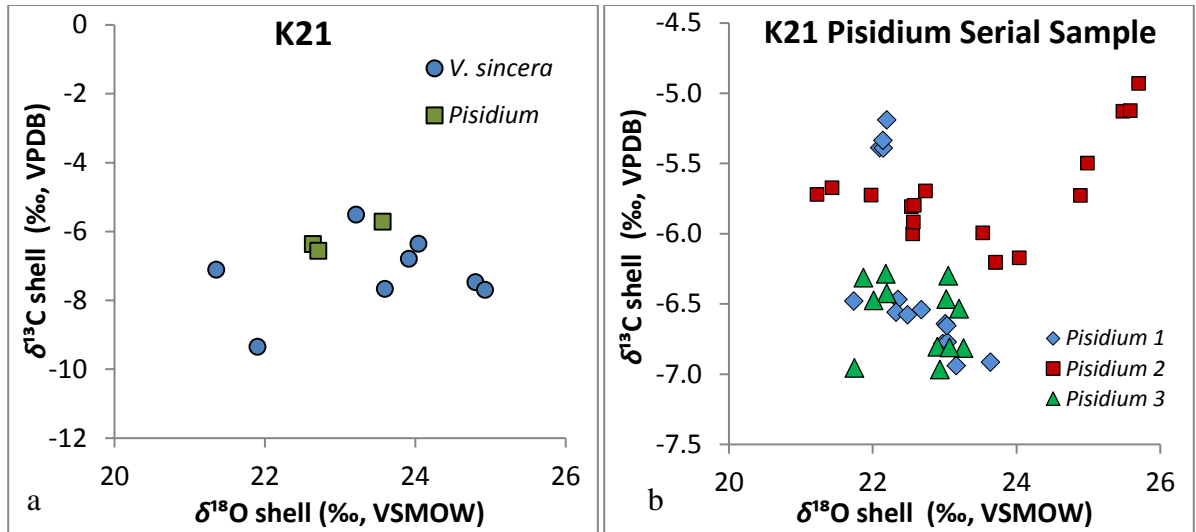


Figure 4.4 - (a) Bulk isotopic results for Algonquin estuarine site K21 shells by species. (b) Isotopic results for serial sampling of three *Pisidium* spp. shells. All results and schematics are provided in Appendix G.

Three *Pisidium* spp. shells were serial sampled for a total of 35 sub-samples (Fig. 4.4b). Shell 1 was sampled twelve times and ranges in $\delta^{18}\text{O}$ from +22.1 to +23.6 ‰ (calculated bulk +22.3 ‰), and in $\delta^{13}\text{C}$ from -6.9 to -5.2 ‰ (calculated bulk -6.6 ‰). Shell 2 was sampled 14 times ($\delta^{18}\text{O}$ ranges from +21.2 to +25.7 ‰, calculated bulk +23.6 ‰; $\delta^{13}\text{C}$ ranges from -6.2 to -4.9 ‰, calculated bulk -5.7 ‰). Shell 3 was sampled nine times ($\delta^{18}\text{O}$ ranges from +21.9 to +23.2 ‰, calculated bulk +22.7 ‰; $\delta^{13}\text{C}$ ranges from -7.0 to -6.3 ‰, calculated bulk -6.6 ‰).

4.3.2 Transitional Phase

4.3.2.1.1 Fluvial Site 51

A total of 24 shells from three species, *Pisidium* spp., *V. sincera*, and *V. tricarinata*, were analysed at site 51 and show a range in $\delta^{18}\text{O}$ of 6.2 ‰, averaging +17.1 ‰ (SD 1.6 ‰), and a range of $\delta^{13}\text{C}$ of 7.0 ‰, averaging -5.2 ‰ (SD 2.1 ‰) (Fig. 4.5a,b: Appendix F).

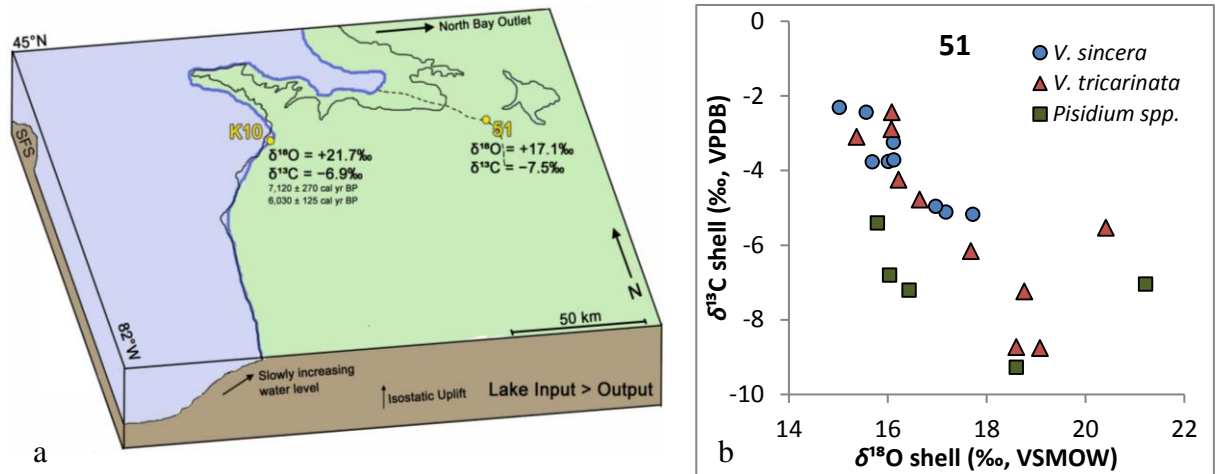


Figure 4.5 - (a) Transitional sites and their average shell $\delta^{18}\text{O}$ and $\delta^{13}\text{C}$. Light blue – Transitional phase lake water. Black lines – modern lake boundary. (b) Isotopic results for site 51 shells by species.

The five *Pisidium* spp. range in $\delta^{18}\text{O}$ from +15.8 to +21.2 ‰ (avg +17.6 ‰, SD 2.3 ‰), and in $\delta^{13}\text{C}$ from -9.3 to -5.4 ‰ (avg -7.1 ‰, SD = 1.4 ‰). The nine *V. sincera* shells have $\delta^{18}\text{O}$ ranging from +15.0 to +17.7 ‰ (avg +16.3 ‰; SD 0.9 ‰), and $\delta^{13}\text{C}$ ranging from -9.9 to -5.5 ‰ (avg -7.2 ‰; SD 1.1 ‰). The $\delta^{13}\text{C}$ and $\delta^{18}\text{O}$ of *V. sincera* at this site show an inverse covariation ($R^2 = 0.873$; $n = 9$). The ten *V. tricarinata* have $\delta^{18}\text{O}$ ranging from +15.4 to +20.4 ‰ (avg +17.5 ‰, SD 1.7 ‰), and $\delta^{13}\text{C}$ ranging from -8.8 to -2.4 ‰ (avg -5.4 ‰, SD 2.3 ‰). The $\delta^{13}\text{C}$ and $\delta^{18}\text{O}$ of *V. tricarinata* at this site show an inverse covariation ($R^2 = 0.585$; $n = 10$)

4.3.2.1.2 Estuarine Site K10

A total of 44 shells from three species, *A. limosa*, *Pisidium* spp., and *V. tricarinata*, were analysed from site K10 and show a $\delta^{18}\text{O}$ range of 4.6 ‰ and average +21.7 ‰ (SD 0.8 ‰); $\delta^{13}\text{C}$ shows a range of 6.0 ‰, and averages -6.9 ‰ (SD 1.4 ‰) (Figs. 4.5a, 4.6; Appendix F).

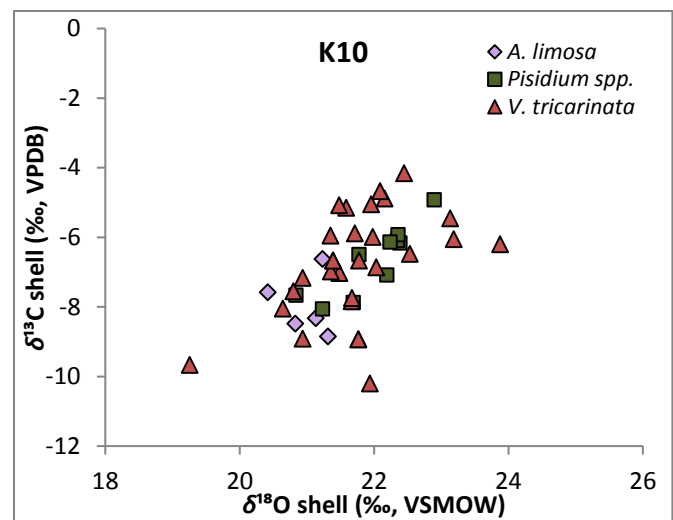


Figure 4.6 - Isotopic results for site K10 shells by species.

The five *A. limosa* shells range in $\delta^{18}\text{O}$ from +20.4 to +21.3 ‰ (avg +21.0 ‰, SD 0.4 ‰), and in $\delta^{13}\text{C}$ from -8.8 to -6.6 ‰ (avg -8.0 ‰, SD 0.9 ‰). The ten *Pisidium* spp. shells range in $\delta^{18}\text{O}$ from +20.8 to +22.9 ‰ (avg +22.0 ‰, SD 0.6 ‰), and in $\delta^{13}\text{C}$ from -8.1 to -4.9 ‰ (avg -6.6 ‰, SD 1.0 ‰). The $\delta^{13}\text{C}$ and $\delta^{18}\text{O}$ of *Pisidium* spp. at this site show a positive covariation (R^2 0.764; n = 10). The twenty-nine *V. tricarinata* range in $\delta^{18}\text{O}$ from +19.3 to +23.9 ‰ (avg +21.8 ‰, SD 0.9 ‰), and in $\delta^{13}\text{C}$ from -9.7 to -4.2 ‰ (avg -6.7 ‰, SD 1.5 ‰). The $\delta^{13}\text{C}$ and $\delta^{18}\text{O}$ of *V. tricarinata* at this site show a positive covariation (R^2 0.237; n = 29).

4.3.3 Nipissing Phase

4.3.3.1 Fluvial Site 52

A total of 32 shells were analysed from site 52 and have a $\delta^{18}\text{O}$ range of 8.9 ‰ (avg +19.1 ‰), and $\delta^{13}\text{C}$ range of 7.7 ‰ (avg -5.9 ‰) (Fig. 4.7a). Three species were analysed, *Pisidium* spp., *V. sincera* and *V. tricarinata*. One *Pisidium* sp. shells was also serial-sampled (Fig. 4.7b; Appendix F).

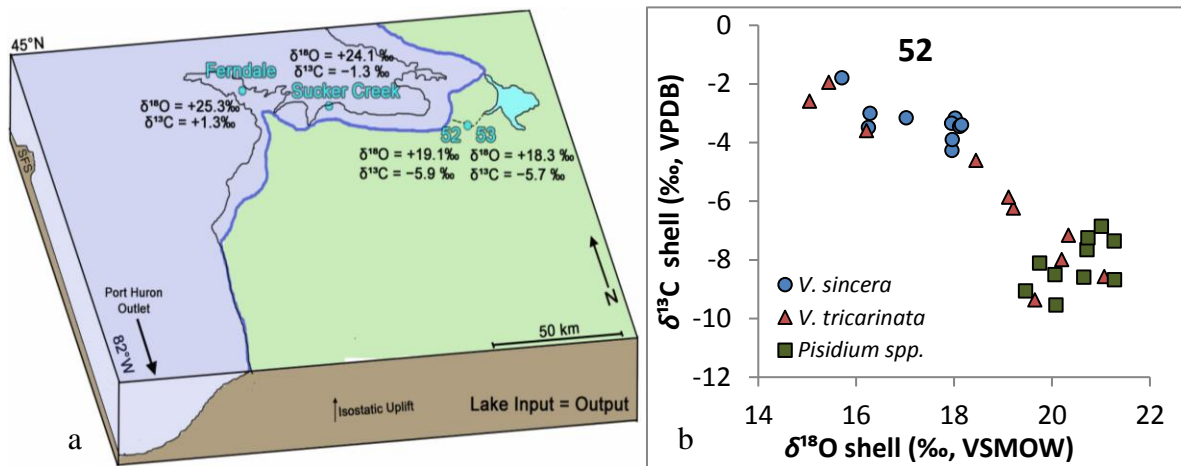


Figure 4.7 - (a) Nipissing sites and their average shell $\delta^{18}\text{O}$ and $\delta^{13}\text{C}$. Light blue – Lake Nipissing water. Black lines – modern lake boundary. (b) Isotopic results for Nipissing phase fluvial site 52 by fauna analysed.

The twelve *V. sincera* range in $\delta^{18}\text{O}$ from +15.7 to +24.0 ‰ (avg +18.4 ‰; SD 2.6 ‰), and in $\delta^{13}\text{C}$ from -8.1 to -1.8 ‰ (avg -4.1 ‰; SD 1.9 ‰). The $\delta^{13}\text{C}$ and $\delta^{18}\text{O}$ of *V. sincera* at this site show an inverse covariation (R^2 0.930; n = 12). The ten *V. tricarinata* range in $\delta^{18}\text{O}$

from +15.0 to +21.1 ‰ (avg +18.5 ‰, SD 2.1 ‰), and in $\delta^{13}\text{C}$ from -9.4 to -2.0 ‰ (avg -5.8 ‰, SD 2.6 ‰). The $\delta^{13}\text{C}$ and $\delta^{18}\text{O}$ of *V. tricarinata* at this site show an inverse covariation (R^2 0.859; $n = 10$). The ten *Pisidium* spp. have a $\delta^{18}\text{O}$ range of +19.5 to +21.3 ‰ (avg +20.4 ‰; SD 0.6 ‰), and $\delta^{13}\text{C}$ range of -9.5 to -7.4 ‰ (avg -8.6 ‰; SD 0.9 ‰). The $\delta^{13}\text{C}$ and $\delta^{18}\text{O}$ of *Pisidium* spp. at this site show a weak positive covariation (R^2 0.320; $n = 10$).

Bulk *Pisidium* sp. shell $\delta^{18}\text{O}$ and $\delta^{13}\text{C}$ are +21.3 ‰ and -7.4 ‰, respectively. The serial sample $\delta^{18}\text{O}$ ranges from +20.7 to +21.0 ‰ (avg +20.8 ‰, SD 0.2 ‰), and the $\delta^{13}\text{C}$ from -7.7 to -6.9 ‰ (avg -7.3 ‰, SD 0.4 ‰) (Fig. 4.8).

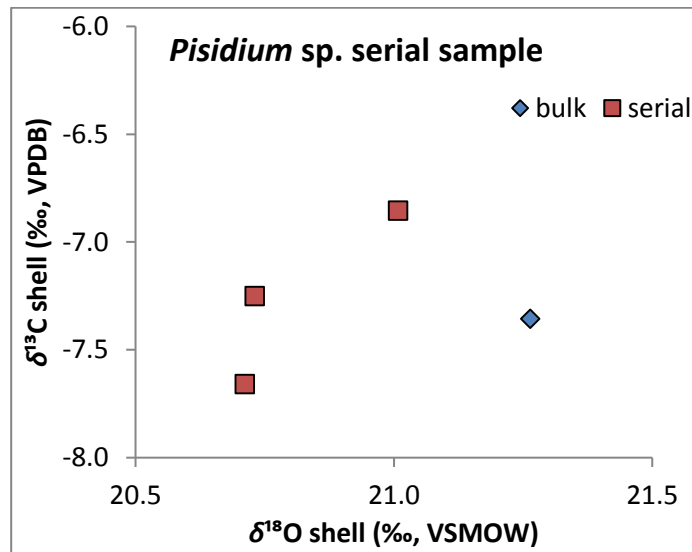


Figure 4.8 - Isotopic results for one serial-sampled *Pisidium* sp. shell from site 52. All results and schematic are [provided in Appendix G.

4.3.3.2 Fluvial Site 53

A total of 53 shells were analysed from site 53, and have a range of $\delta^{18}\text{O}$ of 7.8 ‰ (avg +18.3 ‰), and $\delta^{13}\text{C}$ of 8.7 ‰ (avg -5.7 ‰) (Fig. 4.7; Appendix F). Three species were analysed: *Pisidium* spp., *V. sincera* and *V. tricarinata*. Most shells were bulk sampled but five *Pisidium* spp. shells were serial-sampled (Fig 4.9ab). The weighted isotopic average was calculated for the four *Pisidium* spp. shells for which no bulk analysis could be obtained.

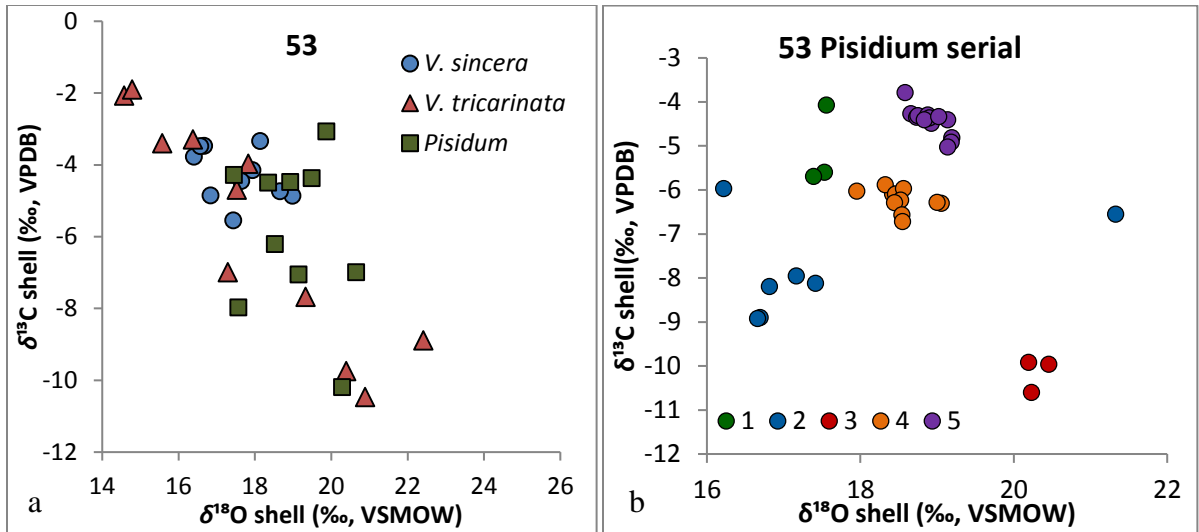


Figure 4.9 - (a) Isotopic results for Nipissing phase fluvial site 53 by fauna analysed. (b) Isotopic results for serial-sampled *Pisidium* spp. shell from site 53. Numbers refer to individual shells analysed. All results and schematics are provided in Appendix G.

The ten *V. sincera* range in $\delta^{18}\text{O}$ from +14.6 to +19.0 ‰ (avg +17.5 ‰; SD 1.1 ‰), and $\delta^{13}\text{C}$ from -5.5 to -3.3 ‰ (avg -4.3 ‰; SD 0.7 ‰). The eleven *V. tricarinata* range in $\delta^{18}\text{O}$ from +14.6 to +22.4 ‰ (avg +17.9 ‰, SD 2.6 ‰), and in $\delta^{13}\text{C}$ from -10.5 to -1.9 ‰ (avg -5.7 ‰, SD 3.1 ‰). The $\delta^{13}\text{C}$ and $\delta^{18}\text{O}$ of *V. tricarinata* at this site show an inverse covariation (R^2 0.848; $n = 11$). The six bulk *Pisidium* spp. have a $\delta^{18}\text{O}$ range of +17.5 to +20.7 ‰ (avg +19.2 ‰; SD = 1.1 ‰), and a $\delta^{13}\text{C}$ range of -7.0 to -3.1 ‰ (avg -5.0 ‰; SD 1.6 ‰).

Five *Pisidium* spp. shells were also serial-sampled for a total of 37 results (Fig. 4.9b: Appendix F). Shell 1 was sampled three times on one half of the shell with a $\delta^{18}\text{O}$ range from +17.4 to +17.6 ‰ (SD 0.1 ‰), and $\delta^{13}\text{C}$ from -5.7 to -4.1 ‰ (SD 0.9 ‰). The other half was bulk sampled with a $\delta^{18}\text{O}$ of +17.5 ‰, and $\delta^{13}\text{C}$ of -4.3‰. Shell 2 was sampled seven times, with a $\delta^{18}\text{O}$ range from +16.2 to +21.3 ‰ (SD 1.7 ‰; calculated bulk +17.6 ‰) and a $\delta^{13}\text{C}$ range from -8.9 to -6.0 ‰ (SD 1.1 ‰; calculated bulk -8.0 ‰). Shell 3 was sampled three times with a $\delta^{18}\text{O}$ range from +20.2 to +20.5 ‰ (SD 0.1 ‰; calculated bulk +20.3 ‰) and $\delta^{13}\text{C}$ range from -10.6 to -9.9 ‰ (SD 0.4 ‰; calculated bulk -10.2 ‰). Shell 4 was sampled eleven times with a $\delta^{18}\text{O}$ range from +18.0 to +19.1 ‰ (SD 0.3 ‰; calculated bulk +18.5 ‰) and $\delta^{13}\text{C}$ range from -6.7 to -5.9 ‰ (SD 0.4 ‰; calculated bulk -6.2 ‰). Shell 5 was sampled thirteen times with $\delta^{18}\text{O}$ range from +18.6 to +19.2 ‰ (SD

0.2 ‰; calculated bulk +18.9 ‰) and $\delta^{13}\text{C}$ range from -5.0 to -3.8 ‰ (SD 0.2 ‰; calculated bulk -4.5 ‰).

4.3.3.3 Ferndale and Sucker Creek - Lacustrine

A total of 34 shells were analysed from the Nipissing phase lacustrine sites at Ferndale and Sucker Creek (Figs. 4.7, 4.10; Appendix F). Three species were analysed, *Pisidium* spp., *V. sincera* and *V. tricarinata*. Together, they vary in $\delta^{18}\text{O}$ and $\delta^{13}\text{C}$ by 2.6 ‰ and 7.0 ‰, respectively.

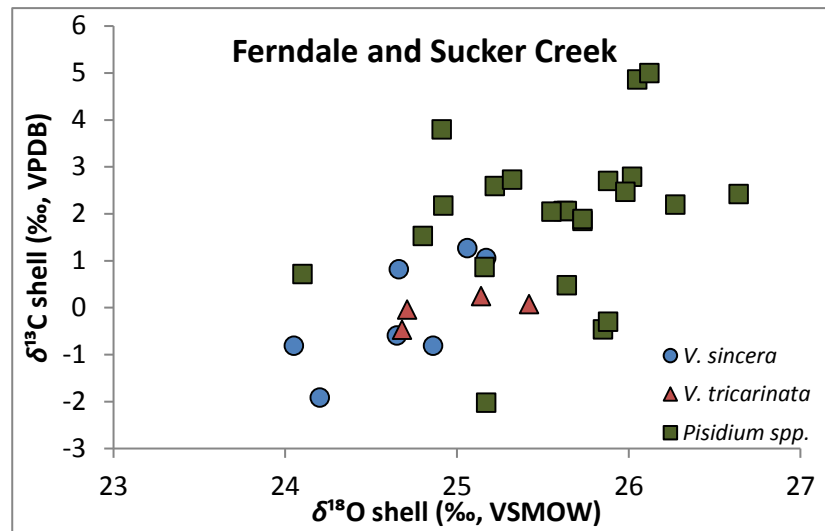


Figure 4.10 - Isotopic results for shells from Nipissing phase lacustrine sites at Ferndale and Sucker Creek.

4.3.3.3.1 Ferndale

The five *V. sincera* range in $\delta^{18}\text{O}$ from $+24.7$ to $+25.2$ ‰ (avg $+24.9$ ‰; SD 0.2 ‰), and in $\delta^{13}\text{C}$ from -0.8 to $+1.3$ ‰ (avg $+0.4$ ‰; SD 1.0 ‰). The four *V. tricarinata* range in $\delta^{18}\text{O}$ from $+24.7$ to $+25.4$ ‰ (avg $+25.0$ ‰, SD 0.4 ‰), and in $\delta^{13}\text{C}$ from -0.5 to $+0.3$ ‰ (avg 0.0 ‰, SD 0.3 ‰). The twenty-three *Pisidium* spp. range in $\delta^{18}\text{O}$ from $+24.1$ to $+26.6$ ‰ (avg $+25.6$ ‰; SD 0.6 ‰), and range in $\delta^{13}\text{C}$ from -2.0 to $+5.0$ ‰ (avg $+1.9$ ‰; SD 1.6 ‰).

4.3.3.3.2 Sucker Creek

The two *V. sincera* shells analysed have $\delta^{18}\text{O}$ of $+24.2$ and $+24.1$ ‰, respectively, and $\delta^{13}\text{C}$ of -1.9 and -0.8 ‰, respectively.

4.4 Consideration of Small Sample Sets ($n \leq 5$)

At several sites, some species were not abundant enough to complete six or more bulk samples. Jones *et al.* (2002) caution that at least six shells should be analysed to approximate the true isotopic variability of an environment. Several sites did not contain the required abundances of individual species. These smaller data sets are not used in the discussion that follows when testing for $\delta^{13}\text{C}$ - $\delta^{18}\text{O}$ trends. The abundance and ubiquity of the genus *Valvata* allows for the necessary numbers of samples to determine the maximum variability of the system.

Chapter 5

5 Discussion

5.1 Vital Effects

The variability of $\delta^{18}\text{O}$ and $\delta^{13}\text{C}$ within single *Pisidium* shells was investigated at sites K21, 52 and 53 to test for vital effects, in addition to understanding variability within and among biological communities. The nine *Pisidium* spp. shells show no systematic enrichment or depletion of ^{13}C or ^{18}O in successive layers of each shell (Fig. 5.1) or along a given layer of shell (Appendix G).

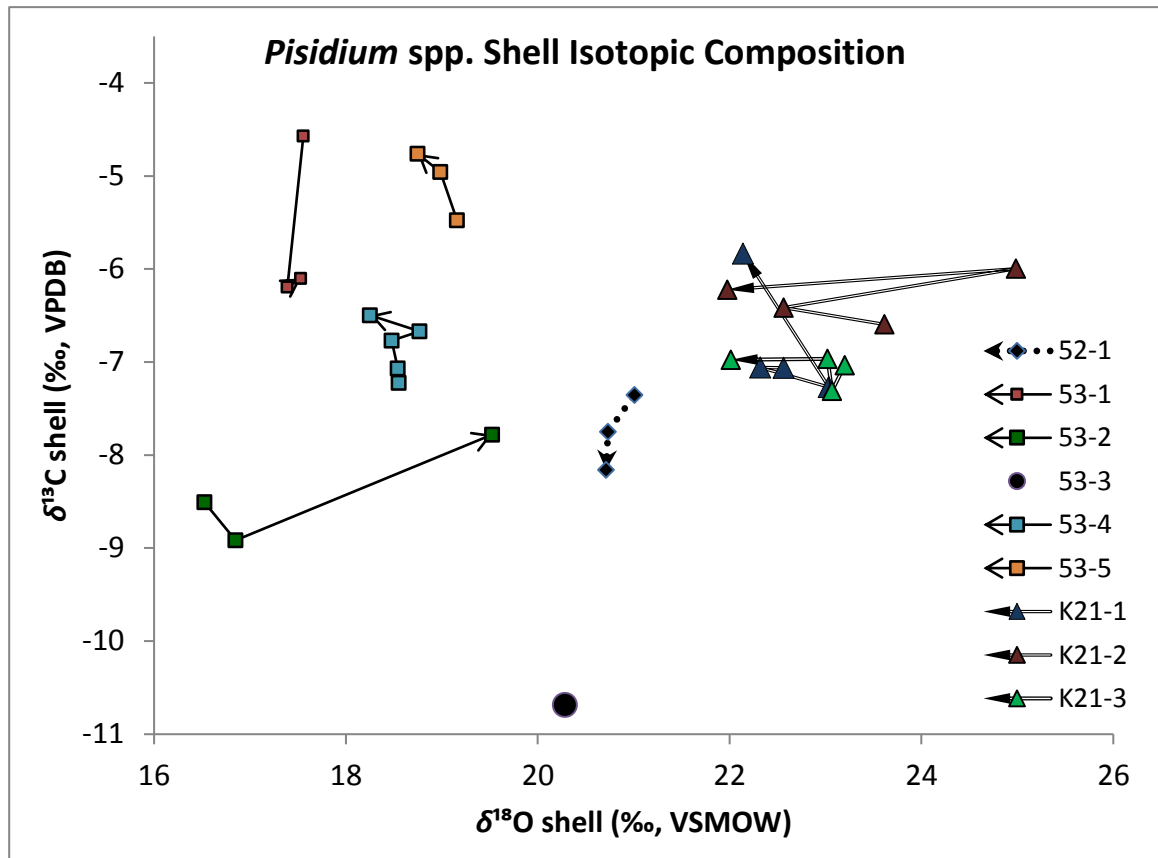


Figure 5.1 - Carbon vs. oxygen isotope compositions of *Pisidium* spp. by calculated weighted mean of successive growth layers. Arrows denote the younging direction. Full schematics and isotopic results are provided in Appendix G.

Many studies have shown that shell oxygen isotopic composition is rarely influenced by vital effects in small, gill-breathing molluscs (Mook and Vogel, 1968; Fritz and Poplawski, 1974; Carpenter and Lohmann, 1995; Leng *et al.*, 1999; Mitchell *et al.*, 1994; Lécuyer *et al.*, 2012; Prendergast and Stevens, 2015). Fritz and Poplawski (1974) reported that *Pisidium* spp. from

southern Ontario precipitated their shells in oxygen isotope equilibrium with ambient water, which is the same conclusion suggested for this thesis.

Figure 5.1 shows that there is no systematic enrichment or depletion of ^{13}C in successive younger layers. This indicates that isotopic disequilibrium did not occur due to this genus incorporating metabolic DIC in their shell growth, or displaying kinetic fractionation due to fast growth of the shell. Determining the age of the *Pisidium* spp. shell was not possible other than recognizing it had reached adulthood. Regardless of the lifespan of the shell, only one shell, 52-1, showed a decreasing $\delta^{13}\text{C}$ with each outward younger layer, allowing us to rule out kinetic fractionation as a general condition by this species.

Keith and Weber (1964) found that bulk shell samples best reflected within-species and within-community differences. The successive younger layer isotopic variations observed in this study are most likely a consequence of local environmental changes during the time of shell growth. Therefore, we have used the calculated bulk isotopic compositions for serial-sampled shells to compare with other bulk shell analyses.

5.2 Indicator Species

Radiocarbon dates were not available for all sites; therefore dating of the locations was completed by combining geological markers with biological markers. Miller *et al.* 1979, 1985 determined that certain species migrated to southern Ontario only after habitable conditions were established. The presence of *P. livescens* at site 53 restricts the age of this site to the Nipissing phase [7.4 to 3.2 ^{14}C ka (8.2 to 3.4 ka cal) BP] (Table 5.1; Goodrich, 1945; Miller *et al.*, 1985; Macdonald and Longstaffe, 2008). Site 52 is situated at a lower elevation (191 masl) than site 53 (195 masl), consistent with fluvial down-cutting into isostatically rebounding crust. In other words, more recently deposited sediment should sit at a lower elevation than later sediments in this setting. The presence of a large unidentified species of *Unionid* clam shell at site 52 can also be used to restrict it to the Nipissing phase (Miller *et al.*, 1985).

Table 5.1 - Relative abundance of species found at each site other than ubiquitous *Valvata* spp. and *Pisidium* spp. and total number of shells counted (n). Sites 52/53 have been considered together because they both represent the same environment and lake phase. I = Nipissing Indicator species. Appendix E lists the species counts and relative abundances for all species.

Depositional Environment	Lake Phase	site	Relative Abundance (%)									Total (n)
			Warm Water					<i>P. gyrina</i>	<i>Ferrissia</i> spp.	<i>S. catascopium</i>	I <i>P. livescens</i>	
			<i>A. limosa</i>	<i>H. anceps</i>	<i>Lymnea</i> spp.	<i>G. parvus</i>	<i>Sphaeriidae</i> spp.					
Fluvial	Algonquin	K6	-	-	-	10	5	-	-	-	-	3
		13	6	-	10	-	2	-	-	-	-	9
	Transitional	51	-	5	25	-	5	-	-	-	-	29
	Nipissing	52/53	4	2	19	3	13	<1	-	-	<1	284
Estuarine	Algonquin	K21	-	4	8	43	15	-	-	-	-	47
	Transitional	K10	44	3	-	13	-	2	8	4	-	240

Magnuson *et al.* (1997) noted that in southeastern Canada, more intense evaporative regimes associated with a warming climate should lead to a general shift in species assemblages favouring more eutrophic conditions. The presence of *H. anceps* is an indicator of eutrophication (van der Schalie and Berry, 1973). Because of its low relative abundance, it can be surmised that conditions examined in the present study were generally not eutrophic. Furthermore, the presence of *Lymnea* spp. is an indicator of relatively oligotrophic waters. Rivers with faster flowing waters receive less cumulative solar radiation, and so generally are cooler than rivers with slower flow rates. The higher abundance of *Lymnea* spp. species during Transitional and Nipissing times compared to Algonquin times may indicate a change in fluvial environments from comparably slower, warmer, and more evaporated to faster, cooler, and less evaporated river systems indicated by the presence of larger grain size of the sandy sediments (Appendix B).

Sediments from Algonquin fluvial site 13 are well-sorted fine-grained sands with planar and rippled laminations (Appendix B), indicating a relatively faster flow than at Algonquin fluvial site K6, which is composed of light brownish-grey silty-clay (Appendix B). The lower abundance of shells at both sites could indicate a shorter depositional time frame relative to the other sites studied. Given the finer grained nature of the sediments at K6 and 13 relative

to the other fluvial sites, however, they may still represent the same length of depositional time. Alternatively, the lower relative abundance of shells may be indicative of reduced productivity or poor preservation of carbonates. We also note that the volume of grab samples at sites 13 and K6 was smaller than for other sites, which may make these samples less representative.

Estuarine sites K21 (Algonquin) and K10 (Transitional) have the highest abundance of the eutrophic water indicator species *G. parvus* and *A. limosa* (Clarke, 1981). *G. parvus* is generally considered to be more associated with water affected by greater amounts of evaporation (Clarke, 1981; Mackie, 2007). It is found in greatest abundance at site K21, which is known to have existed during arid conditions (Edwards *et al.*, 1996; Magnuson *et al.*, 1997). The change from *G. parvus* at site K21 to *A. limosa* at site K10 may indicate a change to a less evaporative regime. The shift may also represent a change in proximity to the lake shoreline, as *A. limosa* is more common in slow moving rivers (Mackie, 2007). Both sites were composed of fine grained silt with small amounts of OM as unidentified roots, indicating a low energy system close to shore. As the lake levels were very low during the Transitional time, what was once in the muddy gyttja zone (K21), may have moved inland toward the pro-deltaic zone (K10).

5.3 Re-evaluating the $\delta^{18}\text{O}$ of Meteoric Water During the Holocene in Southern Ontario

Interpretation of past environmental conditions using $\delta^{18}\text{O}$ of meteoric water has been used in (Burk and Stuvier, 1981; Edwards and Fritz, 1986, 1996). Those studies required assumptions for average air temperature and the latitude-related gradient in precipitation $\delta^{18}\text{O}$. Here we argue that those assumptions may not have been correct and offer an alternative approach.

Edwards and Fritz (1986) used the oxygen and hydrogen isotopic composition of fossil plant cellulose samples from southern Ontario to obtain a record of the historical moisture regime in various localities. Edwards *et al.* (1996) combined data for fossil wood cellulose, fossil aquatic plants, marl, diatoms, and other siliceous microfossils to determine relative changes in annual air temperature, $\delta^{18}\text{O}$ of meteoric water, and relative humidity from six sites in southern Ontario (Fig. 5.2). These two studies, however, have multiple limitations.

While many studies have sought a universally applicable quantitative relationship between the mean annual temperature and humidity with bulk terrestrial plant cellulose (e.g. Burk and Stuiver, 1981) to infer $\delta^{18}\text{O}$ of precipitation, none as yet has been discovered. Schubert and Jahren (2015) argue that this relationship may only be ascertained by the new method of micro-isotopic sampling within each tree ring, which enables relative seasonal changes to be observed.

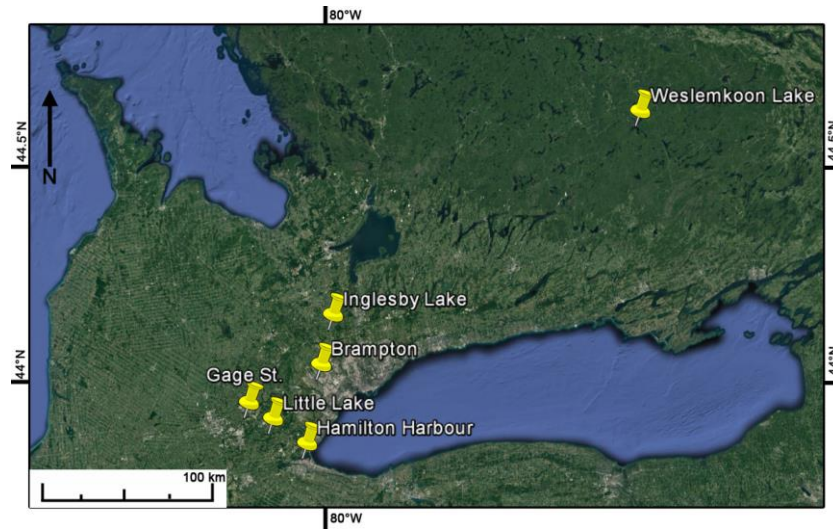


Figure 5.2 - Location of sites studied by Edwards *et al.* (1996) (Google Earth, 2016).

Many studies in southern Ontario agree that there was a warming trend from the Algonquin phase through to the Nipissing, but estimates for the beginning, length, and magnitude of that change vary widely. Entomological evidence suggested that there was a 2 - 3 °C rise in MAT from 11.1 to 9.0 ^{14}C ka (13.0 to 10.2 ka cal) BP (Edwards *et al.*, 1985), whereas Magnuson *et al.* (1997) proposed that the MAT warmed from 10.0 to 8.1 ^{14}C ka (11.5 to 8.9 ka cal) BP.

Studies of fossil pollen, white pine, and hemlock needles estimate that the warming period took place from 9.0 ^{14}C ka (10.2 ka cal) BP (Webb III *et al.*, 1987; Edwards and McAndrews, 1989; Shuman *et al.*, 2002) to 5.0 ^{14}C ka (5.7 ka cal) BP (Edwards and McAndrews, 1989). Edwards *et al.* (1996), however, suggest that warming didn't begin until 6.5 ^{14}C ka (7.5 ka cal) BP. This large variation in timing is likely due to the difference in latitude of locations examined in these studies (Fig. 5.2). Today, for example, average annual temperatures vary by to 3.5 °C when travelling north from Sarnia to Gore Bay, Manitoulin Island (Longstaffe *et al.*, 2013). The length of the modern growing season in present-day Ontario also changes substantially northward (Fig. 5.3a,b). With only a 1 - 2 °C increase, the length of the growing

season on the north shores of Georgian Bay can increase by several weeks (Agriculture and Agri-Food Canada, 2014).

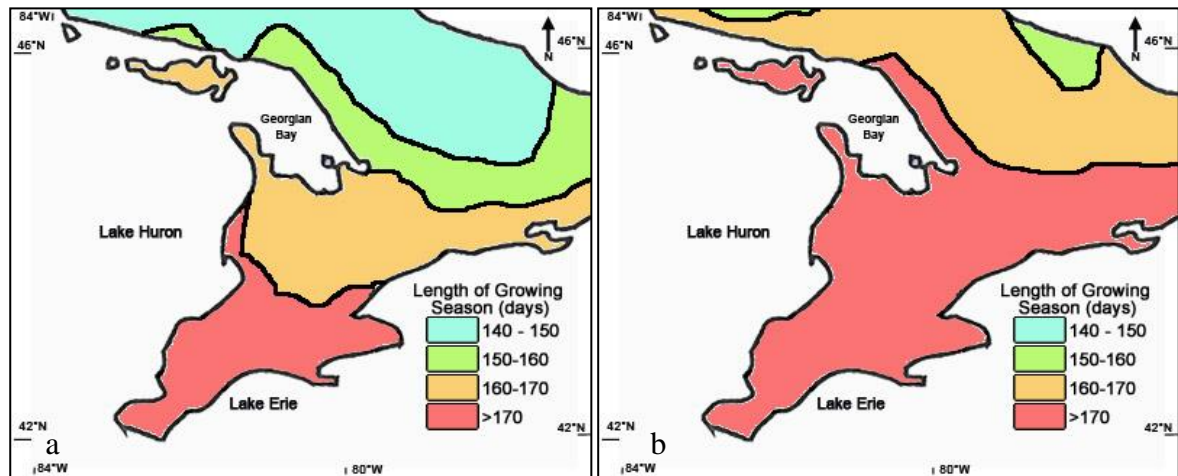


Figure 5.3 - (a) average length of the growing season in Ontario from 1971 - 2000. (b) Estimated growing season length based on a 1 to 2 °C increase in monthly averages from 2010 to 2039 (Agriculture and Agri-Food Canada, 2014).

Precipitation also undergoes a systematic change in $\delta^{18}\text{O}$ in North America for reasons described in section 2.1.2.1 (Fig. 5.4). This corresponds to an average mid- to high-latitude precipitation gradient of 0.65 ‰ / 1 °C. During times of glaciation, however, the initial $\delta^{18}\text{O}$ of tropical air masses travelling northward can be different than during non-glaciated times, affecting the $\delta^{18}\text{O}$ of precipitation at higher latitudes even if there was no change in the $\delta^{18}\text{O}$ / temperature gradient (Fricke and O'Neil, 1999).

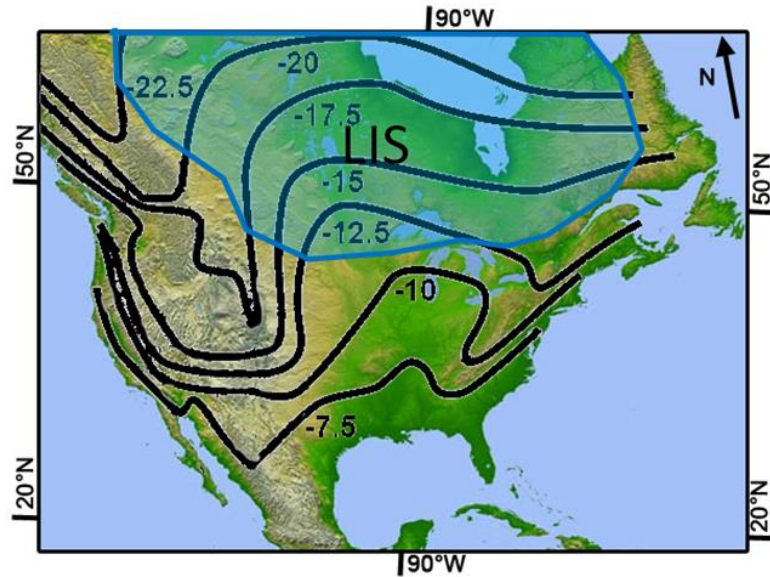


Figure 5.4 – Modern contours of equal $\delta^{18}\text{O}$ for meteoric water (VSMOW) for North America. LIS - Approximate boundary of the Laurentide Ice Sheet at the end of the Main Algonquin phase [10.2 ^{14}C ka (12.1 ka cal) BP] (blue line) after Kohn and Dettman (2007). North American map from Google Earth (2016).

The LIS at the end of the Main Algonquin phase was still present over much of central Canada. This would force the $\delta^{18}\text{O}$ of precipitation to their cold polar values at lower latitudes by shortening the distance between the warm tropics and the boundaries of the ice sheet.

Seasonality also changes the precipitation $\delta^{18}\text{O}$ / temperature gradient; it becomes shallower during summer months, and steepens during winter months (Fricke and O'Neil, 1999). This could skew the average annual $\delta^{18}\text{O}$ of precipitation towards the season having greater amounts of precipitation.

Figure 5.5 shows how a changing $\delta^{18}\text{O}$ / temperature gradient can affect the interpreted mean annual temperature, if a maximum and minimum $\delta^{18}\text{O}$ of precipitation are known. Here we illustrate the present mid- to high-latitude isotopic gradient (0.65 ‰ / 1 °C) and precipitation $\delta^{18}\text{O}$ values from Edwards *et al.* (1996) for southern Ontario during the Holocene ranged from (–16 to –8 ‰), which produces a MAT range of 11 °C, with a maximum inferred temperature of 10 °C. By comparison, a gradient of 2 ‰ / 1 °C produces a MAT range of 4 °C, with a maximum inferred temperature of ~8 °C. A gradient of 0.5 ‰ / 1 °C produces a MAT range of 14 °C, with a maximum inferred temperature of 11 °C.

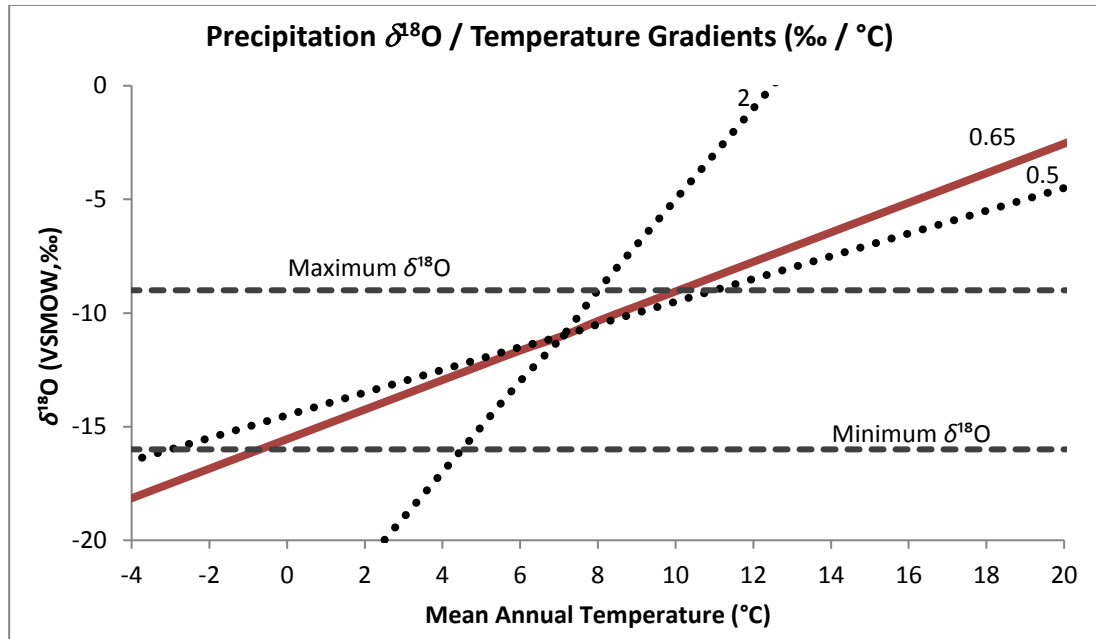


Figure 5.5 - Effect of precipitation $\delta^{18}\text{O}$ / temperature gradient. Red solid line – present mid- to high-latitude isotopic gradient. Dotted lines – other gradients. The intersection point of the example gradients is based on Edwards and Fritz (1986): annual temperature for southern Ontario 7.1 °C and $\delta^{18}\text{O}$ of annual precipitation -11 ‰. Horizontal dashed lines indicate the minimum and maximum precipitation $\delta^{18}\text{O}$ for southern Ontario during the Holocene from Edwards *et al.* (1996).

5.4 Data Sets from Previous (Unpublished) Theses

Interpretation of data collected in the current project can be greatly enhanced by incorporating results reported in two earlier theses that examined this study area or nearby regions (Fig. 5.6; Table 5.2). In 1985, Godwin measured the $\delta^{18}\text{O}$ and $\delta^{13}\text{C}$ of shelly fauna from three sites that represent Algonquin to Transitional fluvial to estuarine environments in southern Ontario. In 2012, Macdonald reported isotopic results for shelly fauna from a lake core situated in the Goderich sub-basin, which record the Algonquin lacustrine environment. She also determined the oxygen isotope shell-water fractionation factors for modern *Amnicola* spp., *Valvata* spp., and *Pisidium* spp. from modern Lake Huron. Results presented in Godwin (1985) for lake water $\delta^{18}\text{O}$ have been recalculated using these fractionation factors.

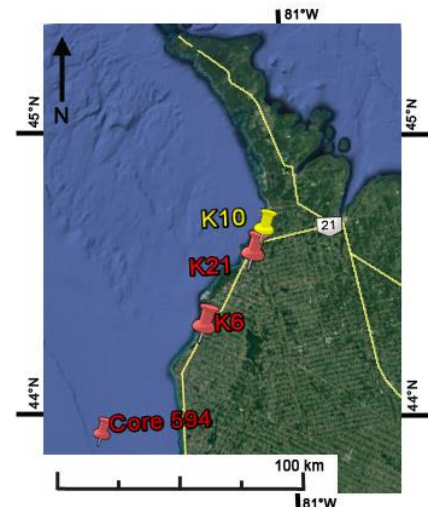


Figure 5.6 - Study areas of Godwin (1985) and Macdonald (2012) (Google Earth, 2016).

Table 5.2 - Summary of isotopic data from Godwin (1985) and Macdonald (2012). All data are provided in Appendices H and I, respectively.

			$\delta^{13}\text{C}$ shell ‰ (VPDB)				Standard Deviation	$\delta^{18}\text{O}$ shell ‰ (VSMOW)			
			Max	Min	Mean	Max		Min	Mean	Standard Deviation	
Macdonald (2012)											
Core 594	Algonquin	Lacustrine	-4.5	-7.5	-5.7	0.8	+27.4	+22.6	+24.8	1.0	
Godwin (1985)											
K6	Algonquin	Fluvial	-4.4	-8.2	-6.8	1.0	+25.8	+19.6	+21.1	1.9	
K21	Algonquin	Estuarine	-3.1	-8.3	-6.4	1.3	+26.6	+19.7	+21.8	1.8	
K10	Transitional	Estuarine	-3.6	-10.5	-7.5	1.7	+25.6	+19.7	+22.8	1.6	

5.5 Water Oxygen Isotope Compositions

Water $\delta^{18}\text{O}$ was calculated for each species using the oxygen isotope shell-water fractionation factors (α) for each analysed species, as described in section 3.2.8. Figure 5.7 suggests that the increasing water oxygen isotopic composition follows geography from upstream river waters, downstream to the estuarine environment, and then into the lake. This trend appears regardless of lake-phase time-period. This indicates that depositional setting may be the stronger control on oxygen isotopic composition than climatic variation. Therefore, comparison of sites will be considered first by depositional environment and then by time.

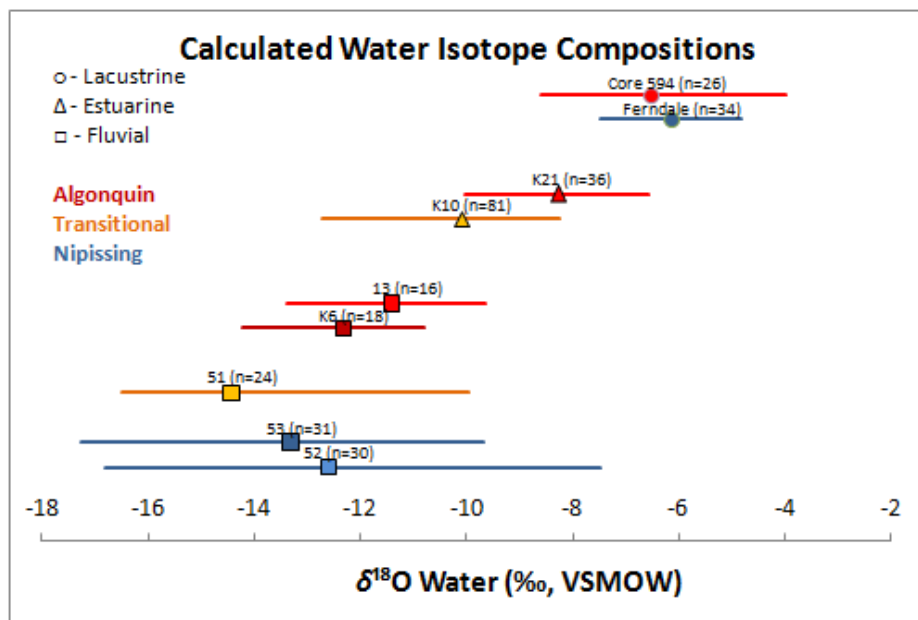


Figure 5.7 - Calculated water $\delta^{18}\text{O}$ for each site using the shell-water oxygen isotope fractionation factors of Macdonald (2012). Shapes indicate the mean water $\delta^{18}\text{O}$. Lines indicate the total range of $\delta^{18}\text{O}$. For

sites 52 and 53, only the weighted mean results for serially-sampled shells are included. Appendix F lists calculated water $\delta^{18}\text{O}$ for each sample.

5.6 Depositional Environments

Calculated water $\delta^{18}\text{O}$ and shell $\delta^{13}\text{C}$ are used in the discussions that follow. All data was categorised by depositional environment and age, as illustrated in Figure 5.8. In subsequent sections, ellipses and associated statistical treatments are then used to identify overlap of data from different settings, which can be inferred to reflect an overlap of environmental conditions. The ellipses used enclose 60 % of all data. A Kruskal-Wallis test, which is a non-parametric ANOVA reported as p values, was completed to elucidate significant differences between univariate data set averages when $p < 0.05$ (Zar, 1996). This test was chosen over a one-way ANOVA because the variances differed between datasets. Statistical analyses were completed using the PAST software (Ryan *et al.*, 1995).

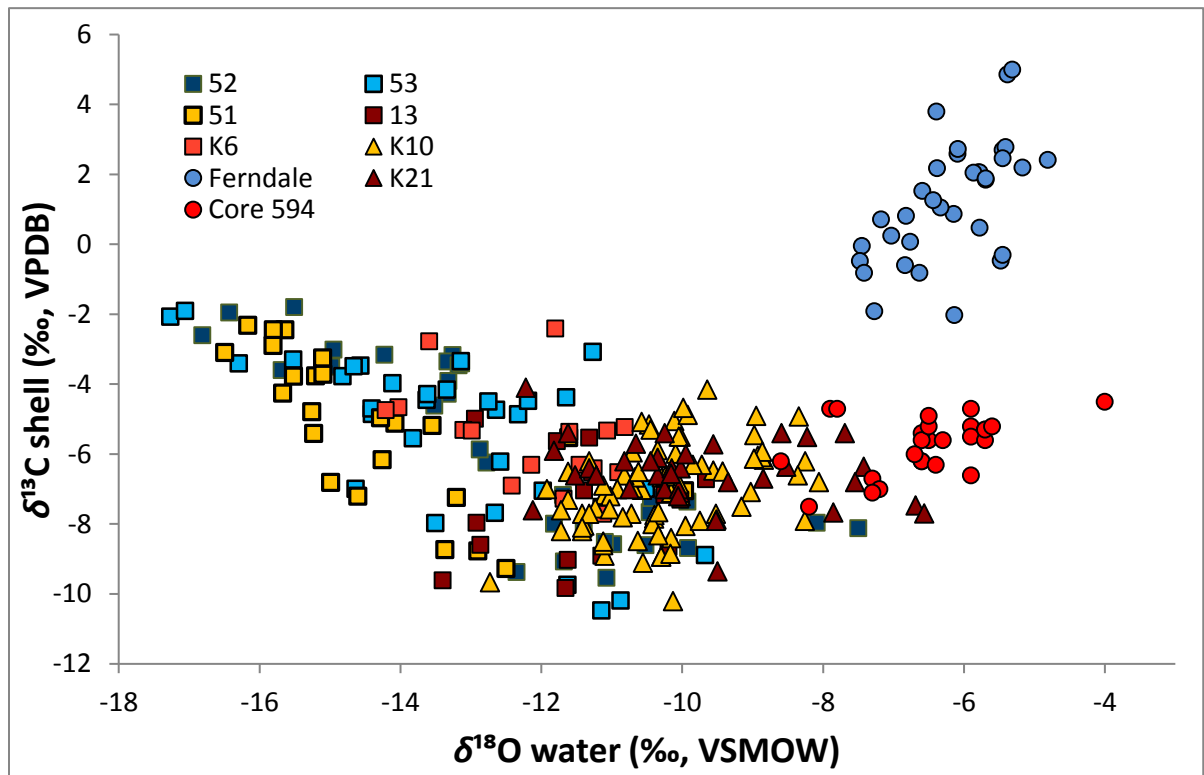


Figure 5.8 - All isotopic data (including Godwin, 1985 and Macdonald, 2012) for shells presented in terms of calculated water oxygen isotopic compositions and shell carbon isotopic compositions. The results have been categorised by lake phase (red - Algonquin; yellow - Transitional; blue - Nipissing) and by depositional environment (square - fluvial, triangle - estuarine; circle - lacustrine).

5.6.1 Lacustrine sites

5.6.1.1 Algonquin - Goderich Sub-basin Core 594

Previous studies suggest that before 10.2 ^{14}C ka (12 ka cal) BP, the Huron basin was a hydrologically open regime with substantial fractions of glacial meltwater despite dropping lake levels (Lewis *et al.* 1994; Rea *et al.* 1994; Moore *et al.*, 1994, 2000; Godsey *et al.*, 1999; Lewis *et al.*, 2007; Macdonald and Longstaffe, 2008; Breckenridge and Johnson 2009). By 10 ^{14}C ka (11.5 ka cal) BP, lake levels had dropped to a level such that the Six Fathom Scarp ridge system that runs from near Point Clark north-west to Thunder Bay began to emerge from the water (Fig. 5.9a; Thomas *et al.*, 1973). This system began to isolate the Goderich sub-basin and acted as a barrier to entry of characteristically low- $\delta^{18}\text{O}$ –high- $\delta^{13}\text{C}$ glacial meltwater from Lake Agassiz in the north (Colman *et al.*, 1990; Macdonald and Longstaffe, 2008; Macdonald, 2012; Hladyniuk and Longstaffe, 2015, 2016). Macdonald (2012) reported isotopic results for *Pisidium* spp. from the base of a sediment core (12.8 to 15.0 m; Fig. 5.9b: Appendix H) from the Goderich sub-basin that dated from 10 to 9.5 ^{14}C ka (11.5 to 10.9 ka cal) BP. Between this reduction of meltwater and the strong evaporative regime in the region, by ~9.9 ^{14}C ka (11.3 ka cal) BP, the Goderich sub-basin lake water became much more enriched in ^{18}O than the northern sub-basins (Fig. 5.10).

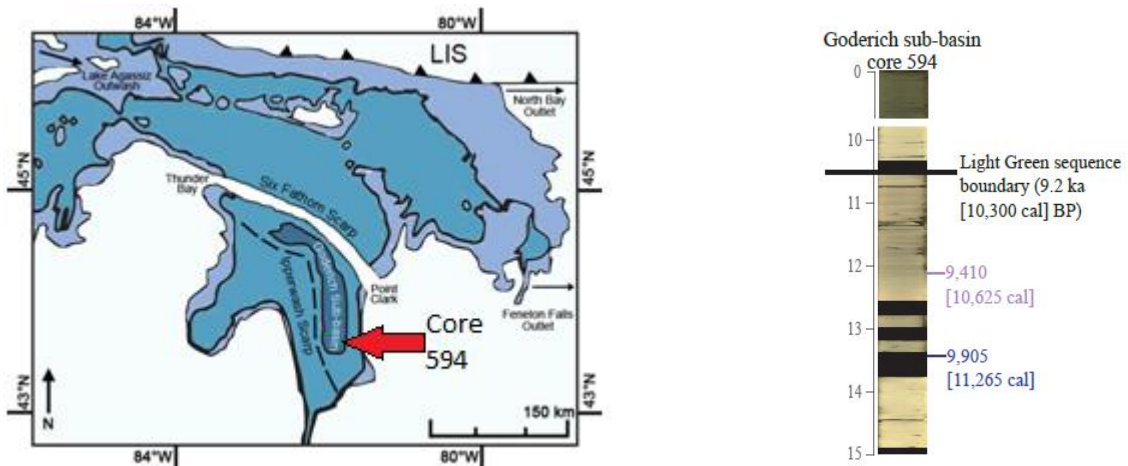


Figure 5.9 - (a) Lake Algonquin shoreline at time of emergence of the Six Fathom Scarp, which isolated the Goderich sub-basin. The Ipperwash scarp to the south may have further isolated the lake during extreme lowstands. (b) Goderich sub-basin core 594 showing interval 9.8 to 15 m. Black intervals are sections lost to radiocarbon dating. *Pisidium* spp. were restricted to 12.8 to 15.0 m depth (from Macdonald, 2012).

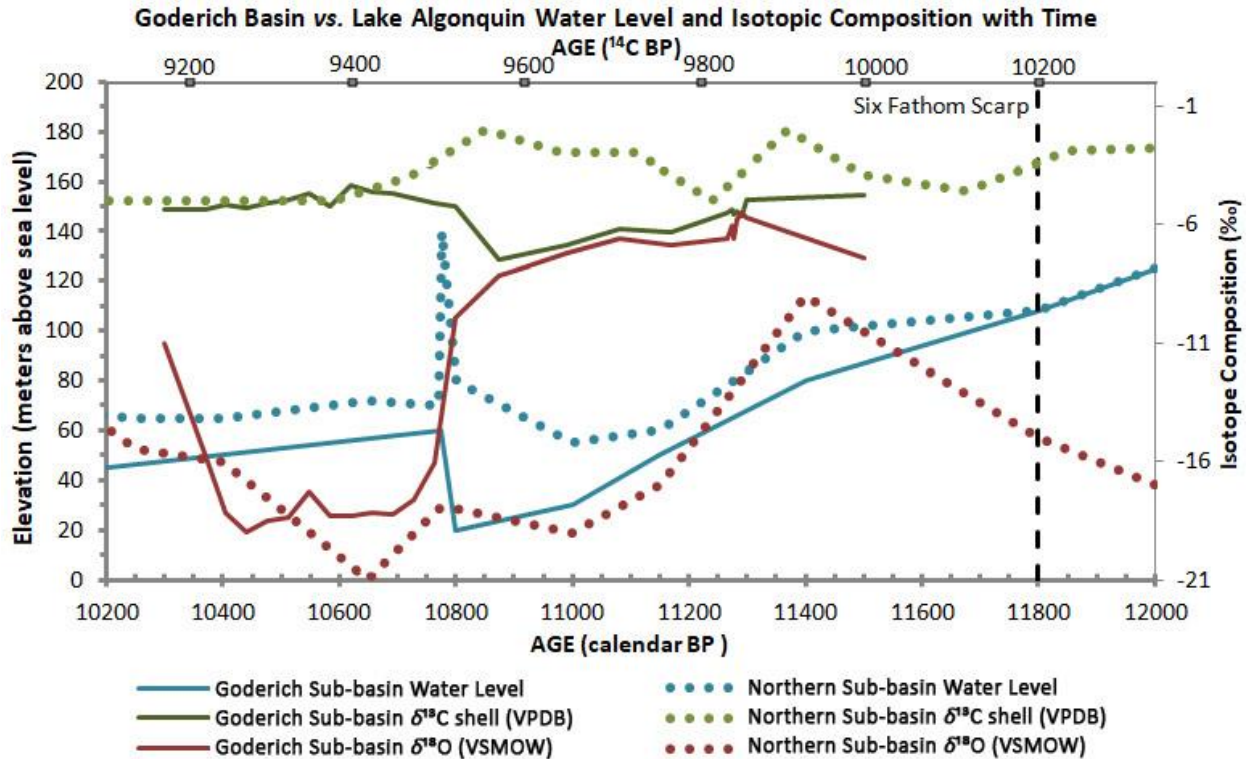


Figure 5.10 - Lake water isotopic variations in the Goderich sub-basin (solid lines) and the northern Manitoulin and Mackinac sub-basins (dotted lines) inferred from ostracodes (Lewis *et al.*, 1994; Moore *et al.*, 2000; Lewis and Anderson, 2012) and *Pisidium* spp. (Macdonald, 2012). Inferred lake level variations are also shown, based on the above references.

Shortly thereafter, the $\delta^{18}\text{O}$ and $\delta^{13}\text{C}$ of the Goderich sub-basin water began a gradual downward trend. These decreases likely reflect slow removal of water from an isolated basin that enhanced contributions from ground water. At lower water levels, a greater fraction of low- ^{18}O ground water was slowly introduced into the lake. In isolated basin environments, isotopic controls associated with regional climate, such as an evaporative regime, can be overprinted by environmental controls, such as low- $\delta^{18}\text{O}$ ground water input. Lower water levels associated with a drier climate can also reduce primary productivity, with attendant effects on DIC $\delta^{13}\text{C}$ when the concentration of decaying OM becomes sufficient to reduce light penetration (Meyers, 1997; Meyers and Lallier-Vergès, 1999; Post, 2002; Routh *et al.*, 2009; Hyodo and Longstaffe, 2011b). The trend to lower $\delta^{13}\text{C}$, however, more likely reflects increased concentrations of decayed terrestrial and aquatic organic matter as lake levels decreased.

Around 9.5 ^{14}C ka (10.8 ka) cal BP, one-third of the remaining Lake Agassiz water was proposed to have been released into the Huron basin in as little as two years (Teller and Thorleifson 1983; Farrand and Drexler 1985; Leverington and Teller 2003, Macdonald and Longstaffe, 2008; Macdonald, 2012). Direct input of glacial meltwater into the Goderich sub-basin is not suggested, however, because the core shows no change in sedimentation type at this time (Fig. 5.9b). Glacial meltwater input is generally associated with larger grain-size deposition (Macdonald, 2012). Nonetheless, this flooding event (Mattawa I) could have been sufficient to overflow the Six Fathom scarp, as suggested by the convergence to similar low- $\delta^{18}\text{O}$ and high- $\delta^{13}\text{C}$ of both Goderich sub-basin core 594 and the northern sub-basin (Fig. 5.10; Lewis *et al.*, 1994; Moore *et al.*, 2000; Macdonald and Longstaffe, 2008; Lewis and Anderson, 2012; Macdonald, 2012).

Further evidence for such inundation is the abrupt disappearance of *Pisidium* spp. shells at 12.8 m [~ 9.5 ^{14}C ka (10.8 ka) cal BP] and the delay in their return until 10.2 m [~ 9.2 ^{14}C ka (10.3 ka) cal BP]. The rising water levels and / or cooling the water temperatures may have reached the point that *Pisidium* spp. could no longer thrive.

5.6.1.2 Ferndale and Sucker Creek

Pisidium casertanum and *compressum*, herein referred to as *Pisidium* spp., *V. sincera* and *V. tricarinata* were analysed from the Ferndale and Sucker Creek sites (Fig. 1.8). Based on geological markers, these sites are known to have been deposited during the Nipissing phase in a lacustrine plain (Karrow and Mackie, 2013).

Macdonald and Longstaffe (2008) used ostracodes and *Pisidium* spp. from offshore cores to estimate the $\delta^{18}\text{O}$ of Nipissing phase lake water to be -6.5 ‰ (Core 594 -7 ‰, Core 146 -6 ‰) (Fig. 5.11). Analyses of shells from the Ferndale and Sucker Creek localities have resulted in estimates of water isotopic compositions that vary around this average. Variation in the $\delta^{18}\text{O}$ of Nipissing phase Lake Huron water likely reflects near-shore depositional environments, which are shallower than the surrounding lake (Fig. 4.7) because of their association with the elevated Niagara escarpment ridge system.

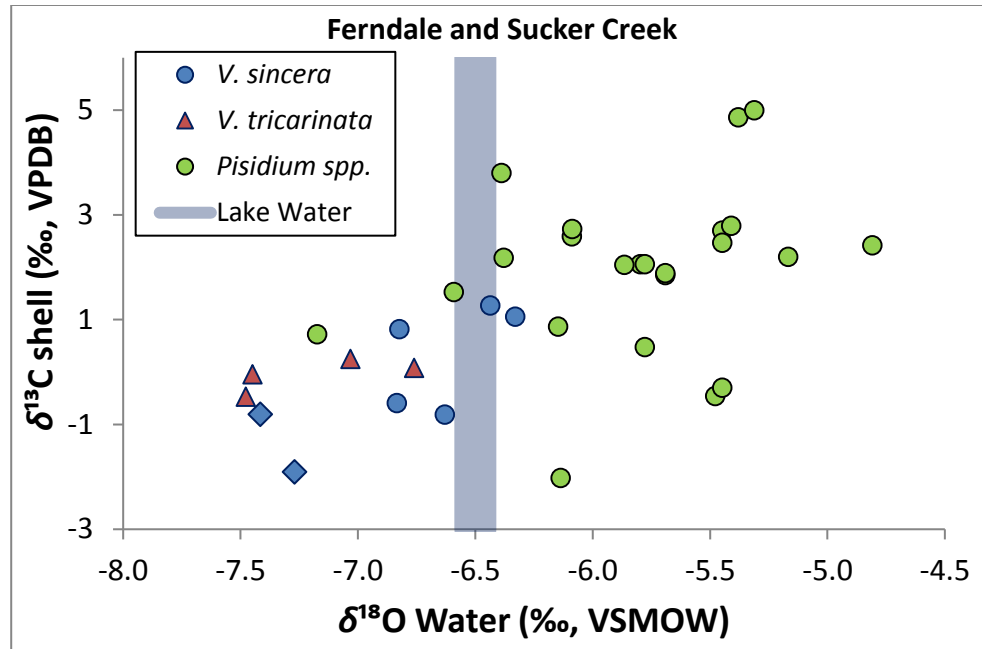


Figure 5.11 - Ferndale and Sucker Creek isotopic compositions of *Valvata* spp. and *Pisidium* spp. Lake water oxygen isotope composition has been determined using ostracode valves from two cores (146: $\delta^{18}\text{O}$ -6 ‰; 594: $\delta^{18}\text{O}$ -7 ‰) in the Goderich sub-basin to the south of Ferndale site, which has been dated to the Nipissing phase [~ 4.4 ^{14}C ka (5 ka cal) BP] (Macdonald and Longstaffe, 2008).

Lake Huron is well mixed, but there can be up to a 1 ‰ difference in $\delta^{18}\text{O}$ between the top 5 m of water and bottom water (Dettman *et al.*, 1995). Overturn and mixing of the lake's more isotopically depleted cooler waters occurs during the winter months, therefore the Ferndale and Sucker Creek *Valvata* spp., which precipitate most of their shell in the late spring-early summer months, could account for their generally lower $\delta^{18}\text{O}$ relative to *Pisidium* spp.. As noted earlier, *Pisidium* spp. can grow over two years and young are produced in spring and fall (Way and Wissing, 1982; von Grafenstein *et al.*, 1999). Those with isotopic compositions similar to the *Valvata* spp. may represent spring offspring, whereas those with higher $\delta^{18}\text{O}$ and $\delta^{13}\text{C}$ may represent fall offspring that would reflect greater evaporation, contributions of summer precipitation, and productivity-related drawdown of ^{12}C . Conversely, the higher $\delta^{18}\text{O}$ *Pisidium* spp. may represent the winter months, as cooler waters precipitate aragonite at a higher $\delta^{18}\text{O}$. This is likely not the case, as the $\delta^{13}\text{C}$ is generally higher and most likely represents local primary productivity, which would be limited in fall/winter months. Additionally, some of the isotopic variation shown in Figure 5.11 may reflect year to year / decade to decade variations in the ages of the shells collected from the sampling horizon.

5.6.1.3 Lacustrine Sites Through Time

Although the range of water $\delta^{18}\text{O}$ inferred from Goderich sub-basin core 594 for the Algonquin phase is similar to the Nipissing phase at Ferndale / Sucker Creek, and their averages shows no significant difference based on Kruskal-Wallis test (p value 0.093; Fig. 5.12), the processes controlling these isotopic compositions were likely different. As mentioned in section 5.6.1.1, low- $\delta^{18}\text{O}$ ground water and glacial meltwater input kept the range of $\delta^{18}\text{O}$ lower than what was expected in the highly evaporative isolated Goderich sub-basin (Edwards and Fritz, 1986). Cooler air temperatures and lower $\delta^{18}\text{O}$ of precipitation would have also played a role in keeping the range lower than expected (Fig. 5.13).

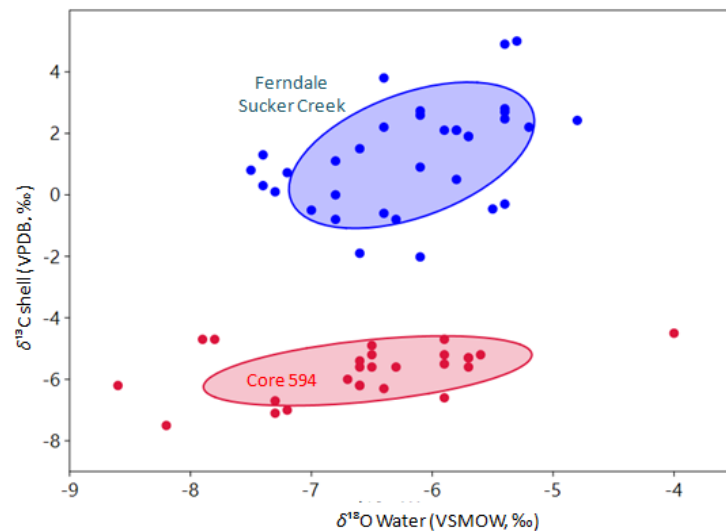


Figure 5.12 – Water oxygen and carbon isotopic compositions calculated for Algonquin phase Core 594 and Nipissing phase Ferndale and Sucker Creek samples.

Controls on Isotopic Composition of Lake Water

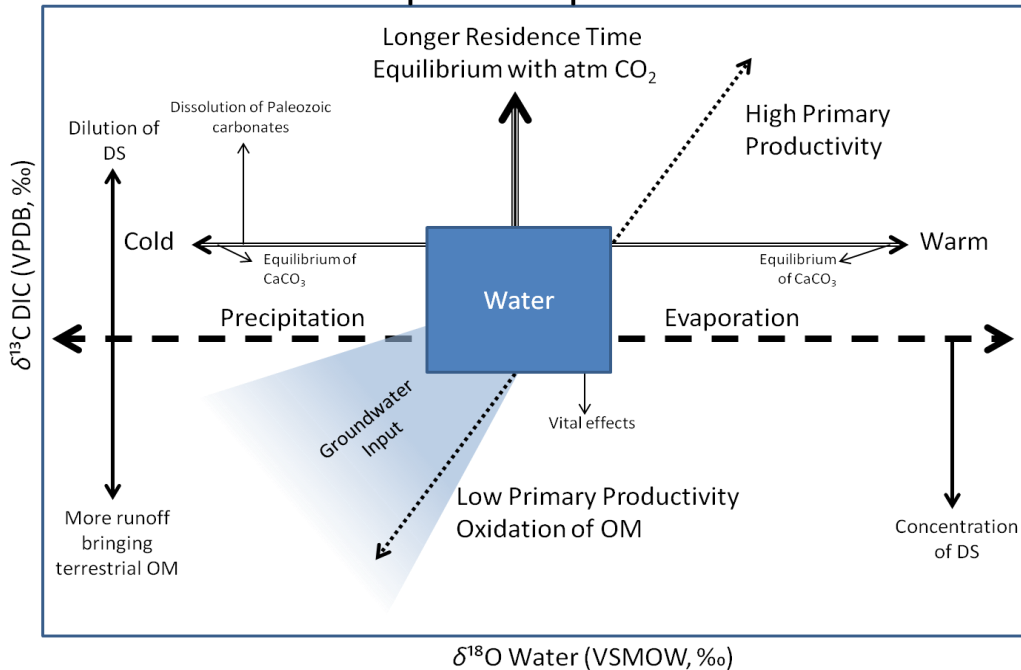


Figure 5.13 - Direction of idealised isotopic change affecting lake water resulting from various processes. OM = organic matter; DS = dissolved solids.

By comparison, lake levels rose during the Nipissing phase, thus reducing the proportion of low- $\delta^{18}\text{O}$ ground water input. Warmer air temperatures were reflected in higher annual $\delta^{18}\text{O}$ of precipitation; however, given the more humid climate at this time, the rate and magnitude of lake water evaporation would have been less than during the Algonquin phase. The slightly higher range of lake water $\delta^{18}\text{O}$ for the Nipissing phase therefore likely reflects these processes rather than evaporation (Fig. 5.13). Depositional setting (e.g. lacustrine) remains the dominant control of lake water $\delta^{18}\text{O}$ in the Huron basin, but climatic differences can still shift those values from that of the original inputs.

The large difference in $\delta^{13}\text{C}$ between the Algonquin phase Goderich sub-basin site and the Nipissing phase Ferndale and Sucker Creek sites likely reflects proximity to the shoreline and depth of the water column. The Algonquin site was located in the deep water of the Goderich sub-basin well below the photic zone, whereas the Nipissing sites were in much shallower water of a lacustrine plain, and well within the photic zone (Karrow and Mackie, 2013). Local photosynthetic activity during the Nipissing phase would have led to ^{13}C -enrichment of the growing-season DIC pool available for shell formation (Fig. 5.13). The larger volume of the lake during the Nipissing phase also likely corresponded to a longer

water residence time, which would have favoured equilibration with atmospheric CO₂ and hence to a relatively higher $\delta^{13}\text{C}$ DIC pool (Fig. 5.13; Li and Ku, 1997). At this time, the relative contribution of decaying terrestrial OM to the system would have been greatly diminished compared to the Algonquin phase, reducing the influence of low- $\delta^{13}\text{C}$ OM on the DIC pool (Fig. 5.13). In short, the $\delta^{13}\text{C}$ of the DIC pool in the lacustrine setting appears to be dominantly controlled by depositional environment (i.e. water depth).

5.6.2 Fluvial Sites

5.6.2.1 Algonquin Phase - Sites K6 and 13

Although there are 150 km separating the two Algonquin fluvial sites (K6, 13; Fig. 5.14), it is assumed here that the regional climate would have been similar at both. There is a 16 m elevation increase from K6 to site 13, and both experienced similar regional uplift; site 13 may have risen slightly higher based on the 25-75 m isobases (Fig. 5.14; Clark *et al.*, 2007). The different elevations may also be a consequence of a difference in the rate of riverbed down-cutting, or it could reflect deposition at somewhat different geological times at each site. Site K6 is dated at 10.8 ± 0.11 ¹⁴C ka (12.8 ka cal) BP (GSC-1904; Miller *et al.*, 1979), and it is assumed in this study that site 13 was deposited concurrently.

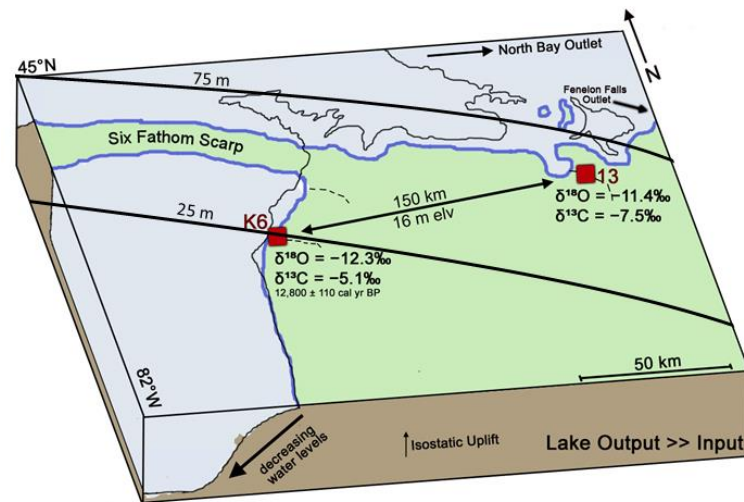


Figure 5.14 – Location of fluvial Algonquin sites with their average water $\delta^{18}\text{O}$ and $\delta^{13}\text{C}$ shell isotopic compositions. Solid black lines indicate isobases representing predicted deformation in meters from 9.9 ka (11.3 ka cal) BP (after Clark *et al.*, 2007).

As mentioned in section 4.4, six or more samples are necessary to estimate the full isotopic variability of a studied site. At both Algonquin fluvial sites only *Valvata* spp. were sufficiently abundant for this purpose. Figure 5.15a illustrates data for all species, as

compared to Figure 5.15b, which illustrates results for only *Valvata* spp.. When small sample sets are excluded, the negative covariation between $\delta^{13}\text{C}$ and $\delta^{18}\text{O}$ for both sites becomes apparent (site K6 R^2 value = 0.725; site 13 R^2 value = 0.559).

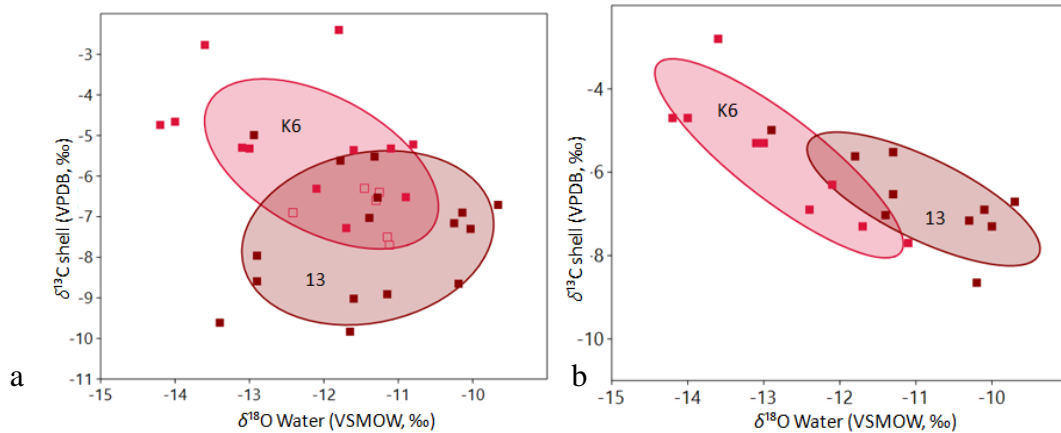


Figure 5.15 – (a) Isotopic composition of all species of Algonquin phase fluvial sites. Godwin (1985) data are shown as open squares. (b) Water isotopic compositions derived from *Valvata* spp. shells for Algonquin-phase fluvial sites.

The elevation map (Fig. 5.16) shows a large barrier (the Niagara escarpment) between sites K6 and 13, and therefore it is assumed that both fluvial systems had different sources of water. The higher $\delta^{18}\text{O}$ of water at site 13 may indicate a more southerly source than site K6.



Figure 5.16 - Topography along transect between K6 and 13 (Google Earth, 2016).

Another possibility is that lower flow rates led to evaporation cumulatively enriching site 13 river water in ^{18}O as it travelled down the river reach. Such a process could account for a +1 to +2 ‰ shift, when taken together with the associated longer interaction with high summer air temperatures (section 1.4.1; Fig. 5.17; Mohseni and Stefan, 1999). Lower flow rates would also concentrate DIC derived from oxidation of aquatic and terrestrial OM, lowering the $\delta^{13}\text{C}$ of the overall DIC pool, producing the lower $\delta^{13}\text{C}$ range at site 13 relative to K6.

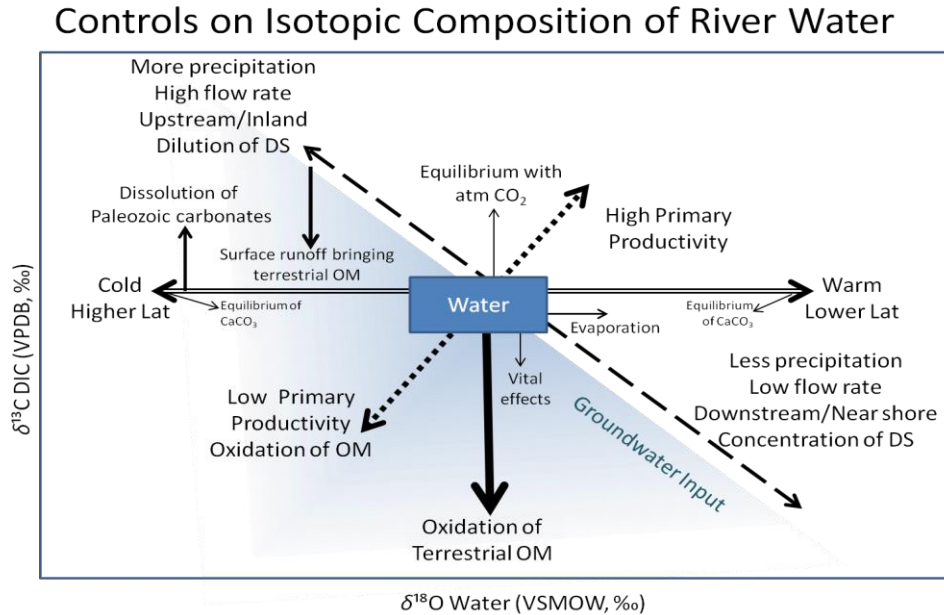


Figure 5.17 - Direction of idealised isotopic change affecting original river water compositions resulting from various processes. OM - organic matter; DS - dissolved solids; Lat - latitude.

5.6.2.2 Transitional and Nipissing Phases - Sites 51 to 53

No radiocarbon dates are available for samples from sites 51- 53; however, they are only six metres apart in elevation (191 masl, 195 masl, and 201 masl respectively) and a few hundred meters apart laterally (Fig. 1.5). Assuming that sedimentation rates remained relatively constant in this river system since the end of the Algonquin phase, the modern elevation of the river (185 masl) and the elevation of the top of the river valley terrace (202 masl) can be used to estimate the age of each site. The top of the valley terrace shows lacustrine sediments, indicating that Lake Algonquin shoreline was once further to the south. Once the lake began to recede, fluvial systems started to develop in the low-lying areas. An estimated date of 10.2 ¹⁴C ka (11.8 ka cal) BP is proposed for the start of this process. That date marked the end of the Main Algonquin Lake phase and the opening of the North Bay outlet, which led to a large drop in lake levels (Fig. 2.12). Dividing this estimated age of 10.2 ¹⁴C ka over 17 m of elevation change yields a relationship of 600 years / meter elevation change. This relationship suggests a Transitional phase date of ~9.6 ¹⁴C ka (11 ka cal) BP for site 51, and Nipissing phase dates of ~6.0 ¹⁴C ka (6.9 ka cal) BP for site 53 and ~3.6 ¹⁴C ka (3.9 ka cal) BP for site 52. The presence of *P. livescens* provides further evidence that site 53 dates to the Nipissing phase (Miller *et al.*, 1979; Karrow and Mackie, 2013).

The isotopic composition of Transitional- and Nipissing-age fluvial sites shows a strong negative co-variation between $\delta^{13}\text{C}$ and $\delta^{18}\text{O}$ (Fig. 5.18) over a very large range of values (8.7 ‰ for $\delta^{13}\text{C}$; 9.0 ‰ for $\delta^{18}\text{O}$). Due to the nature of grab samples, the span of depositional time represented can be difficult to determine and could average changes in the environment that occurred over decades to centuries.

One factor that might explain the large range in $\delta^{18}\text{O}$ is a change in air temperature. To cause a 9 ‰ shift in $\delta^{18}\text{O}$, average air temperature during the shell growing season (May to October) would have to change by $\sim 16^\circ\text{C}$. This is not to say that changes in summer air temperature, and thus the $\delta^{18}\text{O}$ of precipitation, did not account for much of the observed variation, but it is likely that other factors also contributed to this large range.

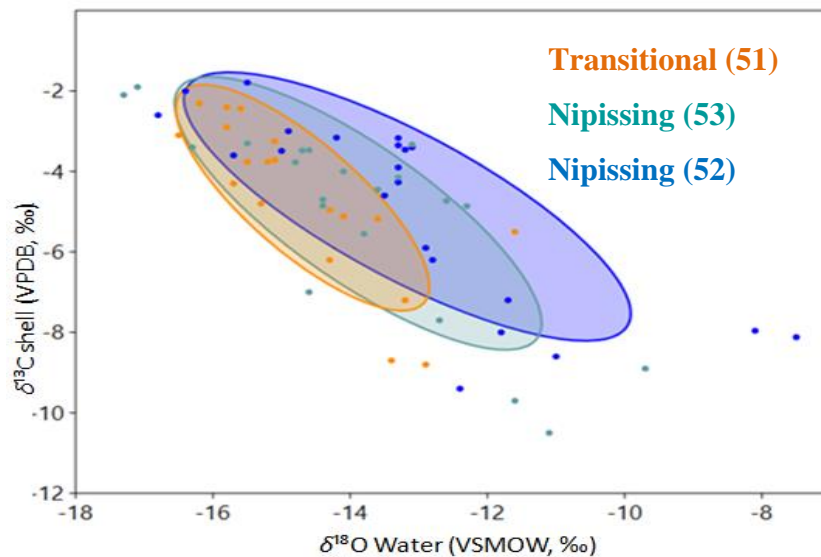


Figure 5.18 – Isotopic composition of all species from Transitional- and Nipissing-phase fluvial sites.

Assuming similar behaviour of the Nottawasaga river during the Transitional to Nipissing phases, some insights into the causes of these variations are possible. Based on the Kruskal-Wallis test (p value 0.824) there is no significant difference between the average $\delta^{13}\text{C}$ for all sites. Based on this result, it is suggested that the mix of carbon sources within the annual cycle has not changed much during the Holocene times represented by these sites.

During the summer months, flow rates can be almost five times lower than during the spring as measured from Baxter, Ontario, which is located 8 km upstream from sites 51 - 53 (Fig. 5.19a,b). Reduced flow rates, and warmer temperatures favour evaporation, which would yield higher water $\delta^{18}\text{O}$ than precipitation. These conditions are also conducive to lowering

DIC $\delta^{13}\text{C}$ by increasing the proportion of decaying OM. This may explain the inverse relationship between $\delta^{13}\text{C}$ and $\delta^{18}\text{O}$. Depletion of ^{13}C can be counteracted by primary productivity removing ^{12}C from the system, via aquatic photosynthesis during the shell-growing season. Drought may explain the few low- $\delta^{13}\text{C}$ -high- $\delta^{18}\text{O}$ results (Fig. 5.18: $\delta^{18}\text{O} = -10$ to -8 , $\delta^{13}\text{C} = -11$ to -8 ‰) as plant growth may have been restricted during this time, keeping the $\delta^{13}\text{C}$ low.

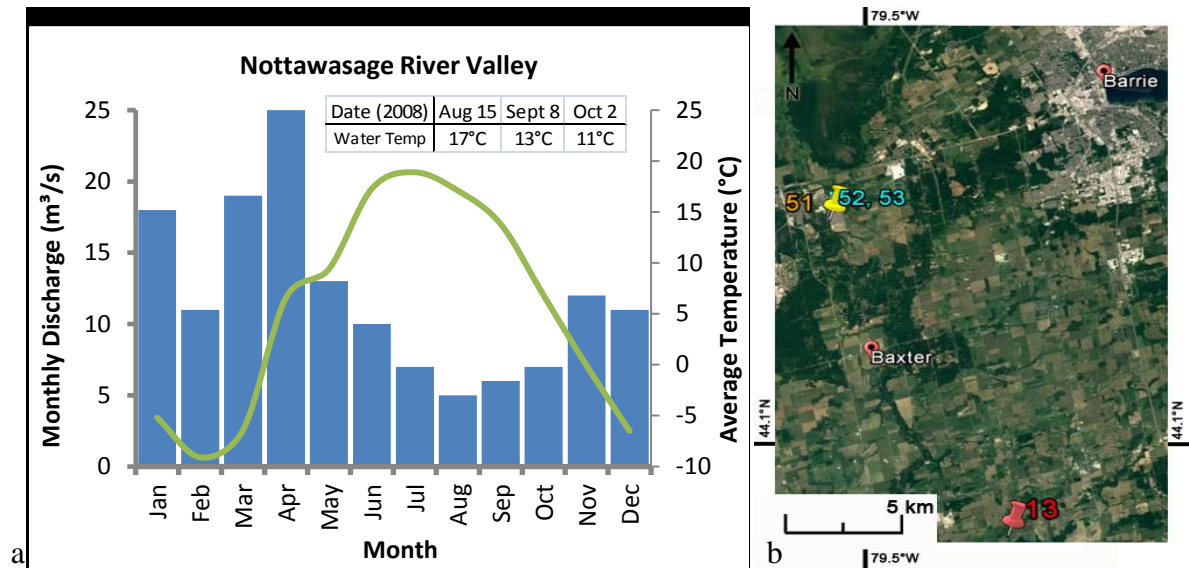


Figure 5.19 - (a) Monthly conditions for the Nottawasaga River. Monthly mean of mean daily discharge for a 4-year period of the Nottawasaga River at Baxter (1992-1996) (Thornbush, 2001). Average monthly temperatures for 2008 recorded at Barrie, Ontario (Government of Canada, 2016). Inset - Water temperature of Nottawasaga River recorded on specific dates in 2008 (Nottawasaga Valley Conservation Authority, 2014). (b) Location of fluvial sites and surrounding towns (Google Earth, 2016).

The Nottawasaga river has a five-year major flood cyclicity that is largely regulated by ice and log jams (MacLaren Plansearch Inc, 1988; Thornbush, 2001). The cyclicity could help explain the high- $\delta^{13}\text{C}$ -low- $\delta^{18}\text{O}$ end-member compositions (Fig. 5.18). In the spring, upstream jamming can reduce water flow; more importantly, these blockages impede sediment transport, including low- $\delta^{13}\text{C}$ OM (MacLaren Plansearch Inc, 1988; Thornbush, 2001). This process causes the $\delta^{13}\text{C}$ of DIC in the downstream river water to increase due to the smaller proportion of low- $\delta^{13}\text{C}$ OM input. These higher values of DIC $\delta^{13}\text{C}$ are magnified by the colder water of the spring, which can lead to greater dissolution of Paleozoic carbonates, which are enriched in ^{13}C ($\delta^{13}\text{C} +1$ to $+4$ ‰) (Guiguer, 2000).

Postponement of peak inflows of winter meltwater may explain why high $\delta^{13}\text{C}$ is associated with $\delta^{18}\text{O}$ as low as -17 ‰. Such water compositions are unexpected during the shell

growth months of May to October. One scenario that could lead to such compositions would be if the upstream dam was not to break until later in the spring or if a flooding event was so large that it required weeks for winter meltwater to leave the system. If so, the isotopic composition of the hatching molluscs could capture the isotopic signal originating from postponed winter snowmelt ($\delta^{18}\text{O}$ -21 to -14 ‰) (Van Beynen and Febroriello, 2006).

Figure 5.20 illustrates the data for the fluvial sites, grouped by species. These data indicate that, although the isotopic compositions of the *Valvata* genus span the widest isotopic range compared to *Pisidium* spp., the range for *V. sincera* appears to be more constrained to relatively high $\delta^{13}\text{C}$ and low $\delta^{18}\text{O}$. This may reflect its habitat. Unlike other members of the *Valvata* genus, *V. sincera* prefers more calcium-rich waters (Massachusetts Division of Fisheries & Wildlife, 2015), such as colder waters containing higher concentrations of dissolved Paleozoic carbonate. Late inundation of this cold water may have been more hospitable for hatching *V. sincera*.

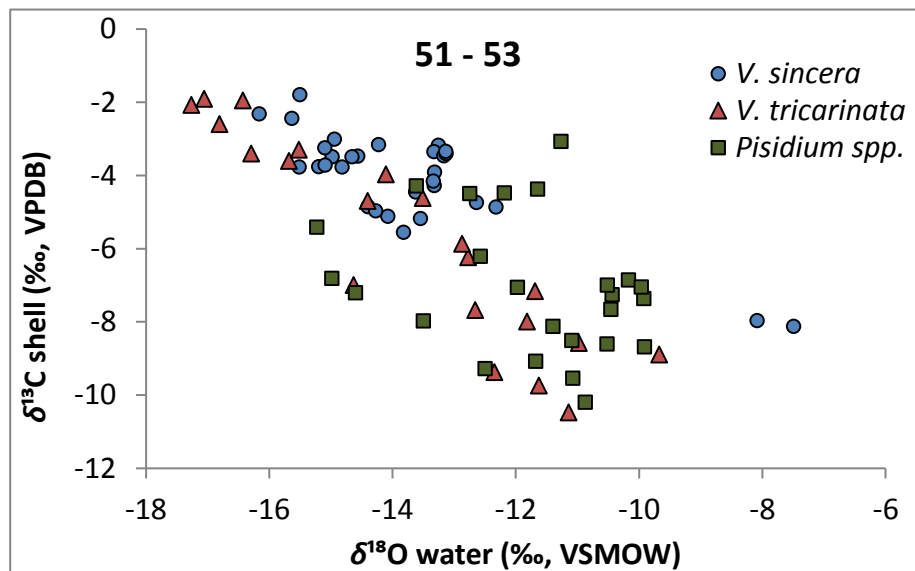


Figure 5.20 - Isotopic results for fluvial sites 51-53 by species.

Fluctuations in the contribution of ground water into the river system may offer another explanation for these unexpected values. As mentioned in section 1.4.1, ground water contributes up to 79 % of river flows in the Great Lakes region, but that percentage decreases downstream, associated with the decreasing land gradient (Rodie and Post, 2009; Lewis, 2016). The fluvial sites studied in this project have experienced different degrees of isostatic rebound since the retreat of the LIS (Clark *et al.*, 2007). The extent of this rebound has

lessened towards present time (Fig. 5.22; Lewis *et al.*, 2005). Therefore, the Transitional site 51 would have received larger contributions of ground water than the Nipissing sites based on the former's steeper land gradients.

In southern Ontario, Pleistocene ground water ($\delta^{18}\text{O}$ -17 to -14 ‰, $\delta^{13}\text{C}$ -8 to -3 ‰) remains present in some localities at depths of 20 to 40 m (Desaulniers *et al.*, 1981; McIntosh and Walter, 2006). Immediately following the retreat of the LIS, when site 51 was being deposited [~ 9.6 ^{14}C ka (11.0 ka cal) BP], this Pleistocene water would have been closer to the surface and contributing more directly to the newly created Nottawasaga river.

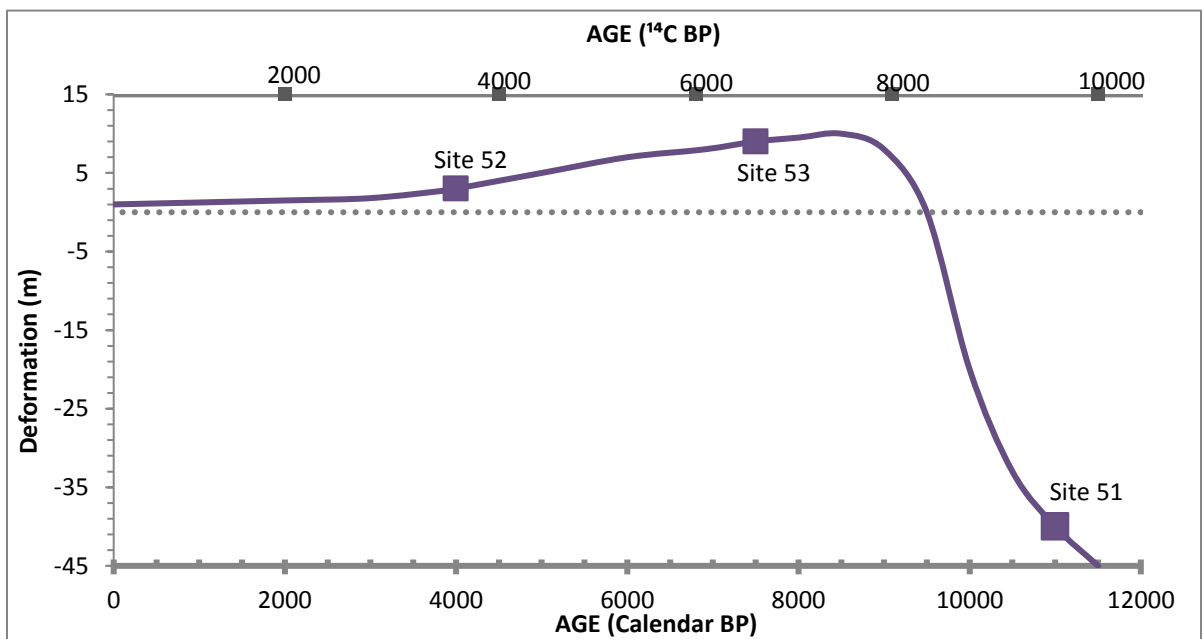


Figure 5.21 - Predicted deformation in the Lake Huron region relative to present due to unloading of the LIS. Fluvial sites 51-53 are shown at the estimated time of deposition (after Clark *et al.*, 2007).

The Nipissing phase [6 ^{14}C ka (6.9 ka cal)] was associated with a 150 mm decrease in annual precipitation compared to Transitional and late Algonquin phase times (Webb III *et al.*, 1987). Greater amounts of ground water likely entered the fluvial system during these drier conditions. It is suggested here that the Transitional sites had a large proportion of ground water input because of the steep gradient of the land at the time of deposition. The Nipissing site also had a large proportion of ground water input, but that was due to the reduced precipitation input. It is difficult to know what proportion of these ground water inflows were sourced from Pleistocene or Holocene age waters, but either would typically have lower

$\delta^{18}\text{O}$ than average precipitation because of preferential sequestering of snowmelt and glacial meltwaters (Clark and Fritz, 1997).

5.6.2.3 Comparison of Fluvial Sites among Lake Phases

In the discussion that follows, results for the Nipissing-phase sites 52 and 53 were combined because of their close proximity, identical depositional setting (the Nottawasaga River) and very similar water systems. Algonquin phase sites K6 and 13 were treated separately for the reasons described in section 5.6.2.1. The genus *Valvata* is used to make this comparison (See section 4.4).

A strong negative trend between shell $\delta^{13}\text{C}$ and water $\delta^{18}\text{O}$ is present at all fluvial sites (Fig. 5.22). Algonquin sites have the smallest range of both $\delta^{18}\text{O}$ and $\delta^{13}\text{C}$ and the Nipissing sites have the largest. Across the three time periods, the average water $\delta^{18}\text{O}$ ranges from -14.4‰ (Transitional) to -10.9‰ (Algonquin). Based on the Kruskal-Wallis test, there are significant differences among site $\delta^{18}\text{O}$ averages (p value $\gg 0.05$), and $\delta^{13}\text{C}$ averages (p value 0.05).

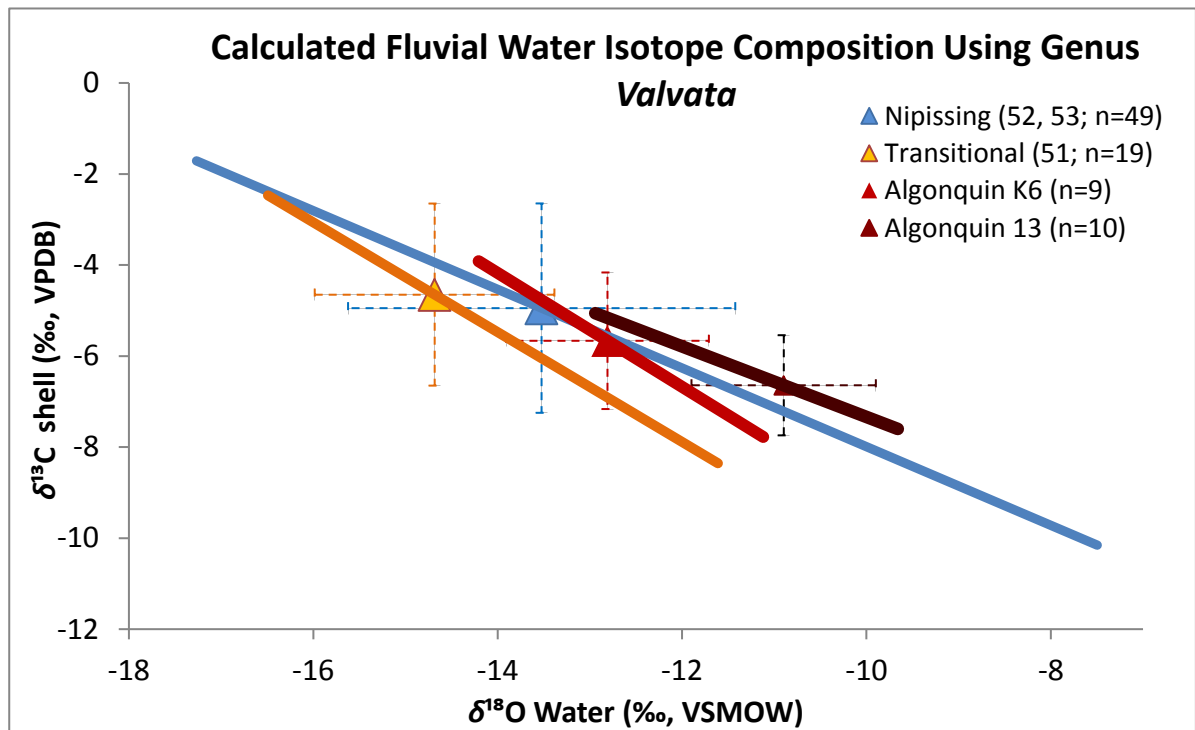


Figure 5.22 - Water oxygen vs. shell carbon isotopic composition averages (triangles) based on results for *V. sincera* and *V. tricarinata*. Solid line represents a linear regression of all data for each time phase. Dashed lines represent one standard deviation for $\delta^{18}\text{O}$ and $\delta^{13}\text{C}$ of each time phase.

The differences shown in Figure 5.22 may reflect a number of processes. First, the grab samples from the fluvial sites likely contain shells formed over decades to centuries. Consequently, their range of isotopic compositions reflect climatic and environmental variations on that time scale. Second, the fractionation factors used to calculate water $\delta^{18}\text{O}$ for *Valvata* spp. were established using modern shells and average Lake Huron water composition (Chapter 3.2.8; Macdonald, 2012). If average shell growth temperatures for *Valvata* spp. were different through the lake phases, then the calculated water $\delta^{18}\text{O}$ would be erroneous. A difference in average growth temperature of 5 °C would produce a change of ~1 ‰ in water $\delta^{18}\text{O}$ at typical surface temperatures. A change in average temperature of ~18 °C would be necessary to account for the variation between average water compositions from the Algonquin phase to the Transitional phase (3.5 ‰), which is well above the maximum average temperature change experienced over this time period (Fig. 2.11; Terasmae, 1961; Edwards *et al.*, 1985, 1996; Edwards and McAndrews, 1989; Magnuson *et al.*, 1997; Shuman *et al.*, 2002).

It is also possible that the length of the shell-forming period was different during each of the studied time periods. The late Transitional and Nipissing phases would have had the longest growing seasons during the warming trend known as the Holocene Hypsithermal (Warner *et al.*, 1984; Edwards *et al.*, 1996), whereas the Algonquin phase had the shortest growing season (Magnuson *et al.*, 1997). During this time, this genus may have adapted to generally cooler growth temperatures. Although this cannot be ruled out, the much lower abundances of all shell species at Algonquin versus Transitional and Nipissing sites (Appendix E) more likely reflects a harsher environment, where fewer species reached adulthood. Nipissing sites have the largest range of $\delta^{18}\text{O}$ and $\delta^{13}\text{C}$, the greatest abundance of shells, and the most diverse species assemblage. These features likely indicate more favourable climatic conditions and a wider window in which shelly fauna could flourish (Miller *et al.*, 1979, 1985).

In the Great Lakes region, winter storms are more frequent and tend to be more intense than summer storms due to the stronger temperature gradient between northern and southern latitudes (Klock *et al.*, 2002). The lower MAT of the Algonquin phase, coupled with the more frequent winter storms over the longer winter season, should have resulted in the average Algonquin water composition being the most negative of all lake phases examined

(Edwards *et al.*, 1996; Magnuson *et al.*, 1998). Instead, both Algonquin sites (K6, 13) have average water $\delta^{18}\text{O}$ higher than Transitional or Nipissing phases. Another apparent anomaly is that the Transitional phase, which was associated with warmer air temperatures, should have the highest average water $\delta^{18}\text{O}$, not the lowest (-14.4‰). Kurtzbach *et al.* (1998) performed a set of paleoclimatic simulations in mid-central North America back to 21 ^{14}C ka (25 ka cal) BP. Their models suggested that summer solar radiation more than doubled in strength during the period 12.8 - 8 ^{14}C ka (15.3 - 8.9 ka cal) BP. This likely led to greater evaporation (see section 5.6.2.1), thus driving Algonquin phase river water $\delta^{18}\text{O}$ to higher average values than later time periods. Evaporation, however, cannot fully explain the high water $\delta^{18}\text{O}$. Figure 5.23 illustrates the variation in river water $\delta^{18}\text{O}$ with temperature, after accounting for a range of precipitation $\delta^{18}\text{O}$ / temperature gradients and 65 – 75 % admixture with then contemporary ground water.

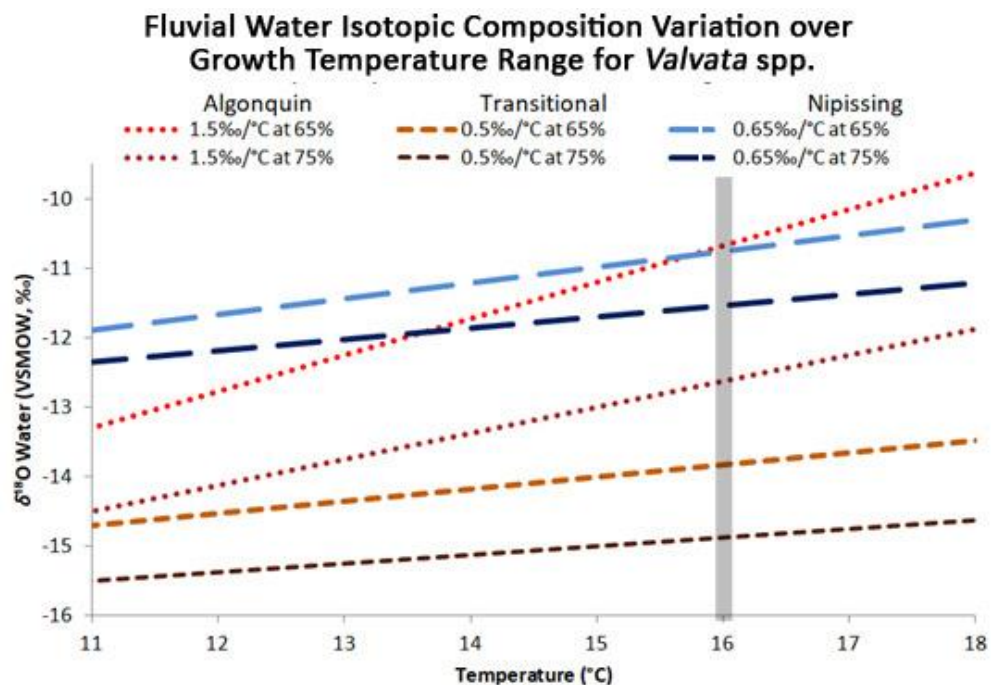


Figure 5.23. River water oxygen isotope composition versus temperature ($\text{‰} / ^\circ\text{C}$) when mixed with 65 % and 75 % ground water (Algonquin and Transitional -17‰ , Nipissing -13‰) over the growth temperature range of *Valvata* spp. Black line represents average growth temperature for *Valvata* spp (Godwin, 1985; Macdonald, 2012). Gradients are based on a southern Ontario modern average annual temperature of $7.1\text{ }^\circ\text{C}$ and average annual precipitation $\delta^{18}\text{O}$ of -11‰ (Edwards and Fritz, 1986).

Changing isotopic gradients and the introduction of ground water greatly affects isotopic composition of river water over the range of temperatures of interest. The Algonquin phase sites should have experienced a steeper precipitation / temperature gradient ($1.5\text{‰} / 1\text{ }^\circ\text{C}$)

because of the presence of the LIS shrinking the distance from warm tropics to cold polar regions (see section 5.3). The Transitional phase sites should have experienced a shallower gradient (0.5 ‰ / 1 °C) because of the Holocene Hypsithermal, with air temperatures as much as 2 - 4 °C above modern by 7 ¹⁴C ka (7.8 ka cal) BP (Edwards *et al.*, 1985, 1996; Magnuson *et al.*, 1997). Increases of air temperature of only 1 - 2 °C can greatly increase the length of the growing season at higher latitudes. The Nipissing phase more closely resembled modern climatic conditions, allowing for the use of the modern mid- to high-latitude gradient (0.65 ‰ / 1 °C). For modern molluscs in southern Ontario, the average growth temperature for gill-breathing gastropods is 16 °C (Godwin, 1985; Macdonald, 2012). Figure 5.23 shows that at 16 °C the Transitional river water $\delta^{18}\text{O}$ range is the lowest; conversely, at this temperature both Algonquin and Nipissing sites have close to the same river water $\delta^{18}\text{O}$ at 65 % ground water contribution. This shows how a cooler Algonquin phase could be characterized by fluvial water $\delta^{18}\text{O}$ comparable to the much warmer Nipissing phase, and how an even warmer Transitional phase could have $\delta^{18}\text{O}$ lower than the other two lake phases.

Several other features could also produce the changes apparent in Figure 5.23. For example, changes in lake boundaries within the Huron basin had a profound effect on the proximity of the fluvial sites to the main body of water. For Lake Algonquin, shoreline mapping showed K6 to be the closest of the studied fluvial sites to a lake shore (Fig. 4.3). Although the shorelines have not been fully mapped near site 13, it is proposed here that its proximity to Lake Algonquin was similar to that of Nipissing sites 52 and 53 to the lake during the that phase (Fig. 4.7). During the Transitional phase, the lake boundary regressed several tens of kilometers to the north (Prest, 1970; Eschman and Karrow, 1985; Karrow, 1986a), which would make site 51 the furthest inland at time of deposition (Fig. 4.5). As discussed in section 2.1.4., proximity of the fluvial system to the lacustrine system affects river water $\delta^{18}\text{O}$ and $\delta^{13}\text{C}$, with upstream waters characterized by high $\delta^{13}\text{C}$ –low $\delta^{18}\text{O}$ and downstream waters trending to low- $\delta^{13}\text{C}$ –high- $\delta^{18}\text{O}$ as the shoreline is approached (Fig. 5.17).

Based on the Kruskal-Wallis test, all but one fluvial site (site 13), show no significant difference among $\delta^{13}\text{C}$ averages, which is interpreted here to indicate that the carbon sources did not change over the time periods investigated for these sites. Average $\delta^{13}\text{C}$ at site 13 is slightly lower than the other fluvial sites. This site may have had a lower flow rate relative to

other sites, or it may have been deposited at an earlier time, when tree cover was less developed (Smol and Boucherle, 1985). During the Algonquin phase, terrestrial organic matter was able to enter the lake and river environments more readily since the surrounding coniferous forests were still immature and deciduous canopies had not yet developed (Smol and Boucherle, 1985; Romanek and Grossman, 1989; Mitchell *et al.*, 1994; Shuman, 2001; Shuman *et al.*, 2002). Water bodies during the Algonquin phase would therefore have had lower $\delta^{13}\text{C}$ because it received more terrestrial OM during the shell growth season, coupled with cooler air temperatures that would have limited primary productivity, relative to later warmer times (Fig. 5.17). In either case, increased terrestrial OM input and / or lower primary productivity would result in lower $\delta^{13}\text{C}$.

5.6.3 Estuarine Sites

The water $\delta^{18}\text{O}$ of the estuarine sites is as expected, given that estuaries connect the fluvial and lacustrine depositional environments (Fig. 5.24a,b). The variability of water $\delta^{18}\text{O}$ at each site is most likely due to seasonal changes in the proportions of water inflows, and weather. In spring and fall months, the estuarine water $\delta^{18}\text{O}$ should be more representative of the downstream fluvial environment, whereas during summer months, when flow rates and precipitation amounts decrease, the water $\delta^{18}\text{O}$ should be closer to that of lake water (Fig. 5.25).

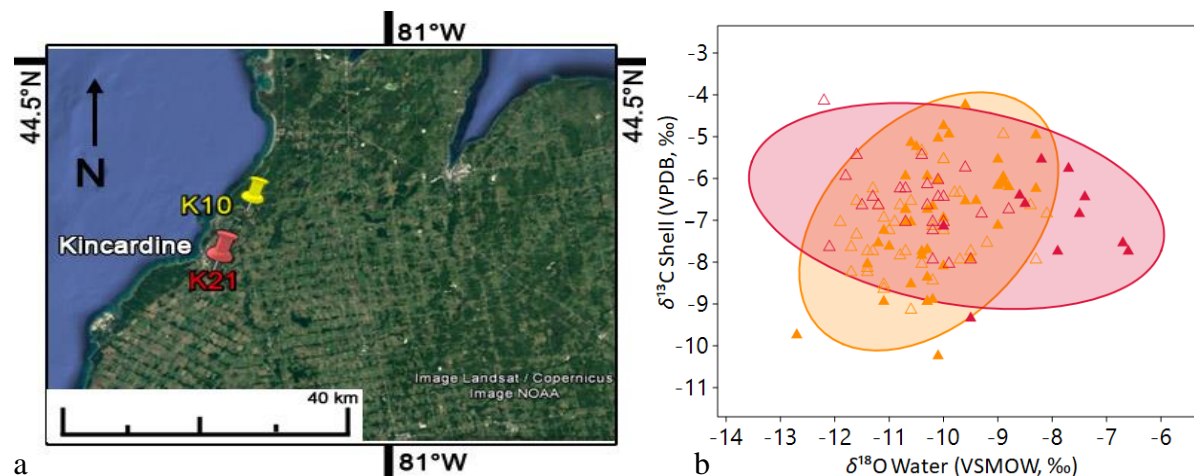


Figure 5.24 - (a) Locations of estuarine sites. (Google Earth, 2016) (b) Water oxygen and shell carbon isotope compositions of all species from estuarine sites. Godwin (1985) shown as open triangles. Red – Algonquin phase; Yellow – Transitional phase.

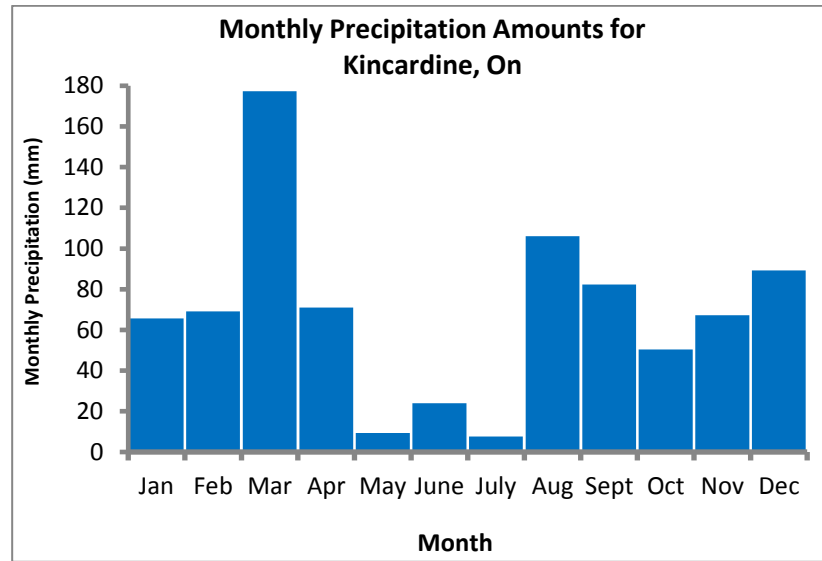


Figure 5.25 - Monthly precipitation for Kincardine, Ontario for 2016 (Government of Canada, 2016).

Based on the Kruskal-Wallis test (p value 0.083), there is no significant difference in the average $\delta^{13}\text{C}$ of this depositional environment from the Algonquin to Nipissing phases, which we interpret to indicate that the sources of carbon have not changed. As discussed in section 1.4.2, virtually all particulate matter, including suspended nutrients, have the potential to be deposited in this setting. This ensures that there is always some input of low- $\delta^{13}\text{C}$ OM to the estuarine environment. The low- $\delta^{13}\text{C}$ of the estuarine environments is seemingly inconsistent with the highly productive nature of this environment, as DIC in these environments tend to become enriched in ^{13}C relative to water bodies with low productivity (Leng and Marshall, 2004; Casey and Post, 2011). In this setting, however, much of the DIC is derived from the oxidation of terrestrial OM (Fuks and Wilkinson, 1998; Wolfe *et al.*, 2007), which drives the DIC $\delta^{13}\text{C}$ pool lower. The range in DIC $\delta^{13}\text{C}$ at these sites is most likely explained by variations in primary productivity over the growing season. Therefore, it is suggested that depositional setting is the strongest control on shell carbon isotopic composition in fresh-water estuarine environments.

5.7 Comparison Between Depositional Environments Over Time: Summary

Figure 5.26 illustrates that depositional setting is the strongest control on water $\delta^{18}\text{O}$ in the study areas, with the fluvial waters being the most depleted of ^{18}O and lacustrine waters the most enriched.

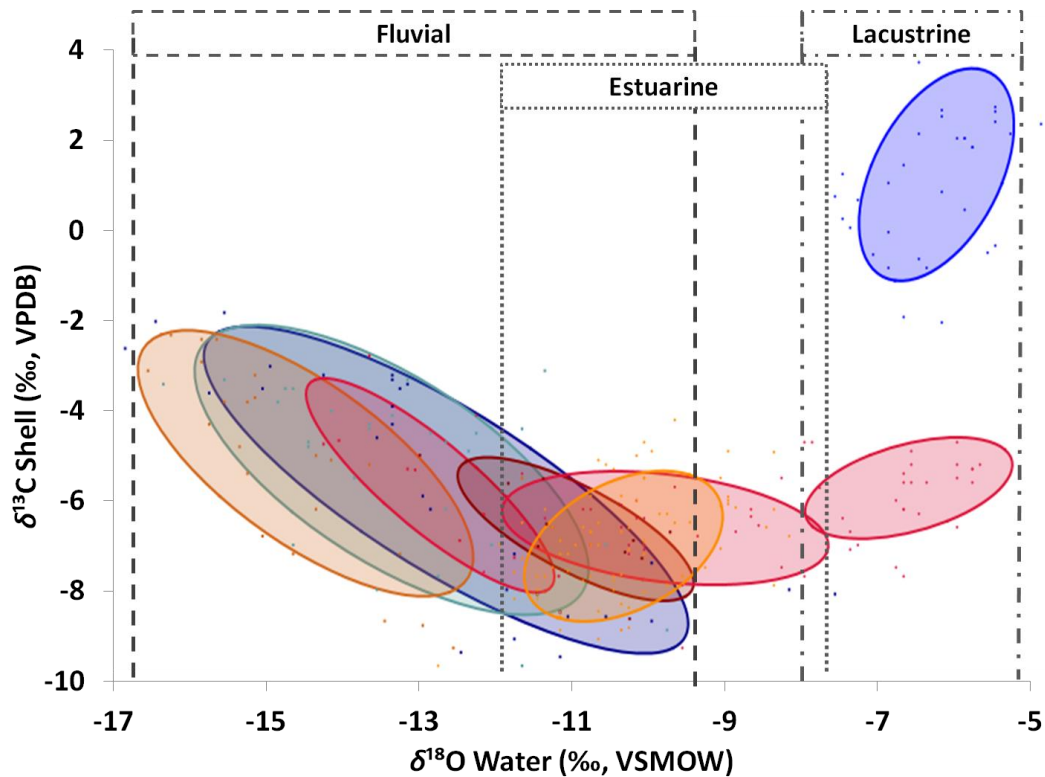


Figure 5.26 - *Valvata* spp. and *Pisidium* spp. $\delta^{13}\text{C}$ shell and $\delta^{18}\text{O}$ water results (for $n \geq 6$) categorized by depositional environment and lake phase. Algonquin phase - red; Transitional phase - orange; Nipissing phase - blue. Dash lines bound the range of $\delta^{18}\text{O}$ for each environment. Ellipses represent 60 % data.

Fluvial environments show the largest range of $\delta^{18}\text{O}$ relative to other environments. This is likely due to a smaller volume of water at any one time being more strongly influenced by climatic variations and local climatic conditions, such as seasonality. By comparison, the lacustrine settings have the narrowest range of $\delta^{18}\text{O}$, because short-term climatic influences are attenuated because of the larger volume of water and its longer residence time compared to fluvial systems. The $\delta^{18}\text{O}$ of the estuarine environment lies between these two end members with a significant amount of overlap. Its variation in $\delta^{18}\text{O}$ is largely controlled by the changing ratio of fluvial to lacustrine water entering the system.

To better elucidate the changes in isotopic composition over the three depositional settings, three Algonquin-phase sites were compared. These sites were deposited within 100 km of each other and considered contemporaneous for this comparison. Figure 5.27a,b shows how the water $\delta^{18}\text{O}$ and shell $\delta^{13}\text{C}$ changes through the three depositional environments during this lake phase interval. It demonstrates how the general trend of isotopic compositions follow deposition environment, with upstream fluvial high- $\delta^{13}\text{C}$ –low- $\delta^{18}\text{O}$, to downstream, estuarine conditions with low- $\delta^{13}\text{C}$ and mid- $\delta^{18}\text{O}$, to open lake water with high $\delta^{13}\text{C}$ and $\delta^{18}\text{O}$. This pattern of $\delta^{18}\text{O}$ from fluvial to lacustrine settings reflects the greater control of watershed and ground water inputs in the upland regions of the fluvial environment and of climatic conditions, particularly evaporative regimes, in the lacustrine setting.

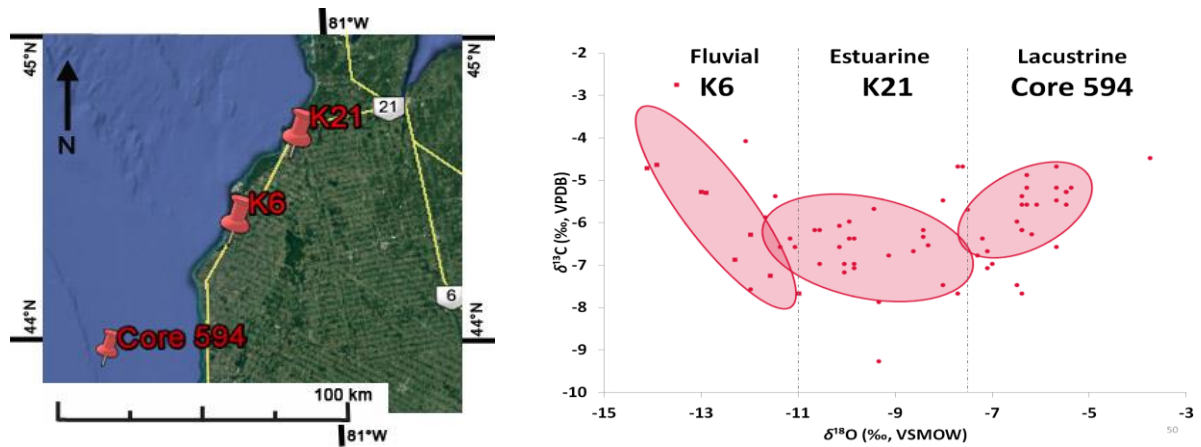


Figure 5.27 - (a) Location of Algonquin phase sites. (b) Three Algonquin phase [~11 to 10.3 ^{14}C ka (12.9 to 12.1 ka cal) BP] sites from three environments on the east shore of modern Lake Huron.

In summary, depositional environment was the dominant control on the oxygen isotopic compositions of shelly fauna in all studied environments over all lake phases examined. The carbon isotopic composition of shelly fauna in the estuarine environment was also more strongly controlled by depositional environment during both the Algonquin phase [~11 to 10.3 ^{14}C ka (12.9 to 12.1 ka cal) BP] and Transitional phase [9 to 7.4 ^{14}C ka (10.2 to 8.2 ka cal) BP]. The oxygen and carbon isotope compositions of the fluvial sites inversely co-vary through all time phases and are affected by both climate and depositional environment. Changes in climatic conditions played a less important role in controlling the oxygen isotopic composition of the Algonquin lacustrine system, but were more dominant by the Nipissing phase [7.4 to 3.2 ^{14}C ka (8.2 to 3.4 ka cal) BP]. The carbon isotopic compositions of the sites were controlled by the main source of carbon at the time of deposition.

Chapter 6

6 Conclusions and Future Work

6.1 Major Conclusions

1. The $\delta^{18}\text{O}$ and $\delta^{13}\text{C}$ of shelly fauna from sediments have shown that:
 - a) Depositional setting exerts the strongest control on the shell and water $\delta^{18}\text{O}$ during all time phases studied.
 - i) Climate conditions at the time of deposition control the variability of $\delta^{18}\text{O}$ but the magnitude of that variability is controlled by the depositional environment.
 - b) The source of carbon and its concentration exerts the strongest control on the shell and DIC $\delta^{13}\text{C}$ during all time phases studied.
 - i) Climate conditions at the time of deposition account for the variability of $\delta^{13}\text{C}$ within the fluvial, estuarine, and open lacustrine sites. Depositional environment account for variability of $\delta^{13}\text{C}$ in isolated basin sites.
 - ii) Of all carbon sources, the proportion of decaying terrestrial organic matter has the strongest influence on DIC $\delta^{13}\text{C}$.
 - c) To properly interpret isotopic compositions of shelly fauna in the Huron basin, care must be taken to recognize and understand the depositional setting in which the mollusc lived.
2. All fluvial environments display a negative $\delta^{13}\text{C}$ - $\delta^{18}\text{O}$ co-variation. Part of the co-variation arises from seasonal precipitation changes, which affects the quantity of low- $\delta^{13}\text{C}$ terrestrial OM entering the system from runoff. The range of this co-variation is likely controlled by the length of the growing season at time of shell formation.
 - a) The $\delta^{18}\text{O}$ is most likely controlled by seasonal variations in precipitation coupled with the admixture of ground water.
 - b) The $\delta^{13}\text{C}$ is most likely controlled by changes in DIC concentration and source, driven by delivery and decay of terrestrial and aquatic organic matter which provides DIC and primary productivity that consumes it. The small volume of water in these systems compared with other settings allows for a greater influence of the low- $\delta^{13}\text{C}$ OM.

3. In the estuarine environments, the variation in water $\delta^{18}\text{O}$ is likely controlled by changing ratios of fluvial / lacustrine water during the shell-formation season. The low shell $\delta^{13}\text{C}$ of this setting reflects continuous input of low- $\delta^{13}\text{C}$ organic matter from the fluvial system. The variation in shell $\delta^{13}\text{C}$ likely arises from changes in primary productivity over the growing season in this setting.
4. The lacustrine environments reflect differences in hydrological regimes at time of shell formation making evaluation of putative climate controls during this time period difficult.
 - a) The Algonquin phase isolated sub-basin showed strong evaporative effects that drove water $\delta^{18}\text{O}$ to higher values than expected for this cold period. The water $\delta^{18}\text{O}$ of the Nipissing phase hydrologically-open lake reflected warmer air temperatures and the higher $\delta^{18}\text{O}$ of precipitation.
 - b) The Algonquin phase isolated-basin shell $\delta^{13}\text{C}$ was controlled by the contribution of DIC from organic matter, possibly in association with reduced local primary productivity, and increased ground water input relative to later lake phases. The Nipissing phase hydrologically-open system acquired shell $\delta^{13}\text{C}$ dominated by exchange with atmospheric CO_2 as a consequence of the longer residence time of the lake during this time period, and possibly increased local primary productivity.

6.2 Future Work

As many of sites in this study were relatively dated, radiocarbon dating of each site is recommended to better understand the climate regime and lake levels it represents, as many conditions can change dramatically in relatively short periods of time. Most sites contained enough organic material, as plant roots or pine needles, that dating would be possible. The accuracy of the comparisons of depositional sites also would be greatly increased with the knowledge of whether the sites were truly deposited concurrently.

Given the large range of isotopic composition of fluvial sites, taking core from these environments would help to ensure the chronology of the samples. This can then be used to elucidate if the large isotopic ranges are due to seasonal variations, or if it represents changes on a scale of decades or longer.

Although very difficult, finding a core that represents the Transitional phase near-shore lacustrine environment would allow for a more complete understanding of how the carbon

and oxygen isotopic compositions co-vary based on open- or closed-basin regimes and how they relate to the Transitional fluvial settings. This time is important to study as it has $\delta^{18}\text{O}$ values that do not readily conform to the known models. This thesis began to give possible mechanisms for these anomalies, but further study is necessary.

The new methods of using CO_2 (Δ_{47}) clumped isotopes to determine the temperature of the water at time of shell precipitation would help to constrain seasonal differences and the fluvial systems $\delta^{18}\text{O}$ anomalies (Ghosh *et al.*, 2006). This method could also add to the accuracy of previously inferred water $\delta^{18}\text{O}$ by ensuring the average growth temperatures of a species had not changed over time. Additionally, this method would help elucidate the magnitude of secondary controls, such as evaporation or location of the site within each depositional setting (e.g. up/down stream, deep/shallow lake).

References

- Anderson, T. W., & Lewis, C. (1992). Climatic influences of deglacial drainage changes in southern Canada at 10 to 8 ka suggested by pollen evidence. *Géographie physique et Quaternaire*, 46(3), 255-272.
- Agriculture and Agri-Food Canada (2014). Length of growing season in Ontario. Retrieved Feb, 2017, from <http://www.agr.gc.ca/eng/science-and-innovation/agricultural-practices/agriculture-and-climate/future-outlook/climate-change-scenarios/length-of-growing-season-in-ontario/?id=1363033977515>
- Baedke, S. J., & Thompson, T. A. (2000). A 4,700-Year Record of Lake Level and Isostasy for Lake Michigan. *Journal of Great Lakes Research*, 26(4), 416-426.
- Baedke, S. J., Thompson, T. A., Johnston, J. W., & Wilcox, D. A. (2004). Reconstructing paleo lake levels from relict shorelines along the Upper Great Lakes. *Aquatic Ecosystem Health & Management*, 7(4), 435-449.
- Baker, R. G., Maher, L. J., Chumbley, C. A., & Van Zant, K. L. (1992). Patterns of Holocene environmental change in the midwestern United States. *Quaternary Research*, 37(3), 379-389.
- Barber, D., Dyke, A., Hillaire-Marcel, C., Jennings, A., Andrews, J., Kerwin, M., et al. (1999). Forcing of the cold event of 8,200 years ago by catastrophic drainage of Laurentide lakes. *Nature*, 400(6742), 344-348.
- Baroni, C., Zanchetta, G., Fallick, A. E., & Longinelli, A. (2006). Mollusca stable isotope record of a core from Lake Frassino, northern Italy: hydrological and climatic changes during the last 14 ka. *The Holocene*, 16(6), 827-837.
- Birks, S. J., Edwards, T. W. D., & Remenda, V. H. (2007). Isotopic evolution of Glacial Lake Agassiz: New insights from cellulose and porewater isotopic archives. *Palaeogeography, Palaeoclimatology, Palaeoecology*, 246, 8-22.
- Böhm, F., Joachimski, M., Lehnert, H., Morgenroth, G., Kretschmer, W., Vacelet, J., & Dullo, W.-C. (1996). Carbon isotope records from extant Caribbean and South Pacific sponges: Evolution of $\delta^{13}\text{C}$ in surface water DIC. *Earth and Planetary Science Letters*, 139(1-2), 291-303.
- Breckenridge, A. (2007). The Lake Superior varve stratigraphy and implications for eastern Lake Agassiz outflow from 10,700 to 8900 cal ybp (9.5–8.0 ^{14}C ka). *Palaeogeography, Palaeoclimatology, Palaeoecology*, 246, 45-61.
- Breckenridge, A., & Johnson, T. C. (2009). Paleohydrology of the upper Laurentian Great Lakes from the late glacial to early Holocene. *Quaternary Research*, 71, 397-408.
- Brenner, M., Whitmore, T. J., Curtis, J. H., Hodell, D. A., & Schelske, C. L. (1999). Stable isotope ($\delta^{13}\text{C}$ and $\delta^{15}\text{N}$) signatures of sedimented organic matter as indicators of historic lake trophic state. *Journal of Paleolimnology*, 22(2), 205-221.

- Brooks, G. R., Medioli, B. E., & Telka, A. M. (2012). Evidence of early Holocene closed basin conditions in the Huron-georgian basins from within the north bay outlet of the upper great lakes. *Journal of Paleolimnology*, 47, 469-492.
- Burch, J. B. (1982). Freshwater snails (Mollusca: Gastropoda) of North America. *United States Environmental Protection Agency-600, Contract no. 68-03-1280*.
- Burch, J. B. (1989). *North American Freshwater Snails*. Hamburg, Michigan: Malacological Publications.
- Burk, R., & Stuiver, M. (1981). Oxygen isotope ratios in trees reflect mean annual temperature and humidity. *Science*, 211(4489), 1417-1419.
- Carpenter, S. J., & Lohmann, K. C. (1995). $\delta^{18}\text{O}$ and $\delta^{13}\text{C}$ values of modern brachiopod shells. *Geochimica Et Cosmochimica Acta*, 59(18), 3749-3764.
- Casey, M. M., & Post, D. M. (2011). The problem of isotopic baseline: reconstructing the diet and trophic position of fossil animals. *Earth-Science Reviews*, 106(1), 131-148.
- Cerling, T. E., Bowman, J. R., & O'Neil, J. R. (1988). An isotopic study of a fluvial-lacustrine sequence: the Plio-Pleistocene Koobi Fora sequence, East Africa. *Palaeogeography, Palaeoclimatology, Palaeoecology*, 63(4), 335-356.
- Chandler, T., & Kostaschuk, R. (1994). Test of selected bed-material load transport models: Nottawasaga River, Ontario. *Canadian Journal of Civil Engineering*, 21(5), 770-777.
- Churcher, C. S., & Karrow, P. F. (2008). The Hamilton Bar Fauna: evidence for a Hypsithermal age. *Canadian Journal of Earth Sciences*, 45(12), 1487-1500. doi: 10.1139/e08-066
- Clark, J. A., Befus, K. M., & Sharman, G. R. (2012). A model of surface water hydrology of the Great Lakes North America during the past 16,000 years. *Physics and Chemistry of the Earth*, 53-54, 61-71.
- Clark, I.D. and Fritz, P. (1997). *Environmental isotopes in hydrogeology*. CRC press.
- Clark, J.A., Zylstra, D.J. and Befus, K.M., 2007. Effects of Great Lakes water loading upon glacial isostatic adjustment and lake history. *Journal of Great Lakes Research*, 33: 627-641.
- Clarke, A. H. (1973). *The freshwater molluscs of the Canadian Interior Basin* (Vol. 13).
- Clarke, A. H. (1981). *The freshwater molluscs of Canada*. Ottawa, Ontario, Canada: National Museum of Natural Sciences.
- Colman, S. M., Keigwin, L. D., & Forester, R. M. (1994). Two episodes of meltwater influx from glacial Lake Agassiz into the Lake Michigan basin and their climatic contrasts. *Geology*, 22(6), 547-550.

- Coniglio, M., Karrow, P. F., & Russell, P. (2006). *Manitoulin Rocks! Rocks, Fossils and Landforms of Manitoulin Island*. Waterloo: Earth Science Museum, University of Waterloo in partnership with the Geological Association of Canada and the Gore Bay Museum (Gore Bay, Manitoulin Island).
- Coplen, T. B. (1996). New guidelines for reporting stable hydrogen, carbon, and oxygen isotope ratio data. *Geochimica Et Cosmochimica Acta*, *17*, 3359-3360.
- Coplen, T. B., Brand, W. A., Gehre, M., Gröning, M., Meijer, H. A., Toman, B., & Verkouteren, R. M. (2006). New guidelines for $\delta^{13}\text{C}$ measurements. *Analytical Chemistry*, *78*(7), 2439-2441.
- Covich, A., & Stuiver, M. (1974). Changes in oxygen 18 as a measure of long-term fluctuations in tropical lake levels and molluscan populations. *Limnology and Oceanography*, *19*(4), 682-691.
- Craig, H. (1961). Isotopic Variations in Meteoric Waters. *Science*, *133*(3465), 1702-1703.
- Craig, H. (1965). The measurement of oxygen isotope paleotemperatures. *Stable isotopes in oceanographic studies and paleotemperatures*, *23*.
- Dansgaard, W. (1964). Stable isotopes in precipitation. *Tellus*, *16*(4), 436-468.
- Desaulniers, D. E., Cherry, J. A., & Fritz, P. (1981). Origin, age and movement of pore water in argillaceous Quaternary deposits at four sites in southwestern Ontario. *Journal of Hydrology*, *50*, 231-257.
- Dettman, D. L. (1994). *Stable isotope studies of fresh-water bivalves (Unionidae) and ostracodes (Podocopida): Implications for Late Cretaceous/Paleogene and Early Holocene paleoclimatology and paleo-hydrology of North America*. (Ph.D. Thesis), University of Michigan.
- Dettman, D. L., Flessa, K. W., Roopnarine, P. D., Schöne, B. R., & Goodwin, D. H. (2004). The use of oxygen isotope variation in shells of estuarine mollusks as a quantitative record of seasonal and annual Colorado River discharge. *Geochimica Et Cosmochimica Acta*, *68*(6), 1253-1263.
- Dettman, D. L., Reische, A. K., & Lohmann, K. C. (1999). Controls on the stable isotope composition of seasonal growth bands in aragonitic fresh-water bivalves (unionidae). *Geochimica Et Cosmochimica Acta*, *63*(7-8), 1049-1057.
- Dettman, D. L., Smith, A. J., Rea, D. K., Moore, T. C., & Lohmann, K. C. (1995). Glacial Meltwater in Lake Huron during Early Postglacial Time as Inferred from Single-Valve Analysis of Oxygen Isotopes in Ostracodes. *Quaternary Research*, *43*(3), 297-310.
- Dillon, R. T. J., T., W. B., Stewart, T. W., & Reeves, W. K. (2006). The freshwater gastropods of North America. Retrieved January, 2015, from <http://www.fwgna.org/>

- Edwards, T., Aravena, R., Fritz, P., & Morgan, A. (1985). Interpreting paleoclimate from ^{18}O and ^2H in plant cellulose: comparison with evidence from fossil insects and relict permafrost in southwestern Ontario. *Canadian Journal of Earth Sciences*, 22(11), 1720-1726.
- Edwards, T., & Fritz, P. (1986). Assessing meteoric water composition and relative humidity from ^{18}O and ^2H in wood cellulose: paleoclimatic implications for southern Ontario, Canada. *Applied Geochemistry*, 1(6), 715-723.
- Edwards, T., & McAndrews, J. H. (1989). Paleohydrology of a Canadian Shield lake inferred from ^{18}O in sediment cellulose. *Canadian Journal of Earth Sciences*, 26(9), 1850-1859.
- Edwards, T. W. D., Wolfe, B. B., & Macdonald, G. M. (1996). Influence of changing atmospheric circulation on precipitation $\delta^{18}\text{O}$ -temperature relations in Canada during the Holocene. *Quaternary Research*, 46(3), 211-218.
- Eschman, D. F., & Karrow, P. F. (1985). Huron Basin Glacial Lakes: A Review. In P. F. Karrow & P. E. Calkin (Eds.), *Geological Association of Canada Special Paper: Quaternary Evolution of the Great Lakes* (Vol. 30, pp. 79-94). Waterloo: Johans Graphics.
- Farrand, W. R., & Drexler, C. W. (1985). Late Wisconsinan and Holocene History of the Lake Superior Basin. In P. F. Karrow & P. E. Calkin (Eds.), *Geological Association of Canada Special Paper: Quaternary Evolution of the Great Lakes* (Vol. 30, pp. 17-32). Waterloo: Johans Graphics.
- Faure, G., & Mensing, T. M. (2005). *Isotopes: principles and applications*. Hoboken, N.J.: Wiley.
- Finamore, P. F. (1985). Glacial Lake Algonquin and the Fenelon Falls Outlet. *Geological Association of Canada Special Paper*, 30, 125-132.
- Finck, L. (2015). Lake Meditation #478: Condé Nast Collections.
- Foltz, S. (2013). Conservation Planning Documents, Species Fact Sheets, Snails and Slugs (Gastropoda): Valvata tricarinata, Three ridge Valvata. *US Forest Service, Interagency Special Status/Sensitive Species Program (ISSSSP)*, 28, 2013.
- Fricke, H. C., & O'Neil, J. R. (1999). The correlation between $^{18}\text{O}/^{16}\text{O}$ ratios of meteoric water and surface temperature: its use in investigating terrestrial climate change over geologic time. *Earth and Planetary Science Letters*, 170(3), 181-196.
- Friedman, I., & O'Neil, J. R. (1977). *Data of geochemistry: Compilation of stable isotope fractionation factors of geochemical interest* (Sixth ed. Vol. 440): US Government Printing Office.
- Friedman, I., & Smith, G. I. (1970). Deuterium content of snow cores from Sierra Nevada area. *Science*, 169(3944), 467-470.

- Fritz, P., Anderson, T. W., & Lewis, C. F. M. (1975). Late-Quaternary Climatic Trends and History of Lake Erie from Stable Isotope Studies. *Science*, 190(4211), 267-269.
- Fritz, P., & Poplawski, S. (1974). ^{18}O and ^{13}C in the shells of freshwater molluscs and their environment. *Earth and Planetary Science Letters*, 24, 91-98.
- Fuks, K. H., & Wilkinson, B. H. (1998). Holocene sedimentation in two western michigan estuaries. *Journal of Great Lakes Research*, 24(4), 822-837.
- Gavin, D. G., Henderson, A. C. G., Westover, K. S., Fritz, S. C., Walker, I. R., Leng, M. J., & Hu, F. S. (2011). Abrupt Holocene climate change and potential response to solar forcing in western Canada. *Quaternary Science Reviews*, 30, 1243-1255.
- Ghosh, P., Adkins, J., Affek, H., Balta, B., Guo, W., Schauble, E.A., Schrag, D. and Eiler, J.M. (2006). ^{13}C - ^{18}O bonds in carbonate minerals: A new kind of paleothermometer. *Geochimica et Cosmochimica Acta*, 70(6): 1439-1456.
- Godsey, H. S., Moore, J., Theodore C, Rea, D. K., & Shane, L. C. (1999). Post-Younger Dryas seasonality in the North American midcontinent region as recorded in Lake Huron varved sediments. *Canadian Journal of Earth Sciences*, 36(4), 533-547.
- Godwin, A. G. (1985). *Stable Isotope Analyses on Postglacial Fluvial and Terrestrial Molluscs from the Kincardine Area of Southern Ontario*. (Master of Science), University of Waterloo.
- Gonfiantini, R. (1986). Environmental isotopes in lake studies. *Handbook of environmental isotope geochemistry*, 2, 113-168.
- Goodrich, C. (1945). *Goniobasis livescens of Michigan* (Vol. 64). Ann Arbor: University of Michigan Press.
- Goodwin, D. H., Schöne, B. R., & Dettman, D. L. (2003). Resolution and Fidelity of Oxygen Isotopes as Paleotemperature Proxies in Bivalve Mollusk Shells: Models and Observations. *PALAIOS*, 18(2), 110-125.
- Google Earth (2016) (Version 7.1.4.1529). Retrieved from <https://www.google.ca/earth>
- Government of Canada (2016). Monthly Climate Summaries. Retrieved Feb, 2017, from http://climate.weather.gc.ca/prods_servs/cdn_climate_summary_e.html
- Gravenor, C. P., & Coyle, D. A. (1985). Origin and magnetic fabric of glacial varves, Nottawasaga River, Ontario, Canada. *Canadian Journal of Earth Sciences*, 22(2), 291-294.
- Grootes, P. (1993). Interpreting continental oxygen isotope records. *Climate change in continental isotopic records*, 37-46.

- Guiguer, K. R. R. D. A. (2000). *Determination of Colpoys Bay (Georgian Bay) benthic community trophic structure and energy flow using stable isotopes and secondary production*. (Ph.D. Thesis), University of Waterloo.
- Haeri-Ardakani, O., Al-Aasm, I., & Coniglio, M. (2013). Petrologic and geochemical attributes of fracture-related dolomitization in Ordovician carbonates and their spatial distribution in southwestern Ontario, Canada. *Marine and Petroleum Geology*, *43*, 409-422.
- Hammarlund, D., Aravena, R., Barnekow, L., Buchardt, B., & Possnert, G. (1997). Multi-component carbon isotope evidence of early Holocene environmental change and carbon-flow pathways from a hard-water lake in northern Sweden. *Journal of Paleolimnology*, *18*(3), 219-233.
- Hansel, A. K., Mickelson, D. M., Schneider, A. F., & Larsen, C. E. (1985). Late Wisconsinan and Holocene History of the Lake Michigan Basin. *Geological Association of Canada Special Paper*, *30*, 39-53.
- Heath, A. J., & Karrow, P. F. (2007). Northernmost (?) Glacial Lake Algonquin Series Shorelines, Sudbury Basin, Ontario. *Journal of Great Lakes Research*, *33*(1), 264-278.
- Hladyniuk, R. and Longstaffe, F.J. (2015). Paleoproductivity and organic matter sources in Late Quaternary Lake Ontario. *Palaeogeography Palaeoclimatology Palaeoecology*, *435*: 13-23.
- Hladyniuk, R. and Longstaffe, F.J. (2016). Oxygen-isotope variations in post-glacial Lake Ontario. *Quaternary Science Reviews*, *134*: 39-50.
- Holmes, J. A. (1996). Trace-element and stable-isotope geochemistry of non-marine ostracod shells in Quaternary palaeoenvironmental reconstruction. *Journal of Paleolimnology*, *15*(3), 223-235.
- Holopainen, I. J. (1980). Growth of Two *Pisidium* (Bivalvia, Sphaeriidae) Species in the Laboratory. *Oecologia*, *45*(1), 104-108.
- Hough, J.L. (1958). *Geology of the Great lakes*. University of Illinois Press.
- Huddart, P., Longstaffe, F. and Crowe, A., 1999. δD and $\delta^{18}O$ evidence for inputs to groundwater at a wetland coastal boundary in the southern Great Lakes region of Canada. *Journal of Hydrology*, *214*(1): 18-31.
- Hunter, R. D., Panyushkina, I. P., Leavitt, S. W., Wiedenhoeft, A. C., & Zawiskie, J. (2006). A multiproxy environmental investigation of Holocene wood from a submerged conifer forest in Lake Huron, USA. *Quaternary Research*, *66*(1), 67-77.
- Hyodo, A., & Longstaffe, F. J. (2011a). The chronostratigraphy of Holocene sediments from four Lake Superior sub-basins. *Canadian Journal of Earth Science*, *48*, 1581-1599.

- Hyodo, A., & Longstaffe, F. J. (2011b). The palaeoproductivity of ancient Lake Superior. *Quaternary Science Reviews*, 30, 2988-3000.
- Hyodo, A., & Longstaffe, F. J. (2012). Variations in the oxygen-isotope composition of ancient Lake Superior between 10,600 and 8,800 cal BP. *Journal of Paleolimnology*, 47, 327-338.
- International Joint Commission (2010). Groundwater in the Great Lakes Basin: Report of the Great Lakes Science Advisory Board to the International Joint Commission 2010. *International Joint Commission, Windsor, Canada*, 155.
- Jokinen, E. (1983). The freshwater snails of Connecticut. *Bulletin Connecticut Geological and Natural History Survey*(109), 1-83.
- Jones, D. S., & Quitmyer, I. R. (1996). Marking time with bivalve shells: oxygen isotopes and season of annual increment formation. *PALAIOS*, 11(4), 340-346.
- Jones, M. D., Leng, M. J., Eastwood, W. J., Keen, D. H., & Turney, C. S. M. (2002). Interpreting stable-isotope records from freshwater snail-shell carbonate: a Holocene case study from Lake Golhisar, Turkey. *The Holocene*, 12(5), 629-634.
- Karrow, P. F. (1986a). Valley terraces and Huron basin water levels, southwestern Ontario. *GSA Bulletin*, 97(9), 1089-1097.
- Karrow, P. F. (1986b). Valley terraces and Lake Algonquin shoreline position, southeast shore of Lake Huron, Canada. *Journal of Great Lakes Research*, 12(2), 132-135.
- Karrow, P. F. (2004). Algonquin-Nipissing Shorelines, North Bay, Ontario. *Géographie physique et Quaternaire*, 58(2-3), 297-304.
- Karrow, P. F., & Mackie, G. L. (2013). Postglacial lake shoreline surveys and lacustrine paleobiotic records in northern Bruce and Grey counties, Ontario, Canada. *Journal of Great Lakes Research*, 39(1), 100-109.
- Keith, M., & Weber, J. N. (1964). Carbon and oxygen isotopic composition of selected limestones and fossils. *Geochimica Et Cosmochimica Acta*, 28(10), 1787-1816.
- Keith, M. L., Anderson, G. M., & Eichler, R. (1964). Carbon and oxygen isotopic composition of mollusk shells from marine and fresh-water environments. *Geochimica Et Cosmochimica Acta*, 28, 1757-1786.
- Kerr-Lawson, L., Karrow, P., Edwards, T., & Mackie, G. (1992). A paleoenvironmental study of the molluscs from the Don Formation (Sangamonian?) Don Valley Brickyard, Toronto, Ontario. *Canadian Journal of Earth Sciences*, 29(11), 2406-2417.
- Kilgour, B. W., & Mackie, G. L. (1991). Relationships between demographic features of a pill clam (*Pisidium casertanum*) and environmental variables. *Journal of the North American Benthological Society*, 10(1), 68-80.

- Kohn, M. J., & Dettman, D. L. (2007). Paleoaltimetry from stable isotope compositions of fossils. *Reviews in Mineralogy and Geochemistry*, 66(1), 119-154.
- Kutzbach, J. E., Guetter, P. J., Behling, P., & Selin, R. (1993). Simulated climatic changes: results of the COHMAP climate-model experiments. *Global climates since the last glacial maximum*, 24-93.
- La Rocque, A. (1974). Non-marine Pleistocene Mollusca. *HOW TO COLLECT SHELLS*.
- Larsen, C. E. (1985). Lake Level, Uplift, and Outlet Incision, the Nipissing and Algoma Great Lakes. In P. F. Karrow & P. E. Calkin (Eds.), *Geological Association of Canada Special Paper: Quaternary Evolution of the Great Lakes* (Vol. 30, pp. 63-78). Waterloo: Johanns Graphics.
- Larsen, C. E. (1987). Geological history of glacial Lake Algonquin and the upper Great Lakes. *U.S. Geological Survey Bulletin*, 1801, 44.
- Larson, G., & Schaetzl, R. (2001). Origin and evolution of the Great Lakes. *Journal of Great Lakes Research*, 27(4), 518-546.
- Lécuyer, C., Hutzler, A., Amiot, R., Daux, V., Grosheny, D., Otero, O., Martineau, F., *et al.* (2012). Carbon and oxygen isotope fractionations between aragonite and calcite of shells from modern molluscs. *Chemical Geology*, 332–333(0), 92-101.
- Leng, M. J., Jones, M. D., Frogley, M. R., Eastwood, W. J., Kendrick, C. P., & Roberts, C. N. (2010). Detrital carbonate influences on bulk oxygen and carbon isotope composition of lacustrine sediments from the Mediterranean. *Global and Planetary Change*, 71(3), 175-182.
- Leng, M. J., Lamb, A. L., Lamb, H. F., & Telford, R. J. (1999). Palaeoclimatic implications of isotopic data from modern and early Holocene shells of the freshwater snail *Melanoides tuberculata*, from lakes in the Ethiopian Rift Valley. *Journal of Paleolimnology*, 21(1), 97-106.
- Leng, M. J., & Lewis, J. P. (2016). Oxygen isotopes in Molluscan shell: Applications in environmental archaeology. *Environmental Archaeology*, 21(3), 295-306.
- Leng, M. J., & Marshall, J. D. (2004). Palaeoclimate interpretation of stable isotope data from lake sediment archives. *Quaternary Science Reviews*, 23(7–8), 811-831.
- Leverington, D., & Teller, J. (2003). Paleotopographic reconstructions of the eastern outlets of glacial Lake Agassiz. *Canadian Journal of Earth Sciences*, 40(9), 1259-1278.
- Lewis, C., & Anderson, T. (1989). Oscillations of levels and cool phases of the Laurentian Great Lakes caused by inflows from glacial Lakes Agassiz and Barlow-Ojibway. *Journal of Paleolimnology*, 2(2), 99-146.
- Lewis, C. F. M. (2016). Understanding the Holocene Closed-Basin Phases (Lowstands) of the Laurentian Great Lakes and Their Significance. *Geoscience Canada*, 43, 179-198.

- Lewis, C. F. M., & Anderson, T. W. (2012). The sedimentary and palynological records of Serpent River Bog, and revised early Holocene lake-level changes in the Lake Huron and Georgian Bay region. *Journal of Paleolimnology*, *47*, 391-410.
- Lewis, C. F. M., Blasco, S. M., & Gareau, P. L. (2005). Glacial Isostatic Adjustment of the Laurentian Great Lakes Basin: Using the Empirical Record of Strandline Deformation for Reconstruction of Early Holocene Paleo-Lakes and Discovery of a Hydrologically Closed Phase. *Géographie physique et Quaternaire*, *59*(2-3), 187-210.
- Lewis, C. F. M., Heil Jr., C. W., Hubeny, J. B., King, J. W., Moore Jr., T. C., & Rea, D. K. (2007). The Stanley unconformity in Lake Huron basin: evidence for a climate-driven closed lowstand about 7900 ¹⁴C BP, with similar implications for the Chippewa lowstand in Lake Michigan basin. *Journal of Paleolimnology*, *37*, 435-452.
- Lewis, C. F. M., Karrow, P., Blasco, S. M., McCarthy, F. M. G., King, J. W., Moore, T., & Rea, D. (2008a). Evolution of lakes in the Huron basin: Deglaciation to present. *Aquatic Ecosystem Health & Management*, *11*(2), 127-136.
- Lewis, C. F. M., King, J. W., Blasco, S. M., Brooks, G. R., Coakley, J. P., Croley II, T. E., *et al.* (2008b). Dry Climate Disconnected the Laurentide Great Lakes. *Eos, Transitions, American Geophysical Union*, *89*(52), 541-542.
- Lewis, C. F. M., Moore, T. C., Rea, D. K., Dettman, D. L., Smith, A. M., & Mayer, L. A. (1994). Lakes of the Huron basin: their record of runoff from the laurentide ice sheet. *Quaternary Science Reviews*, *13*(9-10), 891-922.
- Lewis, C. F. M., Rea, D. K., Hubeny, J. B., Thompson, T. A., Blasco, S. M., King, J. W., *et al.* (2010). Using geological history of the Laurentian Great Lakes to better understand their future. *Aquatic Ecosystem Health & Management*, *13*(2), 118-126.
- Lewis, J., & Leng, M. (2014). Snail shells provide detailed records of environmental change. *Climatica*.
- Li, H.-C. (1995). *Isotope geochemistry of Mono Basin, California: Applications to paleoclimate and paleohydrology*.
- Li, H.-C., Xu, X.-M., Ku, T.-L., You, C.-F., Buchheim, H. P., & Peters, R. (2008). Isotopic and geochemical evidence of palaeoclimate changes in Salton Basin, California, during the past 20 kyr: 1. $\delta^{18}\text{O}$ and $\delta^{13}\text{C}$ records in lake tufa deposits. *Palaeogeography, Palaeoclimatology, Palaeoecology*, *259*(2), 182-197.
- Li, H. C., & Ku, T. L. (1997). $\delta^{13}\text{C}$ – $\delta^{18}\text{C}$ covariance as a paleohydrological indicator for closed-basin lakes. *Palaeogeography, Palaeoclimatology, Palaeoecology*, *133*(1–2), 69-80.
- Liu, W., Li, X., An, Z., Xu, L., & Zhang, Q. (2013). Total organic carbon isotopes: A novel proxy of lake level from Lake Qinghai in the Qinghai–Tibet Plateau, China. *Chemical Geology*, *347*, 153-160.

- Longstaffe, F. J., Ayalon, A., Hladyniuk, R., Hyodo, A., Macdonald, A. R., St. Amout, N., *et al.* (2013). *The Oxygen and Hydrogen Isotope Evolution of the Great Lakes*. Paper presented at the International Atomic Energy Agency, Vienna, Austria.
- Macdonald, R. A. (2012). *The Late Quaternary Histories of Lakes Huron and Michigan: stable isotope investigation of sediment cores and modern biogenic carbonates*. (Doctor of Philosophy Integrated Article), University of Western Ontario.
- Macdonald, R. A., & Longstaffe, F. J. (2008). The Late Quaternary oxygen-isotope composition of Southern Lake Huron. *Aquatic Ecosystem Health & Management*, 11(2), 137-143.
- Mackie, G. L., White, D. S., & Zdeba, T. W. (1980). *A guide to freshwater mollusks of the Laurentian Great Lakes with special emphasis on the genus Pisidium*. University of Guelph: Department of Zoology.
- MacLaren Plansearch Inc. (1988). Watershed hydrology study for Nottawasaga, Pretty and Batteaux Rivers, Black Ash, Silver and Sturgeon Creeks. Volumes I and II. *Ontario Ministry of Natural Resources, and Environment Canada in part of the Canada/Ontario Flood Damage Reduction Program* (Vol. Unpublished report (43347) prepared for the Nottawasaga Valley Conservation Authority).
- MacLeod, N. A., & Barton, D. R. (1998). Effects of light intensity, water velocity, and species composition on carbon and nitrogen stable isotope ratios in periphyton. *Canadian Journal of Fisheries and Aquatic Sciences*, 55(8), 1919-1925.
- Magnuson, J., Webster, K., Assel, R., Bowser, C., Dillon, P., Eaton, J., Evans, H. *et al.* (1997). Potential effects of climate changes on aquatic systems: Laurentian Great Lakes and Precambrian Shield Region. *Hydrological Processes*, 11(8), 825-871.
- Massachusetts Division of Fisheries and Wildlife (2015). Boreal Turret Snail *Valvata sincera*. *Natural Heritage & Endangered Species Program*, 2. Retrieved Feb, 2015 from www.mass.gov/nhesp website:
- Mayer, D. E. B.-Y., Leng, M. J., Aldridge, D. C., Arrowsmith, C., Gümüş, B. A., & Sloane, H. J. (2012). Modern and early-middle Holocene shells of the freshwater mollusc *Unio*, from Çatalhöyük in the Konya Basin, Turkey: preliminary palaeoclimatic implications from molluscan isotope data. *Journal of Archaeological Science*, 39(1), 76-83.
- McAndrews, J., & Campbell, I. (1993). 6 ka mean July temperature in eastern Canada from Bartlein and Webb's (1985) pollen transfer functions.
- McConnaughey, T. (1989a). ^{13}C and ^{18}O isotopic disequilibrium in biological carbonates: I. Patterns. *Geochimica Et Cosmochimica Acta*, 53(1), 151-162.
- McConnaughey, T. (1989b). ^{13}C and ^{18}O isotopic disequilibrium in biological carbonates: II. *In vitro* simulation of kinetic isotope effects. *Geochimica Et Cosmochimica Acta*, 53(1), 163-171.

- McConnaughey, T., & Gillikin, D. P. (2008). Carbon isotopes in mollusk shell carbonates. *Geo-Marine Letters*, 28(5), 287-299.
- McConnaughey, T. A., Burdett, J., Whelan, J. F., & Paull, C. K. (1997). Carbon isotopes in biological carbonates: Respiration and photosynthesis. *Geochimica Et Cosmochimica Acta*, 61(3), 611-622.
- McFadden, M. A., Patterson, W. P., Mullins, H. T., & Anderson, W. T. (2005). Multi-proxy approach to long-and short-term Holocene climate-change: evidence from eastern Lake Ontario. *Journal of Paleolimnology*, 33(3), 371-391.
- McIntosh, J., & Walter, L. (2006). Paleowaters in Silurian-Devonian carbonate aquifers: Geochemical evolution of groundwater in the Great Lakes region since the Late Pleistocene. *Geochimica Et Cosmochimica Acta*, 70(10), 2454-2479.
- Meyers, P. A. (1997). Organic geochemical proxies of paleoceanographic, paleolimnologic, and paleoclimatic processes. *Organic Geochemistry*, 27(5-6), 213-250.
- Meyers, P. A., & Lallier-Vergès, E. (1999). Lacustrine sedimentary organic matter records of Late Quaternary paleoclimates. *Journal of Paleolimnology*, 21(3), 345-372.
- Michener, R. H., Kaufman, L., Michener, R., & Lajtha, K. (2007). Stable isotope ratios as tracers in marine food webs: an update. *Stable isotopes in ecology and environmental science*, 2, 238-282.
- Miller, B. B., Karrow, P. F., & Kalas, L. L. (1979). Late Quaternary mollusks from glacial Lake Algonquin, Nipissing, and transitional sediments from southwestern Ontario, Canada. *Quaternary Research*, 11(1), 93-112.
- Miller, B. B., Karrow, P. F., & Mackie, G. L. (1985). Late Quaternary Molluscan Faunal Changes in the Huron Basin. In P. F. Karrow & P. E. Calkin (Eds.), *Geological Association of Canada Special Paper: Quaternary Evolution of the Great Lakes* (Vol. 30, pp. 95-108). Waterloo: Johanns Graphics.
- Mitchell, L., Fallick, A. E., & Curry, G. B. (1994). Stable carbon and oxygen isotope compositions of mollusc shells from Britain and New Zealand. *Palaeogeography, Palaeoclimatology, Palaeoecology*, 111(3-4), 207-216.
- Mohseni, O., & Stefan, H. (1999). Stream temperature/air temperature relationship: a physical interpretation. *Journal of Hydrology*, 218(3), 128-141.
- Mook, W. G. (1971). Paleotemperatures and chlorinities from stable carbon and oxygen isotopes in shell carbonate. *Palaeogeography, Palaeoclimatology, Palaeoecology*, 9(4), 245-263.
- Mook, W. G., & Vogel, J. C. (1968). Isotopic Equilibrium between Shells and Their Environment. *Science*, 159(3817), 874-875.

- Moore, T., Walker, J., Rea, D. K., Lewis, C., Shane, L., & Smith, A. (2000). Younger Dryas interval and outflow from the Laurentide ice sheet. *Paleoceanography*, *15*(1), 4-18.
- Mortsch, L. D., & Quinn, F. H. (1996). Climate change scenarios for Great Lakes Basin ecosystem studies. *Limnology and Oceanography*, *41*, 903-911.
- Nichols, G. (2009). *Sedimentology and stratigraphy* (Second edition ed.): John Wiley & Sons.
- Nottawasaga Valley Conservation Authority (2014). Healthy Watershed, Healthy Communities. Retrieved Feb, 2017, from <http://www.nvca.on.ca/>
- Perez, K. E., Clark, S. A., & Lydeard, C. (2004). *Freshwater Gastropod Identification Workshop*: University of Alabama.
- Pickering, D. (2016). Discover Life - Molluscs. Retrieved July 21st, 2016
- Post, D. M. (2002). Using stable isotopes to estimate trophic position: models, methods, and assumptions. *Ecology*, *83*(3), 703-718.
- Poulain, C., Lorrain, A., Mas, R., Gillikin, D. P., Dehairs, F., Robert, R., & Paulet, Y.-M. (2010). Experimental shift of diet and DIC stable carbon isotopes: Influence on shell $\delta^{13}\text{C}$ values in the Manila clam *Ruditapes philippinarum*. *Chemical Geology*, *272*(1), 75-82.
- Prendergast, A. L., & Stevens, R. E. (2015). Molluscs (isotopes) – Analyses in environmental archaeology *The Encyclopedia of Global Archaeology*. New York: Springer.
- Prest, V. K. (1970). *Quaternary geology of Canada*: Department of Energy, Mines and Resources.
- Quinn, F. H. (1992). Hydraulic residence times for the Laurentian Great Lakes. *Journal of Great Lakes Research*, *18*(1), 22-28.
- Rea, D. K., Moore Jr., T. C., Lewis, C. F. M., Mayer, L. A., Dettman, D. L., Smith, A. J., & Dobson, D. M. (1994). Stratigraphy and paleolimnologic record of lower Holocene sediments in northern Lake Huron and Georgian Bay. *Canadian Journal of Earth Science*, *31*, 1586-1605.
- Rodie, A., Post, R., & Authority, N. V. C. (2009). Niagara Escarpment baseflow study. *Utopia, ON: Nottawasaga Valley Conservation Authority*, 59.
- Romanek, C. S., & Grossman, E. L. (1989). Stable isotope profiles of *Tridacna maxima* as environmental indicators. *PALAIOS*, 402-413.
- Routh, J., Choudhary, P., Meyers, P. A., & Kumar, B. (2009). A sediment record of recent nutrient loading and trophic state change in Lake Norrviken, Sweden. *Journal of Paleolimnology*, *42*(3), 325-341.

- Rozanski, K., Araguás- Araguás, L., & Gonfiantini, R. (1993). Isotopic patterns in modern global precipitation. *Climate change in continental isotopic records*, 1-36.
- Sackett, W. M., Eckelmann, W. R., Bender, M. L., & Bé, A. W. (1965). Temperature dependence of carbon isotope composition in marine plankton and sediments. *Science*, 148(3667), 235-237.
- Schmitt, J., Schneider, R., Elsig, J., Leuenberger, D., Laurantou, A., Chappellaz, J., Köhler, P., Joos, F., Stocker, T.F. and Leuenberger, M. (2012). Carbon isotope constraints on the deglacial CO₂ rise from ice cores. *Science*, 336(6082): 711-714.
- Schubert, B. A., & Jahren, A. H. (2015). Seasonal temperature and precipitation recorded in the intra-annual oxygen isotope pattern of meteoric water and tree-ring cellulose. *Quaternary Science Reviews*, 125, 1-14.
- Sharp, Z. (2007). *Principles of stable isotope geochemistry*. Upper Saddle River, N.J: Pearson/Prentice Hall.
- Shuman, B., Bartlein, P., Logar, N., Newby, P., & Webb, T. (2002). Parallel climate and vegetation responses to the early Holocene collapse of the Laurentide Ice Sheet. *Quaternary Science Reviews*, 21(16), 1793-1805.
- Shuman, B. N. (2001). *Vegetation response to moisture-balance and abrupt climate change in eastern North America during the late-Quaternary*. (Ph.D. Thesis), Brown University.
- Sinokrot, B. A., & Stefan, H. G. (1993). Stream temperature dynamics: measurements and modeling. *Water resources research*, 29(7), 2299-2312.
- Smol, J. P., & Boucherle, M. M. (1985). Postglacial changes in algal and cladoceran assemblages in Little Round Lake, Ontario. *Archiv fur Hydrobiologie Vo. 103*(1).
- Stott, L. D. (2002). The influence of diet on the $\delta^{13}\text{C}$ of shell carbon in the pulmonate snail *Helix aspersa*. *Earth and Planetary Science Letters*, 195(3), 249-259.
- Stuiver, M. (1968). Oxygen-18 content of atmospheric precipitation during last 11,000 years in the Great Lakes region. *Science*, 162(3857), 994-997.
- Stuiver, M. (1970). Oxygen and carbon isotope ratios of fresh-water carbonates as climatic indicators. *Journal of Geophysical Research*, 75, 5247-5257.
- Szaran, J. (1998). Carbon isotope fractionation between dissolved and gaseous carbon dioxide. *Chemical Geology*, 150(3), 331-337.
- Talbot, M. R. (1990). A review of the palaeohydrological interpretation of carbon and oxygen isotopic ratios in primary lacustrine carbonates. *Chemical Geology: Isotope Geoscience section*, 80(4), 261-279.

- Teller, J. T. (1987). Proglacial lakes and the southern margin of the Laurentide Ice Sheet. *North America and adjacent oceans during the last deglaciation*, 3, 39-69.
- Teller, J. T., & Thorleifson, L. H. (1983). The Lake Agassiz–Lake Superior connection *Glacial Lake Agassiz* (Vol. 26, pp. 261-290): Geological Associations of Canada.
- Terasmae, J. (1961). Notes on the Late-Quaternary Climate Changes in Canada. *Annals of the New York Academy of Sciences*, 95(1), 658-675.
- Thomas, R., Kemp, A., & Lewis, C. (1973). The surficial sediments of Lake Huron. *Canadian Journal of Earth Sciences*, 10(2), 226-271.
- Thompson, T. A., & Baedke, S. J. (1995). Beach-ridge development in Lake Michigan: shoreline behavior in response to quasi-periodic lake-level events. *Marine Geology*, 129(1), 163-174.
- Thornbush, M. J. (2001). *Holocene Floodplain Development and Prehistoric Human Occupation: Lower Nottawasaga River, Southern Ontario, Canada*. (Masters of Science), University of Toronto.
- Torres, I. C., Inglett, P. W., Brenner, M., Kenney, W. F., & Reddy, K. R. (2012). Stable isotope ($\delta^{13}\text{C}$ and $\delta^{15}\text{N}$) values of sediment organic matter in subtropical lakes of different trophic status. *Journal of Paleolimnology*, 47(4), 693-706.
- Turner, J. V. (1982). Kinetic fractionation of carbon-13 during calcium carbonate precipitation. *Geochimica Et Cosmochimica Acta*, 46(7), 1183-1191.
- Turnipseed, D. P., & Sauer, V. B. (2010). Discharge measurements at gaging stations: US Geological Survey.
- Urey, H. C. (1947). The thermodynamic properties of isotopic substances. *Journal of the Chemical Society (Resumed)*, 562-581.
- USEPA. (1995). *The Great Lakes, an environmental atlas and resource book* (Vol. 3rd edition). Chicago: United States Environmental Protection Agency.
- USEPA. (2016). Great Lakes Fact Sheet: Lake Huron. Retrieved Jan, 2016, from <https://www.epa.gov/greatlakes/great-lakes-facts-and-figures>
- Van Beynen, P., & Febroriello, P. (2006). Seasonal isotopic variability of precipitation and cave drip water at Indian Oven Cave, New York. *Hydrological Processes*, 20(8), 1793-1803.
- Van der Schalie, H., & Berry, E. G. (1973). *Effects of temperature on growth and reproduction of aquatic snails*: Office of Research and Monitoring, US Environmental Protection Agency.

- Vogel, J. (1993). Variability of Carbon Isotope Fractionation during Photosynthesis. *Ehleringer JR, Hall AE, Farquhar GD (eds) Stable isotopes and plant carbon-water relations*, 29.
- von Grafenstein, U., Belmecheri, S., Eicher, U., van Raden, U. J., Erlenkeuser, H., Anderson, N., & Ammann, B. (2013). The oxygen and carbon isotopic signatures of biogenic carbonates in Gerzensee, Switzerland, during the rapid warming around 14,685 years BP and the following interstadial. *Palaeogeography Palaeoclimatology Palaeoecology*, 391, 25-32.
- von Grafenstein, U., Erlenkeuser, H., Kleinmann, A., Müller, J., & Trimborn, P. (1994). High-frequency climatic oscillations during the last deglaciation as revealed by oxygen-isotope records of benthic organisms (Ammersee, southern Germany). *Journal of Paleolimnology*, 11(3), 349-357.
- von Grafenstein, U., Erlenkeuser, H., Müller, J., Trimborn, P., & Alefs, J. (1996). A 200 year mid-European air temperature record preserved in lake sediments: an extension of the $\delta^{18}\text{O}_p$ -air temperature relation into the past. *Geochimica Et Cosmochimica Acta*, 60(21), 4025-4036.
- von Grafenstein, U., Erlenkeuser, H., & Trimborn, P. (1999). Oxygen and carbon isotopes in modern fresh-water ostracod valves: assessing vital offsets and autecological effects of interest for palaeoclimate studies. *Palaeogeography, Palaeoclimatology, Palaeoecology*, 148, 133-152.
- Wakabyashi, N. (2010). *An assessment of meltwater influx using oxygen- and carbon-isotope compositions of ostracodes from Holocene sediments of northeastern Lake Huron*. (B.Sc.), University of Western Ontario.
- Walker, R. (2004). Density of Water, Simetric. Retrieved Dec, 2016, from http://www.simetric.co.uk/si_water.htm
- Warner, B. G., Hebda, R. J., & Hann, B. J. (1984). Postglacial paleoecological history of a cedar swamp, Manitoulin Island, Ontario, Canada. *Palaeogeography, Palaeoclimatology, Palaeoecology*, 45, 301-345.
- Way, C. M. (1988). An analysis of life histories in freshwater bivalves (Mollusca: Pisidiidae). *Canadian Journal of Zoology*, 66(5), 1179-1183.
- Way, C. M., & Wissing, T. E. (1982). Environmental heterogeneity and life history variability in the freshwater clams, *Pisidium variabile* (Prime) and *Pisidium compressum* (Prime) (Bivalvia: Pisidiidae). *Canadian Journal of Zoology*, 60(11), 2841-2851.
- Webb III, T., Bartlein, P. J., & Kutzbach, J. E. (1987). Climatic change in eastern North America during the past 18,000 years; comparisons of pollen data with model results. *North America and adjacent oceans during the last deglaciation. Geological Society of America, Boulder*, 447-462.

- Wefer, G., & Berger, W. H. (1991). Isotope paleontology: growth and composition of extant calcareous species. *Marine Geology*, *100*(1), 207-248.
- Wolfe, B. B., Karst- Riddoch, T. L., Hall, R. I., Edwards, T. W., English, M. C., Palmieri, R., *et al.* (2007). Classification of hydrological regimes of northern floodplain basins (Peace–Athabasca Delta, Canada) from analysis of stable isotopes ($\delta^{18}\text{O}$, $\delta^2\text{H}$) and water chemistry. *Hydrological Processes*, *21*(2), 151-168.
- Woszczyk, M., Grassineau, N., Tylman, W., Kowalewski, G., Lutynska, M., & Bechtel, A. (2014). Stable C and N isotope record of short term changes in water level in lakes of different morphometry: Lake Anastazewo and Lake Skulskie, central Poland. *Organic Geochemistry*, *76*, 278-287.
- Yu, Z. (2000). Ecosystem response to Lateglacial and early Holocene climate oscillations in the Great Lakes region of North America. *Quaternary Science Reviews*, *19*, 1723-1747.
- Yu, Z., & Eicher, U. (1998). Abrupt climate oscillations during the last deglaciation in central North America. *Science*, *282*(5397), 2235-2238.
- Yu, Z., McAndrews, J. H., & Siddiqi, D. (1995). Influences of Holocene climate and water levels on vegetation dynamics of a lakeside wetland. *Canadian Journal of Botany*, *74*, 1602-1615.
- Yu, Z., & Wright, H. (2001). Response of interior North America to abrupt climate oscillations in the North Atlantic region during the last deglaciation. *Earth-Science Reviews*, *52*(4), 333-369.
- Zar, J. H. (1996). *Biostatistical analysis* (3rd ed.). Prentice Hall.
- Zuppi, G. M. (1981). *Statistical treatment of environmental isotope data in precipitation*: International Atomic Energy Agency.

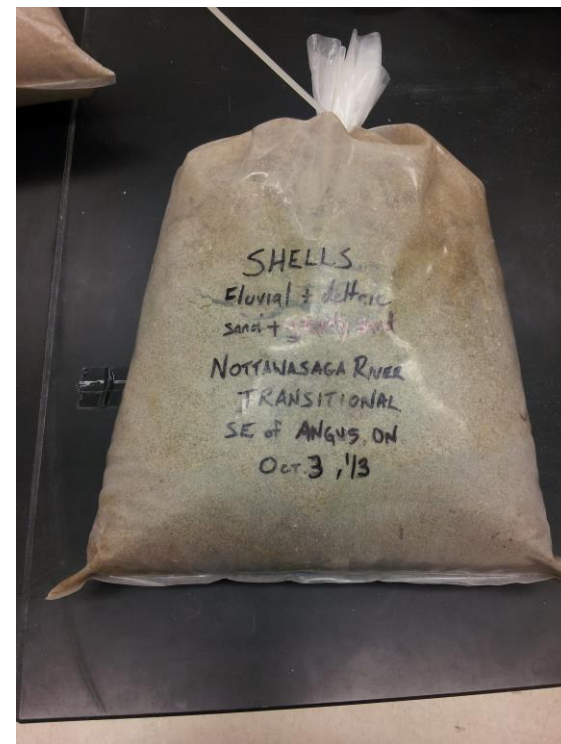
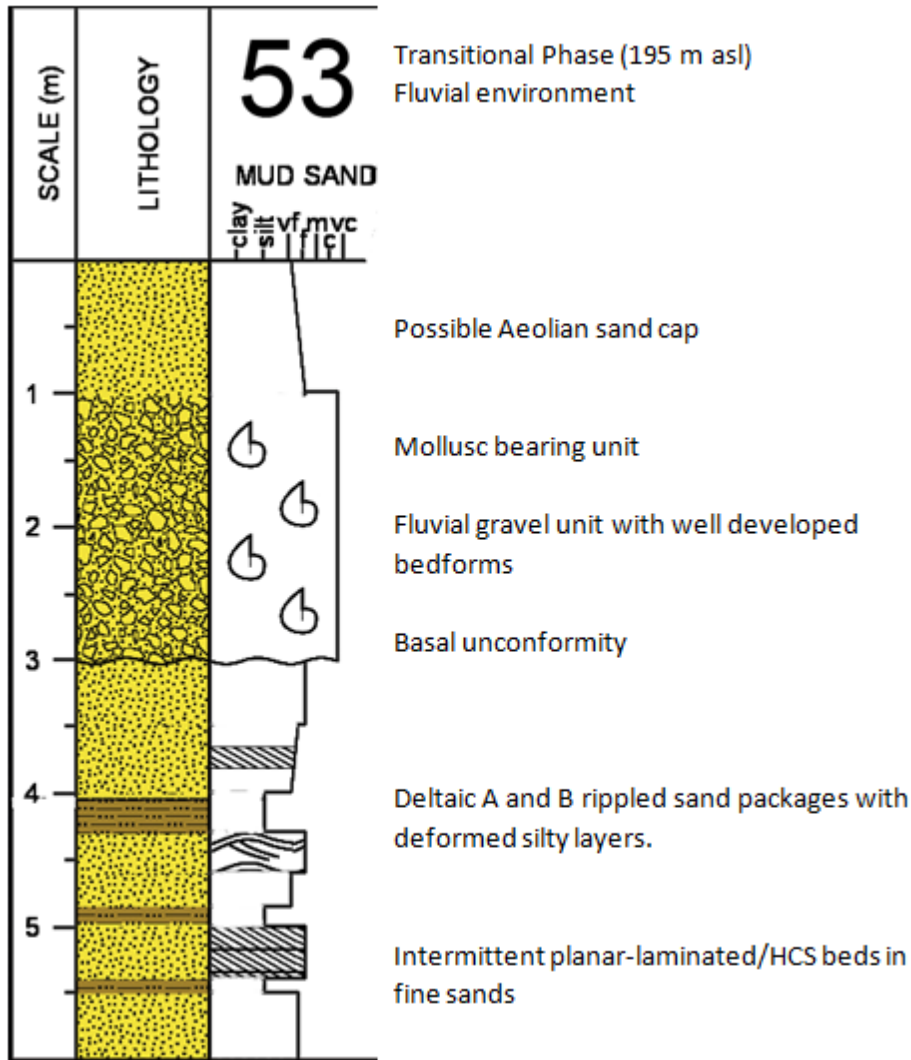
Appendices

Appendix A - Site Descriptions and Locations

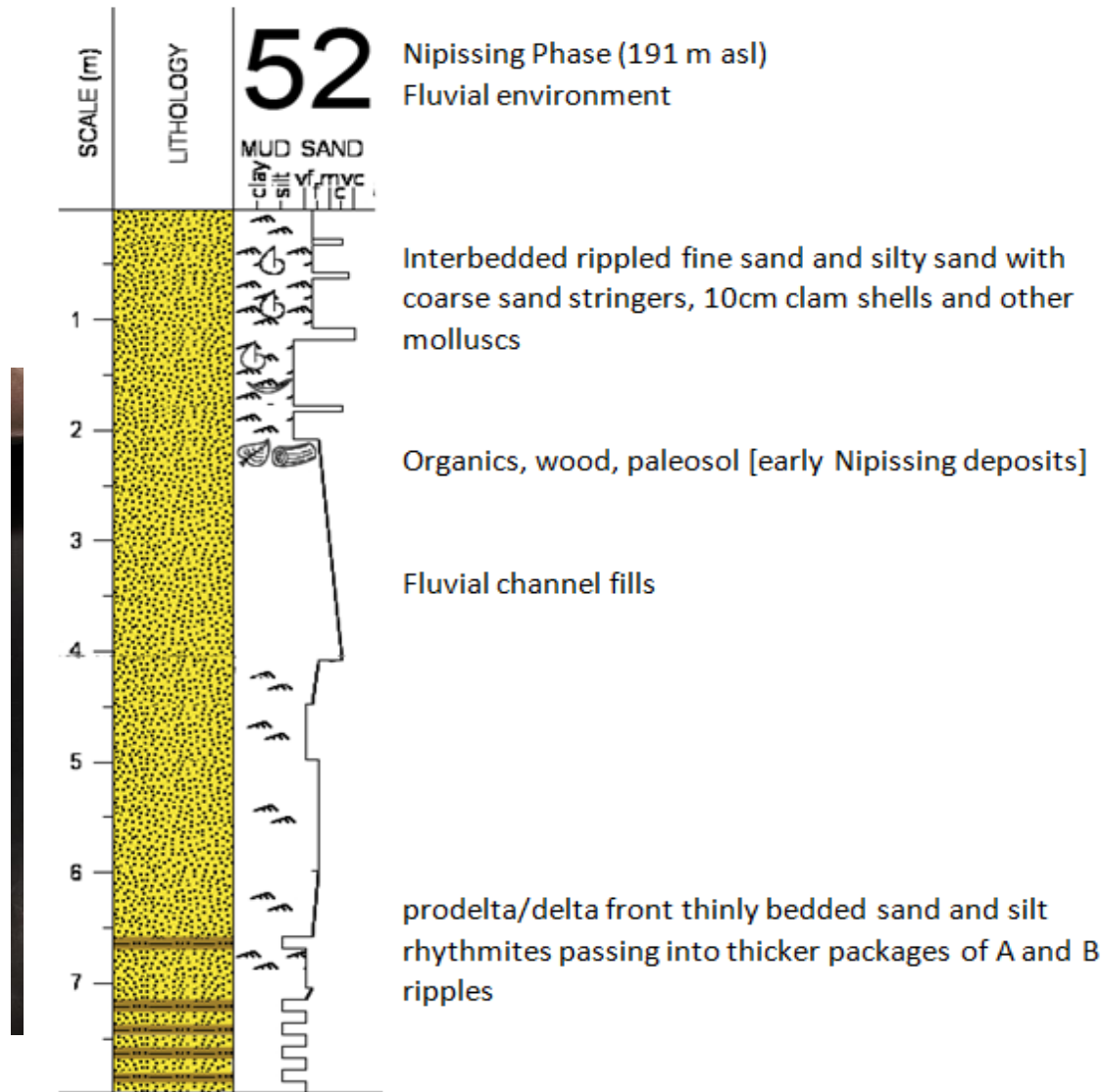
Sample Number	Previous Publications	Location	Lat/Long (DMS)		Elv. (top) (masl)	Samples Collected By
			N°	W°		
Nipissing						
Ferndale	Karrow and Mackie, 2013	2.5 km NW of Ferndale along Budvet rd	44°59'14"	81°18'08"	187	Karrow, 2012
Sucker Creek	FN-1,2,8 Sucker Creek	Canadian Armed Forces Base	44°42'50"	80°43'19"	190	Karrow, 2012
52	-	End of Nadmarc ct. to the north-west, Angus	44°18'58"	79°51'42"	191	Bajc, 2013
53	-	Nottawasaga Dr. to the south-east, Angus	44°18'52"	79°52'11"	195	Bajc, 2013
Transitional						
K10	Miller <i>et al.</i> , 1979 K10 (19)*	North Bank of Saugeen River. NE of Southampton, S of Saugeen Reserve end of closed road to Indian Agent Road. Waypoint #8.	44°30'18"	81°19'11"	193	Longstaffe, 2014
		Hwy 21 just north of Southampton at Chippawa Hill, Turn southeast past Indian reserve. Continue 0.5km past gravel pit to river bank, section on the north bank approximately 100m west of Denny's Dam	44°30'20"	81°14'45"	193	Godwin, 1985
51	-	End of Nadmarc ct. to the south-west, Angus	44°18'52"	79°51'35"	201	Bajc, 2013
Algonquin						
K21	Miller <i>et al.</i> , 1985 K21 (15)	Mill Ck. N Bank E of S end of Port Elgin on Hwy 21. Behind the bar in an embayment. Waypoint #9	44°24'36"	81°22'48"	211	Longstaffe, 2014
		Highway 21 N, turn east after rail crossing just south of Port Elgin. First right (south) crosses Mill Creek. Section on North Bank.	44°24'35"	81°21'50"	205	Godwin, 1985
		North bank Mill Creek, east of township road, 1.6km west of Saugeen River and 3 km south south-east of Port Elgin, Bruce County, Ontario.	-	-	-	Miller <i>et al.</i> , 1985
K6	Miller <i>et al.</i> , 1979 K6 (12)*	Algonquin terraces E of Hwy 21. Dug in roadcut South side of road (Kincardine Ave). Waypoint #11	44°09'26"	81°37'23"	199	Longstaffe, 2014
		Highway 21 in Kincardine, E on Kincardine Ave. (by greenhouses), site in ditch on south side of road approximately 200 m from turn	44°09'35"	81°37'25"	197	Godwin, 1985
Core 594	Macdonald, 2012		43°48'02"	82°06'57"	88.5 ^a	Macdonald, 2004
13	-	Algonquin Sand (13th Line)	44°09'06"	79°44'59"	215	Bajc, 2013

* - Radiocarbon dated α - Water depth

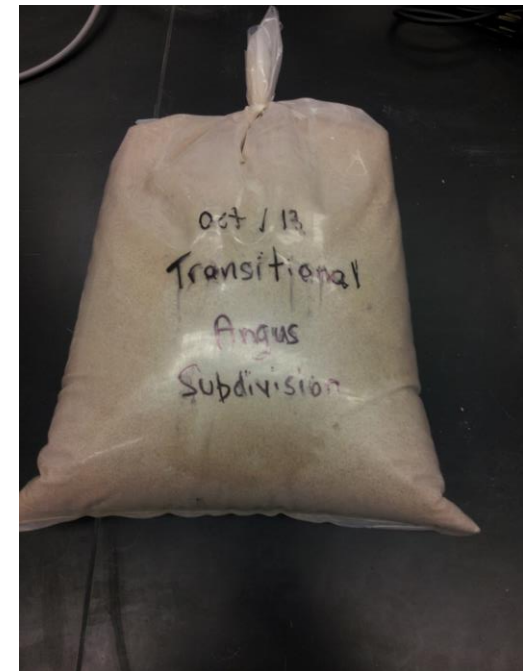
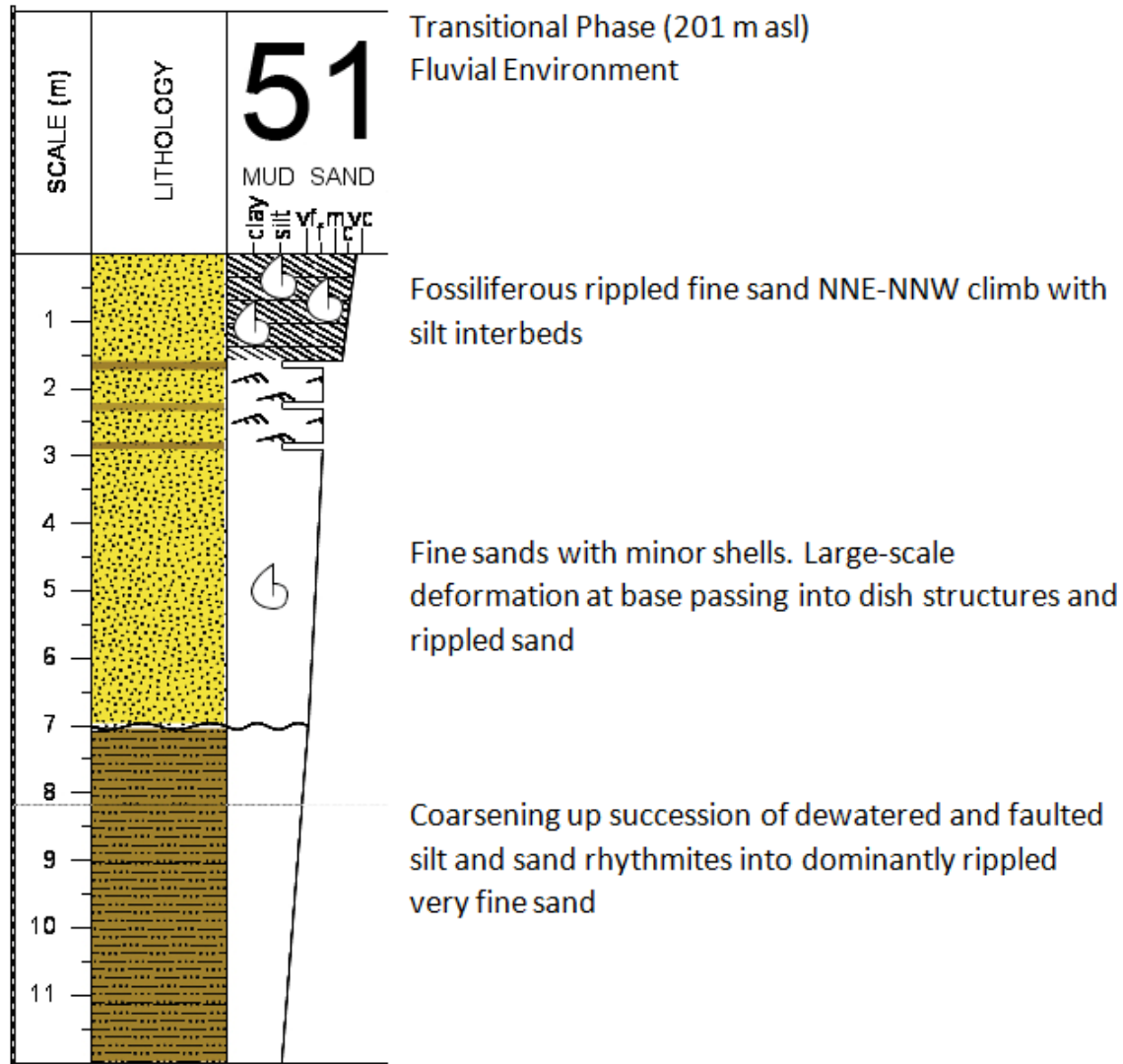
Appendix B - Sediment Columns



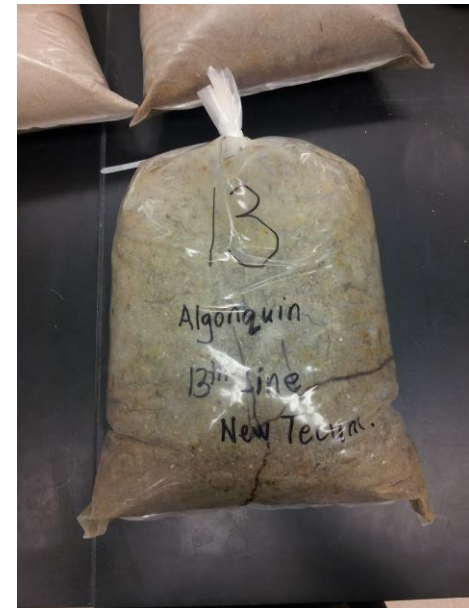
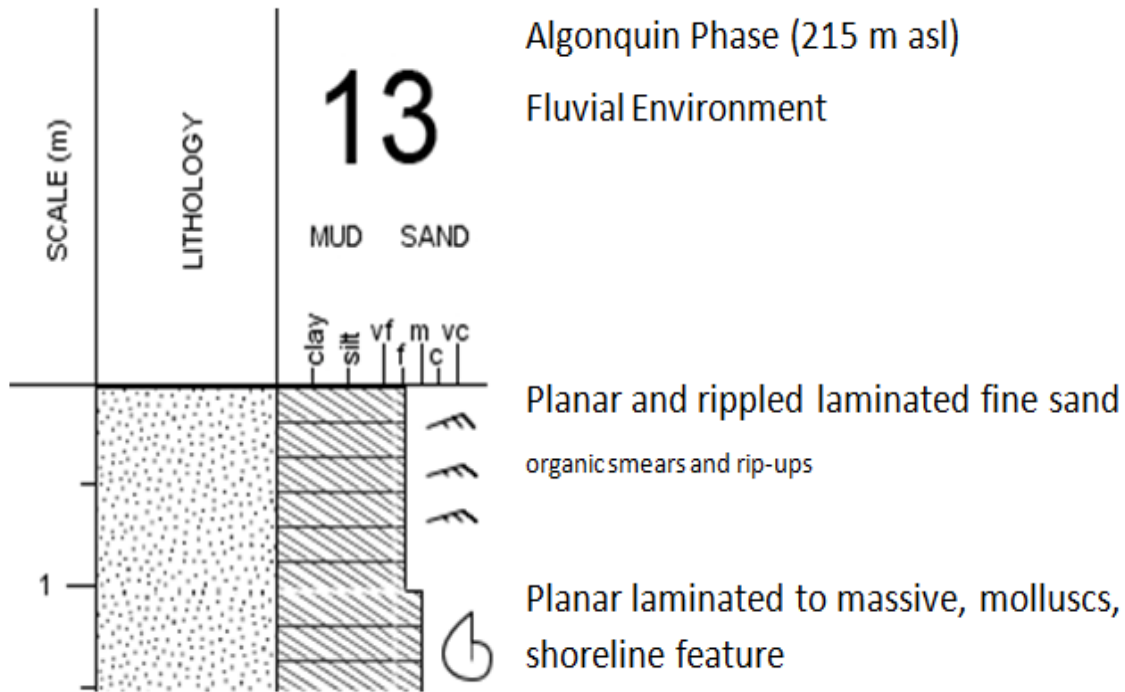
Appendix B (cont'd) Sediment Columns



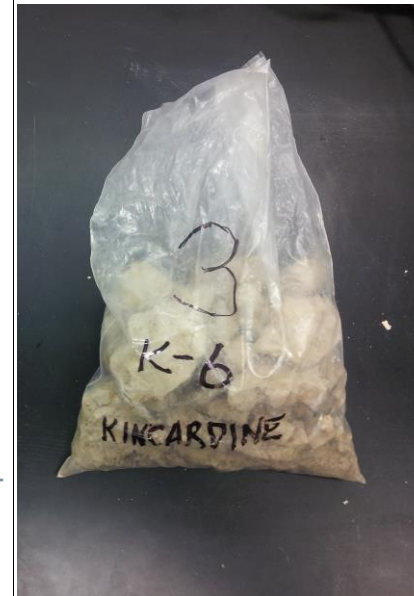
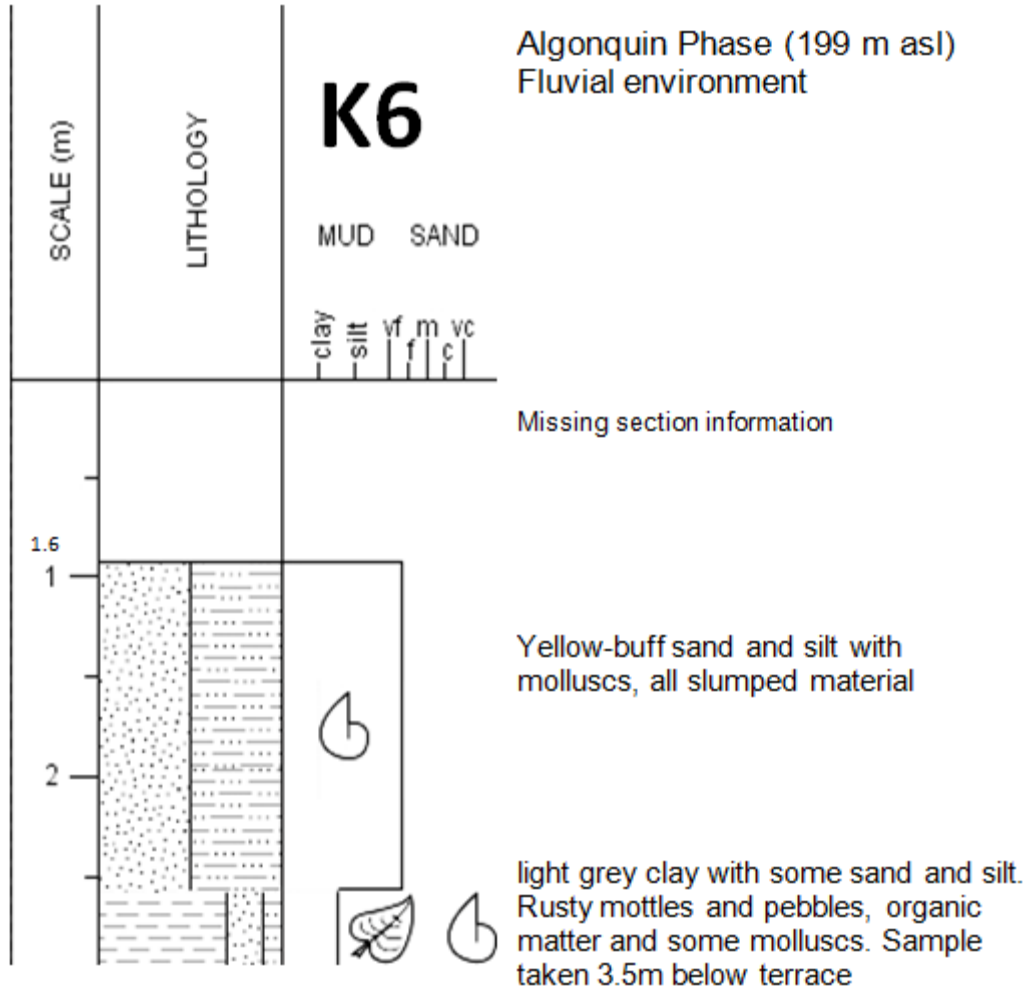
Appendix B (cont'd) Sediment Columns



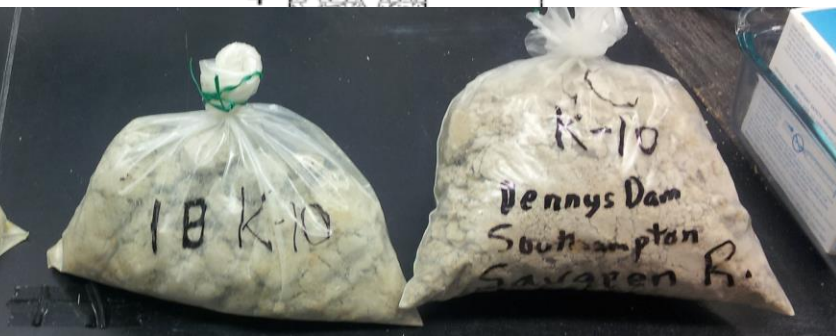
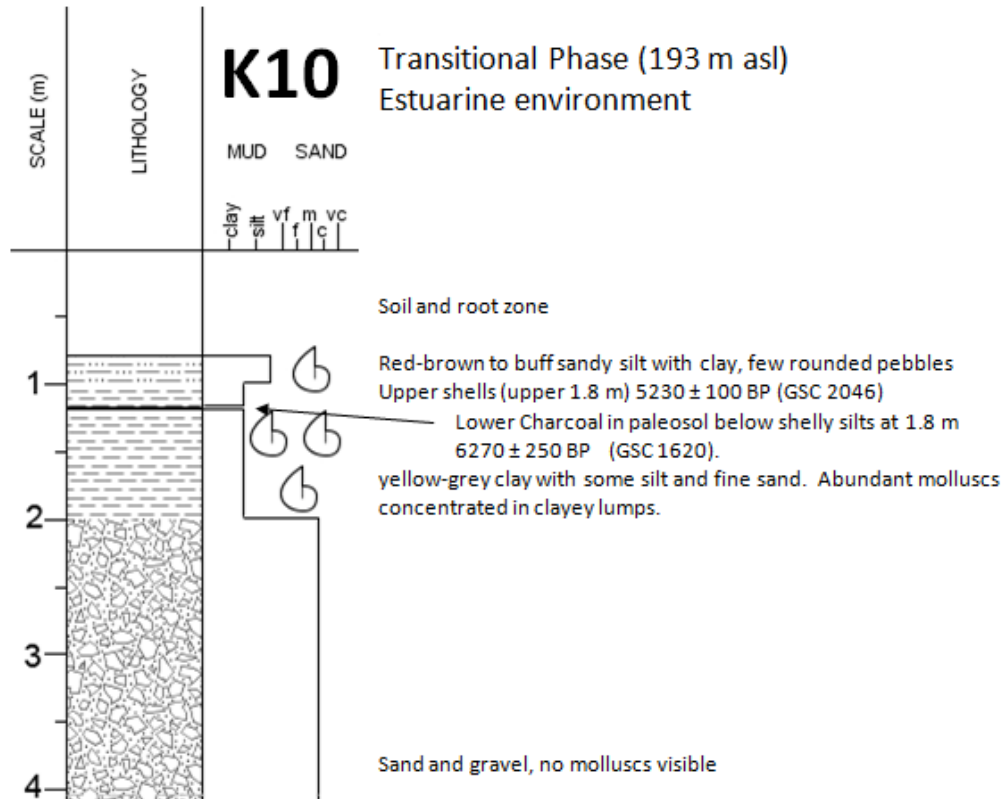
Appendix B (cont'd) Sediment Columns



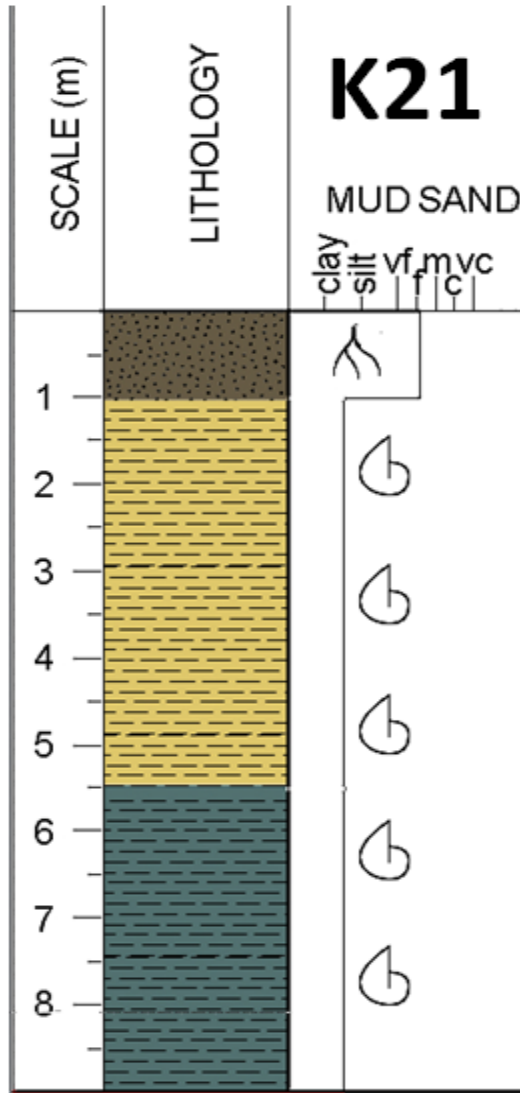
Appendix B (cont'd) Sediment Columns



Appendix B (cont'd) Sediment Columns



Appendix B (cont'd) Sediment Columns

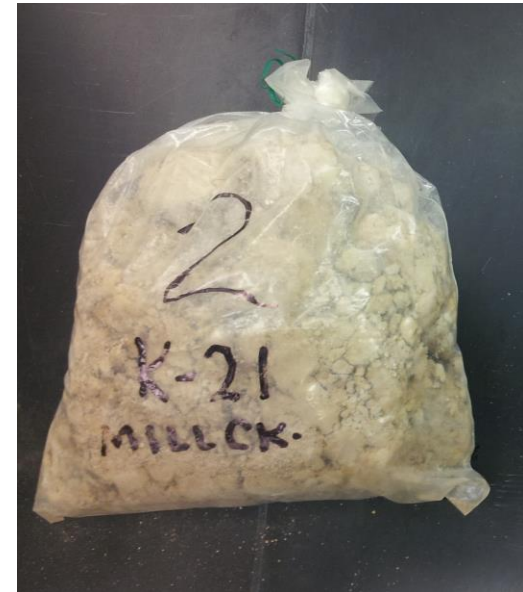


Algonquin Phase (211 m asl)
Estuarine Environment

Large exposure with shells on surface.

Mottled silty clay and worm holes.

When surface is freshly eroded, thin
laminae of plant debris are visible along
bedding planes



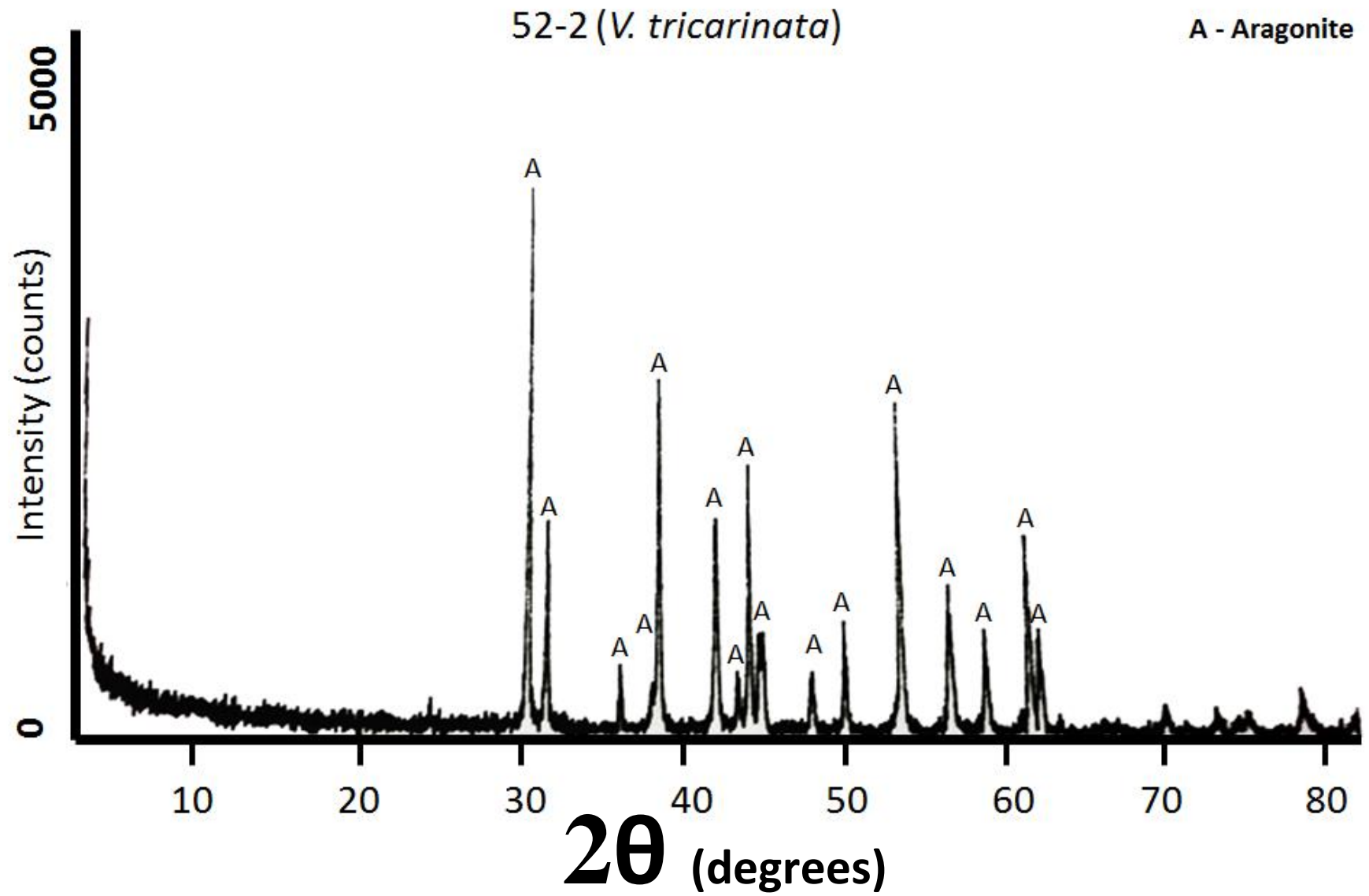
Appendix C - Isotopic Results for Standards

Standard	$\delta^{13}\text{C}$ (VPDB)	$\delta^{18}\text{O}$ (VSMOW)	Standard	$\delta^{13}\text{C}$ (VPDB)	$\delta^{18}\text{O}$ (VSMOW)	Standard	$\delta^{13}\text{C}$ (VPDB)	$\delta^{18}\text{O}$ (VSMOW)
NBS-18	-5.19	7.25	NBS-19	1.96	28.58	WS-1	0.77	26.25
NBS-18	-5.11	7.22	NBS-19	1.96	28.59	WS-1	0.77	26.31
NBS-18	-5.19	7.15	NBS-19	1.98	28.66	WS-1	0.74	26.20
NBS-18	-5.25	7.18	NBS-19	1.93	28.52	WS-1	0.75	26.31
NBS-18	-5.14	7.23	NBS-19	1.94	28.65	WS-1	0.77	26.29
NBS-18	-4.98	7.14	NBS-19	1.93	28.58	WS-1	0.90	26.56
NBS-18	-5.13	7.21	NBS-19	1.97	28.70	WS-1	0.86	26.36
NBS-18	-5.09	7.22	NBS-19	1.93	28.67	WS-1	0.75	26.19
NBS-18	-4.95	7.81	NBS-19	1.98	28.65	WS-1	0.80	26.34
NBS-18	-5.12	7.16	NBS-19	1.93	28.64	WS-1	0.61	25.97
NBS-18	-5.02	7.25	NBS-19	2.08	28.84	WS-1	0.72	26.13
NBS-18	-5.05	7.15	NBS-19	1.99	28.75	WS-1	0.76	26.28
NBS-18	-5.10	7.21	NBS-19	1.81	28.38	WS-1	0.77	26.34
NBS-18	-5.10	7.18	NBS-19	1.91	28.63	WS-1	0.77	26.23
NBS-18	-5.06	7.32	NBS-19	1.93	28.71	WS-1	0.83	26.44
NBS-18	-5.12	7.14	NBS-19	1.97	28.68	WS-1	0.84	26.41
NBS-18	-5.10	7.15	NBS-19	1.95	28.62	WS-1	0.81	26.37
NBS-18	-5.11	7.22	NBS-19	1.96	28.59	WS-1	0.69	26.16
NBS-18	-5.18	7.15	NBS-19	1.83	28.53	WS-1	0.69	26.30
NBS-18	-5.61	7.15	NBS-19	1.97	28.75	WS-1	0.77	26.29
NBS-18	-5.64	7.30	NBS-19	1.97	28.68	WS-1	0.71	26.42
NBS-18	-5.03	7.46	NBS-19	1.91	28.66	WS-1	0.72	26.39
NBS-18	-5.08	7.08	NBS-19	2.34	28.62	WS-1	0.73	26.27
NBS-18	-4.95	7.06	NBS-19	1.92	28.62	WS-1	0.70	26.38
NBS-18	-5.13	7.23	NBS-19	1.97	28.57	WS-1	0.89	26.39
NBS-18	-4.86	7.10	NBS-19	1.93	28.61	WS-1	0.76	26.22
NBS-18	-5.05	7.17	NBS-19	1.97	28.69	WS-1	0.70	26.27
NBS-18	-4.95	7.25	NBS-19	1.95	28.65			
NBS-18	-5.02	7.26	NBS-19	1.89	28.70			
NBS-18	-4.87	7.12	NBS-19	2.01	28.60			
NBS-18	-5.09	7.22	NBS-19	1.97	28.78			
NBS-18	-5.09	7.25	NBS-19	1.93	28.52			

Appendix C (cont'd) - Isotopic Results for Standards

Standard	$\delta^{13}\text{C}$ (VPDB)	$\delta^{18}\text{O}$ (VSMOW)	Standard	$\delta^{13}\text{C}$ (VPDB)	$\delta^{18}\text{O}$ (VSMOW)
LSVEC	-47.24	4.06	Suprapur	-36.06	13.32
LSVEC	-45.96	4.27	Suprapur	-36.21	13.20
LSVEC	-46.32	4.39	Suprapur	-36.24	13.44
LSVEC	-46.62	4.04	Suprapur	-35.68	13.30
LSVEC	-46.86	3.65	Suprapur	-35.60	13.22
LSVEC	-46.48	4.13	Suprapur	-35.66	13.25
LSVEC	-46.68	3.88	Suprapur	-35.50	13.39
LSVEC	-46.64	3.83	Suprapur	-35.65	13.08
LSVEC	-46.62	4.09	Suprapur	-35.66	13.25
LSVEC	-46.56	4.08	Suprapur	-35.66	13.11
LSVEC	-46.62	4.07	Suprapur	-35.64	13.20
LSVEC	-46.72	4.03	Suprapur	-35.64	13.20
LSVEC	-46.48	4.05	Suprapur	-35.66	13.22
LSVEC	-46.53	4.04	Suprapur	-35.72	13.20
LSVEC	-46.67	3.90	Suprapur	-35.63	13.18
LSVEC	-46.59	4.08	Suprapur	-35.52	13.16
LSVEC	-46.53	3.97	Suprapur	-34.83	13.09
LSVEC	-46.69	3.90	Suprapur	-35.40	13.41
LSVEC	-46.44	4.03	Suprapur	-35.38	13.26
LSVEC	-46.67	3.93	Suprapur	-35.53	13.37
LSVEC	-46.67	3.95	Suprapur	-35.54	13.25
LSVEC	-46.62	3.96	Suprapur	-35.61	13.19
LSVEC	-46.58	3.95			
LSVEC	-46.66	3.84			
LSVEC	-46.56	3.97			

Appendix D - XRD Pattern



Appendix E - Absolute and Relative Percent Shell Abundances

Fluvial

52 Nipissing			53 Nipissing			51 Transitional		
Species Identified	Number	Percent	Species Identified	Number	Percent	Species Identified	Number	Percent
<i>Sphaeriidae</i> spp.	80	46.8	<i>Valvata sincera</i>	164	30.0	<i>Valvata tricarinata</i>	24	28.6
<i>Pisidium</i> spp.	26	15.2	<i>Lymnea</i> spp.	122	22.3	<i>Lymnea decampi</i>	21	25.0
<i>Valvata sincera</i>	25	14.6	<i>Pisidium</i> spp.	100	18.3	<i>Valvata sincera</i>	16	19.0
<i>Valvata tricarinata</i>	23	13.5	<i>Valvata tricarinata</i>	79	14.4	<i>Pisidium</i> spp.	15	17.9
<i>Fossaria decampi</i>	13	7.6	<i>Amnicola limosa</i>	26	4.8	<i>Helisoma anceps</i>	4	4.8
<i>Helisoma anceps</i>	3	1.8	<i>Gyraulus parvus</i>	23	4.2	<i>Sphaeriidae</i> spp.	4	4.8
<i>Physa gyrina</i>	1	0.6	<i>Sphaeriidae</i> spp.	15	2.7	Total	84	100
Total	171	100	<i>Helisoma anceps</i>	10	1.8			
			<i>Pleurocera livescens</i>	4	0.7			
			<i>Physa gyrina</i>	4	0.7			
			Total	547	100			

K6 Algonquin			13 Algonquin		
Species Identified	Number	Percent	Species Identified	Number	Percent
<i>Pisidium</i> spp.	10	50	<i>Valvata tricarinata</i>	21	42.9
<i>Valvata tricarinata</i>	7	35	<i>Pisidium</i> spp.	7	14.3
<i>Gyraulus parvus</i>	2	10	<i>Valvata sincera</i>	12	24.5
<i>Sphaeriidae</i> spp.	1	5	<i>Lymnea decampi</i>	5	10.2
Total	20	100	<i>Amnicola limosa</i>	3	6.1
			<i>Sphaeriidae</i> spp.	1	2.0
			Total	49	100

Estuarine

K21 Algonquin			K10 Transitional		
Species Identified	Number	Percent	Species Identified	Number	Percent
<i>Gyraulus parvus</i>	29	43.3	<i>Amnicola limosa</i>	142	43.6
<i>Sphaeriidae</i> spp.	10	14.9	<i>Valvata tricarinata</i>	67	20.6
<i>Valvata sincera</i>	9	13.4	<i>Gyraulus parvus</i>	41	12.6
<i>Pisidium</i> spp.	10	14.9	<i>Ferrissia</i> spp.	26	8.0
<i>Lymnea decampi</i>	5	7.5	<i>Pisidium</i> spp.	19	5.8
<i>Helisoma anceps</i>	3	4.5	<i>Stagnicola catascopium</i>	13	4.0
<i>Valvata tricarinata</i>	1	1.5	<i>Helisoma anceps</i>	10	3.1
Total	67	100	<i>Physa gyrina</i>	8	2.5
			Total	326	100

Appendix F – All Isotopic Results for Samples

Site 13 - Algonquin – Fluvial

Species	$\delta^{13}\text{C}$ Shell (VPDB)	$\delta^{18}\text{O}$ Shell (VSMOW)	$\delta^{18}\text{O}$ Water (VSMOW)	$\delta^{13}\text{C}$ Shell (VPDB)	Max	Min	Range	Average	St Dev
<i>Amnicola limosa</i>	-9.8	19.8	-11.7*	All Data	-5.0	-9.8	-4.8	-7.5	1.5
<i>Amnicola limosa</i>	-8.9	20.3	-11.1*	<i>Amnicola limosa</i>	-8.9	-9.8	-0.9	-9.4	0.7
<i>Valvata sincera</i>	-5.5	20.0	-11.3*	<i>Valvata sincera</i>	-5.0	-8.6	-3.7	-6.6	1.1
<i>Valvata sincera</i>	-7.0	19.9	-11.4*	<i>Valvata tricarinata</i>	-8.0	-9.6	-1.6	-8.8	0.7
<i>Valvata sincera</i>	-5.6	19.5	-11.8*						
				$\delta^{18}\text{O}$ Shell (VSMOW)	Max	Min	Range	Average	St Dev
<i>Valvata sincera</i>	-5.0	18.3	-12.9*	All Data	21.7	18.3	3.4	20.1	1.0
<i>Valvata sincera</i>	-6.7	21.7	-9.7*	<i>Amnicola limosa</i>	20.3	19.8	0.5	20.0	0.4
<i>Valvata sincera</i>	-7.2	21.1	-10.3*	<i>Valvata sincera</i>	21.7	18.3	3.4	20.5	1.0
<i>Valvata sincera</i>	-8.6	21.2	-10.2*	<i>Valvata tricarinata</i>	20.4	18.6	1.8	19.3	0.8
<i>Valvata sincera</i>	-6.9	21.2	-10.1*						
<i>Valvata sincera</i>	-6.5	20.1	-11.3*						
<i>Valvata sincera</i>	-7.3	21.4	-10.0*		Max	Min	Average		
<i>Valvata tricarinata</i>	-8.6	19.1	-12.9*	River Water $\delta^{18}\text{O}$ *	-9.7	-13.4	-11.4		
<i>Valvata tricarinata</i>	-8.0	19.1	-12.9*						
<i>Valvata tricarinata</i>	-9.6	18.6	-13.4*						
<i>Valvata tricarinata</i>	-9.0	20.4	-11.6*						
				Species Identified	Relative Percent				
Count (n value)				<i>Valvata tricarinata</i>	43				
<i>Amnicola limosa</i>	2			<i>Valvata sincera</i>	24				
<i>Valvata sincera</i>	10			<i>Pisidium</i> spp.	14				
<i>Valvata tricarinata</i>	4			<i>Lymnea decampi</i>	10				
				<i>Amnicola limosa</i>	6				
				<i>Sphaeriidae</i> spp.	2				

* - calculated values

Appendix F (cont'd) - All Isotopic Results for Samples

Site 13 - Algonquin - Fluvial (cont'd)

Count (n value)	
<i>Pisidium</i> spp.	5
<i>Valvata tricarinata</i>	7

Species Identified	Relative Percent
<i>Pisidium</i> spp.	50
<i>Valvata tricarinata</i>	35
<i>Gyraulus parvus</i>	10
<i>Sphaeriidae</i> spp.	5

$\delta^{13}\text{C}$ (‰, VPDB)	Max	Min	St Dev
All Data	-2.4	-7.3	1.4
<i>Pisidium</i> spp.	-2.4	-6.5	1.5
<i>Valvata tricarinata</i>	-2.8	-7.3	1.4

$\delta^{18}\text{O}$ (‰, VSMOW)	Max	Min	St Dev
All Data	20.3	17.7	0.9
<i>Pisidium</i> spp.	20.3	19.3	0.5
<i>Valvata tricarinata</i>	20.3	17.7	1.0

	Max	Min	
River Water $\delta^{18}\text{O}$ *	-10.8	-14.2	* - Calculated values

Appendix F (cont'd) - All Isotopic Results for Samples

Site K6 - Algonquin - Fluvial

Species	$\delta^{13}\text{C}$ Shell (VPDB)	$\delta^{18}\text{O}$ Shell (VSMOW)	$\delta^{18}\text{O}$ Water (VSMOW)	$\delta^{13}\text{C}$ Shell (VPDB)	Max	Min	Range	Average	St Dev
<i>Pisidium</i> spp.	-9.3	18.6	-12.5*	All Data	-2.3	-9.3	-7.0	-5.2	2.1
<i>Pisidium</i> spp.	-5.4	15.8	-15.2*	<i>Pisidium</i> spp.	-5.4	-9.3	-3.9	-7.1	1.4
<i>Pisidium</i> spp.	-6.8	16.0	-15.0*	<i>Valvata sincera</i>	-2.3	-5.2	-2.9	-3.8	1.1
<i>Pisidium</i> spp.	-7.2	16.4	-14.6*	<i>Valvata tricarinata</i>	-2.4	-8.8	-6.3	-5.4	2.3
<i>Pisidium</i> spp.	-7.0	21.2	-10.0*						
				$\delta^{18}\text{O}$ Shell (VSMOW)	Max	Min	Range	Average	St Dev
<i>Valvata sincera</i>	-3.8	16.0	-15.2*	All Data	21.2	15.0	6.2	17.1	1.6
<i>Valvata sincera</i>	-5.2	17.7	-13.6*	<i>Pisidium</i> spp.	21.2	15.8	5.4	17.6	2.3
<i>Valvata sincera</i>	-3.7	16.1	-15.1*	<i>Valvata sincera</i>	17.7	15.0	2.7	16.3	0.9
<i>Valvata sincera</i>	-2.3	15.0	-16.2*	<i>Valvata tricarinata</i>	20.4	15.4	5.0	17.5	1.7
<i>Valvata sincera</i>	-5.1	17.2	-14.1*						
<i>Valvata sincera</i>	-3.2	16.1	-15.1*	Count (n value)					
<i>Valvata sincera</i>	-2.4	15.6	-15.6*	<i>Pisidium</i> spp.	5				
<i>Valvata sincera</i>	-3.8	15.7	-15.5*	<i>Valvata sincera</i>	9				
<i>Valvata sincera</i>	-5.0	17.0	-14.3*	<i>Valvata tricarinata</i>	10				
<i>Valvata tricarinata</i>	-8.8	19.1	-12.9*	Species Identified	Relative Percent				
<i>Valvata tricarinata</i>	-5.5	20.4	-11.6*	<i>Valvata tricarinata</i>	29				
<i>Valvata tricarinata</i>	-3.1	15.4	-16.5*	<i>Lymnea decampi</i>	25				
<i>Valvata tricarinata</i>	-6.2	17.7	-14.3*	<i>Valvata sincera</i>	19				
<i>Valvata tricarinata</i>	-2.4	16.1	-15.8*	<i>Pisidium</i> spp.	18				
<i>Valvata tricarinata</i>	-8.7	18.6	-13.4*	<i>Helisoma anceps</i>	5				
<i>Valvata tricarinata</i>	-4.8	16.7	-15.3*	<i>Sphaeriidae</i> spp.	5				
<i>Valvata tricarinata</i>	-4.3	16.2	-15.7*						
<i>Valvata tricarinata</i>	-7.2	18.8	-13.2*						
<i>Valvata tricarinata</i>	-2.9	16.1	-15.8*						
				River Water $\delta^{18}\text{O}$ *	-10.0	-16.5	-14.4		

* - Calculated values

Appendix F (cont'd) - All Isotopic Results for Samples
Site K21 - Algonquin - Estuarine

Species	Serial	$\delta^{13}\text{C}$ (‰, VPDB)	$\delta^{18}\text{O}$ (‰, VSMOW)	$\delta^{18}\text{O}$ (‰, VSMOW)	Species	Serial	$\delta^{13}\text{C}$ (‰, VPDB)	$\delta^{18}\text{O}$ (‰, VSMOW)	$\delta^{18}\text{O}$ (‰, VSMOW)*	
<i>Pisidium</i> spp.	1	1.1	-5.4	22.1	<i>Pisidium</i> spp.	2	3.1	-6.0	22.6	
<i>Pisidium</i> spp.	1	1.2	-5.2	22.2	<i>Pisidium</i> spp.	2	3.2	-5.8	22.6	
<i>Pisidium</i> spp.	1	1.3	-5.4	22.1	<i>Pisidium</i> spp.	2	3*	-5.9*	22.6*	
<i>Pisidium</i> spp.	1	1*	-5.3*	22.1*	<i>Pisidium</i> spp.	2	4.1	-6.0	23.5	
<i>Pisidium</i> spp.	1	2.1	-6.8	23.0	<i>Pisidium</i> spp.	2	4.2	-6.2	23.7	
<i>Pisidium</i> spp.	1	2.2	-6.9	23.6	<i>Pisidium</i> spp.	2	4*	-6.1	23.6	
<i>Pisidium</i> spp.	1	2.3	-6.5	22.4	<i>Pisidium</i> spp.	2	Bulk*	-5.7*	23.6*	-7.7*
<i>Pisidium</i> spp.	1	2.4	-6.6	23.0	<i>Pisidium</i> spp.	3	1.1	-6.4	22.2	
<i>Pisidium</i> spp.	1	2.5	-6.9	23.2	<i>Pisidium</i> spp.	3	1.2	-6.3	21.9	
<i>Pisidium</i> spp.	1	2*	-6.8*	23.0*	<i>Pisidium</i> spp.	3	1.3	-6.3	22.2	
<i>Pisidium</i> spp.	1	3.1	-6.5	21.7	<i>Pisidium</i> spp.	3	1.4	-7.0	21.7	
<i>Pisidium</i> spp.	1	3.2	-6.7	23.0	<i>Pisidium</i> spp.	3	1*	-6.5*	22.0*	
<i>Pisidium</i> spp.	1	3*	-6.6*	22.3*	<i>Pisidium</i> spp.	3	2.1	-7.0	22.9	
<i>Pisidium</i> spp.	1	4.1	-6.5	22.7	<i>Pisidium</i> spp.	3	2.2	-6.3	23.1	
<i>Pisidium</i> spp.	1	4.1 DUP	-6.6	22.5	<i>Pisidium</i> spp.	3	2*	-6.5*	23.0*	
<i>Pisidium</i> spp.	1	4*	-6.6*	22.6*	<i>Pisidium</i> spp.	3	3.1	-6.8	23.3	
<i>Pisidium</i> spp.	1	Bulk*	-6.4*	22.6*	<i>Pisidium</i> spp.	3	3.2	-6.8	22.9	
				-8.6*	<i>Pisidium</i> spp.	3	3*	-6.8*	23.1*	
<i>Pisidium</i> spp.	2	1.1	-5.7	22.7	<i>Pisidium</i> spp.	3	4.1	-6.5	23.2	
<i>Pisidium</i> spp.	2	1.2	-5.8	22.5	<i>Pisidium</i> spp.	3	Bulk*	-6.56*	22.71*	-8.5*
<i>Pisidium</i> spp.	2	1.3	-5.7	21.4	<i>Valvata sincera</i>			-7.7	23.6	-7.9*
<i>Pisidium</i> spp.	2	1.4	-5.7	21.2	<i>Valvata sincera</i>			-7.1	21.4	-10.0*
<i>Pisidium</i> spp.	2	1*	-5.7*	22.0*	<i>Valvata sincera</i>			-5.5	23.2	-8.2*
<i>Pisidium</i> spp.	2	2.1	-5.7	24.9	<i>Valvata sincera</i>			-7.5	24.8	-6.7*
<i>Pisidium</i> spp.	2	2.2	-5.1	25.5	<i>Valvata sincera</i>			-9.3	21.9	-9.5*
<i>Pisidium</i> spp.	2	2.3	-4.9	25.7	<i>Valvata sincera</i>			-7.7	24.9	-6.6*
<i>Pisidium</i> spp.	2	2.4	-6.2	24.0	<i>Valvata sincera</i>			-6.4	24.0	-7.4*
<i>Pisidium</i> spp.	2	2.5	-5.1	25.6	<i>Valvata sincera</i>			-6.8	23.9	-7.5*
<i>Pisidium</i> spp.	2	2.6	-6.2	23.7						
<i>Pisidium</i> spp.	2	2*	-5.5*	25.0*						

* - Calculated value; DUP - Duplicate sample

Appendix F (cont'd) - All Isotopic Results for Samples

Site K21 - Algonquin - Estuarine (cont'd)

$\delta^{13}\text{C}$ Shell (‰, VPDB)	Max	Min	Range	Average	St Dev
All Data	-4.9	-9.3	-4.4	-6.4	0.8
<i>Pisidium</i> spp.	-4.9	-7.0	-2.0	-6.2	0.6
<i>Valvata sincera</i>	-5.5	-9.3	-3.8	-7.2	1.1

$\delta^{18}\text{O}$ Shell (‰, VSMOW)	Max	Min	Range	Average	St Dev
All Data	25.7	21.2	4.5	23.1	1.1
<i>Pisidium</i> spp.	25.7	21.2	4.5	23.0	1.1
<i>Valvata sincera</i>	24.9	21.4	3.6	23.5	1.3

Count (n value)

<i>Pisidium</i> spp.	35
<i>Valvata sincera</i>	8

Species Identified

<i>Gyraulus parvus</i>	43
<i>Pisidium</i> spp.	15
<i>Sphaeriidae</i> spp.	15
<i>Valvata sincera</i>	13
<i>Lymnea decampi</i>	7
<i>Helisoma anceps</i>	4

Appendix F (cont'd) - All Isotopic Results for Samples

Site 51 - Transitional - Fluvial

Species	$\delta^{13}\text{C}$ Shell (VPDB)	$\delta^{18}\text{O}$ Shell (VSMOW)	$\delta^{18}\text{O}$ Water (VSMOW)	$\delta^{13}\text{C}$ Shell (VPDB)	Max	Min	Range	Average	St Dev
<i>Pisidium</i> spp.	-9.3	18.6	-12.5*	All Data	-2.3	-9.3	-7.0	-5.2	2.1
<i>Pisidium</i> spp.	-5.4	15.8	-15.2*	<i>Pisidium</i> spp.	-5.4	-9.3	-3.9	-7.1	1.4
<i>Pisidium</i> spp.	-6.8	16.0	-15.0*	<i>Valvata sincera</i>	-2.3	-5.2	-2.9	-3.8	1.1
<i>Pisidium</i> spp.	-7.2	16.4	-14.6*	<i>Valvata tricarinata</i>	-2.4	-8.8	-6.3	-5.4	2.3
<i>Pisidium</i> spp.	-7.0	21.2	-10.0*						
<i>Valvata sincera</i>	-3.8	16.0	-15.2*	$\delta^{18}\text{O}$ Shell (VSMOW)	Max	Min	Range	Average	St Dev
<i>Valvata sincera</i>	-5.2	17.7	-13.6*	All Data	21.2	15.0	6.2	17.1	1.6
<i>Valvata sincera</i>	-3.7	16.1	-15.1*	<i>Pisidium</i> spp.	21.2	15.8	5.4	17.6	2.3
<i>Valvata sincera</i>	-2.3	15.0	-16.2*	<i>Valvata sincera</i>	17.7	15.0	2.7	16.3	0.9
<i>Valvata sincera</i>	-5.1	17.2	-14.1*	<i>Valvata tricarinata</i>	20.4	15.4	5.0	17.5	1.7
<i>Valvata sincera</i>	-3.2	16.1	-15.1*						
<i>Valvata sincera</i>	-2.4	15.6	-15.6*	Count (n value)					
<i>Valvata sincera</i>	-3.8	15.7	-15.5*	<i>Pisidium</i> spp.	5				
<i>Valvata sincera</i>	-5.0	17.0	-14.3*	<i>Valvata sincera</i>	9				
<i>Valvata tricarinata</i>	-8.8	19.1	-12.9*	<i>Valvata tricarinata</i>	10				
<i>Valvata tricarinata</i>	-5.5	20.4	-11.6*						
<i>Valvata tricarinata</i>	-3.1	15.4	-16.5*	Species Identified	Relative Percent				
<i>Valvata tricarinata</i>	-6.2	17.7	-14.3*	<i>Valvata tricarinata</i>	29				
<i>Valvata tricarinata</i>	-2.4	16.1	-15.8*	<i>Lymnea decampi</i>	25				
<i>Valvata tricarinata</i>	-8.7	18.6	-13.4*	<i>Valvata sincera</i>	19				
<i>Valvata tricarinata</i>	-4.8	16.7	-15.3*	<i>Pisidium</i> spp.	18				
<i>Valvata tricarinata</i>	-4.3	16.2	-15.7*	<i>Helisoma anceps</i>	5				
<i>Valvata tricarinata</i>	-7.2	18.8	-13.2*	<i>Sphaeriidae</i> spp.	5				
<i>Valvata tricarinata</i>	-2.9	16.1	-15.8*						
	Max	Min	Average						
Lake Water $\delta^{18}\text{O}$ *	-10.0	-16.5	-14.4						

* - Calculated value

Appendix F (cont'd) - All Isotopic Results for Samples

Site K10 - Transitional - Estuarine

Species	$\delta^{13}\text{C}$ Shell (VPDB)	$\delta^{18}\text{O}$ Shell (VSMOW)	$\delta^{18}\text{O}$ Water (VSMOW)	Species	$\delta^{13}\text{C}$ Shell (VPDB)	$\delta^{18}\text{O}$ Shell (VSMOW)	$\delta^{18}\text{O}$ Water (VSMOW)
<i>Ammicola limosa</i>	-8.5	20.8	-10.6*	<i>Valvata tricarinata</i>	-4.9	22.2	-9.9*
<i>Ammicola limosa</i>	-8.3	21.1	-10.3*	<i>Valvata tricarinata</i>	-4.7	22.1	-10.0*
<i>Ammicola limosa</i>	-7.6	20.4	-11.0*	<i>Valvata tricarinata</i>	-10.2	21.9	-10.1*
<i>Pisidium</i> spp.	-7.9	21.7	-9.5*	<i>Valvata tricarinata</i>	-8.0	20.6	-11.4*
<i>Pisidium</i> spp.	-8.1	21.2	-10.0*	<i>Valvata tricarinata</i>	-7.0	21.4	-10.7*
<i>Pisidium</i> spp.	-6.2	22.4	-8.8*	<i>Valvata tricarinata</i>	-8.9	20.9	-11.1*
<i>Pisidium</i> spp.	-4.9	22.9	-8.3*	<i>Valvata tricarinata</i>	-5.2	21.6	-10.5*
<i>Pisidium</i> spp.	-6.1	22.4	-8.9*	<i>Valvata tricarinata</i>	-5.1	21.5	-10.6*
<i>Pisidium</i> spp.	-5.9	22.4	-8.9*	<i>Valvata tricarinata</i>	-8.9	21.8	-10.3*
<i>Pisidium</i> spp.	-6.5	21.8	-9.4*	<i>Valvata tricarinata</i>	-6.7	21.4	-10.7*
<i>Pisidium</i> spp.	-7.1	22.2	-9.0*	<i>Valvata tricarinata</i>	-6.0	22.0	-10.1*
<i>Pisidium</i> spp.	-6.1	22.2	-9.0*	<i>Valvata tricarinata</i>	-6.7	21.8	-10.3*
<i>Valvata tricarinata</i>	-6.5	22.5	-9.6*	<i>Valvata tricarinata</i>	-5.9	21.4	-10.7*
<i>Valvata tricarinata</i>	-7.8	21.7	-10.4*	<i>Valvata tricarinata</i>	-6.2	23.9	-8.3*
<i>Valvata tricarinata</i>	-7.2	20.9	-11.1*				
<i>Valvata tricarinata</i>	-7.7	21.7	-10.4*				
<i>Valvata tricarinata</i>	-6.9	22.0	-10.0*				
<i>Valvata tricarinata</i>	-5.0	22.0	-10.1*				
<i>Valvata tricarinata</i>	-5.5	23.1	-9.0*				
<i>Valvata tricarinata</i>	-7.0	21.5	-10.6*				
<i>Valvata tricarinata</i>	-9.7	19.3	-12.7*				
<i>Valvata tricarinata</i>	-6.7	21.4	-10.7*				
<i>Valvata tricarinata</i>	-7.5	20.8	-11.2*				
<i>Valvata tricarinata</i>	-4.2	22.4	-9.6*				

* - Calculated Value

Appendix F (cont'd) - All Isotopic Results for Samples

Site K10 - Transitional - Estuarine (cont'd)

$\delta^{13}\text{C}$ Shell (VPDB)	Max	Min	Range	Average	St Dev
All Data	-4.2	-10.2	-6.0	-6.9	1.4
<i>Amnicola limosa</i>	-6.6	-8.8	-2.2	-8.0	0.9
<i>Pisidium</i> spp.	-4.9	-8.1	-3.1	-6.6	1.0

$\delta^{18}\text{O}$ Shell (VSMOW)	Max	Min	Range	Average	St Dev
All Data	23.9	19.3	4.6	21.7	0.8
<i>Amnicola limosa</i>	21.3	20.4	0.9	21.0	0.4
<i>Pisidium</i> spp.	22.9	20.8	2.1	22.0	0.6
<i>Valvata tricarinata</i>	23.9	19.3	4.6	21.8	0.9

Species Identified	Relative Percent		Max	Min	Average
		Estuarine Water			
<i>Amnicola limosa</i>	44	$\delta^{18}\text{O}^*$	-8.3	-12.7	-10.1
<i>Valvata tricarinata</i>	21				
<i>Gyraululus parvus</i>	13				
<i>Ferrissia</i> spp.	8				
<i>Pisidium</i> spp.	6				
<i>Amnicola walkeri</i>	4				
<i>Helisoma anceps</i>	3				
<i>Physa gyrina</i>	2				
Count (n value)					
<i>Amnicola limosa</i>	5				
<i>Pisidium</i> spp.	10				
<i>Valvata tricarinata</i>	29				

* - Calculated value

Appendix F (cont'd) - All Isotopic Results for Samples
Site 52 - Nipissing - Fluvial

Species	Serial	$\delta^{13}\text{C}$ (VPDB)	$\delta^{18}\text{O}$ Shell (VSMOW)	$\delta^{18}\text{O}$ Water (VSMOW)	Species	Site	$\delta^{13}\text{C}$ Shell (VPDB)	$\delta^{18}\text{O}$ Shell (VSMOW)			
<i>Pisidium</i> spp.		-9.1	19.5	-11.7*	<i>Valvata tricarinata</i>	-4.6	18.4	-13.5			
<i>Pisidium</i> spp.		-8.7	21.3	-9.9*	<i>Valvata tricarinata</i>	-8.6	21.1	-11.0			
<i>Pisidium</i> spp.		-8.6	20.6	-10.5*	<i>Valvata tricarinata</i>	-2.6	15.0	-16.8			
<i>Pisidium</i> spp.		-8.5	20.1	-11.1*	<i>Valvata tricarinata</i>	-5.9	19.1	-12.9			
<i>Pisidium</i> spp.		-8.1	19.7	-11.4*							
<i>Pisidium</i> spp.		-9.5	20.1	-11.1*	$\delta^{13}\text{C}$ Shell (VPDB)	Max	Min	Range	Average	St Dev	
<i>Pisidium</i> spp.	1	Bulk	-7.4	21.3	-9.9*	All Data	-1.8	-9.5	-7.7	-5.9	2.5
<i>Pisidium</i> spp.	1	1	-7.7	20.7		<i>Pisidium</i> spp.	-7.4	-9.5	-2.2	-8.6	0.9
<i>Pisidium</i> spp.	1	2	-7.3	20.7		<i>Valvata sincera</i>	-1.8	-8.1	-6.3	-4.1	1.9
<i>Pisidium</i> spp.	1	3	-6.9	21.0		<i>Valvata tricarinata</i>	-2.0	-9.4	-7.4	-5.8	2.6
<i>Valvata sincera</i>		-4.3	18.0	-13.3*	$\delta^{18}\text{O}$ Shell (VSMOW)	Max	Min	Range	Average	St Dev	
<i>Valvata sincera</i>		-1.8	15.7	-15.5*	All Data	24.0	15.0	8.9	19.1	2.2	
<i>Valvata sincera</i>		-3.2	18.0	-13.3*	<i>Pisidium</i> spp.	21.3	19.5	1.8	20.4	0.6	
<i>Valvata sincera</i>		-3.0	16.3	-14.9*	<i>Valvata sincera</i>	24.0	15.7	8.3	18.4	2.6	
<i>Valvata sincera</i>		-3.2	17.0	-14.2*	<i>Valvata tricarinata</i>	21.1	15.0	6.0	18.5	2.1	
<i>Valvata sincera</i>		-3.3	17.9	-13.3*		Max	Min	Average			
<i>Valvata sincera</i>		-3.5	16.2	-15.0*	River water $\delta^{18}\text{O}$ *	-7.5	-16.4	-12.4			
<i>Valvata sincera</i>		-3.9	18.0	-13.3*	Count (n values)						
<i>Valvata sincera</i>		-8.0	23.4	-8.1*	<i>Pisidium</i> spp.	10					
<i>Valvata sincera</i>		-3.5	18.1	-13.2*	<i>Valvata sincera</i>	12					
<i>Valvata sincera</i>		-3.4	18.1	-13.1*	<i>Valvata tricarinata</i>	10					
<i>Valvata sincera</i>		-8.1	24.0	-7.5*	Species Identified	Relative Percent					
<i>Valvata tricarinata</i>		-3.6	16.2	-15.7*	<i>Sphaeriidae</i> spp.	47					
<i>Valvata tricarinata</i>		-8.0	20.2	-11.8*	<i>Pisidium</i> spp.	15					
<i>Valvata tricarinata</i>		-6.2	19.2	-12.8*	<i>Valvata sincera</i>	15					
<i>Valvata tricarinata</i>		-9.4	19.6	-12.4*	<i>Valvata tricarinata</i>	13					
<i>Valvata tricarinata</i>		-7.2	20.3	-11.7*	<i>Lymnea decampi</i>	8					
<i>Valvata tricarinata</i>		-2.0	15.4	-16.4*	<i>Helisoma anceps</i>	2					
					<i>Physa gyrina</i>	< 1					

* - Calculated value

Appendix F (cont'd) - All Isotopic Results for Samples
Site 53 - Nipissing - Fluvial (cont'd)

Species	Serial	$\delta^{13}\text{C}$ (VPDB)	$\delta^{18}\text{O}$ Shell (VSMOW)	$\delta^{18}\text{O}$ Water (VSMOW)	Species	Serial	$\delta^{13}\text{C}$ (VPDB)	$\delta^{18}\text{O}$ Shell (VSMOW)	$\delta^{18}\text{O}$ Water (VSMOW)*
<i>Pisidium</i> spp.		-4.4	19.5	-11.6*	<i>Pisidium</i> spp.	4 1.1	-6.0	18.0	
<i>Pisidium</i> spp.		-7.0	19.1	-12.0*	<i>Pisidium</i> spp.	4 1.2	-6.1	18.4	
<i>Pisidium</i> spp.		-4.5	18.3	-12.8*	<i>Pisidium</i> spp.	4 1.3	-5.9	18.3	
<i>Pisidium</i> spp.		-7.0	20.7	-10.5*	<i>Pisidium</i> spp.	4 1*	-6.0*	18.3*	
<i>Pisidium</i> spp.		-3.1	19.9	-11.3*	<i>Pisidium</i> spp.	4 2.1	-6.3	19.1	
<i>Pisidium</i> spp.	1 Bulk	-4.3	17.5	-13.6*	<i>Pisidium</i> spp.	4 2.2	-6.3	19.0	
<i>Pisidium</i> spp.	1 1	-5.6	17.5		<i>Pisidium</i> spp.	4 2.3	-6.1	18.5	
<i>Pisidium</i> spp.	1 2	-5.7	17.4		<i>Pisidium</i> spp.	4 2.4	-6.0	18.6	
<i>Pisidium</i> spp.	1 3	-4.1	17.6		<i>Pisidium</i> spp.	2*	-6.2*	18.8*	
<i>Pisidium</i> spp.	2 1.1	-8.1	17.4		<i>Pisidium</i> spp.	4 3.1	-6.2	18.5	
<i>Pisidium</i> spp.	2 1.2	-6.6	21.3		<i>Pisidium</i> spp.	4 3.2	-6.3	18.4	
<i>Pisidium</i> spp.	2 1*	-5.6*	17.5*		<i>Pisidium</i> spp.	3*	-6.3*	18.5*	
<i>Pisidium</i> spp.	2 2.1	-8.2	16.8		<i>Pisidium</i> spp.	4 4.1	-6.6	18.5	
<i>Pisidium</i> spp.	2 2.2	-8.9	16.7		<i>Pisidium</i> spp.	4 5.1	-6.7	18.6	
<i>Pisidium</i> spp.	2 2.3	-8.0	17.2		<i>Pisidium</i> spp.	4 Bulk*	-6.2*	18.5*	-12.6*
<i>Pisidium</i> spp.	2 2*	-8.4*	16.9*		<i>Pisidium</i> spp.	5 1.1	-4.3	18.7	
<i>Pisidium</i> spp.	2 3.1	-8.9	16.7		<i>Pisidium</i> spp.	5 1.2	-4.4	18.7	
<i>Pisidium</i> spp.	2 3.2	-6.0	16.2		<i>Pisidium</i> spp.	5 1.3	-3.8	18.6	
<i>Pisidium</i> spp.	2 3*	-8.0*	16.5*		<i>Pisidium</i> spp.	5 1.4	-4.3	18.7	
<i>Pisidium</i> spp.	2 Bulk*	-8.0*	17.6*	-13.5*	<i>Pisidium</i> spp.	5 1.5	-4.3	18.9	
<i>Pisidium</i> spp.	3 1.2	-10.6	20.2		<i>Pisidium</i> spp.	1*	-4.3*	18.7*	
<i>Pisidium</i> spp.	3 1.2	-10.0	20.5		<i>Pisidium</i> spp.	5 2.1	-4.5	18.9	
<i>Pisidium</i> spp.	3 1.3	-9.9	20.2		<i>Pisidium</i> spp.	5 2.2	-4.4	18.9	
<i>Pisidium</i> spp.	3 Bulk*	-10.2*	20.3*	-10.9*	<i>Pisidium</i> spp.	5 2.3	-4.4	18.8	

Appendix F (cont'd) - All Isotopic Results for
Samples

Site 53 - Nipissing - Fluvial (cont'd)

Species	Serial	$\delta^{13}\text{C}_{\text{Shell}}$ (VPDB)	$\delta^{18}\text{O}_{\text{Shell}}$ (VSMOW)	$\delta^{18}\text{O}_{\text{Water}}$ (VSMOW)	$\delta^{13}\text{C}$ (VPDB)	Max	Min	Range	Average	St Dev	
<i>Pisidium</i> spp.	5	2.4	-4.8	19.2	All Data	-1.9	-10.6	-8.7	-5.7	2.1	
<i>Pisidium</i> spp.	5	2.5	-4.4	19.1	<i>Pisidium</i> spp.	-3.1	-10.6	-7.5	-6.5	1.8	
<i>Pisidium</i> spp.	5	2.6	-4.3	19.0	<i>Valvata sincera</i>	-3.3	-5.5	-2.2	-4.3	0.7	
<i>Pisidium</i> spp.		2*	-4.5*	19.0*	<i>Valvata tricarinata</i>	-1.9	-10.5	-8.6	-5.7	3.1	
<i>Pisidium</i> spp.	5	5.3	-4.9	19.2	$\delta^{18}\text{O}$ (VSMOW)	Max	Min	Range	Average	St Dev	
<i>Pisidium</i> spp.	5	5.3 DUP	-5.0	19.1	All Data	22.4	14.6	7.8	18.3	1.5	
<i>Pisidium</i> spp.		3*	-5.0*	19.2*	<i>Pisidium</i> spp.	21.3	16.2	5.1	18.5	1.1	
<i>Pisidium</i> spp.	5	Bulk*	-4.5*	18.9*	-12.2*	<i>Valvata sincera</i>	19.0	14.6	4.4	17.5	0.9
<i>Valvata sincera</i>			-5.5	17.4	-13.8*	<i>Valvata tricarinata</i>	22.4	14.6	7.8	17.9	2.6
<i>Valvata sincera</i>			-3.3	18.1	-13.1*						
<i>Valvata sincera</i>			-4.9	19.0	-12.3*	Count (n value)					
<i>Valvata sincera</i>			-3.8	16.4	-14.8*	<i>Pisidium</i> spp.	32				
<i>Valvata sincera</i>			-4.1	17.9	-13.3*	<i>Valvata sincera</i>	10				
<i>Valvata sincera</i>			-4.4	17.6	-13.6*	<i>Valvata tricarinata</i>	11				
<i>Valvata sincera</i>			-4.8	16.8	-14.4*	Species Identified	Relative Percent				
<i>Valvata sincera</i>			-4.7	18.7	-12.6*	<i>Valvata sincera</i>	30				
<i>Valvata sincera</i>			-3.5	16.7	-14.6*	<i>Lymnea</i> spp.	22				
<i>Valvata sincera</i>			-3.5	16.6	-14.7*	<i>Pisidium</i> spp.	18				
<i>Valvata tricarinata</i>			-9.7	20.4	-11.6*	<i>Valvata tricarinata</i>	14				
<i>Valvata tricarinata</i>			-7.0	17.3	-14.6*	<i>Amnicola limosa</i>	5				
<i>Valvata tricarinata</i>			-8.9	22.4	-9.7*	<i>Gyraulus parvus</i>	4				
<i>Valvata tricarinata</i>			-10.5	20.9	-11.1*	<i>Sphaeriidae</i> spp.	3				
<i>Valvata tricarinata</i>			-4.0	17.8	-14.1*	<i>Pleurocera livescens</i>	< 1				
<i>Valvata tricarinata</i>			-3.3	16.4	-15.5*	<i>Physa gyrina</i>	< 1				
<i>Valvata tricarinata</i>			-3.4	15.6	-16.3*		Max	Min	Average		
<i>Valvata tricarinata</i>			-7.7	19.3	-12.7*	River water $\delta^{18}\text{O}$ *	-9.7	-17.3	-13.3		
<i>Valvata tricarinata</i>			-1.9	14.8	-17.1*						

* - Calculated value DUP - Duplicate Sample

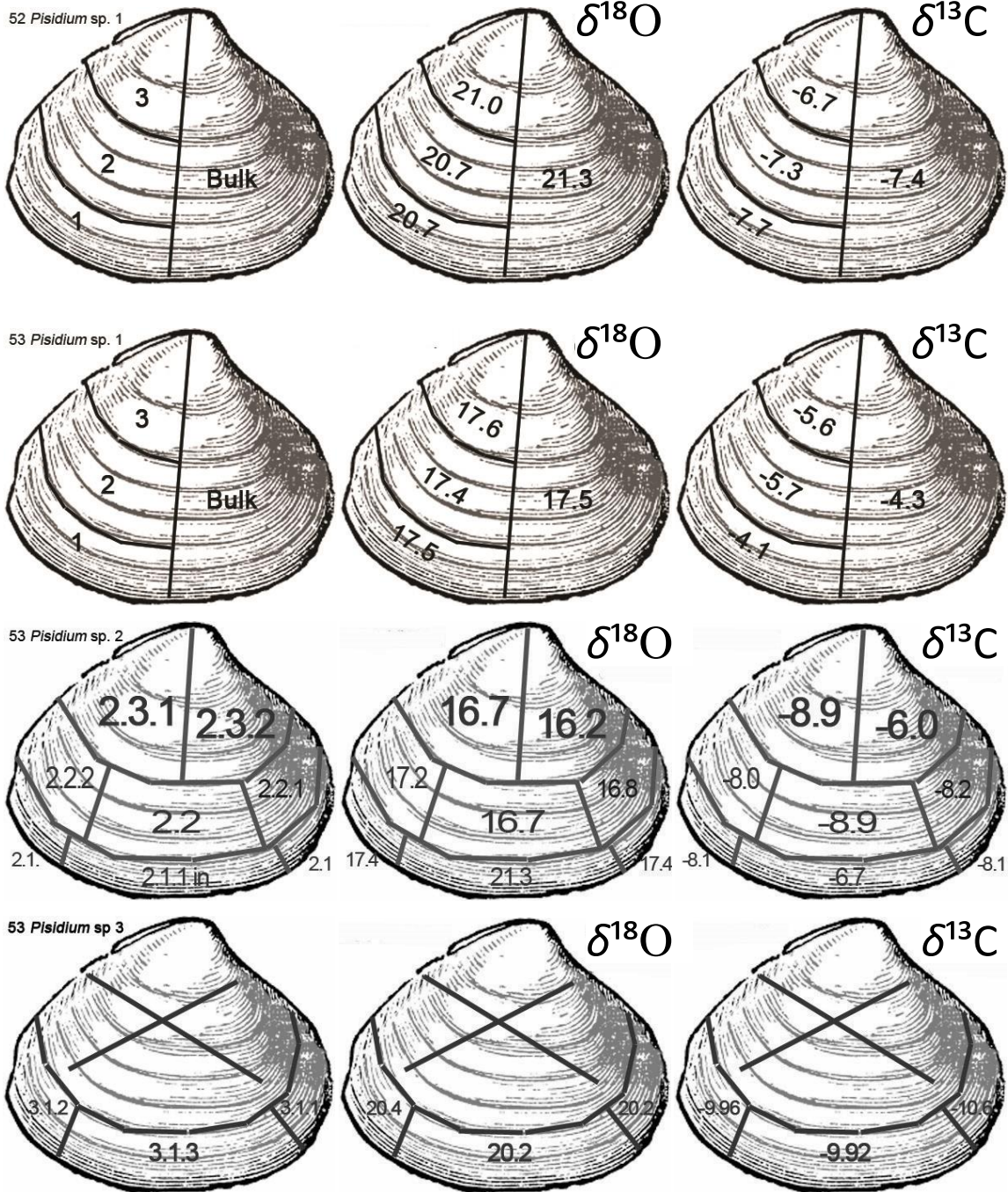
Appendix F (cont'd) -

Site: Ferndale/Sucker Creek - Nipissing - Lacustrine

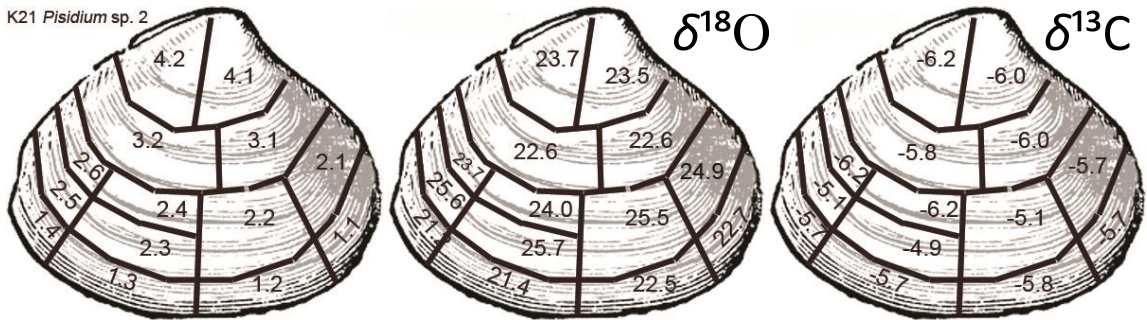
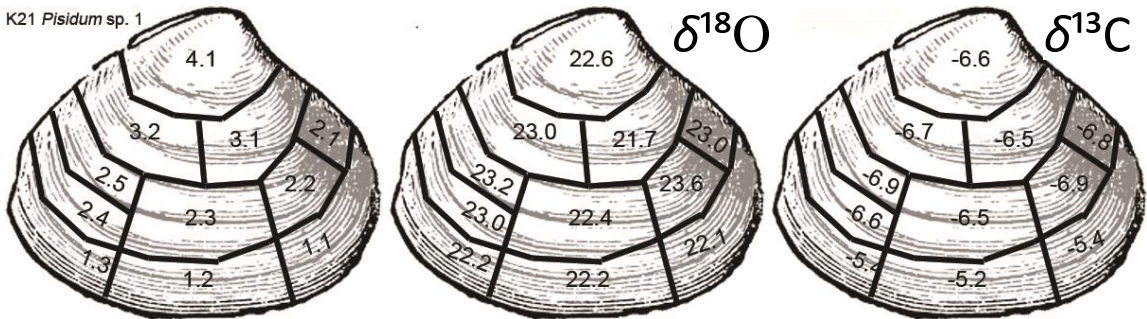
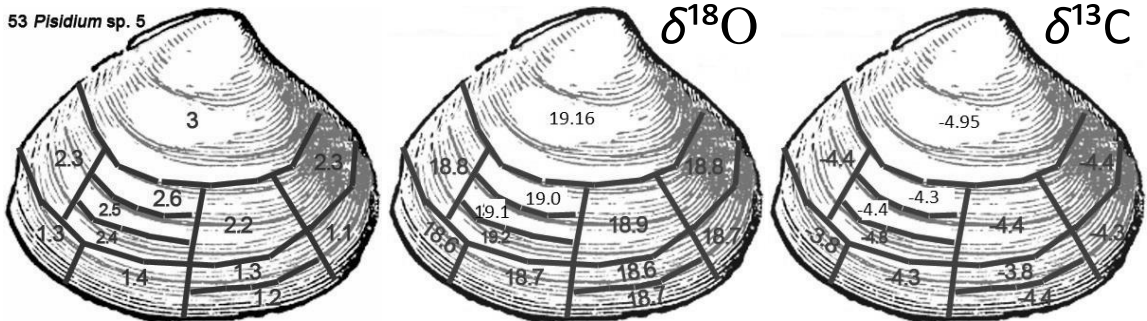
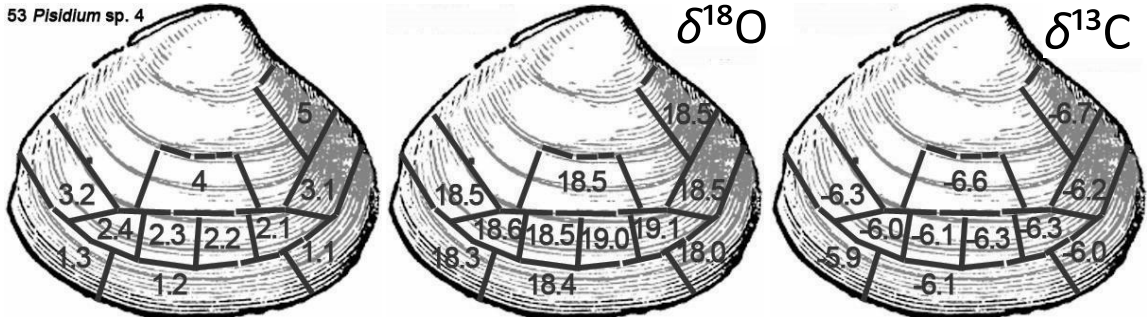
Species	Site	$\delta^{13}\text{C}$			Species	Site	$\delta^{13}\text{C}$			Species	Site	$\delta^{18}\text{O}$		
		Shell (VPDB)	$\delta^{18}\text{O}$ Shell (VSMOW)	$\delta^{18}\text{O}$ Water (VSMOW)			Shell (VPDB)	$\delta^{18}\text{O}$ Shell (VSMOW)	$\delta^{18}\text{O}$ Water (VSMOW)			Shell (VPDB)	$\delta^{18}\text{O}$ Shell (VSMOW)	$\delta^{18}\text{O}$ Water (VSMOW)
<i>Pisidium casertanum</i>	FN 2A	2.7	25.9	-5.4*	<i>Valvata sincera</i>	FN 2B	-0.8	24.9	-6.6*					
<i>Pisidium casertanum</i>	FN 2A	2.2	24.9	-6.4*	<i>Valvata sincera</i>	FN 2B	-0.6	24.7	-6.8*					
<i>Pisidium casertanum</i>	FN 2A	0.9	25.2	-6.1*	<i>Valvata sincera</i>	FN 2A	1.1	25.2	-6.3*					
<i>Pisidium casertanum</i>	FN 2	2.6	25.2	-6.1*	<i>Valvata sincera</i>	FN 2A	1.3	25.1	-6.4*					
<i>Pisidium casertanum</i>	FN 2	-0.5	25.9	-5.5*	<i>Valvata sincera</i>	FN 2A	0.8	24.7	-6.8*					
<i>Pisidium casertanum</i>	FN 2	-0.3	25.9	-5.4*	<i>Valvata tricarinata</i>	FN 2A	0.0	24.7	-7.4*					
<i>Pisidium casertanum</i>	FN 8	0.7	24.1	-7.2*	<i>Valvata tricarinata</i>	FN 2A	-0.5	24.7	-7.5*					
<i>Pisidium casertanum</i>	FN 8	-2.0	25.2	-6.1*	<i>Valvata tricarinata</i>	FN 2A	0.1	25.4	-6.8*					
<i>Pisidium casertanum</i>	FN 8	3.8	24.9	-6.4*	<i>Valvata tricarinata</i>	FN 2A	0.3	25.1	-7.0*					
<i>Pisidium compressum</i>	FN8	2.8	26.0	-5.4*	<i>Valvata sincera</i>	Sucker Creek	-1.9	24.2	-7.3*					
<i>Pisidium compressum</i>	FN8	1.5	24.8	-6.6*	<i>Valvata sincera</i>	Sucker Creek	-0.8	24.1	-7.4*					
<i>Pisidium compressum</i>	FN8	4.9	26.1	-5.4*	$\delta^{13}\text{C}$ (VPDB)	Max	Min	Range	Average	St Dev				
<i>Pisidium compressum</i>	FN8	5.0	26.1	-5.3*	All	5.0	-7.2	12.2	1.6	2.4				
<i>Pisidium compressum</i>	FN 2B	2.1	25.6	-5.8*	<i>Pisidium</i> spp.	5.0	-2.0	7.0	1.9	1.6				
<i>Pisidium compressum</i>	FN 2B	2.1	25.6	-5.8*	<i>Valvata sincera</i>	1.3	-0.8	2.1	0.4	1.0				
<i>Pisidium compressum</i>	FN 2B	0.5	25.6	-5.8*	<i>Valvata tricarinata</i>	0.3	-0.5	0.7	0.0	0.3				
<i>Pisidium compressum</i>	FN 2A	2.1	25.6	-5.9*	$\delta^{18}\text{O}$ (VSMOW)	Max	Min	Range	Average	St Dev				
<i>Pisidium compressum</i>	FN 2A	1.9	25.7	-5.7*	All	26.6	-5.8	32.4	24.3	6.4				
<i>Pisidium compressum</i>	FN 2A	1.9	25.7	-5.7*	<i>Pisidium</i> spp.	26.6	24.1	2.5	25.6	0.6				
<i>Pisidium compressum</i>	FN 2A	2.2	26.3	-5.2*	<i>Valvata sincera</i>	25.2	24.7	0.5	24.9	0.2				
<i>Pisidium compressum</i>	FN 1	2.7	25.3	-6.1*	<i>Valvata tricarinata</i>	25.4	24.7	0.7	25.0	0.4				
<i>Pisidium compressum</i>	FN 1	2.5	26.0	-5.4*	Count (n value)									
<i>Pisidium compressum</i>	FN 1	2.4	26.6	-4.8*	<i>Pisidium</i> spp.	23								
	Max	Min	Average		<i>Valvata sincera</i>	5								
Lake Water $\delta^{18}\text{O}$ *	-4.8	-7.2	-5.8		<i>Valvata tricarinata</i>	4								

* - Calculated value

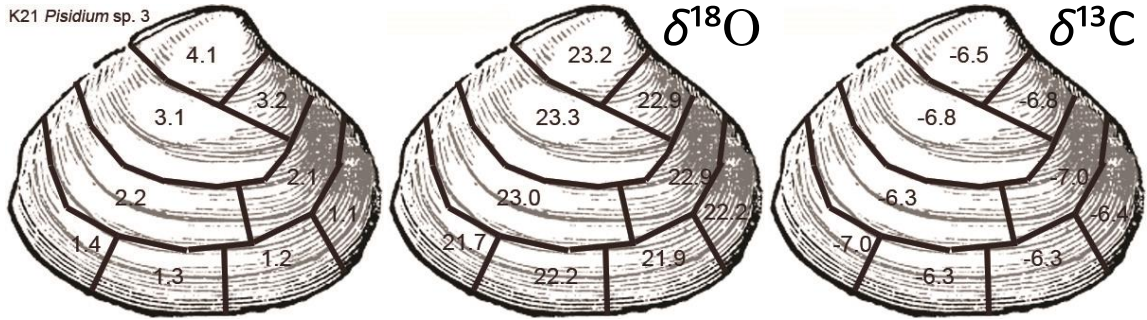
Appendix G - Serial Sampling Schematics and Isotopic Results



Appendix G (cont'd) - Serial Sampling Schematics and Isotopic Results



Appendix G (cont'd) - Serial Sampling Schematics and Isotopic Results

K21 *Pisidium* sp. 3

Appendix H - Oxygen and Carbon Isotope Data from Core 594 from Macdonald (2012)

Species	Depth (m)	$\delta^{13}\text{C}$ Shell (‰, VPDB)	$\delta^{18}\text{O}$ Shell (‰, VSMOW)	$\delta^{18}\text{O}$ Water (‰, VSMOW)*
<i>Pisidium</i> spp.	12.8	-7.5	23.1	-8.2
<i>Pisidium</i> spp.	12.8	-6.2	22.6	-8.6
<i>Pisidium</i> spp.	13.0	-6.7	24.0	-7.3
<i>Pisidium</i> spp.	13.0	-7.0	24.0	-7.2
<i>Pisidium</i> spp.	13.2	-6.2	24.7	-6.6
<i>Pisidium</i> spp.	13.2	-6.2	24.7	-6.6
<i>Pisidium</i> spp.	13.4	-7.1	24.0	-7.3
<i>Pisidium</i> spp.	13.4	-5.6	24.8	-6.5
<i>Pisidium</i> spp.	13.6	-5.4	24.7	-6.6
<i>Pisidium</i> spp.	13.6	-5.6	24.7	-6.6
<i>Pisidium</i> spp.	13.8	-5.2	25.5	-5.9
<i>Pisidium</i> spp.	13.8	-5.6	25.0	-6.3
<i>Pisidium</i> spp.	14.0	-5.2	24.8	-6.5
<i>Pisidium</i> spp.	14.0	-6.0	24.6	-6.7
<i>Pisidium</i> spp.	14.2	-5.3	25.6	-5.7
<i>Pisidium</i> spp.	14.2	-5.5	25.4	-5.9
<i>Pisidium</i> spp.	14.2	-5.6	25.4	-5.7
<i>Pisidium</i> spp.	14.4	-4.5	27.4	-4.0
<i>Pisidium</i> spp.	14.4	-5.3	25.7	-5.7
<i>Pisidium</i> spp.	14.4	-6.3	24.9	-6.4
<i>Pisidium</i> spp.	14.4	-6.6	25.4	-5.9
<i>Pisidium</i> spp.	14.6	-4.7	25.4	-5.9
<i>Pisidium</i> spp.	14.6	-5.2	25.8	-5.6
<i>Pisidium</i> spp.	14.8	-4.7	23.3	-7.9
<i>Pisidium</i> spp.	14.8	-4.9	25.8	-6.5
<i>Pisidium</i> spp.	14.8	-4.7	23.4	-7.8

* - Calculated value

Appendix I - Oxygen and Carbon Isotope Data from Godwin (1985)

Species	Site	$\delta^{13}\text{C}$ Shell (‰, VPDB)	$\delta^{18}\text{O}$ Shell (‰, VPDB)	$\delta^{18}\text{O}$ Water (‰, VSMOW)*
<i>Amnicola</i> sp.	K6	-6.6	-10.5	20.1
<i>Amnicola</i> sp.	K21	-5.4	-9.6	21.0
<i>Amnicola</i> sp.	K21	-8.0	-9.1	21.5
<i>Amnicola</i> sp.	K21	-7.9	-9.4	21.2
<i>Amnicola</i> sp.	K10	-5.3	-9.6	21.0
<i>Amnicola</i> sp.	K10	-5.5	-9.2	21.4
<i>Amnicola</i> sp.	K10	-4.9	-8.1	22.6
<i>Amnicola</i> sp.	K10	-7.8	-10.0	20.6
<i>Amnicola</i> sp.	K10	-6.3	-9.0	21.6
<i>Amnicola</i> sp.	K10	-7.9	-8.9	21.7
<i>Pisidium</i> spp.	K6	-6.3	-10.9	19.7
<i>Pisidium</i> spp.	K6	-6.4	-10.7	19.9
<i>Pisidium</i> spp.	K10	-9.1	-10.0	20.6
<i>Pisidium</i> spp.	K10	-8.4	-9.6	21.0
<i>Pisidium</i> spp.	K10	-7.5	-8.6	22.1
<i>Pisidium</i> spp.	K10	-6.6	-7.8	22.9
<i>Pisidium</i> spp.	K10	-6.8	-7.5	23.2
<i>Pisidium</i> spp.	K10	-7.9	-7.7	23.0
<i>Pisidium</i> spp.	K10	-7.1	-9.6	21.0
<i>Pisidium</i> spp.	K21	-5.7	-9.0	21.6
<i>Pisidium</i> spp.	K21	-7.2	-9.6	21.0
<i>Pisidium</i> spp.	K21	-6.2	-10.1	20.5
<i>Pisidium</i> spp.	K21	-6.0	-9.5	21.1
<i>Valvata sincera</i>	K6	-7.5	-10.4	20.2
<i>Valvata sincera</i>	K21	-6.8	-8.6	22.1
<i>Valvata sincera</i>	K21	-6.7	-8.1	22.6
<i>Valvata sincera</i>	K21	-6.6	-9.6	21.0
<i>Valvata sincera</i>	K21	-7.0	-10.0	20.6
<i>Valvata sincera</i>	K21	-6.4	-9.4	21.2
<i>Valvata sincera</i>	K21	-7.0	-9.3	21.3
<i>Valvata sincera</i>	K21	-6.1	-9.6	21.0
<i>Valvata sincera</i>	K21	-7.0	-9.5	21.1
<i>Valvata tricarinata</i>	K6	-6.9	-11.0	19.6
<i>Valvata tricarinata</i>	K6	-7.7	-9.7	20.9

Appendix I (cont'd) - Oxygen and Carbon Isotope Data from Godwin (1985)

Species	Site	$\delta^{13}\text{C}$ Shell (‰, VPDB)	$\delta^{18}\text{O}$ Shell (‰, VPDB)	$\delta^{18}\text{O}$ Water (‰, VSMOW)*
<i>Valvata tricarinata</i>	K10	-8.6	-9.7	20.9
<i>Valvata tricarinata</i>	K10	-6.6	-9.4	21.2
<i>Valvata tricarinata</i>	K10	-6.6	-9.8	20.8
<i>Valvata tricarinata</i>	K10	-6.5	-10.2	20.4
<i>Valvata tricarinata</i>	K10	-6.2	-9.9	20.7
<i>Valvata tricarinata</i>	K10	-7.0	-9.5	21.1
<i>Valvata tricarinata</i>	K10	-7.7	-10.0	20.6
<i>Valvata tricarinata</i>	K10	-8.2	-10.0	20.6
<i>Valvata tricarinata</i>	K10	-7.3	-10.2	20.4
<i>Valvata tricarinata</i>	K10	-7.0	-10.5	20.1
<i>Valvata tricarinata</i>	K10	-8.2	-10.3	20.3
<i>Valvata tricarinata</i>	K10	-7.7	-9.3	21.3
<i>Valvata tricarinata</i>	K10	-6.3	-8.3	22.4
<i>Valvata tricarinata</i>	K10	-7.6	-10.3	20.3
<i>Valvata tricarinata</i>	K10	-6.5	-9.2	21.4
<i>Valvata tricarinata</i>	K10	-7.2	-9.6	21.0
<i>Valvata tricarinata</i>	K10	-7.7	-9.9	20.7
<i>Valvata tricarinata</i>	K10	-8.5	-9.7	20.9
<i>Valvata tricarinata</i>	K10	-8.1	-10.0	20.6
<i>Valvata tricarinata</i>	K10	-6.9	-9.7	20.9
<i>Valvata tricarinata</i>	K10	-7.2	-8.6	22.1
<i>Valvata tricarinata</i>	K10	-5.5	-8.6	22.1
<i>Valvata tricarinata</i>	K10	-7.7	-8.8	21.8
<i>Valvata tricarinata</i>	K10	-8.0	-9.0	21.6
<i>Valvata tricarinata</i>	K21	-6.4	-8.6	22.1
<i>Valvata tricarinata</i>	K21	-6.2	-9.4	21.2
<i>Valvata tricarinata</i>	K21	-7.9	-8.1	22.6
<i>Valvata tricarinata</i>	K21	-6.4	-9.9	20.7
<i>Valvata tricarinata</i>	K21	-5.9	-10.4	20.2
<i>Valvata tricarinata</i>	K21	-4.1	-10.8	19.8
<i>Valvata tricarinata</i>	K21	-7.6	-10.7	19.9
<i>Valvata tricarinata</i>	K21	-6.6	-9.8	20.8
<i>Valvata tricarinata</i>	K21	-5.4	-10.2	20.4
<i>Valvata tricarinata</i>	K21	-6.6	-10.1	20.5

* - Calculated value

Curriculum Vitae

- Name:** Jane L.M.D. Wilson
- Post-secondary Education and Degrees:** The University of Western Ontario
London, Ontario, Canada
2014 – 2017 M.Sc. in Geology
- The University of Western Ontario
London, Ontario, Canada
2010 – 2014 B.Sc. in Professional Geology
- Honours and Awards:** Graduate Student Teaching Award (2016)
Canadian Mineral Industry Education Foundation Scholarship (2011, 2012, 2013)
Dean's Honour List (2012, 2013)
Laurene Patterson Estate Scholarship (2012)
Robert and Ruth Lumsden Undergraduate Awards in Earth Sciences (2012)
The J.P. Bickell Foundation Mining Scholarship (2012)
- Related Work Experience** Teaching Assistant
The University of Western Ontario
2014 – 2016
- Abstracts and Presentations:** Wilson, J.L.M.D, Longstaffe, F.J. (2017) Carbonate isotopes of shelly fauna describe Late Pleistocene-Holocene depositional environment in the Huron basin, Ontario, Canada. Advances in Earth Science Research conference, London, Ontario [poster presentation]
- Wilson, J.L.M.D, Longstaffe, F.J. (2016) Using carbonates to discover Mid-Holocene climate variability in the Huron Basin. Northeastern Geological Society of America conference, Albany, New York [oral presentation]